U.S. Department
of Commerce

Volume 114
Number 3
July 2016

Fishery Bulletin

Fishery Bulletin

***Fishery Bulletin* web site: www.fisherybulletin.noaa.gov**

The *Fishery Bulletin* (ISSN 0090-0656) is published quarterly by the Scientific Publications Office, National Marine Fisheries Service, NOAA, 7600 Sand Point Way NE, Seattle, WA 98115-0070.

The Secretary of Commerce has determined that the publication of this periodical is necessary according to law for the transaction of public business of this Department. Use of funds for printing of this periodical has been approved by the Director of the Office of Management and Budget.

For Sale by the Superintendent of Documents, U.S. Government Printing Office, Washington, DC 20402. Subscription price per year: $32.00 domestic and $44.80 foreign. Cost per single issue: $19.00 domestic and $26.60 foreign. **See back for order form.**

The *Fishery Bulletin* carries original research reports on investigations in fishery science, engineering, and economics. It began as the Bulletin of the United States Fish Commission in 1881; it became the Bulletin of the Bureau of Fisheries in 1904 and the *Fishery Bulletin* of the Fish and Wildlife Service in 1941. Separates were issued as documents through volume 46; the last document was no. 1103. Beginning with volume 47 in 1931 and continuing through volume 62 in 1963, each separate appeared as a numbered bulletin. A new system began in 1963 with volume 63 in which papers are bound together in a single issue. Beginning with volume 70, number 1, January 1972, *Fishery Bulletin* became a periodical, issued quarterly. In this form, it is available by subscription from the Superintendent of Documents, U.S. Government Printing Office, Washington, DC 20402. It is also available free in limited numbers to libraries, research institutions, state and federal agencies, and in exchange for other scientific publications.

U.S. Department
of Commerce
Seattle, Washington

Volume 114
Number 3
July 2016

Fishery Bulletin

Contents

Articles

Short communication

NOAA
National Marine
Fisheries Service

Fishery Bulletin
established 1881

Spencer F. Baird
First U.S. Commissioner
of Fisheries and founder
of *Fishery Bulletin*

Assessing the use of a camera system within an autonomous underwater vehicle for monitoring the distribution and density of sea scallops (*Placopecten magellanicus*) in the Mid-Atlantic Bight

Justin H. Walker[1]
Arthur C. Trembanis (contact author)[1,2]
Douglas C. Miller[2]

Email address for contact author: art@udel.edu

[1] Department of Geological Sciences
University of Delaware
109 Penny Hall
Newark, Delaware 19716

[2] School of Marine Science and Policy
University of Delaware
Lewes, Delaware 19958

Abstract—The sea scallop (*Placopecten magellanicus*) fishery in the Atlantic is assessed during annual surveys by using both dredging and surface-deployed imaging techniques. In this pilot study in the Mid-Atlantic Bight, we used an autonomous underwater vehicle (AUV) to photograph the seafloor and to evaluate its use for determining scallop density and size. During 22 surveys in 2011, 257 km of seafloor were photographed, resulting in over 203,000 color images. Using trained annotators and photogrammetric software, we determined scallop density and shell heights for 15,252 scallops. The inshore scallop grounds near Long Island (at depths <40 m) had a density of 0.077 scallops per m^2, whereas the inshore grounds of the New York Bight had a density of 0.012 scallops per m^2. Shell heights derived from images were found to agree well with measurements from scallops collected with a commercial dredge. We show that images obtained with an AUV can be used to reliably estimate both density and shell height consistent with direct sampling from the same area. Moreover, side-scan sonar images obtained with an AUV can be used to detect dredge scars and, therefore, can provide a simultaneous, relative estimate of fishing effort in that area. AUVs provide a highly accurate suite of data for each survey site and therefore allow the design of experimental studies of fishing practices.

Manuscript submitted 9 April 2015.
Manuscript accepted 22 March 2016.
Fish. Bull. 114:261–273 (2016).
Online publication date: 26 April 2016.
doi: 10.7755/FB.114.3.1

The sea scallop (*Placopecten magellanicus*, Gmelin 1791) of the Mid-Atlantic Bight Atlantic fishery has been commercially active for over 100 years, and in recent years has consistently ranked in the top five most valuable domestic U.S. fisheries at around a half billion dollars (NMFS, 2009–2013). To promote the sustainability of the sea scallop fishery, the National Marine Fisheries Service (NMFS) monitors the fishery annually through a combination of survey approaches (Stokesbury et al., 2004; Kelly[1]; DuPaul and Rudders[2]; NEFSC[3]; Rudders and DuPaul[4]). The results of these monitoring efforts are used to determine annual catch limits that balance overfishing and sustainability against potentially unnecessary economic loss (Rosenberg, 2003; Naidu and Robert, 2006).

The sea scallop fishery stock is monitored by means of both dredge surveys (DuPaul and Rudders[2]; NEFSC[3]), and drop-camera surveys (Jacobson et al., 2010; Carey and Stokesbury 2011; Stokesbury, 2012; Hart et al., 2013). Dredging is performed by towing either a commercial or scientific survey dredge across the seafloor and has a direct impact on scallops, bycatch organisms, and

[1] Kelly, K. H. 2007. Results from the 2006 Maine sea scallop survey, 34 p. Maine Dep. Mar. Res., W. Boothbay Harbor, ME. [Available at website.]

[2] DuPaul, W. D., and D. B. Rudders. 2008. An assessment of sea scallop abundance and distribution in selected closed areas: Georges Bank area I and II, Nantucket Lightship and Elephant Trunk. VIMS Mar. Res. Rep. 2008-3, 47 p. Virginia Institute of Marine Science, College of William and Mary, Gloucester Point, VA. [Available at website.]

[3] NEFSC (Northeast Fisheries Science Center). 2010. 50th northeast regional stock assessment workshop (50th SAW) assessment report. Northeast Fish. Sci. Cent. Ref. Doc. 10-17, 844 p. [Available at website.]

[4] Rudders, D. B., and W. D. DuPaul. 2012. An assessment of sea scallop abundance and distribution in open access areas: New York Bight and the southern New England area. VIMS Mar. Res. Rep. 2012-8, 48 p. Virginia Institute of Marine Science, College of William and Mary, Gloucester Point, VA. [Available at website.]

the seafloor itself. Imagery-based surveys have fewer direct impacts on the seafloor and its inhabitants and have the advantage of covering large areas efficiently. Early studies were performed with cameras mounted on a rigid stationary pyramid-shaped platform that was lowered from a vessel to the seafloor (Stokesbury, 2002). More recently the HabCam system has been developed, which is a towed camera sled tethered to a ship, and it can photograph long stretches of the seafloor (Rosenkranz et al., 2008). In 2010, the National Marine Fisheries Service (NMFS) formally expressed the need to develop and apply new approaches to stock assessment of sea scallop in the Mid-Atlantic Bight (NMFS, 2010). A recent NOAA-sponsored workshop (NOAA[5]) gathered numerous researchers engaged in seabed imaging to highlight the development of a variety of imaging platforms, and among their findings, the potential value of autonomous imaging platforms was recognized for future survey efforts. The present study is a an application of those recommendations by extending previous smaller scale camera studies with the use of autonomous underwater vehicles (AUVs) in Iceland (Singh et al., 2013 and 2014) to a larger spatial scale study through surveys conducted within the Mid-Atlantic Bight.

AUVs have been shown to be an effective platform for mapping benthic habitat (Tolimieri et al., 2008; Forrest et al., 2012; Raineault et al., 2012; Seiler et al., 2012; Raineault et al., 2013) by coupling images obtained by underwater camera with highly accurate preprogrammed navigation. In this study, we used an AUV to assess sea scallop shell height and abundance, as well to estimate biomass in the shallow (< 40 m) open scallop fishing grounds within the Mid-Atlantic Bight. Because shallow grounds are not typically within the scope of the annual NMFS survey, this study offers unique findings of the sea scallop populations in such areas. Moreover, our results show that an AUV is a suitable platform for collecting images as part of the sea scallop stock assessment process. Our goal in this pilot study was to test and show the feasibility of the AUV platform by using synchronous commercial dredging samples to illustrate the efficacy of the underwater camera system for what could be scaled up to be a useful tool for a full stock assessment process.

Materials and methods

Field sampling

The Mid-Atlantic Bight is the shallow portion of the continental shelf that extends from Cape Hatteras, NC, to Cape Cod, MA. Our study area was selected to fulfill the needs of the Mid-Atlantic Fishery Management Council's Research Set-Aside (RSA) program to survey heavily fished inshore scallop grounds (<40 m depth) that are not regularly monitored. All of the AUV surveys reported here were conducted in the New York Bight (NYB) and Long Island (LI) regions during July 2011 (Fig. 1).

As part of their survey sampling design, the National Marine Fisheries Service uses a 30×30 minute latitude/longitude grid system. Our AUV surveys were executed at randomly selected sites within each block area of an 8-block grid. They involved photographically surveying at least 37,500 m^2 of seafloor at two or more sites within each grid. Sites were either chosen from recent NMFS survey sites for scallop stocks or were randomly chosen from within each grid to meet the predetermined total area. All of the surveys were conducted within 70 km of the coast of Delaware, New Jersey, or New York, and the water depths sampled ranged from 20 to 50 m (Table 1), which is within the normal habitable zone for the sea scallop (Merrill[6]; Hart and Chute, 2004). Extensive details of the sampling design were compiled in the master's thesis for the pilot study (Walker, 2013) and were reviewed and approved by both an internal and external panel of scientists selected by NMFS as part of the final project review process.

Survey design

At each site, we deployed the AUV on a preplanned path that ranged from 3 to 16 kilometers of contiguous survey trackline. Surveys lasted up to 3 hours, an operational limit imposed by the life of a single battery pack. The AUV was programmed in a terrain-following mode with a commanded altitude of 2.2 m. Postprocessing analysis of the survey logs showed that the AUV remained within a 16 cm standard deviation of the 2.2 m commanded altitude, a deviation that is consistent with previous studies in which the same vehicle system has been used (e.g., Forrest et al., 2012; Raineault et al., 2012). Precise navigation of the vehicle is accomplished by using a DVL-aided (Doppler Velocity Log) INS (Inertial Navigation System), which has been shown in the literature to provide a positional drift rate of 0.5 m/h (Patterson et al., 2008) or 0.1% of distance traveled (Rankey and Doolittle, 2012). Comparison of known targets (such as stationary man-made objects on the seafloor) in side-scan sonar imagery from repeated passes showed positional precision of within 2 m from one survey to the next—a level that is consistent with results from other published benthic habitat mapping studies conducted with this same vehicle system (e.g., Forrest et al., 2012; Raineault et al., 2013).

Because this was a pilot study, several trackline designs were tested to determine the most effective geometric design for image and acoustic sampling. The survey design that we used most often comprised a series of parallel boustrophedon lines, commonly known

[5] NOAA. 2014. Undersea Imaging Workshop: workshop report; Red Bank, N.J., 14–15 January, 34 p. New Jersey Sea Grant Consortium, NOAA, Fort Hancock, NJ. [Available at website.]

[6] Merrill, A. S. 1971. The sea scallop. *In* Annual report for 1970, p. 24–27. Am. Malacol. Union Inc.

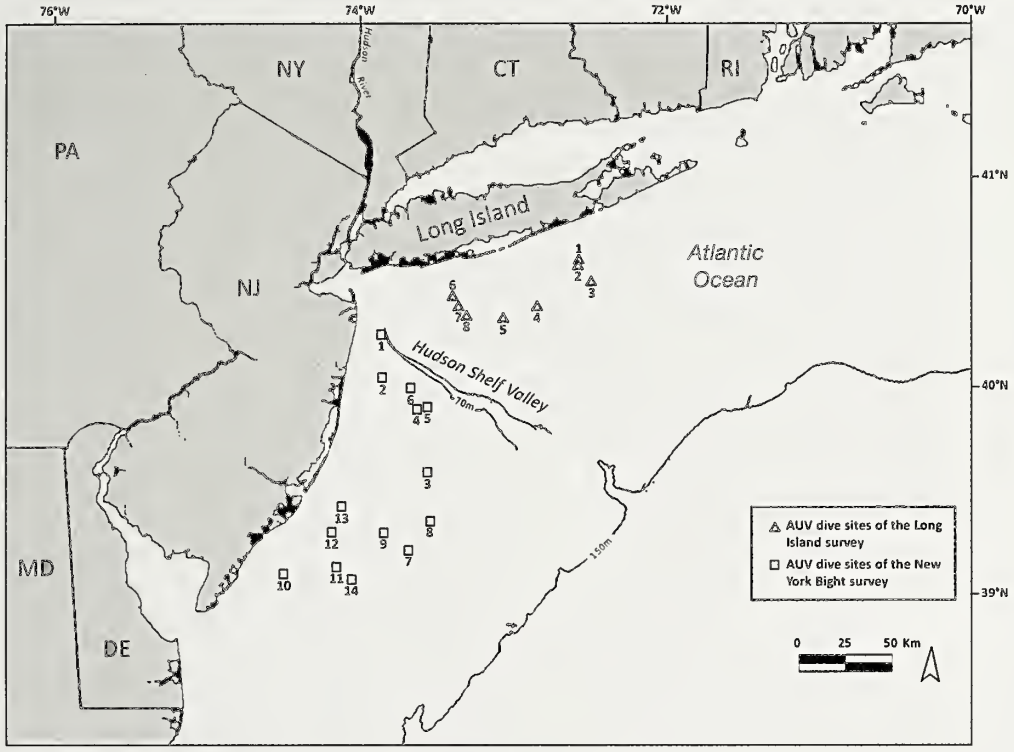

Figure 1

A map of the Mid-Atlantic Bight showing the sites where photographs of the sea bottom and sea scallops (*Placopecten magellanicus*) were taken with an underwater camera from an autonomous underwater vehicle (AUV) at 22 survey sites in 2011.

as a "lawn mower" pattern. Multiple equidistant transects were run parallel to each other at a commanded even spacing that ranged between 2 to 40 m laterally. This method had the advantage of allowing 100% imaging and side-scan sonar coverage depending on transect spacing. Less frequently, our survey design consisted of equidistant oblique transects that propagated along only one of the transect axes in a slalom path. This design would be most useful for sampling an elongated bed of scallops. The third most used survey design consisted of equidistant orthogonal transects that propagated along both transect axes (in the profile of a staircase). This design provided the largest extent of geographic coverage from a single battery charge.

Equipment

Our surface vessel was the FV *Christian and Alexa*, a 30-m eastern rig, commercial fishing ship with port and starboard New Bedford style 15-ft (4.57-m) scallop dredges. For comparison of the AUV imagery data, each survey site was dredged immediately after the AUV survey with the starboard scallop dredge by towing for 15 minutes at 4.5 to 5.0 knots at every site along the initial AUV transect line. The dredges were fitted with 4-inch (10.2-cm) interlocking rings to coincide with commercial fishing requirements, along with an 11-inch (27.9-cm) twine mesh top and turtle chains. Shell-height-frequency data were collected on the deck from the dredged contents by using standard survey methods for sizing a randomly selected bushel of scallops.

The photographic imaging platform used was a Teledyne Gavia AUV that has an operational depth limit of 500 m. The AUV was run in an imaging and sonar mapping configuration consisting (from front to back) of a nose cone camera, lithium ion battery module, GeoSwath phase measuring bathymetric sonar (500 kHz) module, Kearfott T-24 inertial navigation system (INS) and Doppler velocity log (DVL), command module (900/1800 kHz Marine Sonic side-scan sonar), and a propulsion module. During a survey, the AUV can simultaneously optically image the seafloor, map the seafloor with side-scan sonar and phase measuring bathymetric sonar, log depth and altitude of the vehicle, and measure water temperature, dissolved oxygen saturation, turbidity, and salinity.

The nose cone camera was a Point Grey Scorpion 20SO research camera, equipped with a Sony ICX274 Type 1/1.8" (8.923 mm diagonal) CCD camera, with a resolution of 800×600 pixels. This camera was configured to acquire images at a rate of 3.75 images per second. Illumination was provided by LED strobe array, positioned obliquely aft of the camera. The camera has a Fujinon DF6HA-1B 6-mm focal length lens and a horizontal viewing angle of 44.65° in salt water based on a salinity of 35 (PSU). Calibration results determined

Table 1

Summary of environmental data and measurements of sea scallops (*Placopecten magellanicus*) derived from photographs taken with an underwater camera within an autonomous underwater vehicle (AUV) during surveys within the Long Island (LI) and New York Bight (NYB) areas.

	AUV survey site	Latitude (°)	Longitude (°)	Water depth (m)	Bottom water temperature (°C)	Survey distance (m)	Survey area (m^2)	Number of bottom images	Number of scallops	Scallop density (scallops/m^2)	Mean shell height (mm)	Mean meat weight (g/scallop)
Long Island area	LI1	40.5529	-72.5899	41.9	8.8	15,904	26,834	14,742	2,172	0.081	121.1	37.0
	LI2	40.5503	-72.5872	43.5	8.8	3,015	5,280	2,387	894	0.169	119.6	35.2
	LI3	40.4712	-72.5294	45.4	8.5	10,337	18,135	8,065	3,706	0.204	103.7	23.7
	LI4	40.3449	-72.8817	45.8	8.6	12,280	21,689	9,992	1,365	0.063	101.4	21.8
	LI5	40.3111	-73.0825	42.1	8.9	10,773	19,085	8,338	1,850	0.097	102.8	23.6
	LI6	40.3961	-73.3818	31.7	11.9	14,211	23,473	11,329	422	0.018	100.0	25.3
	LI7	40.3551	-73.3483	33.7	10.8	12,271	20,384	10,163	227	0.011	112.6	33.5
	LI8	40.3213	-73.2749	35.3	9.8	12,154	21,328	9,780	1,403	0.066	104.2	26.5
Summary				Mean 39.3	Mean 9.6	Total 90,945	Total 156,208	Total 74,796	Total 12,039	Mean 0.077	Mean 107.7	Mean 27.3
New York Bight area	NYB1	40.2368	-73.7828	35.5	11.0	10,398	17,684	9,141	82	0.005	106.4	28.4
	NYB2	40.0279	-73.8078	27.7	11.5	12,511	21,000	9,523	16	0.001	112.5	37.0
	NYB3	39.5942	-73.5386	41.5	8.4	11,691	19,079	9,544	508	0.027	116.4	35.5
	NYB4	39.8873	-73.6105	32.8	9.1	12,181	19,069	9,479	212	0.011	130.2	51.4
	NYB5	39.9019	-73.5318	36.9	9.2	11,752	20,440	9,425	801	0.039	117.2	36.7
	NYB6	39.9793	-73.6383	37.9	9.4	12,133	20,036	9,281	331	0.017	119.7	37.7
	NYB7	39.2332	-73.6423	46.6	8.0	12,196	18,228	12,068	506	0.028	121.0	35.9
	NYB8	39.3621	-73.5099	50.7	8.2	12,149	20,006	9,572	140	0.007	120.6	37.2
	NYB9	39.3266	-73.7925	40.0	9.5	13,086	21,704	10,950	523	0.024	128.9	45.8
	NYB10	39.1000	-74.4470	21.9	11.6	11,791	19,740	9,170	3	<0.001	92.2	23.3
	NYB11	39.1431	-74.0397	38.7	10.0	13,499	23,559	7,050	1	<0.001	86.8	14.0
	NYB12	39.1431	-74.0397	28.2	11.6	12,207	20,700	7,345	0	0	–	–
	NYB13	39.4200	-74.0267	20.1	12.7	8,292	13,494	6,285	0	0	–	–
	NYB14	39.0950	-73.984	42.0	9.2	12,331	21,334	9,437	90	0.004	126.7	43.6
Summary				Mean 36.2	Mean 9.9	Total 166,218	Total 276,073	Total 128,270	Total 3,213	Mean 0.012	Mean 120.8	Mean 38.9

from a set of images taken within a test tank described below show that scale distortions in relation to the image center were less than 2 pixels over 65% of the full frame (Fig. 2). Each image had a metadata header that contained navigation (i.e. latitude, longitude, altitude, depth, etc.) and near seafloor environmental conditions corresponding to the capture time of the photo from the sensors of the AUV.

Calibration of the camera system was conducted with photos gathered with the AUV camera system in a saltwater tank. The calibration process entailed a sequence of images of a standard planar checkerboard pattern viewed from multiple angles and processed by using the Camera Calibration Toolbox for Matlab developed by Bouguet (2011) and based on the models of Zhang (2000) and Heikkila and Silven (1997). The analysis (Fig. 2) provided a direct quantitative measure of the camera field of view (FOV) and showed that minimal radial and tangential lens distortion affected the camera. These results agreed closely with previously published results from the same AUV and camera systems (Guðmundsson, 2012; Singh et al. 2013; Singh et al., 2014) and were further confirmed by independent analysis of the images (Rzhanov[7]).

The camera calibration (Fig. 2) showed the spatial pattern as that of the AUV camera, namely the impact of spherical and tangential lens distortion at each pixel point within the full image frame. Most of the area within each image (65%) exhibits distortion of less than 2 pixels (~5 mm in ground distance), except for the upper and lower left corners, which have 7 or more pixels of displacement (~16 mm in on the ground distance), representing a maximum error of <1% of total pixel width. These distortions will have generally less than 1% impact on the estimation of scallop shell height because the average distortion of 1–2 pixels translates to

[7] Rzhanov, Y. 2015. Personal commun. Center for Coastal and Ocean Mapping, Univ. New Hampshire, Durham, NH 03824.

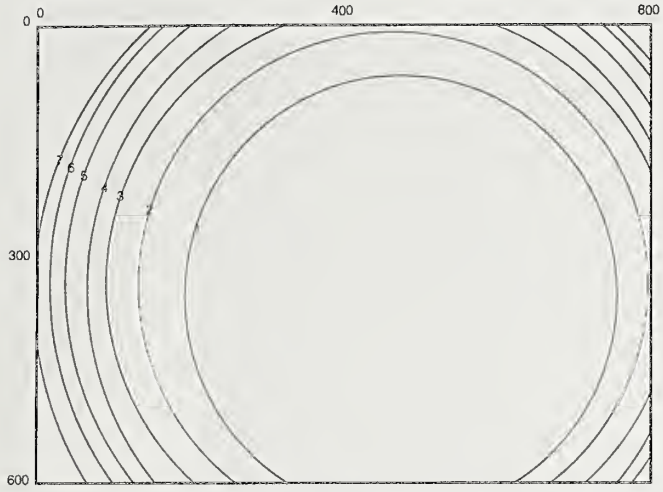

Figure 2

Distortion contours (measured from 1 to 7 pixels) in relation to the center of an image for the AUVs underwater camera used in a study of the distribution and abundance of the sea scallop (*Placopecten magellanicus*) during 2011.

between 0.23 and 0.46 cm in distance on the ground. This distortion uncertainty is approximately within <5% of the average shell height directly measured in the dredge tow samples, with which the image-based measurements were favorably compared. It is important to note, however, that camera distortions have no impact on the enumeration of scallops and the resulting analysis of scallop counts. In previously published studies of sea scallop shell height and abundance, this same combination of AUV camera was used and calibrated camera distortions along with both pitch and roll of the AUV were found to be negligible (Guðmundsson, 2012; Singh et al. 2013; Singh et al., 2014). Our study, therefore, is consistent with the findings of the previous research cited above, suggesting that the influence of roll bias (< 1%), camera distortions (< 1%), and manual digitization (< 1%) overall contributes less than 5% uncertainty for estimates of shell height. The width (W) of a single image was determined by using the image metadata collected by the AUV navigational system and sensors.

$$W = 2\tan\left(\frac{\alpha_h}{2}\right)[z - 1.3\sin(-\theta_p)], \qquad \text{(Eq. 1)}$$

where W = seafloor image width in meters;
α_h = horizontal viewing angle (degrees) of the camera in water;
z = height above the seafloor in meters; and
θ_p = pitch of the AUV in degrees.

Knowing the horizontal viewing angle of the camera in water (α_h=44,65°), and the height above the seafloor (z), we were able to calculate real world dimensions on the seafloor in each image. The pitch of the AUV (θ_p) and the arm length (1.3 m) from the camera to the AUV navigational reference point were known and used to correct the calculation, although in other studies (Guðmundsson, 2012; Singh et al., 2013, 2014) both pitch and roll were found to be negligible factors. Not accounting for pitch would have resulted in a potential 3% (mean) overestimation of image height for all of the photos. For Equation 1, the AUV is assumed to image a flat seafloor over the area of the full frame, and the equation also does not account for roll of the vehicle. The roll-induced error associated with image width is less than 1.0% (at 2 m altitude) if vehicle roll is less than 10° from horizontal, and log data showed that the AUV operated with roll characteristics of $\bar{x}$=4.01°C and σ=1.11° for all survey sites. Singh et al. (2013 and 2014) reported a similar ground distance error (<2%) due to both AUV pitch and roll for the same Scorpion 20SO camera when surveying at an altitude of 2 m. Similarly, Guðmundsson (2012) performed as detailed a calibration of the same AUV camera system as that used in our study and reported negligible effects of camera distortion, pitch, and roll.

Scallop counts and sizing

The 22 AUV surveys resulted in 203,066 images of the seafloor; see Figure 3 for a selection of representative images. In order to process all of the images, we engaged a team of graduate students and interns to count and size scallops using software written in-house for this project. Each scallop annotator received training on identifying sea scallops in benthic images, and was required to successfully identify at least 95% of the scallops from a standardized image data set before being allowed to annotate the rest of the images. Repeated digital measurement of the same scallop by the same annotator (N=53, where N is the number of sea scallops) yielded a standard deviation of 5.0 mm in shell height measurement. This value of annotation repeatability for size determination is in agreement with the 5 mm annotator measurement error reported by Singh et al. (2014). Furthermore, it is worth noting that in comparison with manually sized scallops from dredge samples, manually sizing was itself segmented into 5-mm bin intervals and thus the discretization of image-based sizes was on par with the discretization from physical samples. The protocol used for image selection and sizing was the following:

1 All images that were taken at a height between 1.5 m and 2.5 m above the seafloor were counted (removing the starting descent and ending ascent portions of each survey).
2 Each sea scallop in an image was counted individually, unless it had already been counted from the previous image that overlapped the same section of seafloor. Annotators examined photos sequentially and were trained to recognize overlapped images, so that scallops were not counted more than once.
3 Each scallop shell height was sized on the basis of the distance from the shell umbo to the ventral margin by using a pixel-measuring tool. The projected

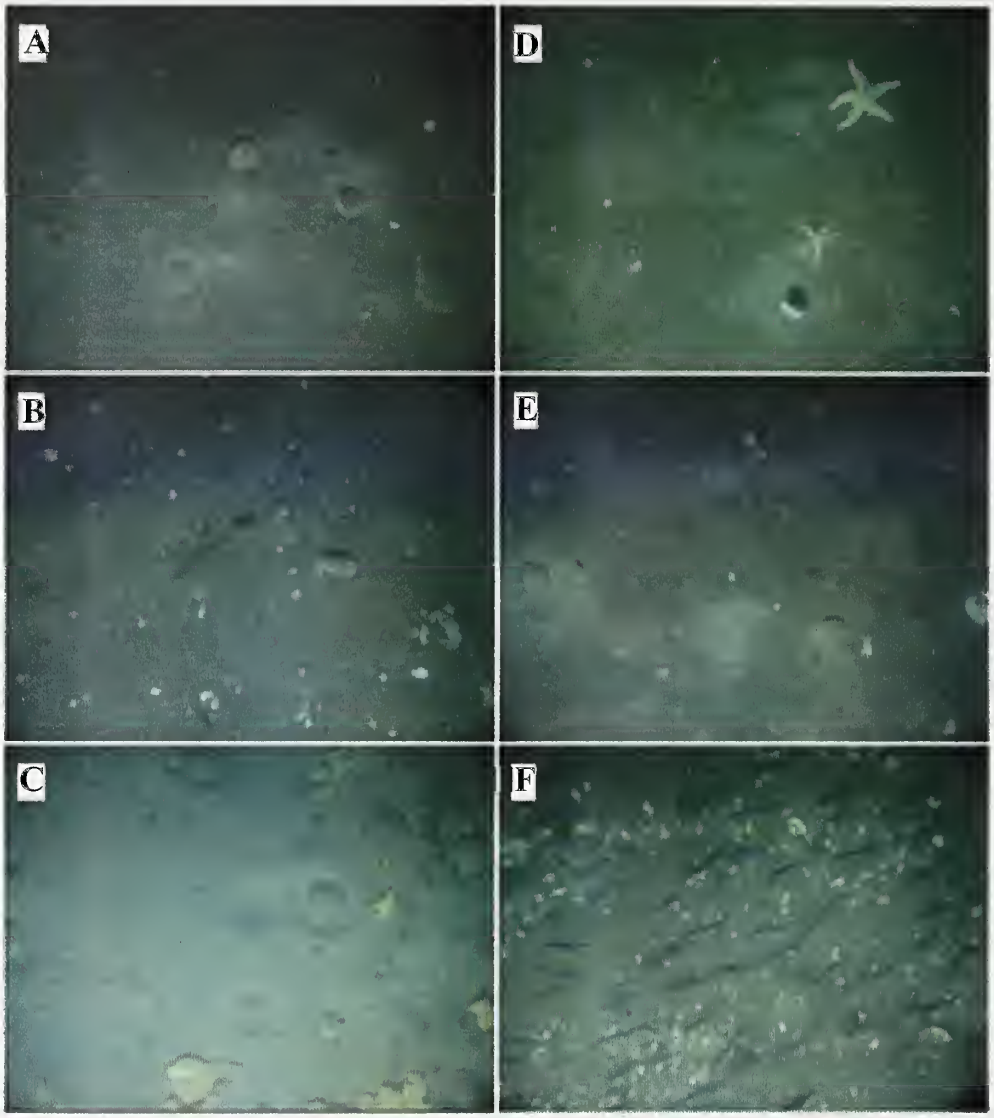

Figure 3

Representative examples of images from the database of photographs from the 2011 survey of sea scallops (*Placopecten magellanicus*) in the Long Island and New York Bight areas. The sea bottom was photographed with an underwater camera mounted inside the nose cone of an autonomous underwater vehicle. Images A, C, D, and E show sea scallops resting on the seafloor. Images B and F show other species incidentally photographed during the AUV surveys including crabs, fish, and skates.

on-the-ground length represented by the pixels was then calculated from the metadata of each image (e.g., altitude, pitch, and camera FOV) with Equation 1.

4 Shell height was not recorded if more than half of the entire scallop was not contained within the frame.

5 Scallops identified as disarticulated shells were neither counted nor sized.

6 The final count for a survey was the number of scallops that could be sized.

Scallop densities were calculated for each survey site. The number of scallops that were identified and sized for each survey were summed and divided by the area of the seafloor that had been photographed. In order to limit the effect of image overlap (as much as 5% in the current surveys), the AUV transect length was calculated from the global positioning system (GPS) start and end point of each survey line. The transect length was then multiplied by the mean image width for that transect, and the vehicle control kept the AUV to within 16 cm standard deviation of the 2.2 m alti-

tude set point along the trackline. As part of the image analysis and review process, annotators classified the quality of each image on the basis of whether the image was out of focus, too dark, or the water was too turbid for scallops to be recognized. More than 95% of all the images were of sufficient quality for the annotators to recognize, count, and size the scallops. It is worth noting that many towed camera systems have only a fractional portion of the images annotated, whereas we were able to annotate all of our images. Additionally, the stability of the AUV platform ensured that fewer images (<5%) were removed with altitude or image quality filtering.

Biomass

Because our project methods were based on seabed images, we used an empirical relationship from the literature to estimate the meat weight of scallops for comparative purposes. This parameter has been shown to vary on the basis of a number of geographical and environmental factors and decreases with depth (Hennen and Hart, 2012). The equation chosen from Rothschild et al. (2009) is based on meat-weight measurements of sea scallops dredged from within the Mid-Atlantic Bight (the study area) and therefore was not further corrected for latitude and longitude. The meat-weight biomass was calculated for each scallop by using the photogrammetrically measured shell height of each scallop and the depth recorded for each image with the following equation:

$$W_m = e^{-8.94+2.94\ln H_S-0.43\ln d} \quad \text{(Eq. 2)}$$

where W_m = meat-weight biomass of the sea scallop in grams;
H_S = shell height of the sea scallop in millimeters;
d = depth of the sea scallop in meters.

Fishing effort

Commercial fishing dredges create distinctive patterns of sediment disturbance on the seafloor, and these dredge scars are visible with side scan sonar (Dickson et al., 1978; NRC, 2002; Lucchetti and Sala, 2012; Krumholz and Brennan, 2015). For each survey, the dredge marks were determined from the side-scan data collected by the AUV at the same time that the photos were gathered. SonarWiz 5 (Chesapeake Technology Inc., Mountain View, CA) was used to process the acoustic data collected by the 900 kHz side-scan sonar and gridded at a 0.25×0.25 m horizontal resolution for inspection. Each dredge scar was then manually traced in each side-scan mosaic by using the SonarWiz digitizing tool. The track length was then multiplied by the measured width of the dredge scar (4.57 m) to determine the total area of the dredge scar. The area dredged was compared with the area acoustically surveyed (survey track length multiplied by a 20-m swath width) to give a ratio that represented a measure of recent fishing effort. For one site, we ran the AUV both before and after the dredge and verified that our dredge track was visible in the side-scan imagery. In most of the sonar mosaic images there were many dredge marks visible such that our sampling mark was only a small fraction of the total estimated dredge area.

Results

Over the 10-day cruise in July 2011, we completed 22 surveys with the AUV and covered 257 km of track line for a combined surveyed area of 490,000 m^2. In all, 203,000 images of the seafloor were produced, from which annotators identified and digitally sized 15,252 sea scallops.

Scallop density

The New York Bight (NYB) region was surveyed over 14 discrete sites and sea scallops were identified from images collected from 12 of those sites (i.e., 2 survey sites had no scallops). Overall, 276,000 m^2 of seafloor were surveyed (optically and acoustically) in the NYB, and densities for each survey ranged from 0 to 0.039 scallops per m^2 (Table 1). The area-weighted mean scallop density for the region was 0.012 scallops per m^2. The 6 sites that had scallop densities <<0.01 scallops per m^2 were the shallowest surveys (20.1–35.5 m) and also coincided with the warmest near bottom temperatures (10.0–12.7°C). We also observed that these sites typically had dense sand dollar populations.

The histogram in Figure 4A shows the shell-height frequency for all of the photogrammetrically sized sea scallops within the NYB. Taken together, 1.5% (48) of the 3,213 sized scallops fell into the recruit size class (<70 mm), and 13.8% were of a size larger than that of recruits but smaller than the 4″ dredge rings (>70 mm and <101.6 mm). The harvestable size class accounted for the remaining 84.7%, which results in an exploitable (harvestable) scallop density of 0.010 scallops per m^2 for NYB. The mean shell height for the NYB region was found to be 121 mm. These results indicate that the NYB had a size population dominated by large harvestable scallops.

The Long Island (LI) region was surveyed at 8 distinct sites, and an area of over 156,000 m^2 of seafloor was photographed in the region. The sea scallop density was 0.077 scallops per m^2, and there was a large variability in densities ranging from 0.01 to 0.20 scallops per m^2 (Table 1). As found in the NYB region, the denser scallop populations were found at near bed temperatures of 8–9°C, whereas the warmer (>10°C), shallower survey sites had the lowest population densities.

The distribution of shell heights in the LI region is shown in Figure 4B. Of the 12,039 scallops that were sized, 61.2% (7,368) were classified as harvestable and

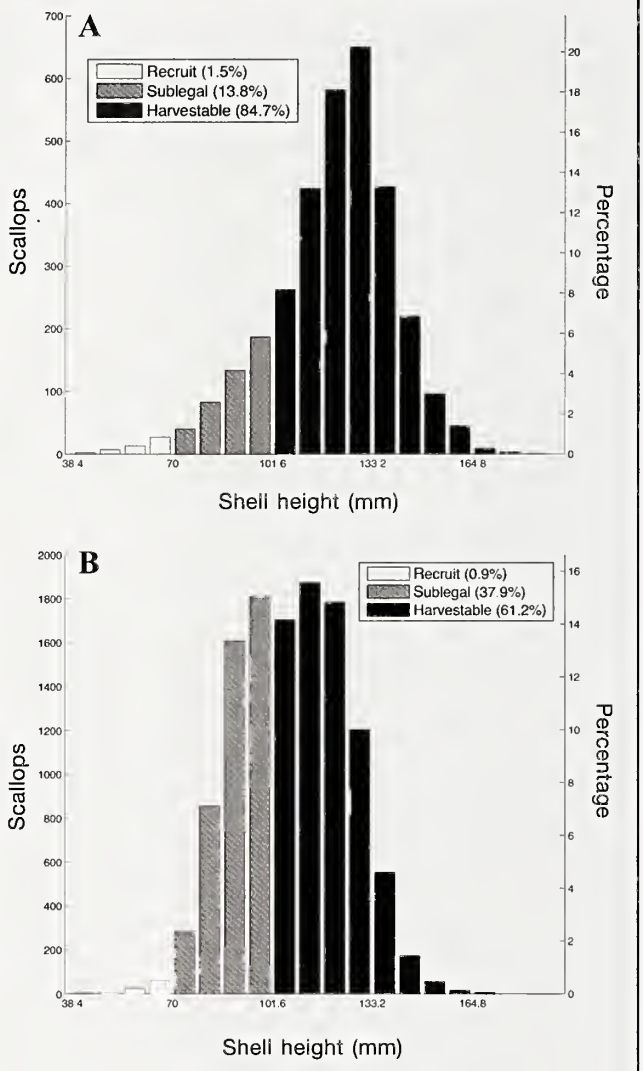

Figure 4

Frequency histograms of digitally sized shell heights (in millimeters) of sea scallops (*Placopecten magellanicus*) within (**A**) New York Bight (3213 sea scallops) and (**B**) Long Island areas (12,039 sea scallops).

37.9% (4,563) were classified as larger than the size of recruits but smaller than the 4″ rings. This distribution yields an exploitable scallop density (of harvestable size scallops) of 0.047 scallops per m^2. The remaining 0.9% (108) scallops were classified as recruits. The mean shell height for the region was 108 mm. As with the NYB sites, the scallop population was found to be dominated by scallops with a large shell height and only a small number of recruit-size scallops were observed (Fig. 5).

Comparisons of results from dredge tows with those from camera imagery were performed for a subset of the surveys from the NYB region (NYB4-8). The dredged scallops were manually sized into 5-mm bins. The dredged scallop sizes were compared with shell-height sizes obtained with the AUV from the same surveys by using size-class distribution plots (Fig. 6). The means of the manually measured scallop shell heights obtained with dredging (range of mean values 122–135 mm, N=54–22,) were found to be within 6% of the co-located AUV image-sized shell height means (range of mean values 117–130 mm, N=140–801, Fig. 6). The lower means of the AUV image-sized scallops are expected because recruit-size scallops are included within the distribution. By design, dredges do not accurately sample scallops under 101.6 mm (4″ diameter ring), thereby skewing the shell height distribution toward larger sizes (Yochum and DuPaul, 2008).

Biomass

Using a published equation (Eq. 2) we calculated the meat weight of each individual scallop from the shell height measurements derived from AUV images and the results are plotted in Figure 7. The majority of sea scallop biomass off LI is due to a high frequency of smaller meat weights (10–30 g each). The highest density sites in the LI region were typically coincident with smaller shell heights. The bulk of sea scallop biomass in the NYB region is due to a higher frequency of meat weights ranging from 30–50 g each.

Fishing effort

Digitized dredge scars in the side-scan mosaics revealed that over 174,000 m^2 or 35.5% of the total surveyed seafloor area showed signs of dredging. We found that higher dredging effort (>7% of the bottom area dredged) coincided with the highest scallop densities, whereas a low scallop density area typically showed little or no dredging. It was not uncommon for a site to have a single dredge scar from a commercial vessel— perhaps the mark of a test dredge tow that did not yield a large enough catch for continued fishing effort.

There was a noticeable difference between fishing efforts in LI and NYB. We found that the NYB had significantly less dredging (5% overall) than that found in the LI region. The scallop densities at all NYB sites were considerably less than those at LI counterparts. NYB8 had the most concentrated dredging in the region with 11.9% of the area dredged. In addition, the shell height distributions for the heavily fished sites were positively skewed because of the size selectivity of the commercial scallop dredge (Fig. 5).

The LI sites had an overall density 7 times that of the NYB region. As a result, the LI region had significant commercial dredging >18% of the total area dredged for 5 out of the 8 survey sites. Operationally, digitizing dredge scars did not add significant processing time of the data. After side-scan sonar mosaics had been produced for each site, it took a total of 8 man-hours to manually digitize and calculate the area dredged for all 22 survey sites.

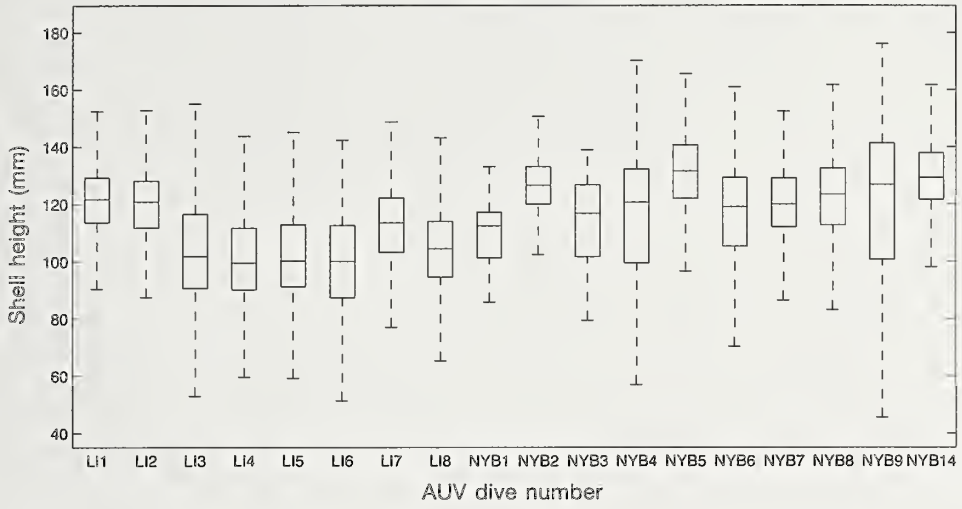

Figure 5

Boxplots of shell heights of sea scallops (*Placopecten magellanicus*) obtained from photographs taken with an underwater camera of an autonomous underwater vehicle with the Long Island (LI) and New York Bight (NYB) areas. Surveys where <16 sea scallops were collected were not plotted.

Discussion

Automated underwater vehicle as an image-producing survey platform

The AUV is an efficient platform that allows surveys from images (optical and acoustical simultaneously) over 15 km of seafloor on a single battery charge, and allows the noninvasive study of benthic organisms over any bed type, including rocky or uneven terrain that would be difficult or impossible for dredges. For sea scallops, we found that an altitude of 2.2 m allowed for the largest image area, while still maintaining visibility and resolution to size scallops. Particulate matter in the water column drastically decreased visibility of the seafloor for altitudes over 4 m. Continual logging of geographic and environmental conditions allowed accurate sizing and enumeration of scallops after processing. The highly accurate navigation—typically a 1-m drift over 1 km of trackline of the AUV—allowed precise repeatability of survey lines. Targets visible in overlapping side-scan sonar imagery exhibited horizontal offsets of less than 2 m—a finding that is consistent with numerous other AUV benthic and geomorphic survey studies (e.g. Patterson et al., 2008; Forrest et al., 2012; Rankey and Doolittle, 2012; Raineault et al., 2013). This navigational precision allowed for the reoccupation of survey lines.

A variety of survey designs were evaluated in our study. Although we believe designs that propagate in a continuous linear direction (e.g., in a stair-case pattern) have a use for surveying an extremely elongated bed of scallops, we did not find those designs suited this type of study or fully incorporated the strengths of the AUV. The boustrophedon survey design, or a more regular and approximately rectangular pattern design, was found to be most useful in simultaneously photographing the seafloor and acoustically mapping it. Surveys were designed to allow complete coverage of a rectangular survey site (~1.75 km×0.3 km) with side-scan sonar. The use of the geo-referenced data of each image also made it possible to plot the precise location of each scallop and to evaluate the distribution of individuals within the population (Trembanis et al., 2012; Walker, 2013).

Logistically, the AUV offers an effective and productive platform for the collection of sea scallop images as part of a larger stock assessment effort. The ability to quickly deploy and retrieve the AUV from a support vessel allows the rapid acquisition of photographic and acoustic data that can be analyzed at sea during transit time or after the completion of the cruise. Imaging the seafloor is a noninvasive way to survey the scallop population and gather data about the small-scale spatial structuring of the population, seafloor texture and morphological features, and water quality. Photogrammetric sizing of the scallops was rapid, requiring only a few seconds once a scallop had been located in an image. We found that the digital sizes agreed favorably with the measurements of dredged specimens from the survey sites.

One of the major advantages of the AUV is the high volume of data that can be collected in a few hours, but this high volume also results in a significant challenge for data processing. However, we showed that with the aid of sizing software, a team of trained scallop annota-

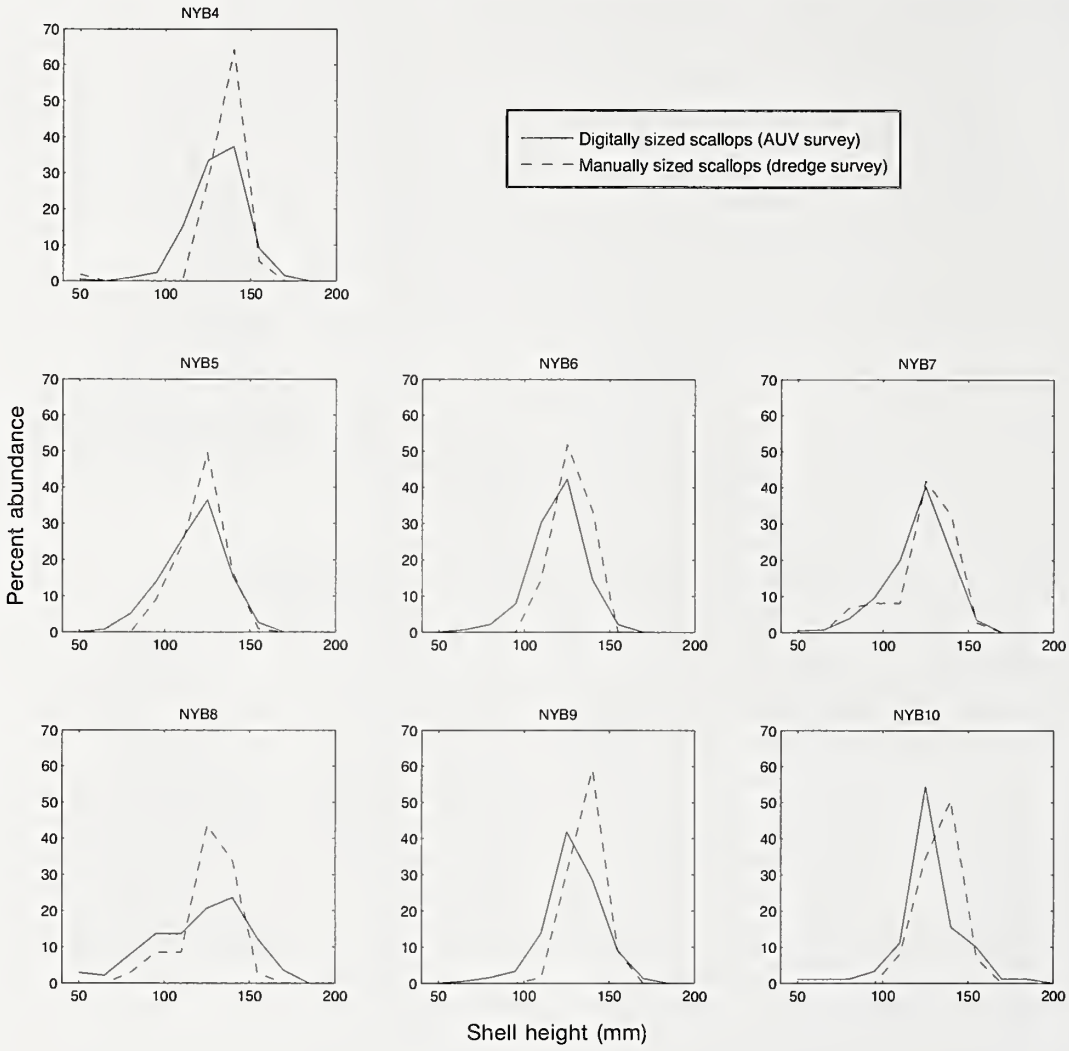

Figure 6

Histographs of shell height distribution for digitally sized sea scallops (*Placopecten magellanicus*) photographed with an underwater camera of an autonomous underwater vehicle (AUV) and for sea scallops collected with a commercial dredge in fishing operations undertaken at the same time and at the same locations in the New York Bight area.

tors could complete the observation of 203,000 images in 98 man-hours (a rate of 2,000 images per hour). Walker (2013) showed that the hours required to complete annotation of a set of images were directly related to the number of scallops and associated fauna.

Over 200,000 bottom photographs were obtained in this study, and all were examined by annotators trained to count scallops and measure their shell height. We found this manual step to require many hours of effort and some expense. We investigated statistical approaches by repeated random sampling simulations and text book formulae (Zar 1999, p. 109) that can be used to gauge the loss in precision by examining only a random subset of images. Overall, we found the mean density to be 0.075 scallops/image, with a standard deviation of 0.35. These values were sufficient to compute the standard error of the mean density from a smaller random subset of images with the formula for the standard error, $SE = s/\sqrt{n}$, where s is the standard deviation and n is the number of photos. For example, a random subset of 40,000 images would have a standard error of $0.35/\sqrt{40{,}000}=0.00175$, giving a 95% confidence interval (i.e., twice the standard error) of ±0.0035. This bound is at ±5% of the mean value (i.e., the relative error) obtained from all photographs and can be the expected precision when examining a random sample of only 20% of the images that we collected. Sampling half that number (20,000) increases the relative error to 6.6%, while doubling it to 80,000 decreases the relative error to 3.3%. Because imagery-based assessments typically generate large numbers of images,

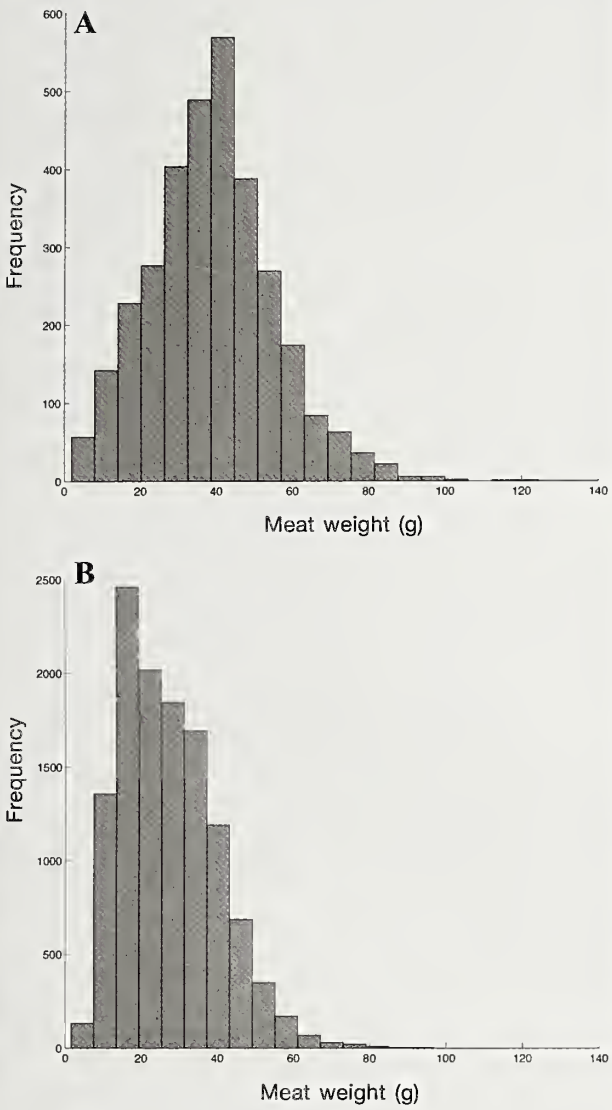

Figure 7

Histograms of calculated biomass based on meat weight (g) of sea scallops (*Placopecten magellanicus*) collected in 2011 from (**A**) the New York Bight (NYB) and (**B**) Long Island (LI) areas.

the examination of a much smaller random subset may yield sufficiently precise density values and substantial savings in time and effort.

Sea scallop stock assessment

The results of the inshore surveys showed that the LI region had an overall density of 0.077 scallops per m^2, which agrees with the density of 0.061 scallops per m^2 reported by Rudders and DuPaul[4] for dredge-based survey of the LI region in 2011. The NYB inshore sites were only slightly less populated (0.013 scallops per m^2) in comparison both with the density of 0.015 scallops per m^2 reported by Rudders and Dupaul[4] for the deeper NYB waters and with the population density in the LI region in general. The higher population level of the LI region has been hypothesized by Law (2007) to be due to seeding from the Georges Bank area. Conversely, the lower NYB region densities could be explained by the interruption of scallop larvae transport from the LI region caused by the influx of freshwater from the Hudson River (Law, 2007). Additionally, the Hudson Shelf Valley forms a natural bathymetric divide between the two regions. The two scallop populations were also different in their shell height distributions. The LI population was skewed toward smaller shell heights in contrast with the more symmetrical distribution of the NYB population. Both regions had very few recruit-size class scallops (<1.5%) and were found overall to possess large-size scallop populations. We also noted that the largest scallop populations occurred around the 9°C ocean water isotherm, which corresponds well with the optimal scallop growth temperature of 10°C reported by Posgay (1953).

Dredging effort and sea scallop density

The combined optical and acoustic AUV method used in this study was found to be an efficient way to further use commonly collected side-scan data to quantify dredging effort. This method could be used to assess the effects of dredging effort on other benthic organisms, particularly on common bycatch species in the scallop fishery. As would be expected, a direct comparison of dredging effort with scallop density revealed that fishermen concentrated dredging in only the most populated sites, and that size-selective dredges had a noticeable impact on the shell height distribution of the remaining scallop population (see Fig. 5).

The effects of dredging on the substrate of the seafloor have been investigated in multiple studies (Margetts and Bridger[8]; Caddy, 1973; Krost, 1990; Hall-Spencer and Moore, 2000; Jenkins et al. 2001; NRC, 2002; Lucchetti and Sala, 2012; Krumholz and Brennan, 2015). These studies have found that substrate texture and fishing effort are the leading variables in the preservation of trawl marks. Finer grained sediment (muddy sediment versus sandy bottom) allows the gear to penetrate further into the substrate due to lower mechanical resistance between the substrate and the gear (Krost, 1990). Researchers have reported dredge marks remaining for up to 1.5 years on continually fished substrate (Hall-Spencer and Moore, 2000). In the absence of dredging, disturbed bed contouring effects last for significantly longer periods of time; Hall-Spencer and Moore (2000) reported dredge scars can remain for up to 2.5 years without further fishing efforts and Bernhard (reported by Krost, 1990) reported a single trawl scar remaining for up to 5 years

[8] Margetts, A. R., and J. P. Bridger. 1971. The effect of a beam trawl on the sea bed. ICES Council Meeting (C.M.) Documents 1971/B:8, 9 p. [Available at website.]

in a bay setting devoid of fishing and strong near-bed tidal currents.

The fine-sand seabed of the study site allows for the formation of relatively shallow dredge scars. The limited seasonal time scale for discernibility of the dredge scars is due to ongoing fishing efforts that rework the surface sediment and the reworking of sediment from wave driven near-bed currents. As such, side-scan surveys at our study sites can be a useful tool for quantifying fishing effort but only for a current season.

Acknowledgments

This project was funded by the NOAA Research Set-Aside Program (award number: NA11NMF4540011). The authors are grateful to the crew of the FV *Christian and Alexa*: Co-Captain A. Ochse, Co-Captain K. Ochse, M. Newman, D. Crosson, and R. Adams; the late W. Phoel; D. Hart at NMFS; V. Schmidt; C. DuVal, A. Norton, AUV Team: J. Gutsche and B. Keller; and the Digital Image Scallop Annotator Team: V. Amrutia, B. Reed, M. Christie, T. Santangelo, and D. Wessell.

Literature cited

Bouguet, J.-Y.
2011. Camera Calibration Toolbox for Matlab. [Available at website, accessed October 2011.]

Caddy, J. F.
1973. Underwater observations on tracks of dredges and trawls and some effects of dredging on a scallop ground. J. Fish. Res. Board Can. 30:173–180.

Carey J. D., and K. D. E. Stokesbury.
2011. An assessment of juvenile and adult sea scallop, *Placopecten magellanicus*, distribution in the northwest Atlantic using high-resolution still imagery. J. Shellfish Res. 30:569–582.

Dickson, R. R., D. N. Langhorne, R. S. Millner, and E. G. Shreeve.
1978. An examination of a dredged channel using sector scanning sonar in side-scan mode. J. Cons. Int. Explor. Mer 38:41–47.

Forrest, A. L., M. E. Wittmann, V. Schmidt, N. A. Raineault, A. Hamilton, W. Pike, S. G. Schladow, J. E. Reuter, B. E. Laval, A. C. Trembanis.
2012. Quantitative assessment of invasive species in lacustrine environments through benthic imagery analysis. Limnol. Oceanogr. Methods 10:65–74.

Guðmundsson, E. O.
2012. Detecting scallops in images from an AUV. M.Sc. thesis, 82 p. Univ. Iceland, Reykjavik, Iceland. [Available at website.]

Hart, D. R., and A. S. Chute.
2004. Essential Fish Habitat Source Document: sea scallop, *Placopecten magellanicus*, life history and habitat characteristics, 2nd ed. NOAA Tech. Memo. NMFS-NE-189, 21 p

Hart, D. R., L. D. Jacobson, and J. Tang.
2013. To split or not to split: assessment of Georges Bank sea scallops in the presence of marine protected areas. Fish. Res. 144:74–83..

Hall-Spencer, J. M., and P. G. Moore.
2000. Scallop dredging has profound, long-term impacts on maerl habitats. ICES J. Mar. Sci. 57:1407–1415.

Heikkilä, J. and O. Silvén.
1997. A four-step camera calibration procedure with implicit image correction. *In* Proceedings of the 1997 IEEE Computer Society Conference on Computer Vision and Pattern Recognition; San Juan, Puerto Rico, 17–19 June, p. 1106–1112. IEEE Computer Soc., Los Alamitos, CA.

Hennen, D. R., and D. R. Hart.
2012. Shell height-to-weight relationships for Atlantic sea scallops (*Placopecten magellanicus*) in offshore U.S. waters. J. Shellfish Res. 31:1133–1144.

Jacobson, L. D., K. D. E. Stokesbury, M. A. Allard, A. Cute, B. P. Harris, D. Hart, T. Jaffarian, M. C. Marino II, J. I. Nogueria, and P. Rago.
2010. Measurement errors in body size of sea scallops (*Placopecten magellanicus*) and their effect on stock assessment models. Fish. Bull. 108:233–247.

Jenkins, S. R., B. D. Beukers-Stewart, and A. R. Brand.
2001. Impact of scallop dredging on benthic megafauna: a comparison of damage levels in captured and non-captured organisms. Mar. Ecol. Prog. Ser. 215:297–301.

Krost, P.
1990. The impact of otter-trawl fishery on nutrient release from the sediment and macrofauna of Kieler Bucht (western Baltic). Ber. Inst. Meereskd. Christian-Albrechts-Univ. Kiel 200, 150 p.

Krumholz, J. S. and M. L. Brennan.
2015. Fishing for common ground: investigations of the impact of trawling on ancient shipwreck sites uncovers a potential for management synergy. Mar. Policy 61:127–133.

Law, C. G., III.
2007. The impacts of spatial and temporal variability of larval transport on the distribution and population dynamics of the sea scallop (*Placopecten magellancius*). Ph.D. dissertation, 120 p. Rutgers Univ., New Brunswick, NJ.

Lucchetti, A., and A. Sala.
2012. Impact and performance of Mediterranean fishing gear by side-scan sonar technology. Can. J. Fish. Aquat. Sci. 69:1806–1816.

NMFS (National Marine Fisheries Service).
2009. Fisheries of the United States 2008. Current Fishery Statistics No. 2008, 103 p. Natl. Mar. Fish. Serv., NOAA, Silver Spring, MD. [Available at website.]
2010. Fisheries of the United States 2009. Current Fishery Statistics No. 2009, 103 p. Natl. Mar. Fish. Serv., NOAA, Silver Spring, MD. [Available at website.]
2011. Fisheries of the United States 2010. Current Fishery Statistics No. 2010, 103 p. Natl. Mar. Fish. Serv., NOAA, Silver Spring, MD. [Available at website.]
2012. Fisheries of the United States 2011. Current Fishery Statistics No. 2011, 124 p. Natl. Mar. Fish. Serv., NOAA, Silver Spring, MD. [Available at website.]
2013. Fisheries of the United States 2012. Current Fishery Statistics No. 2012, 124 p. Natl. Mar. Fish. Serv., NOAA, Silver Spring, MD. [Available at website.]

Naidu, K. S., and G. Robert.
2006. Fisheries sea scallop, *Placopecten magellanicus*. Dev. Aquac. Fish. Sci. 35:869–905.

National Research Council (NRC).
2002. Effects of trawling and dredging on seafloor habitat, 136 p. National Academy Press, Washington, D.C.

Patterson, M., T. Hiller, and A. Trembanis.
2008. Exploring coral reef sustainability. HydroInternational Newsletter 12(7):10–15. [Available at website.]

Posgay, J. A.
1953. Sea scallop investigations. *In* Sixth report on investigations of methods of shellfisheries of Massachusetts, p. 9–24. Div. Mar. Fish., Mass. Dep. Conserv., Boston, MA.

Raineault, N. A., A. C. Trembanis, and D. C. Miller.
2012. Mapping benthic habitats in Delaware Bay and the coastal Atlantic: acoustic techniques provide greater coverage and high resolution in complex, shallow-water environments. Estuaries and Coasts 35:682–689.

Raineault, N. A., A. C. Trembanis, D. C. Miller, and V. Capone.
2013. Interannual changes in seafloor surficial geology at an artificial reef site on the inner continental shelf. Cont. Shelf Res. 58:67–78.

Rankey, E. C., and D. F. Doolittle.
2012. Geomorphology of carbonate platform-marginal uppermost slopes: insights from a Holocene analogue, Little Bahama Bank, Bahamas. Sedimentology 59:2146–2171.

Rosenberg, A. A.
2003. Managing to the margins: the overexploitation of fisheries. Front. Ecol. Environ. 1:102–106.

Rosenkranz, G. E., S. M. Gallager, R. W. Shepard, and M. Blakeslee.
2008. Development of a high-speed, megapixel benthic imaging system for coastal fisheries research in Alaska. Fish. Res. 92:340–344.

Rothschild, B. J., C. F. Adams, C. L. Sarro, and K. D. E. Stokesbury.
2009. Variability in the relationship between sea scallop shell height and meat weight. ICES J. Mar. Sci. 66:1972–1977.

Seiler, J., A. Williams, and N. Barrett.
2012. Assessing size, abundance and habitat preferences of the Ocean Perch *Helicolenus percoides* using a AUV-borne stereo camera system. Fish. Res. 129–130:64–72.

Singh W., E.B. Örnólfdóttir, and G. Stefansson.
2013. A camera-based autonomous underwater vehicle sampling approach to quantify scallop abundance. J. Shellfish Res. 32:725–732.

Singh W., E. B. Örnólfdóttir E.B., and G. Stefansson.
2014. A small-scale comparison of Iceland scallop size distributions obtained from a camera based autonomous underwater vehicle and dredge survey. PLoS ONE 9(10):e109369.

Stokesbury, K. D. E.
2002. Estimation of sea scallop abundance in closed areas of Georges Bank, USA. Trans. Am. Fish. Soc. 131:1081–1092.
2012. Stock definition and recruitment: implications for the U.S. sea scallop (*Placopecten magellanicus*) fishery from 2003 to 2011. Rev. Fish. Sci. 20:154–164.

Stokesbury, K. D. E., B. P. Harris, M. C. Marino II, and J. L. Nogueira.
2004. Estimation of sea scallop abundance using a video survey in off-shore US waters. J. Shellfish Res. 23:33–40.

Tolimieri, N., M. E. Clarke, H. Singh, and C. Goldfinger.
2008. Evaluating the SeaBED AUV for monitoring groundfish in untrawlable habitat. *In* Marine habitat mapping technology for Alaska (J. R. Reynolds and H. Gary Greene, eds.), p. 129–141. Univ. Alaska Fairbanks, Alaska Sea Grant College Program Rep. AK-SG-08-03.

Trembanis, A., J. Walker, D. Miller, B. Phoel.
2012. A high-density image analysis of sea scallop habitat in the Mid-Atlantic Bight [Abstract]. *In* Proceedings of the GeoHab 2012 Eleventh International Symposium; Orcas Island, WA, 1–4 May, p. 60. GeoHab, Eastsound, WA. [Available at website.]

Walker, J. H.
2013. Abundance and size of the sea scallop population in the Mid-Atlantic Bight. Master's thesis, 272 p. Univ. Delaware, Newark, DE.

Yochum, N., and W. D. DuPaul.
2008. Size-selectivity of the northwest Atlantic sea scallop (*Placopecten magellanicus*) dredge. J. Shellfish Res. 27:265–271.

Zhang, Z.
2000. A flexible new technique for camera calibration. IEEE Trans. Pattern Anal. Mach. Intell. 22:1330–1334.

Zar, J. H.
1999. Biostatistical analysis, 4th ed, 663 p. Prentice Hall, Upper Saddle River, NJ.

NOAA
National Marine
Fisheries Service

Fishery Bulletin
established 1881

Spencer F. Baird
First U.S. Commissioner
of Fisheries and founder
of *Fishery Bulletin*

Oceanographic influences on the diet of 3 surface-migrating myctophids in the eastern tropical Pacific Ocean

Joel E. Van Noord (contact author)[1,4]
Robert J. Olson[2]
Jessica V. Redfern[3]
Leanne M. Duffy[2]
Ronald S. Kaufmann[1]

Email address for contact author: joel.vannoord@noaa.gov
Present address: California Wetfish Producers Association
P.O. Box 1951
Buellton, California 93427

[1] Marine Science and Environmental Studies Department
University of San Diego
5998 Alcalá Park
San Diego, California 92110

[2] Inter-American Tropical Tuna Commission
8901 La Jolla Shores Drive
La Jolla, California 92037

[3] Southwest Fisheries Science Center
National Marine Fisheries Service, NOAA
8901 La Jolla Shores Drive
La Jolla, California 92037

Abstract—We examined the stomach contents of 3 vertically migrating myctophid fish species from the eastern tropical Pacific (ETP) Ocean and used a classification tree to examine the influence of spatial, biological, and oceanographic predictor variables on diet. *Myctophum nitidulum* (n=299), *Symbolophorus reversus* (n=199), and *Gonichthys tenuiculus*, (n=82) were collected with dip nets from surface waters, and prey taxa were quantified from bongo net tows from August through November 2006. A classification tree produced splits with longitude and sea surface salinity (SSS), thereby separating 3 geographically and oceanographically distinct regions of the ETP (offshore, nearshore, and intermediate), where diet was similar among the 3 species. Myctophids consumed, primarily, ostracods offshore (76.4% mean percentage by number [MN_i]), euphausiids nearshore (45.0%), and copepods (66.6%) in the intermediate region. The offshore region was characterized by a greater abundance of ostracods in the zooplankton community (17.5% by number) and within a deep mixed-layer depth (MLD) (mean 52.6 m, max 93.0 m). SSS was low in the nearshore region (<32.9 psu) and the MLD was shallow. The intermediate region represented a transition zone between the oceanographic condition of the offshore and nearshore regions. Our results indicate that these 3 myctophid species share a similar regional diet that is strongly influenced by longitude, ostracod availability, SSS, and MLD.

Manuscript submitted 13 May 2015.
Manuscript accepted 6 April 2016.
Fish. Bull. 114:274–287 (2016).
Online publication date: 28 April 2016.
doi: 10.7755/FB.114.3.2

The Myctophidae (lanternfishes) comprise a family of fishes whose members are both extremely abundant and distributed throughout the world's oceans (Gjosaeter and Kawaguchi, 1980; Irigoien et al., 2014). Species making up this family of fish serve roles as both important predators (Pakhomov et al., 1996) and prey (Naito et al., 2013); furthermore myctophids transfer energy from lower to higher trophic levels in food webs (Brodeur et al., 1999). Myctophids are also influential in the transfer of carbon to the deep sea because they feed in surface waters and return to the mesopelagic zone (Davison et al., 2013). The family is speciose, with as many as 250 species in 33 genera (Catul et al., 2011). In some instances, as many as 50 species can be found in close proximity, simultaneously feeding on similar prey (Hopkins and Gartner, 1992).

Resource partitioning, broadly defined as differences in resource use among co-occurring species (Schoener, 1974), has been used to explain how diverse myctophid assemblages can co-occur without competitively excluding one another (Hopkins and Gartner, 1992). Myctophids have been shown to partition resources by size (myctophid size) (Shreeve et al., 2009; Saunders et al., 2015), migration depth, and prey type (Hopkins and Gartner, 1992; Pepin, 2013). Co-occurring myctophid species of similar size that are found in the same habitat either partition dietary resources or feed opportunistically on prey in the proportions that are available. For example, dietary resource partitioning has been de-

scribed in myctophids in the Gulf of Mexico (Hopkins and Gartner, 1992; Hopkins and Sutton, 1998), Central Pacific (Clarke, 1980), western tropical Pacific (Van Noord 2013), Kuroshio Current (Watanabe et al., 2002), California Current (Suntsov and Brodeur, 2008), Southern Ocean (Cherel et al., 2010; Shreeve et al., 2009), and North Atlantic (Pusch et al., 2004). Conversely, generalist behavior has been described by Kinzer and Schulz (1985), who found that 7 myctophid species in the equatorial Atlantic fed opportunistically on similar calanoid copepods. Pakhomov et al. (1996) also found that 4 myctophid species in the Southern Ocean fed opportunistically on the same mesozooplankton, whereas Tyler and Pearcy (1975) found that myctophids in the California Current fed on a diverse and overlapping diet. These previous studies, although valuable, were primarily descriptive in nature, did not provide measurements of prey availability, were restricted to geographically small areas, and therefore do not provide a broad picture of myctophid feeding and the variables that govern their diet. Understanding the factors that influence the diet of myctophid fishes will provide insight into food-web dynamics and the structure of related communities. If myctophids are opportunistic feeders, for example, bottom-up forcing or environmental changes in the system would have a dynamic effect on their feeding patterns, which, in turn, would reverberate throughout the food web (Fiedler et al., 2013).

Little is known about the ecology or biology of myctophids from the eastern tropical Pacific (ETP) but in surveys of larval fish in the ETP, high densities, as well as a diversity, of myctophid species have been encountered (Ahlstrom, 1972, 1971). Studies investigating the ecological role of myctophids in this region have lumped species together as a forage base for top predators (e.g., Pitman et al.[1]; Maas et al. 2014) and myctophids have been documented as prey for cetaceans (Perrin et al., 1973; Scott et al., 2012), tunas, swordfish, and other large pelagic fish (Moteki et al., 2001), squids (Shchetinnikov, 1992), and seabirds (Spear et al., 2007) in the ETP. Given their importance as prey, their feeding behavior can have ramifications on how energy is transferred from lower to higher trophic levels.

The eastern tropical Pacific Ocean encompasses areas of upwelling and oligotrophy (Fiedler and Talley, 2006), and this oceanographic variability produces diverse zooplankton prey assemblages (Fernández-Álamo and Färber-Lorda, 2006). There are also diverse and abundant communities of myctophids (Ahlstrom, 1972, 1971). With the abundance of myctophids and their zooplankton prey in this region, the ETP presents an opportunity to assess feeding strategies for these fish.

Using samples collected across a productivity gradient along the North Equatorial Countercurrent (NECC), we quantified the diets of 3 common surface-migrating myctophids, and assessed the availability of prey for these species from zooplankton net hauls. Then, using a bagged (i.e., bootstrap aggregating, where classifications of randomly generated training sets are combined to improve overall model performance) classification tree (Kuhnert et al., 2012), we investigated the influence of spatial, oceanographic, and biologic (prey and predator) variables on myctophid diets. We postulate that, if dietary resources were partitioned, the diets of each species would be unique, whereas if feeding was opportunistic, myctophid diets would be related to broad-scale patterns of prey availability and oceanography.

Materials and methods

Study area and data collection

The study area is located in the ETP between the subtropical gyres of the North and South Pacific (Fiedler and Talley, 2006). The ETP contains 3 major surface currents: the North Equatorial Current (NEC), North Equatorial Countercurrent (NECC), and the South Equatorial Current (SEC [Fig. 1]). The NECC is a warm, eastward flowing current in which upwelling causes shoaling of the thermocline along an east-to-west gradient near 5°N (Fiedler and Talley, 2006). Two eastern boundary currents at the northern (California Current) and southern (Peru Current) extent of the ETP bring cold, nutrient-rich water into the system (Fiedler and Talley, 2006). Nearshore waters associated with the Gulf of Panama have characteristically low sea-surface-salinity (SSS) values owing to high local rainfall (Amador et al., 2006).

Myctophids (n=580) were collected aboard National Oceanic and Atmospheric Administration (NOAA) research vessels RV *MacArthur II* and RV *David Starr Jordan* during surveys conducted in the ETP by NOAA's Southwest Fisheries Science Center (SWFSC) from August to November 2006. Myctophids were systematically collected every night in dip nets at predetermined stations (Fig. 2) located on line transects (Fig. 3). A randomized subsample of myctophids captured at 32 stations was available for this study. Dipnet sampling began one hour after local sunset and lasted for 1 hour. Long-handled (~6-m) dip nets with 1-m wide baskets and 0.5-cm mesh size were used to catch myctophids under deck lights that illuminated approximately 10 m^2 of the water surface (Coad, 1998). Researchers at the SWFSC have collected specimens using this standardized method for decades (Fiedler et al., 2013; Pitman et al.[1]). The dipnet method is unique in comparison with that of traditional net tows because fish are collected from the ocean environment individually and not retained in a net, thus excluding the possibility of postcapture feeding. Net avoidance associated with the bow-wave of large towed equipment is also negated with handheld dip nets. Myctophids exhibit size-related

[1] Pitman, R. L., L. T. Ballance, and P. C. Fiedler. 2002. Temporal patterns in distribution and habitat associations of prey fishes and squids. NOAA, Natl. Mar. Fish. Serv., Southwest Fish. Sci. Cent. Admin. Rep. LJ-02-19, 52 p. [Available at website.]

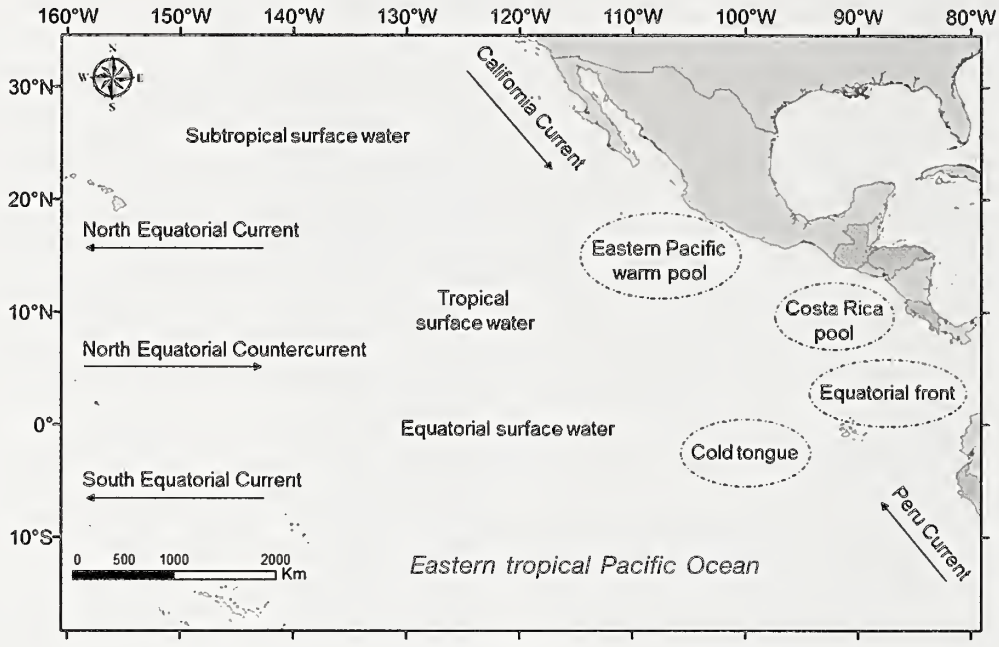

Figure 1

Major currents and oceanographic features in the eastern tropical Pacific Ocean. Arrows indicate direction of the currents. Dashed ovals signify distinct oceanographic features.

depth stratification throughout the water column, and certain, often larger, individuals remain deeper in the column (Collins et al., 2008; Saunders et al., 2015). Additionally, not all members of a surface-migrating population migrate each night, and surface-migration is likely spurred by feeding. Therefore, our samples are not representative of all size classes within this population; instead, we focused entirely on the surface-migrating myctophids that were found in surface waters during the time of capture. Specimens were frozen whole at sea.

Zooplankton were sampled with a bongo net (0.6-m mouth diameter, 333-μm mesh) towed obliquely to a depth of 200 m at an average ship speed of 1.75 kn. A flow meter was attached to the net to determine the amount of filtered seawater. We analyzed only net tows at the 32 stations where myctophids were collected (Fig. 2). The sampling depth of the bongo tows does not cover the entire depth range for myctophids because our study focused exclusively on the surface-migrating members of the population and we were interested in the prey that might be available to this subset of the fish community. Zooplankton also conduct diel vertical migrations from deep-water to near-surface waters and it is likely that some zooplankton had migrated from deeper than 200 m (Longhurst and Harrison, 1988). Depth-integrated zooplankton samples were used because myctophids feed during migration (Watanabe et al., 1999). Net tows commenced 30 min after the conclusion of dipnet sampling and the zooplankton samples were preserved at sea in 3.7% buffered formalin.

Systematic oceanographic sampling was conducted during the surveys (for details, see Fiedler and Philbrick[2]). Sea surface temperature (SST) and SSS values were recorded with a thermosalinograph at 2-min intervals along transects (Fig 3). Surface chlorophyll-*a* (SCHL) concentrations were measured at approximately 55-km intervals along transects by using a fluorometer. Mixed layer depth (MLD), i.e. the depth at the top of the thermocline, was estimated as the depth (m) at which the temperature is 0.5°C less than the surface temperature. MLDs were derived from data obtained from expendable bathythermograph (XBT) and conductivity, temperature, and depth (CTD) casts. XBT casts were made at approximately 55-km intervals along transects to a depth of 760 m. CTD casts were undertaken at sunrise and sunset each day to a depth of 1000 m. Using these data, Barlow et al. (2009) created smoothed (using the Kriging method) maps of SST, SSS, MLD, and SCHL data (Fig. 3) and are presented here with permission. In the classification tree model we considered, only variables coinciding with the 32 dipnet stations at which myctophids were collected.

In the laboratory, myctophids were thawed individually, identified (by using keys devised by Wisner, 1974 and Gago and Ricord, 2005), blotted, weighed to the nearest mg, and measured to the nearest mm (standard length, SL). Stomachs were dissected whole from each

[2] Fiedler, P. C., and V. A. Philbrick. 2002. Environmental change in the eastern tropical Pacific Ocean: observations in 1986–1990 and 1998–2000. NOAA, Natl. Mar. Fish. Serv., Southwest Fish. Sci. Cent. Admin. Rep. LJ-02-15, 16 p. [Available at website.]

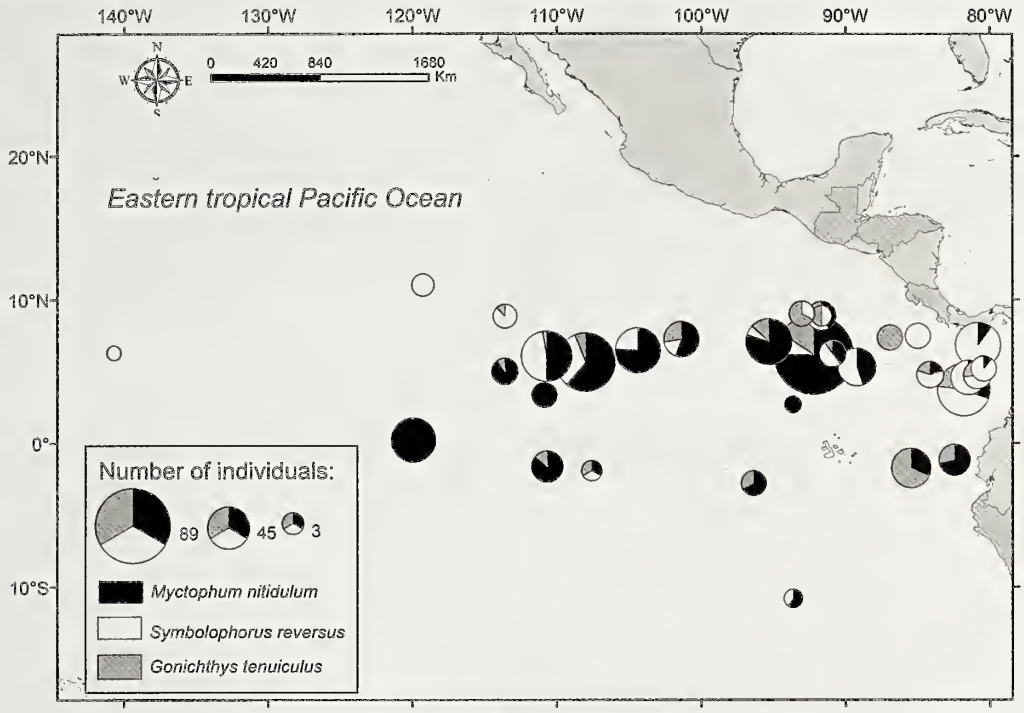

Figure 2

Species distribution of the 580 myctophid individuals of 3 myctophid species collected from the eastern tropical Pacific Ocean by dip net during 2006.

fish, weighed, fixed in 3.7% formalin, and stored in 70% ethyl alcohol. The amount of time specimens were left either unfrozen or unpreserved was minimized to avoid degradation of stomach contents.

Displacement volumes of small zooplankton from oblique net tows were measured in the laboratory. This measurement excluded all fishes, large cephalopods, pelagic crabs, and large plankters (>5 mm), including Thaliacea and medusae (Ohman and Smith, 1995). Net samples were split to a one-eighth volume by using a Folsom plankton splitter, and individuals were identified under a dissecting microscope to the taxonomic level of order. Identifications were made to order level for comparison with the taxonomic resolution of most gut-content identifications. This taxonomic resolution restricted our diet analysis because we could not exclude the possibility that resource partitioning occurs at a lower taxonomic level. Zooplankton densities were standardized as numbers of individuals per m^3 of water filtered at each station by using methods of Smith and Richardson (1977) and were converted to numeric percentages for comparison with gut contents.

Diet composition

We identified stomach contents to the lowest possible taxon and enumerated and weighed contents by taxonomic group. Pieces of plastic found in stomachs were not included in the analysis of the natural diet. Stomachs void of all material, including unidentifiable substance, were classified as empty.

We calculated mean percentage by number (MN_i) by using the following equation:

$$N_i = \frac{1}{P}\sum_{j=1}^{P}\left(\frac{N_{ij}}{\sum_{i=1}^{Q} N_{ij}}\right)\times 100, \quad (1)$$

where N_{ij} = the count of prey type i in fish j;
Q = the number of prey types in the stomach of fish j; and
P = the number of fish with food in their stomachs in any particular sampling stratum (Chipps and Garvey, 2007).

We calculated mean percentage by weight (MW_i) similarly, substituting prey weights (W) for counts (N). Percent occurrence (O_i) was calculated as the number of fish containing a specific prey item i, divided by the total number of fish sampled, including those myctophids with empty stomachs, and multiplied by 100. We focused our analysis on the numeric predation data for comparison with the numeric zooplankton prey data.

Classification tree analysis

We applied Classification and Regression Tree (CART) analysis to the myctophid diet data, using the modified approach of Kuhnert et al. (2012 [see also Olson et al., 2014]). CART is a nonparametric modeling approach described by Breiman et al. (1984). Diet data are partitioned by forming successive splits on predictor variables in order to minimize an error criterion, in this case the Gini index, which represents a mea-

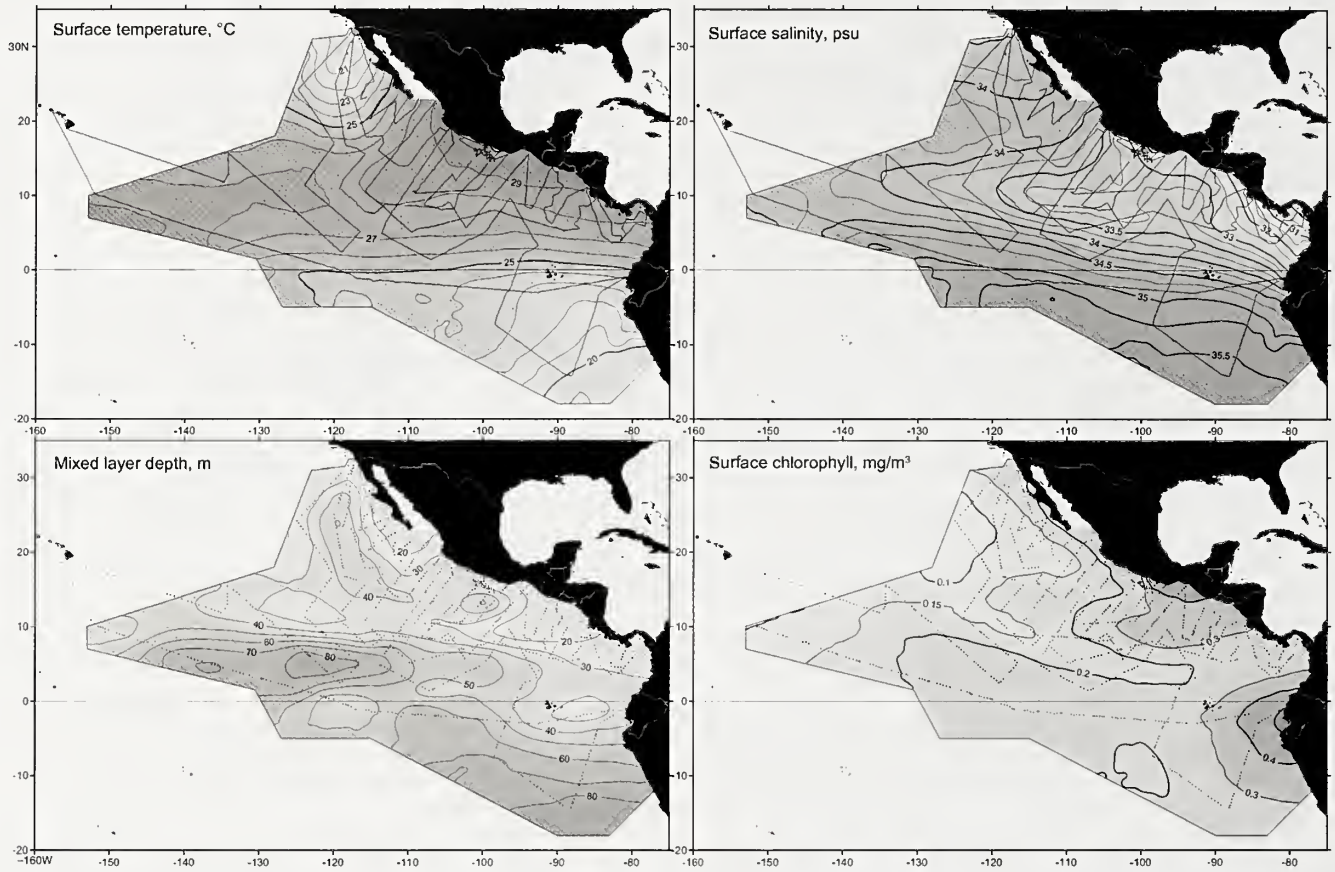

Figure 3

Oceanographic maps smoothed (with the Kriging method) and created by Barlow et al. (2009) and used with permission, displaying (clockwise from top left) surface temperature, surface salinity, surface chlorophyll, and mixed layer depth values in the eastern tropical Pacific (shaded region). Ship track-lines are shown with solid or dashed lines. Solid lines indicate sampling was continuous. Dashed lined indicated sampling was conducted at 55-km intervals. Numbers along isopleths indicate values for the variable represented in each map. Only variables coinciding with the 32 dipnet stations were used in the classification and regression tree (CART) analysis.

sure of diet diversity ranging from 0 (no diet diversity) to 1 (high diet diversity) among predicted prey categories. A large tree is produced and 10-fold cross-validation is used to prune the tree to within one standard error of the tree yielding the minimum error (i.e., the "1 SE" rule [Breiman et al., 1984; Kuhnert et al., 2012]). Predictions are made by partitioning a new observation down the tree until it resides in a terminal node. The prey group with the greatest numeric proportion among a suite of prey in the diet is displayed at each terminal node. The vector of prey proportions, in numbers of prey eaten by an individual predator is represented as a univariate categorical response variable of prey type (class), with observation (case) weights equal to the proportion of the prey type eaten by the predator. Fish with empty stomachs were omitted from this analysis because we were interested in how predictor variables influenced prey type. Rankings of variable importance are computed to identify which predictor variables are most important in the model. In addition, Kuhnert et al. (2012) implemented a spatial bootstrapping technique to account for spatial dependence in the data and to assess uncertainty in the predicted diet composition at each node in the classification tree. The classification was implemented in R software, vers. 3.1.1 (R Core Team, 2014) with the 'rpart' package (Therneau et al., 2013); further details can be found in Kuhnert et al. (2012).

We used CART analysis to explore the relationship among 12 dependent spatial, oceanographic, and biological predictor variables (Table 1) and the response variable, diet composition. Spatial predictors included latitude and longitude, oceanographic predictors consisted of MLD, SSS, SST, and SCHL concentration, and biological predictors contained information on the zooplankton prey community by using data from the net samples and the myctophid predators. Data representing the zooplankton community (potential prey) included ostracod, copepod, and euphausiid numeric composition and zooplankton displacement volume in the net samples (Table 2). Standard fish length was used to assess the effects of ontogenetic diet. We used species as a predictor variable to assess resource-partitioning among species.

Table 1

Geographic, oceanographic, and biologic predictor variables used in the analysis to determine the diet of 3 myctophids in the eastern tropical Pacific Ocean. Fish were collected from August through November 2006.

Predictor variable	Type of variable	Mean (Min.–Max)
Longitude	Spatial	140.7°W to 80.4°W
Latitude	Spatial	11.0°S to 10.8°N
Myctophid species	Biological	*Myctophum nitidulum*, *Symbolophorus reversus*, *Gonichthys tenuiculus*
Myctophid standard length	Biological	50.4 mm (25–80)
Ostracod zooplankton (ZP) composition	Biological	10.9% (1.2–37.0)
Copepod ZP composition	Biological	72.2% (45.0–87.3)
Euphausiid ZP composition	Biological	4.4% (1.8–20.7)
Zooplankton volume	Biological	97.5 mL (1,000)/m^3 (44–241)
Mixed layer depth (MLD)	Oceanographic	38.1 m (6–93)
Sea surface salinity (SSS)	Oceanographic	33.25 psu (31.21–35.58)
Sea surface temperature (SST)	Oceanographic	21.2°C (21.9–29.2)
Surface chlorophyll (SCHL)	Oceanographic	0.184 mg/m^3 (0.002–0.382)

We categorized the myctophid diet into 17 prey groups in the CART analysis (14 are shown in Table 3). These groups ranged in taxonomic level from family (e.g., Euchaetidae) to phylum (e.g., Mollusca) because the taxonomic resolution of prey identifications varied and because some rare prey were combined into broader taxa along with unidentifiable specimens. For the CART analysis, all mollusks were grouped together, as were all euphausiids, and all cyclopoid copepods. Rare calanoid copepods, defined as types contributing less than 1% MN_i to all 3 myctophid species were grouped as "other copepods." Rare amphipods, defined as types contributing less than 0.3% in MN_i were grouped as "other amphipods." The "other" copepod and amphipod groups contained a majority of unidentifiable specimens. Decapods (0.5% combined mean MN_i), fish eggs (0.3%), and the one cephalopod (<0.1%) were not included in the analysis because of their scarcity.

Results

Oceanographic variables

The MLD, SSS, SST, and SCHL concentrations each showed distinct geographic patterns within the study area. MLD deepened from east to west along the NECC, between the equator and 10°N (Fig. 3). At its shallowest, MLD (mean 38.1 ±20.5 m standard deviation [SD], averaged over the 32 dipnet stations) was 6 m deep nearshore (8°N, 91°W) and reached 93 m at the station farthest offshore (6°N, 140°W). SSS (mean 33.3 ±1.20 practical salinity units [psu]) was lowest (31.21 psu) near the coast of Central America, and became more saline farther offshore and south of the equator (max. of 35.5 psu). SST (mean 21.2 ±1.90° C) showed little variation along the NECC, where the majority of stations occurred. Surface chlorophyll-*a* values (mean 0.20 ±0.08 mg/m^3) were greatest along the coast of southern Mexico and Ecuador and decreased offshore (Fig. 3).

Myctophid size-composition

The individuals collected at the surface nightly by dip net differed morphologically (Fig. 4). *Symbolophorus reversus* (n=199; 172 with identifiable prey remains) was the largest of the 3 species in length (mean=55.9 ±8.8 mm SD) and weight (2.66 ±1.27 g SD). *Myctophum nitidulum* (n=299; 275 with identifiable prey remains) was intermediate in length (47.9 ±6.6 mm) and weight (1.82 ±0.80 g). *Gonichthys tenuiculus* (n=82; 26 with identifiable prey remains), was the smallest species in length (37.8 ±4.3 mm) and weight (0.54 ±0.21 g [Fig. 4]).

Diet composition

Prey composition data for each of the 3 species are summarized by the 3 diet indices, MN_i, MW_i, and O_i in Table 2. We focused our data analysis on the numeric diet index for consistency with the numeric data on prey availability. We included the weight and occurrence indices in Table 2, however, so that our data are comparable with other published data.

Zooplankton community

Seventeen unique taxonomic groups of zooplankton were identified and enumerated (n=178,090 individuals) in the net tows. Copepods were by far the most abundant group, representing as much as 87.3% of the community sampled and never less than 45.0% at any station (Table 3, Fig. 5). Ostracods were the second most abundant group overall (8.65 ±10.1%). Euphausiids and amphipods each contributed <5% of the sampled community.

Table 2

Percentages of the prey composition for 3 myctophids collected at 32 stations in the eastern tropical Pacific Ocean. Samples of zooplankton prey were taken with an oblique haul of a bongo net. Offshore, intermediate, and nearshore regions were identified by a classification tree analysis (Fig. 7). Standard deviations are shown in parentheses.

Latitude	Longitude	Amphipods (%)	Copepods (%)	Euphausiids (%)	Euphausiids (%)	Other prey (%)	Nonprey items (%)
6.30°N	140.72°W	0.55	72.9	2.37	12.1	3.29	8.78
0.23°N	119.92°W	1.52	76.6	3.07	3.09	2.79	13.0
11.03°N	119.28°W	1.43	82.8	2.92	1.80	4.06	7.00
5.02°N	113.58°W	1.62	61.0	2.58	22.3	2.38	10.1
8.25°N	113.17°W	1.38	45.0	5.98	33.6	2.66	11.3
3.37°N	110.85°W	2.17	67.5	2.35	9.74	4.00	14.3
6.07°N	110.70°W	2.05	45.2	4.61	37.0	5.17	6.04
1.62°S	110.65°W	1.07	69.8	4.94	5.16	1.38	17.6
5.65°N	108.00°W	1.45	61.1	5.54	19.7	6.29	5.84
1.90°S	107.58°W	1.73	76.7	4.36	2.78	0.36	14.1
6.48°N	104.38°W	1.02	49.3	3.12	32.9	2.00	11.6
6.33°N	101.73°W	1.15	70.5	3.89	15.4	1.78	7.30
7.25°N	101.37°W	1.35	65.0	5.13	17.6	2.19	8.68
2.78°S	96.37°W	1.24	78.4	3.87	3.11	1.67	11.7
7.07°N	95.32°W	0.82	82.5	2.35	1.53	3.55	9.20
2.68°N	93.65°W	0.82	81.8	2.50	5.18	4.36	5.29
10.8°S	93.62°W	0.76	61.7	20.7	1.48	1.58	13.8
9.02°N	93.05°W	2.56	82.1	3.63	2.00	7.57	2.14
6.15°N	92.20°W	1.91	79.9	4.37	3.21	3.01	7.64
8.37°N	91.68°W	1.76	79.8	4.01	1.66	2.60	10.2
6.23°N	90.90°W	2.15	76.2	3.07	3.73	2.86	12.0
5.30°N	89.20°W	1.57	75.8	4.20	3.06	1.14	14.3
7.35°N	86.93°W	1.15	72.7	5.51	5.49	1.09	14.1
1.73°S	85.45°W	1.72	80.7	3.29	1.21	4.98	8.04
7.47°N	85.00°W	1.15	81.2	3.74	1.21	1.77	10.9
4.77°N	84.15°W	1.22	77.4	4.41	3.54	0.83	12.6
1.17°S	82.45°W	0.48	87.3	1.78	1.45	3.22	5.73
3.72°N	81.82°W	1.08	77.0	3.73	4.58	1.72	11.9
4.57°N	81.52°W	1.07	76.7	4.07	2.76	5.76	9.64
4.73°N	80.88°W	1.34	69.6	5.29	6.40	2.60	14.8
6.83°N	80.83°W	1.23	75.5	4.21	5.23	1.14	12.7
5.18°N	80.43°W	0.61	70.5	5.44	6.62	3.83	12.9
Region							
Offshore		1.40	63.9	3.90	17.5	3.20	10.1
Intermediate		1.50	80.5	3.30	2.60	3.50	8.60
Nearshore		1.11	75.1	4.55	4.48	2.34	12.5
Mean		1.35 (±0.49)	72.2 (±10.7)	4.41 (±3.16)	8.65 (±10.1)	2.93 (±1.69)	10.5 (±3.46)

Classification tree analysis

The classification tree analysis produced a tree with 2 splits and 3 terminal nodes (Fig. 6A) and yielded a cross-validated error rate of 0.73 (standard error [SE]=0.04, coefficient of multiple determination [R^2]=~27%). The rankings of variable importance (Fig. 6B) indicated that longitude was the most important variable (i.e., rank=1.00) for predicting the diet composition of these myctophids. The ostracod numeric composition of the zooplankton (rank=0.74), the copepod composition of the zooplankton (rank=0.61), MLD (rank=0.61), and SSS (rank=0.50) were the next most important. Myctophid species (rank=0.08) was a less important predictor variable in the classification tree given our collection of surface-migrating fishes and at the taxonomic level possible in this study. Latitude, myctophid length, SST, SCHL, zooplankton volume, and euphausiid composition in the zooplankton net samples yielded an importance rank of zero.

The initial split in the tree provided the greatest reduction in deviance over the entire data set and par-

Table 3

Summary of stomach contents (including pieces of plastic) of 3 myctophid species collected in the eastern tropical Pacific Ocean during 2006. Diet indices include mean percentages by number (MN_i), weight (MW_i), and percent occurrence (O_i). Fourteen of the 17 prey groups used in the classification tree analysis are designated with an "X." Unidentifiable and rare individuals (generally contributing <1% MN_i to the diet) within the broader taxonomic group are not displayed. CART=classification and regression tree analysis. Bold font represents total values for a subclass and order of prey.

	Used (X) in CART	*Myctophum nitidulum*			*Symbolophorus reversus*			*Gonichthys tenuiculus*		
		MN_i	MW_i	O_i	MN_i	MW_i	O_i	MN_i	MW_i	O_i
Copepoda		**42.7**	**39.1**	**69.6**	**32.5**	**28.3**	**50.3**	**18.6**	**17.6**	**7.3**
Calanoida		36.4	37.5	62.5	27.1	23.3	45.2	18.6	17.6	7.3
Calanidae	X	1.01	1.44	10.7	0.29	0.15	1.51	3.85	4	1.22
Candaciidae—*Candacia* spp.	X	1.47	1.84	14.4	5.53	5.04	16.1	0	0	0
Eucalanidae	X	1.79	2.51	14.4	0.12	0.27	1	0	0	0
Euchaetidae	X	7.33	10.2	32.1	6.94	15	15.1	3.85	4	1.22
Pontellidae	X	0.5	0.64	6.69	0	0	0	3.01	2.44	2.44
Cyclopoida		6.26	2.89	35.5	5.33	4.99	14.1	0.55	0	1.22
Corycaeidae—*Corycaeus* spp.	X	1.43	0.56	12.7	0.37	0	1.51	0	0	0
Oncaeidae—*Onceaea* spp.	X	4.8	2.33	27.4	4.73	1.81	13.6	0	0	0
Ostracoda		**41.5**	**39.1**	**45.5**	**24.4**	**18.1**	**26.1**	**34.6**	**36**	**11**
Cypridinidae—*Cypridina americana*	X	41.3	38.8	45.1	24.4	18.1	26.1	34.6	36	11
Euphausiacea	X	**3.29**	**3.42**	**13**	**29.6**	**34.5**	**47.2**	**19.4**	**16.4**	**7.32**
Euphausia diomedeae		0		0	2.86		6.53	0		0
E. mutica		0.08		0.67	4.15		10.1	0		0
E. tenera		0.16		2.01	2.34		8.04	0		0
Euphausia spp.		2.18		10	19.6		7	19.4		7.32
Amphipoda		**8.38**	**12.1**	**35.8**	**7.58**	**9.61**	**20.1**	**27.3**	**30**	**9.76**
Hyperiidae	X	3.86	5.42	20.1	4.6	5.32	15.1	9.34	11.5	3.66
Pronoidae	X	1.23	2.54	8.36	0.24	0.37	3.02	4.81	6	2.44
Platyscellidae	X	0.32	1.11	3.34	0.3	1.09	3.02	0	0	0
Mollusca	X	**2.98**	**4.35**	**14.7**	**2.48**	**3.59**	**8.54**	**0**	**0**	**0**
Atlantidae		0.12	0.32	2.01	0.39	0.75	2.51	0	0	0
Janthinidae		1.44	1.99	8.01	1.42	1.8	2.51	0	0	0
Limacinidae—*Limacina* spp.		0.4	0.48	1	0	0	0	0	0	0
Cavoliniidae—*Diacria schmidti*		0.03	0.16	0.67	0.03	0.16	0.5	0	0	0
Unidentified Mollusk		0.98	1.35	5.69	0.64	0.88	3.02	0	0	0
Larval fish	X	**0.12**	**0.19**	**0.33**	**2.09**	**3.63**	**7.04**	**0**	**0**	**0**
Decapoda		**0.33**	**0.47**	**3.01**	**1.09**	**1.86**	**3.02**	**0**	**0**	**0**
Fish egg		**0.78**	**0.16**	**3.34**	**0.08**	**1.21**	**0.5**	**0**	**0**	**0**
Cephalopoda		**0**	**0**	**0**	**0.19**	**0.3**	**0.5**	**0**	**0**	**0**
Plastic				**2.01**			**0**			**1.22**
Total stomachs		299			199			82		

titioned the diet composition for 271 myctophids sampled east of 100°W, on the left side of the tree (node 2), from the diet composition of 196 myctophids sampled west of 100°W, on the right side of the tree (i.e., terminal node 3) (Figs. 6 and 7). Ostracod composition in the zooplankton was a strong competitor-split variable, i.e, ostracod composition in the zooplankton preformed only 2% worse than longitude at this partition (node 2). The diet composition of the myctophids east of 100°W was variable, and the tree further separated 169 samples caught in waters of relatively high salinity, SSS ≥32.86, east of 100°W (terminal node 4) from 102 samples caught in waters of relatively low salinity, SSS <32.86, east of 100°W and near the Panama Bight (terminal node 5 [Figs. 6 and 7]).

Terminal node 3 All myctophids in the offshore region (Fig. 7) consumed large proportions of the ostracod *Cypridina americana* (mean MN_i: 76.4%) and small numbers of several other prey (Fig. 7). The diet diversity (0.22) of the myctophids in this region (terminal node 3) was lowest among all terminal nodes. Ostracods were the most numerically abundant and the MLD was the deepest at the 13 stations within the offshore region.

Terminal node 4 The 169 myctophids residing in terminal node 4 consumed large proportions of copepods (mean MN_i: 66.6%) that were identifiable as euchaetids. These myctophids were captured at 9 stations at intermediate distances from the coast, between 100°W

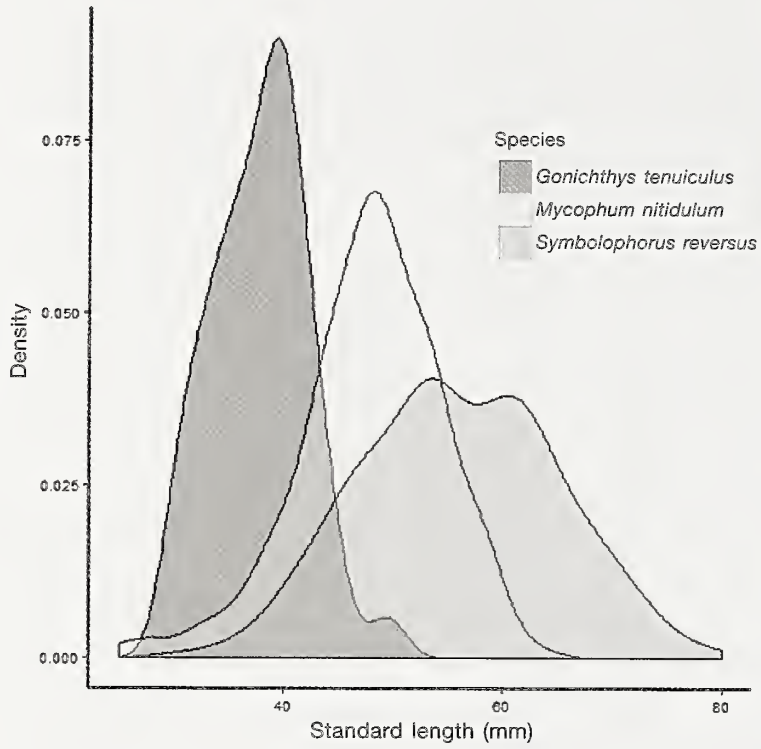

Figure 4

Length-frequency plot for the 3 myctophid species captured from surface waters in the eastern tropical Pacific during 2006. Sizes reflect our unique specimen collection and are not representative of the entire population because only surface-migrants were targeted.

and 89°W, and nearshore off Ecuador (Fig. 7). Net samples revealed copepods were the most numerically abundant zooplankton (80.5%, compared with 63.9 and 75.1% in the offshore and nearshore regions) in this region (Table 3). This intermediate region was characterized by moderate values of MLD, SSS, and SCHL (Fig. 3), and it appears to represent a transition zone between the offshore and nearshore regions.

Terminal node 5 The myctophids sampled at 8 nearshore stations near the Panama Bight, east of 87°W and north of 3°N, (Fig. 7) consumed primarily euphausiids (mean MN_i: 45.0%). SSS in this region was low (<32.86 [Fig. 3]), the MLD was shallow (mean MLD: 22.9 m), and SCHL concentrations (0.22 mg/m^3) were greater than those at stations identified within the other regions.

Interspecific patterns

Collectively, the predominant prey of these myctophids came from 4 groups, copepods (MN_i=37.7%), ostracods (34.9%), euphausiids (13.7%), and amphipods (9.1%), which accounted for more than 95% of the diet, by number. The remaining 5% comprised mollusks (pteropods and heteropods, 2.6%), larval fishes, decapods, fish eggs, one squid paralarva, and one terrestrial insect (Table 2).

Interspecific dietary differences were apparent and might have been more definitive if the prey were identified at a lower taxonomic level. Previous research has, for example, indicated that these species are selective feeders (Van Noord et al., 2013b). We further assessed these previous findings by including a broad suite of predictor variables and found that "myctophid species" ranked relatively low in explaining diet patterns across the ETP. *Myctophum nitidulum* fed on copepods (42.7%) and ostracods (41.5% [Table 2]). *Symbolophorus reversus* fed primarily on copepods (32.5%), euphausiids (29.6%), and ostracods (24.4%). *Gonichthys tenuiculus* took prey from only 4 groups, primarily ostracods (34.6%) and amphipods (27.3% [Table 2]).

Distribution patterns differed somewhat among the 3 myctophids. Figure 2 displays spatial trends in abundance; greater numbers of *S. reversus* and *G. tenuiculus* occurred in the nearshore and intermediate areas, respectively. The individuals in this study, however, represent subsamples of the captured myctophids, and no quantitative distribution analysis was possible. However, representatives of each species were captured across the entire sampling region, resulting in adequate distributional overlap, but the tree analysis did not indicate that myctophid species are an important variable in characterizing the diet of the fishes in this study.

Discussion

We used a classification tree to examine the influence of spatial, biological, and oceanographic predictors on diet and found that feeding by the collection of surface-migrating myctophids in this study was controlled by prey distribution and resource-driven processes, such as mixed-layer depth, productivity, and sea surface salinity, whereas the influence of dietary resource partitioning was a minor controlling factor. These myctophids shared a similar diet, consisting primarily of copepods, ostracods, euphausiids, and amphipods. Diet of all 3 species changed geographically, and with oceanographic conditions and zooplankton prey composition. Myctophids consumed ostracods offshore where the mixed layer depth was deep and ostracods were more abundant in the prey community, euphausiids nearshore where the MLD was shallow, and copepods at intermediate stations between those stations where they were most abundant. Understanding myctophid feeding behavior can provide insight into how these

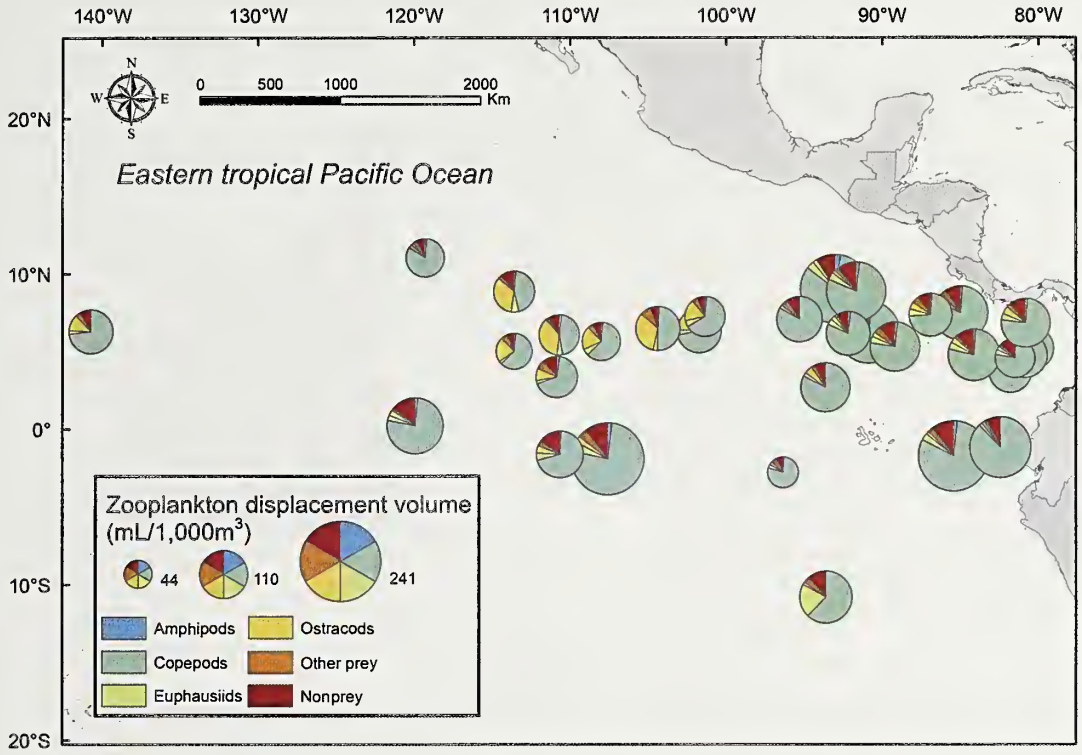

Figure 5

Distribution of the prey community sampled with an oblique bongo net in the eastern tropical Pacific Ocean. Each color represents a zooplankton prey species, other prey species, or non-prey species. Circle size reflects zooplankton displacement volume. The numbers 44, 110, and 241 indicate zooplankton displacement volume (mL/1000m^3).

communities are structured and how energy is transferred through the food web.

Longitude had the greatest variable importance ranking among all predictors, and this is likely because water masses and prey composition co-varied geographically along the NECC. The NECC is characterized by a shoaling thermocline and by increased productivity from west to east (Fiedler and Talley, 2006), and the classification tree allowed us to identify distinct regions along the NECC where myctophid diet was different. The zooplankton samples collected from the stations in each of the 3 geographic regions had different percentages of prey groups that contributed to myctophid diet patterns.

The offshore region was defined by a high abundance of pelagic ostracods in myctophid diets. This region was oceanographically distinct because of its mixed layer depth, low productivity, and high abundance of ostracods in contrast to the other regions. A deep MLD corresponds to reduced mixing, lower nutrient availability in surface waters, and oligotrophic conditions (Fiedler and Talley, 2006). Pelagic ostracods are typically most abundant in such oligotrophic conditions because of their greater ability to exploit environments low in food availability (Le Borgne and Rodier, 1997; Angel et al., 2007).

The nearshore region was defined by a high abundance of euphausiids in myctophid diets. This region was oceanographically distinct because of its shallow MLD and low saline waters. It typically displays elevated primary productivity and low oxygen levels (Fiedler and Talley, 2006). Extreme local rainfall and westward transport of water vapor across the Isthmus of Panama contribute to the low-salinity water mass in this location (Amador et al., 2006). Euphausiid abundance is typically greatest in productive, nearshore waters (Brinton, 1979; Simard et al., 1986), and that is the case here. Upwelling and biological production are greatest near the coast in the ETP, particularly the Gulf of Panama and the Costa Rica Dome than in other regions in the ETP (Lavín et al., 2006). Additionally, an oxygen minimum zone exists in the ETP; low oxygen values extend south into the Gulf of Panama (Fiedler and Talley, 2006). Some euphausiids, such as *Euphausia diomedeae* and *E. mutica* that were consumed by the myctophids in this study, are tolerant of low oxygen (Brinton, 1979).

Myctophids in the intermediate region had high numbers of copepods in their diets. This region, a transition zone between the nearshore and offshore, showed moderate mixed layer depths, salinities, and surface chlorophyll values in comparison with the higher and lower values of the other regions, respectively. Copepods were abundant throughout the study area but

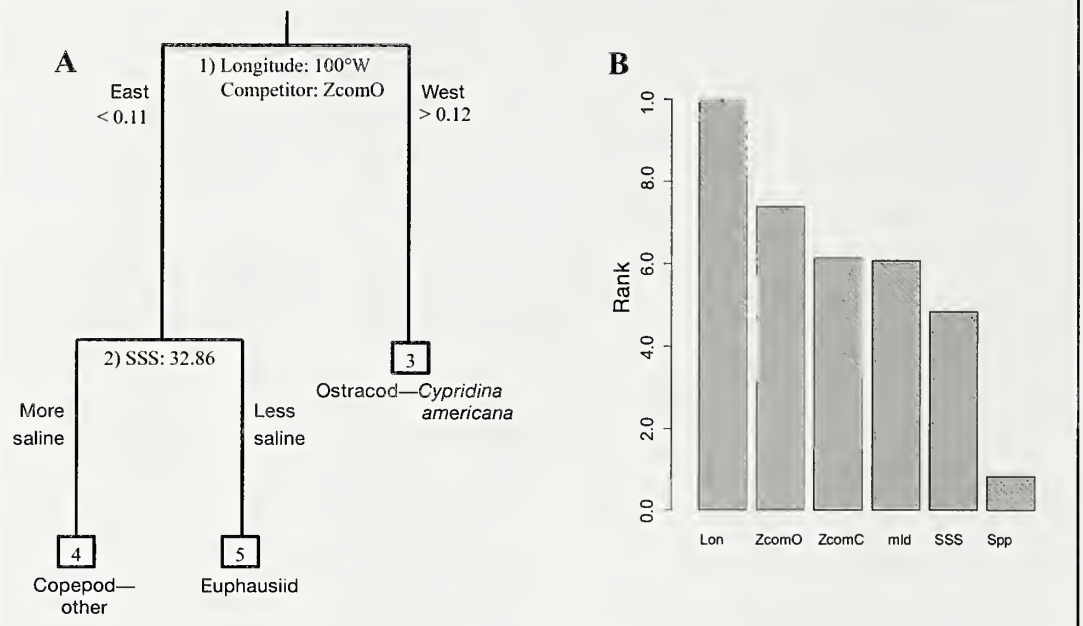

Figure 6

(**A**) The classification tree (at a 1 SE resolution) used to predict myctophid (*Myctophum nitidulum*, *Symbolophorus reversus*, *Gonichthys tenuiculus*) diet composition from geographic, oceanographic, and biologic predictor variables (see *Materials and methods* section for further explanation). The prey group identified at each terminal node is that with the highest proportional numeric composition among all the prey in the myctophid samples that were mapped to each terminal node. (**B**) A variable importance plot showing rankings of each nonzero predictor variable used in the classification tree model. Lon=longitude; ZcomO=ostracod composition in the zooplankton net samples; ZcomC=copepod composition in the zooplankton net samples; mld=mixed layer depth; SSS=sea surface salinity; Spp=myctophid species

made up more than 80% of the community in the intermediate region, perhaps reflecting a competitive advantage that various copepods have in moderately oceanographic conditions (McGowan and Walker, 1985; Turner, 2004). In contrast, ostracods were limited in their range to oligotrophic conditions, and euphausiids were more dominant in productive nearshore environments (Brinton, 1979).

Previous research has indicated that *M. nitidulum* selects amphipods and ostracods and that *S. reversus* prey on euphausiids and amphipods (Van Noord et al. 2013b), and in fact dietary resource partitioning among myctophids has commonly been reported (e.g., Hopkins and Gartner 1992: Hopkins and Sutton 1998: Cherel et al., 2010), but the influence of oceanography on diet is less often considered. The selective feeding behavior observed by Van Noord et al, (2013b) is indicative of resource partitioning, but the current study expands on these initial findings and presents a more complete ecosystem-based analysis by including spatial, biological, and oceanographic variables in addition to dietary information. The current study indicates a very low level of resource partitioning among these species, as evidenced by the low importance of myctophid species in the ranking of variables. Indeed, when considering a fuller compliment of oceanographic, spatial, and prey composition data, we found that resource partitioning between species is not the most important aspect controlling diet. Therefore, dietary resource partitioning and competition among these species played minor roles in regulating feeding behavior, and spatial and oceanographic predictor variables outweighed resource partitioning. The importance of considering spatial, biological, and oceanographic variables when evaluating feeding behavior is clear, and the findings obtained from these variables have implications for interpreting previous results.

A diverse fish community structured through dietary resource partitioning can be affected by disturbance events and bottom-up forcing. For example, flying fish in the ETP consume many of the same prey that are consumed by myctophids, which could introduce a level of food competition (Van Noord et al., 2013a). During the course of our investigations, (August–November 2007), a tropical storm bisected the sampling area (15–17 October), resulting in enhanced upwelling, productivity, and zooplankton biomass in the wake of the storm. The flying fish community reflected these changes. Feeding success increased and diet composition changed in accordance with storm-induced chang-

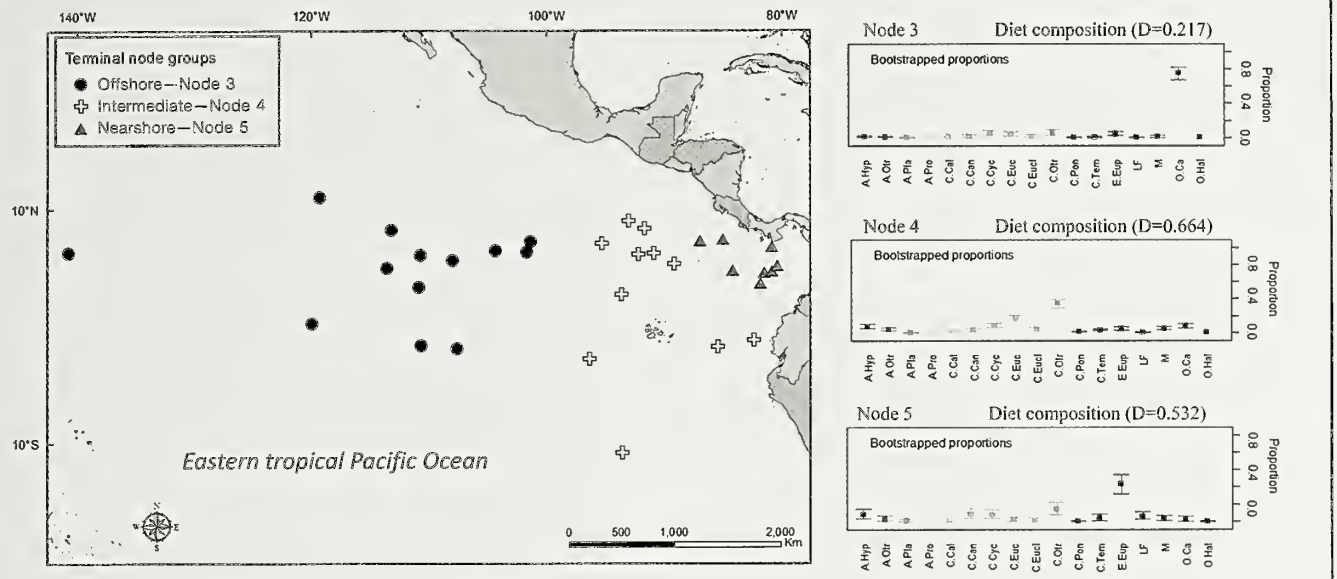

Figure 7

Map of terminal node groups 3, 4, and 5 in the classification tree of myctophid prey composition and showing the bootstrapped diet proportions for the myctophids grouped at each terminal node. Map displays symbols, which indicate the sampling stations where myctophids were feeding similarly according to the classification tree analysis. All stations occurred in waters >3000 m and bathymetric contours (in m) are displayed to show the depth ranges of our sampling. Diet diversity (D) values ranging from 0 (no diet diversity) to 1 (high diet diversity), are shown above each graph. Color gradients are provided for ease of viewing. Abbreviations are as follows: A=amphipod; C=copepod; E=euphausiid; A.Hyp=hyperiid amphipods; A.Otr=unidentifiable and rare amphipod types; A.Pla=platyscellid amphipods; A.Pro=pronoid amphipods; C.Cal=calanid copepods; C.Can=candaciid copepods; C.Cyc=cyclopoid copepods; C.Euc=euchaetid coepods; C.Eucl=eucalanid copepods;"C. Otr=unidentifiable and rare copepod types; C.Pon=pontellid copepods; C.Tem=temorid copepods; E.Eup=euphausiids,; LF=larval fishes; M=mollusks, O.Ca=*Cypridina americana* (ostracod); O.Hal=Halocyprida ostracods.

es in the prey community (Fiedler et al., 2013). These studies document the dynamic nature of the feeding habits of fish, and show that feeding patterns are not necessarily static; fish clearly respond to oceanographic conditions, in addition to displaying intrinsic behaviors that result in a more typical pattern of resource partitioning. This dynamic feeding behavior highlights the necessity of obtaining samples that adequately cover both temporal and spatial scales.

We sampled only surface migrating myctophids and therefore the interpretation of our data and implications for the broader myctophid community are limited. We did not include deeper dwelling individuals, and this limitation could alter both the feeding patterns observed and the size class of myctophids encountered. Sampling a broader spectrum of the myctophid population by using a suite of sampling gear that would cover the entire depth range for these fish could help to elucidate distributional patterns in the ETP and better address the role of resource partitioning in this fish community. As with all studies of fish feeding habits, taxonomic resolution of stomach contents impacts interpretation of the results. A finer taxonomic resolution may reveal a more subtle species-level diet partitioning among the myctophids. Prey size is also a function of the resolution of stomach samples and because we were unable to consistently quantify prey size in this study, it is possible that some species of myctophids partition diets on the basis of prey size rather than species, or some combination of size and species. As with most studies, a greater temporal sampling resolution would be beneficial for addressing longer term nuances in feeding ecology, and future work would benefit from seasonal and yearly sampling. Both these improvements are reinforced by the fact that our current analysis has shown the importance of physical variables in fish diet studies and highlights the need to include spatial, oceanographic and biological factors when evaluating feeding patterns of myctophids and of fish in general.

Acknowledgments

This research was partially funded by the University of San Diego and a Stephen Sullivan Memorial Scholarship. We thank the many scientists at the Southwest Fisheries Science Center, NOAA, who made these samples available, including: L. Ballance, P. Fiedler, V. Andreassi, C. Hall, M. Kelley, R. Pitman, and G. Wat-

ters. We thank W. Watson for laboratory space and W. Walker for identifying the myctophid samples. We thank J. Barlow and P. Fiedler for use of smoothed oceanographic maps and 3 anonymous reviewers for their comments and editorial suggestions to improve this article at the manuscript stage.

Literature cited

Ahlstrom, E. H.
1971. Kinds and abundance of fish larvae in the eastern tropical Pacific, based on collections made on EASTROPAC I. Fish. Bull. 69:3–77.
1972. Kinds and abundance of fish larvae in the eastern tropical Pacific on the second multivessel EASTROPAC survey, and observations on the annual cycle of larval abundance. Fish. Bull. 70:1153–1242.

Amador, J. A., E. J. Alfaro, O. G. Lizano and V. O. Magaña.
2006. Atmospheric forcing of the eastern tropical Pacific: a review. Prog. Oceanogr. 69:101–142.

Angel, M. V., K. Blachowiak-Samolyk, I. Drapun, and R. Castillo, R.
2007. Changes in the composition of planktonic ostracod populations across a range of latitudes in the North-east Atlantic. Prog. Oceanogr. 73:60–78.

Barlow, J., M. C. Ferguson, E. A. Becker, J. V. Redfern, K. A. Forney, I. L. Vilchis, P. C. Fiedler, T. Gerrodette, and L. T. Ballance.
2009. Predictive modeling of cetacean densities in the Eastern Pacific Ocean. NOAA Tech. Memo. NMFS-SWFSC-444, 206 p.

Breiman, L., J. H. Friedman, R. A. Olshen, and C. J. Stoned.
1984. Classification and regression trees, 358 p. Chapman and Hall, Boca Raton, FL.

Brinton, E.
1979. Parameters relating to the distributions of planktonic organisms, especially euphausiids in the eastern tropical Pacific. Prog. Oceanogr. 8:125–189.

Brodeur, R., S. McKinnell, K. Nagasawa, W. Pearcy, V. Radchenko, and S. Takagi.
1999. Epipelagic nekton of the North Pacific Subarctic and Transition Zones. Prog. Oceanogr. 43:365–397.

Catul, V., M. Gauns, M., and P. K. Karuppasamy.
2011. A review on mesopelagic fishes belonging to family Myctophidae. Rev. Fish Biol. Fish. 21:339–354.

Cherel, Y., C. Fontaine, P. Richard, and J.-P. Labat.
2010. Isotopic niches and trophic levels of myctophid fishes and their predators in the Southern Ocean. Limnol. Oceanogr. 55:324–332.

Chipps, S. R., and J. E. Garvey.
2007. Assessment of diets and feeding patterns. *In* Analysis and interpretation of freshwater fisheries data (C. S. Guy and M. L. Brown, eds.), 473–514. Am. Fish. Soc., Bethesda, MD.

Clarke, T. A.
1980. Diets of fourteen species of vertically migrating mesopelagic fishes in Hawaiian waters. Fish. Bull. 78:619–640.

Coad, B. W.
1998. Expedition field techniques: fishes, 2nd ed., 97 p. Geography Outdoors, Royal Geographical Society, London.

Collins, M. A., J. C. Xavier, N. M. Johnston, A. W. North, P. Enderlein, G. A. Tarling, C. M. Waluda, E. J. Hawker, and N. J. Cunningham.
2008. Patterns in the distribution of myctophid fish in the northern Scotia Sea ecosystem. Polar Biol. 31:837–851.

Davison, P. C., D. M. Checkley Jr., J. A. Koslow, and J. Barlow.
2013. Carbon export mediated by mesopelagic fishes in the northeast Pacific Ocean. Prog. Oceanogr. 116:14–30.

Fernández-Álamo, M. A., and J. Färber-Lorda.
2006. Zooplankton and the oceanography of the eastern tropical Pacific: a review. Prog. Oceanogr. 69:318–359.

Fiedler, P. C., and L. D. Talley.
2006. Hydrography of the eastern tropical Pacific: a review. Prog. Oceanogr. 69:143–180.

Fiedler, P., J. V. Redfern, J. Van Noord, C. Hall, R. L. Pitman, and L. T. Ballance.
2013. Effects of a tropical cyclone on a pelagic ecosystem from the physical environment to top predators. Mar. Ecol. Prog. Ser. 484:1–16.

Gago, F. J., and R. C. Ricord.
2005. *Symbolophorus reversus*: a new species of lanternfish from the eastern Pacific (Myctophiformes: Myctophidae). Copeia 2005:138–145.

Gjosaeter, J., and K. Kawaguchi.
1980. A review of the world resources of mesopelagic fish. FAO Fish. Tech. Pap. 193, 151 p. FAO, Rome.

Hopkins, T. L., and J. V. Gartner Jr.
1992. Resource-partitioning and predation impact of a low-latitude myctophid community. Mar. Biol. 114:185–197.

Hopkins, T. L., and T. T. Sutton.
1998. Midwater fishes and shrimps as competitors and resource partitioning in low latitude oligotrophic ecosystems. Mar. Ecol. Prog. Ser. 164:37–45.

Irigoien, X., T. A. Klevjer, A. Røstad, U. Martinez, G. Boyra, J. L. Acuña, A. Bode, F. Echevarria, J. I. Gonzalez-Gordillo, S. Hernandez-Leon, S. Agusti, D. L. Aksnes, C. M. Duarte, and S. Kaartvedt.
2014. Large mesopelagic fishes biomass and trophic efficiency in the open ocean. Nat. Commun. 5:3271.

Kinzer, J., and K. Schulz.
1985. Vertical distribution and feeding patterns of midwater fish in the central equatorial Atlantic. Mar. Biol. 85:313–322.

Kuhnert, P. M., L. M. Duffy, J. W. Young, and R. J. Olson.
2012. Predicting fish diet composition using a bagged classification tree approach: a case study using yellowfin tuna (*Thunnus albacares*). Mar. Biol. 159:87–100.

Lavin, M. F., P. C. Fiedler, J. A. Amador, L. T. Ballance, J. Färber-Lorda, and A. M. Mestas-Nuñez.
2006. A review of eastern tropical Pacific oceanography: summary. Prog. Oceanogr. 69:391–398.

Le Borgne, R., and M. Rodier.
1997. Net zooplankton and the biological pump: a comparison between the oligotrophic and mesotrophic equatorial Pacific. Deep Sea Res. (II Top. Stud. Oceanogr.) 44:2003–2023.

Longhurst, A. R., and W. G. Harrison.
1988. Vertical nitrogen flux from the oceanic photic zone by diel migrating zooplankton and nekton. Deep-Sea Res., A. 35:881–889.

Maas, A. E., S. L. Frazar, D. M. Outram, B. A. Seibel, and K. F. Wishner.
2014. Fine-scale vertical distribution of macroplankton and micronekton in the Eastern Tropical North Pacific in

association with an oxygen minimum zone. J. Plankton Res. 36:1557–1575.

McGowan, J. A., and P. W. Walker.
1985. Dominance and diversity maintenance in an oceanic ecosystem. Ecol. Monogr. 55:103–118.

Moteki, M., M. Arai, K. Tsuchiya, and H. Okamoto.
2001. Composition of piscine prey in the diet of large pelagic fish in the eastern tropical Pacific Ocean. Fish. Sci. 67:1063–1074.

Naito, Y., D. P. Costa, T. Adachi, P. W. Robinson, M. Fowler, and A. Takahashi.
2013. Unravelling the mysteries of a mesopelagic diet: a large apex predator specializes on small prey. Funct. Ecol. 27:710–717.

Ohman, M. D., and P. E. Smith.
1995. A comparison of zooplankton sampling methods in the CalCOFI time series. CalCOFI Rep. 36:153–158.

Olson, R. J., L. M. Duffy, P. M. Kuhnert, F. Galván-Magaña, N. Bocanegra-Castillo, V. Alatorre-Ramírez.
2014. Decadal diet shift in yellowfin tuna *Thunnus albacares* suggests broad-scale food web changes in the eastern tropical Pacific Ocean. Mar. Ecol. Prog. Ser. 497:157–178.

Pakhomov, E. A., R. Perissinotto, and C. D. McQuaid.
1996. Prey composition and daily rations of myctophid fishes in the Southern Ocean. Mar. Ecol. Prog. Ser. 134:1–14.

Pepin, P.
2013. Distribution and feeding of *Benthosema glaciale* in the western Labrador Sea: fish–zooplankton interaction and the consequence to calanoid copepod populations. Deep Sea Res. (I Oceanogr. Res. Pap.) 75:119–134.

Perrin, W. F., R. R. Warner, C. H. Fiscus, and D. B. Holts.
1973. Stomach contents of porpoise, *Stenella* spp., and yellowfin tuna, *Thunnus albacares*, in mixed-species aggregations. Fish. Bull. 71:1077–1092.

Pusch, C., S. Schnack-Schiel, E. Mizdalski, and H. von Westernhagen.
2004. Feeding ecology of three myctophid species at the Great Meteor Seamount (North-east Atlantic). Arch. Fish. Mar. Res. 51:251–271.

R Core Team.
2014. R: a language and environment for statistical computing. R Foundation for Statistical Computing, Vienna, Austria. [Available at website. org, accessed July 2014.]

Rissik, D., and I. M. Suthers.
2000. Enhanced feeding by pelagic juvenile myctophid fishes within a region of island-induced flow disturbance in the Coral Sea. Mar. Ecol. Prog. Ser. 203:263–273.

Saunders, R., M. A. Collins, P. Ward, G. Stowasser, R. Shreeve, and G. A. Tarling.
2015. Distribution, population structure and trophodynamics of Southern Ocean *Gymnoscopelus* (Myctophidae) in the Scotia Sea. Polar Biol. 38:287–308.

Schoener, T. W.
1974. The compression hypothesis and temporal resource partitioning. Proc. Natl. Acad. Sci. 71:4169–4172.

Scott, M. D., S. J. Chivers, R. J. Olson, P. C. Fiedler, and K. Holland.
2012. Pelagic predator associations: tuna and dolphins in the eastern tropical Pacific Ocean. Mar. Ecol. Prog. Ser. 458:283–302.

Shchetinnikov, A. S.
1992. Feeding spectrum of squid *Sthenoteuthis oulaniensis* (Oegopsida) in the eastern Pacific. J. Mar. Biol. Ass. U. K. 72:849–860.

Shreeve, R. S., M. A. Collins, G. A. Tarling, C. E. Main, P. Ward, and N. M. Johnston.
2009. Feeding ecology of myctophid fishes in the northern Scotia Sea. Mar. Ecol. Prog. Ser. 386:221–236.

Simard, Y., R. de Ladurantaye, and J. C. Therriault.
1986. Aggregation of euphausiids along a coastal shelf in an upwelling environment. Mar. Ecol. Prog. Ser. 32:203–215.

Smith, P. E., and S. L. Richardson.
1977. Standard techniques for pelagic fish egg and larva surveys. FAO Fish. Tech. Pap. 175, 108 p.

Spear, L. B., D. G. Ainley, and W. A. Walker.
2007. Foraging dynamics of seabirds in the eastern tropical Pacific Ocean. Stud. Avian Biol. 35:1–99.

Suntsov, A. V., and R. D. Brodeur.
2008. Trophic ecology of three dominant myctophid species in the northern California Current region. Mar. Ecol. Prog. Ser. 373:81–96.

Therneau, T., B. Atkinson, and B. Ripley.
2013. rpart: recursive partitioning and regression trees. R package vers. 4.1-3. [Available at website, accessed October 2013.]

Turner, J. T.
2004. The importance of small planktonic copepods and their roles in pelagic marine food webs. Zool. Stud. 43:255–266.

Tyler, H. R., Jr., and W. G. Pearcy.
1975. The feeding habits of three species of lanternfishes (family myctophidae) off oregon, USA. Mar. Biol. 32:7–11.

Van Noord, J. E.
2013. Diet of five species of the family Myctophidae caught off the Mariana Islands. Ichthyol. Res. 60:89–92.

Van Noord, J. E., E. A. Lewallen, and R. L. Pitman.
2013a. Flyingfish feeding ecology in the eastern Pacific: prey partitioning within a speciose epipelagic community. J. Fish Biol. 83:326–342.

Van Noord, J. E., R. J. Olson, J. V. Redfern, and R. S. Kaufmann.
2013b. Diet and prey selectivity in three surface-migrating myctophids in the eastern tropical Pacific. Ichthyol. Res. 60:287–290.

Watanabe, H., K. Kawaguchi, and A. Hayashi.
2002. Feeding habits of juvenile surface-migratory myctophid fishes (family Myctophidae) in the Kuroshio region of the western North Pacific. Mar. Ecol. Prog. Ser. 236:263–272.

Watanabe, H., M. Moku, K. Kawaguchi, K. Ishimaru, and A. Ohno.
1999. Diel vertical migration of myctophid fishes (Family Myctophidae) in the transitional waters of the western North Pacific. Fish. Oceanogr. 8:115–127.

Wisner, R. L.
1974. The taxonomy and distribution of lanternfishes (family Myctophidae) of the eastern Pacific ocean. Navy Ocean Research and Development Activity (NORDA), Rep. 3, 229 p. U.S. Govt. Print. Off., Washington, D.C.

NOAA
National Marine
Fisheries Service

Fishery Bulletin
established 1881

Spencer F. Baird
First U.S. Commissioner
of Fisheries and founder
of *Fishery Bulletin*

Evaluation of nucleic acids and plasma IGF1 levels for estimating short-term responses of postsmolt Atlantic salmon (*Salmo salar*) to food availability

Elaine M. Caldarone[1]
Sharon A. MacLean[1]
Brian R. Beckman (contact author)[2]

Email address for contact author: brian.beckman@noaa.gov

[1] Narragansett Laboratory
Northeast Fisheries Science Center
National Marine Fisheries Service, NOAA
28 Tarzwell Drive
Narragansett, Rhode Island 02882

[2] Environmental and Fisheries Sciences Division
Northwest Fisheries Science Center
National Marine Fisheries Service, NOAA
2725 Montlake Boulevard East
Seattle, Washington 98112

Abstract—We evaluated 4 potential indices obtained by nonlethal sampling for use in determining nutritional state and short-term growth rate in postsmolt Atlantic salmon (*Salmo salar*): the ratio of RNA to DNA, both RNA and DNA normalized to protein, and plasma levels of insulin-like growth factor 1 (IGF1). Fish reared in the laboratory for 27 days were fed, fasted, or refed. Short-term growth rates (7 to 23 day intervals) were calculated on a wet-weight basis. RNA/DNA values were highly correlated to growth rates, responded rapidly to changes in food availability and were the best able to consistently distinguish between the fasted and fed treatments. RNA/protein values were also well correlated with growth rate; however, within any one sampling day, feeding groups could not be differentiated with this index. DNA/protein increased during fasting but was neither strongly correlated with growth rate nor an accurate discriminator of nutritional state. IGF1 values were positively correlated with growth rates and responded rapidly with refeeding but changed little during the 3 weeks of fasting—a result that may have been influenced by sampling serially. We propose that RNA/DNA is a useful nonlethal technique for estimating recent growth rates and for identifying the nutritional condition of individual postsmolt Atlantic salmon exposed to short-term changes in food availability.

Manuscript submitted 15 May 2015.
Manuscript accepted 31 March 2016.
Fish. Bull. 114:288–301 (2106).
Online publication date: 3 May 2016.
doi: 10.7755/FB.114.3.3

The ability to measure the growth rate of a fish can be a powerful tool for evaluating the survival potential of an individual. The ability to assess the nutritional state of a fish, whether the animal is feeding or fasting and for how long the fish has been in that state (hours to days to weeks) is also highly desirable information because variation in nutritive state leads to variation in growth rate. Currently, there are a limited number of nonlethal techniques available for estimating growth rates or nutritional state (or both) in field-caught juvenile fish. Longitudinal cohort analysis is a direct approach to assessing changes in size (growth); however obtaining multiple samples of the same cohort in the field can be challenging. Biochemical indices that indirectly yield estimates of growth rate or nutritional state have the advantage of providing estimates within a single sampling. This point estimate allows an investigation of the connectivity between nutritional state and environmental parameters on relevant temporal and spatial scales.

In this study we evaluated 4 potential biochemical indices of short-term growth-rate or nutritional state in postsmolt Atlantic salmon (*Salmo salar*): the ratio of RNA to DNA (RNA/DNA), both RNA and DNA on a protein basis (RNA/pro and DNA/pro, respectively) and circulating plasma insulin-like growth factor 1 (IGF1). Considerable effort has been directed toward hatchery-based restoration of Atlantic salmon to 8 rivers in Maine, where the population has been listed as endangered since 2009 under the United States Endangered Species Act (Federal Register, 2009). Restoration managers require tools to both assess whether hatchery-reared fish are thriving in the natural environment and to assess the condition of native postsmolts. Identifying a minimally invasive, nonlethal method to provide an index of growth rate or nutritional state in postsmolt Atlan-

tic salmon would allow restoration managers to evaluate the condition of field-captured fish.

Since their first application in the 1970s, RNA-based indices have been used to determine the nutritional state and growth rates of larval and juvenile fish in both the laboratory and field (Bulow, 1970; Buckley, 1979; Buckley et al., 1999; Gwak and Tanaka, 2001; Vasconcelos et al., 2009; Ciotti et al., 2010; among many other studies). Juvenile fish grow rapidly through accretion of protein, and the amount of RNA in a cell is a measure of the capacity of a cell to synthesize protein (Millward et al., 1973). MacLean et al. (2008) evaluated 4 tissues in Atlantic salmon postsmolts and determined that RNA/DNA values from muscle tissue were those that were the most highly correlated with growth rate, and that muscle tissue samples could be obtained by nonlethal means with a biopsy punch. DNA/protein has been shown to increase during fasting (Bulow, 1970; Mathers et al., 1993; Fukuda et al., 2001) and thus could provide useful information about the nutritional state of a fish. Circulating plasma insulin-like growth factor 1 (IGF1) is a polypeptide that is involved in a number of regulatory processes, including differentiation and proliferation of cells. The preponderance of evidence indicates a significant relation between growth rates and the plasma level of IGF1 in fish within some constraints (see review by Beckman, 2011). Pierce et al. (2001) have shown that blood can be drawn by nonlethal means to obtain samples for this index. In most studies of juvenile fish, sampling has been too infrequent to establish the response time of nucleic-acid–based indices or of IGF1 to food variability. Because our field recaptures of hatchery-reared postsmolts occur 2 to 3 weeks after their release, we designed our experiment to focus on nutritive responses to short-term changes in food availability rather than to longer term changes. Results presented here are part of a larger laboratory study designed to evaluate a variety of nonlethal techniques for detecting short-term changes in the nutritional status of postsmolt Atlantic salmon. Results regarding proximate body composition, Fulton's K, and bioelectrical impedance analysis (BIA) of the same individuals reported in the present study can be found in Caldarone et al. (2012).

Materials and methods

Smolts used in this study were progeny of field-caught Atlantic salmon from the Penobscot River, Maine. They had been spawned at Craig Brook National Fish Hatchery, East Orland, Maine, and reared at the Green Lake National Fish Hatchery, Ellsworth, Maine, for 13–15 months. In 2008, 80 randomly selected smolts (52–113 g, 16–21 cm) were anesthetized in buffered tricaine methane sulfonate (MS-222, 150 mg/L) and were implanted intramuscularly with a passive integrated transponder tag (PIT tag, Biomark, Boise, ID[1]) to permit identification of individuals. The smolts were then returned to the hatchery tank to allow time for full recovery, resumption of feeding, and removal of any tagging-related mortalities (5 fish). Twenty-five days later the fish were transported to the University of Rhode Island's Blount Aquarium facility in Narragansett, Rhode Island, where they were randomly placed in two aerated, flow-through tanks (360-L capacity) initially filled with freshwater trucked from the hatchery. Over a period of 5 to 6 hours, freshwater was gradually replaced with sand-filtered seawater (10°C, 30 ppt). During the next 3 weeks, while the fish were recovering from the transfer and acclimating to seawater, the water temperature was gradually raised to 12°C. During this period fish were fed to satiation twice per day with a commercial feed (Corey Optimum Hatchery Feed for Salmonids, Corey Nutrition Co., Fredericton, NB, Canada), supplemented with freeze-dried krill (*Euphausia pacifica*, Aquatic Eco-Systems, Inc., Apopka, FL). Twenty-five days after the initial transfer to seawater, when the now postsmolts appeared to be acclimated and feeding well, the experiment commenced (day 0).

Throughout the experiment, water temperature in each flow-through tank was recorded hourly with an HOBO® data logger (Onset Computer Corp., Bourne, MA), and ammonia levels and salinity were tested weekly. Water temperatures averaged 12.0°C, standard deviation (SD)=0.2; salinity averaged 31 ppt, SD=1; and the photoperiod was 15 hours of light to 9 hours of dark. Part (two-thirds) of each tank surface was covered with black plastic to provide a low-light refuge, and the remaining third was exposed to overhead fluorescent lighting that was covered with red plastic to better mimic natural light.

Feeding treatments and sampling schedule

Five fish were randomly selected on day 0 from the acclimation tanks, sacrificed, and sampled to provide baseline biochemical data. The remaining 70 postsmolts were subdivided into 3 feeding treatments (tanks): fed, fasted, and fasted then refed. The purpose of the different feeding regimens was to produce fish growing at a range of rates, not to test the effect of ration on growth rate. By measuring and sampling tagged fish we were able to assess the relation of the biochemical indices to growth rate on an individual basis.

The fed treatment (n=24) was fed ad libitum, the fasted treatment (n=24) received no food, and the refed treatment (n=22) received no food for 11 days followed by feeding for 16 days. Before being placed in 360-L flow-through treatment tanks on day 0, all individuals were anesthetized with buffered MS-222 (150 mg/L) in chilled (12°C) seawater, blotted dry, measured for initial weight (wet weight, WW_{init}, nearest 0.1 g) and for fork length (FL, nearest 0.1 cm), examined for any gross external abnormalities, and their PIT tag number

[1] Mention of trade names or commercial companies is for identification purposes only and does not imply endorsement by the National Marine Fisheries Service, NOAA.

Table 1

Sampling schedule for postsmolt Atlantic salmon (*Salmo salar*) reared in the laboratory at 12°C under 3 feeding regimens (fed; fasted; fasted then refed) in order to determine the response time to varyhing food availability. Condition indices obtained by nonlethal sampling techniques (RNA/DNA; RNA/protein; DNA/protein; IGF1) and wet-weight–based growth rate were determined for each fish. The refed group was fasted for 11 days and then fed for 16 days. Numbers listed are number of fish sampled.

	Sampling day and feeding regimen											
		Day 0			Day 3			Day 7			Day 11		
	Baseline	Fed	Fasted	Refed	Fed	Fasted	Refed	Fed	Fasted	Refed	Fed	Fasted	Refed
Length, weight	5	24	24	22	4	4	0	4	4	0	4	4	22
Muscle plugs for nucleic acid and protein	5	0	24	0	4	4	0	4	4	0	4	4	22
Blood sample for IGF1 measurement	5	0	24	0	4	4	0	4	4	0	4	4	22
		Day 15			Day 19			Day 23			Day 27		
		Fed	Fasted	Refed	Fed	Fasted	Refed	Fed	Fasted	Refed	Fed	Fasted	Refed
Length, weight		4	4	5	4	4	5	4	4	5	0	0	7
Muscle plugs for nucleic acid and protein		4	4	5	4	4	5	4	4	5	0	0	7
Blood sample for IGF1 measurement		4	4	5	4	4	5	4	4	5	0	0	7

was recorded. Additionally, 2 muscle plugs and a blood sample were obtained from fish assigned to the fasting treatment in order to track individual response times to fasting. Fish in the group of refed postsmolts were again weighed and measured and then sampled on day 11 to obtain individual baseline fasting values before fish were refed. Total time needed for the biochemical sampling was less than 1 minute per fish. From day 3 onward, 5 fish from the fasted and fed treatments were sampled and sacrificed every 4 days for 20 days. From day 15 onward, 5 fish from the refed treatment were sampled and sacrificed every 4 days until day 27 when 7 fish were sacrificed (Table 1). Final wet weight, FL, 2 muscle plugs for biochemical analysis, and a blood sample for IGF1 determination were obtained from all sacrificed fish. All fish were also sampled for bioelectrical impedance analysis (BIA) indices and proximate body composition (see Caldarone et al., 2012). All aspects of this experiment were conducted in accordance with guidelines established by the Institutional Animal Care and Use Committee (IACUC) at the University of Rhode Island

Sampling protocol and biochemical analyses

IGF1 Blood samples (0.3 mL) for IGF1 analysis were obtained from the caudal vein using a sterile heparinized syringe (23-ga×25-mm needle). Samples were immediately transferred to a microfuge vial, stored on wet ice for < 0.5 hour, and centrifuged at 5000×g for 5 minutes. Plasma was removed by pipet, transferred to a 1.5 mL microfuge vial and stored at –80°C until further analysis. Samples were analyzed at the National Marine Fisheries Service, Northwest Fisheries Science Center by using an immunoassay to measure the concentration of IGF1. Briefly, IGF1 was isolated from plasma by acid-ethanol extraction, and measured by TRF immunoassay by using a modification of the methods described by Small and Peterson (2005). Each sample was analyzed in duplicate, and samples with low (<30%) or high (> 85%) binding, as well as those with a coefficient of variation exceeding 10%, were reanalyzed or excluded. IGF1 values are reported as ng/mL plasma.

Nucleic acids and protein A 2-mm diameter biopsy punch (MacLean et al., 2008) was used to remove 2 muscle samples for analysis of nucleic acids and protein. Samples were taken from the epaxial muscle between the lateral line and dorsal fin. Each muscle plug was immediately placed in a microfuge vial, stored on wet ice for <0.5 hour and then transferred to –80°C until analysis. Nucleic acid levels were measured by using a 2-enzyme (RNase, DNase) ethidium bromide fluorometric microplate method. On the day of analysis, each muscle plug was transferred to a cold glass slide and any fat layer, skin, or blood was removed. The top 2 mm of the muscle plug was transferred to

a microfuge vial containing 150 µL 1% N-lauroylsarcosine. The vial was placed in an ice slurry and the sample was sonicated for three 5-second pulses followed by 45 minutes of vortexing at room temperature. From that point onward, we followed the protocol of Caldarone et al.[2] for nucleic acid analysis. Results from duplicate plugs were averaged. The ratio of the slope of the DNA standards to the slope of the RNA standards was mean=2.5, SD=0.05 (n=7 microplates). This value can be used to convert the reported RNA/DNA data for direct comparison with other published studies (Caldarone et al., 2006). The remaining extract was stored frozen and later analyzed for protein content by using a bicinchoninic-acid–based assay adapted for a microplate format (Caldarone, 2005). Nucleic acids (µg) are expressed as a RNA to DNA ratio (RNA/DNA; µg/µg), RNA to protein ratio (RNA/pro; µg/mg) and DNA to protein ratio (DNA/pro; µg/mg).

Calculations of growth rates Individual instantaneous weight-based growth rates (per d) were calculated with the following formula:

$$growth\ rate\ (G) = (\ln WW_{t2} - \ln WW_{t1})/(t_2 - t_1) \quad \text{(Ricker, 1979)}, \qquad (1)$$

where WW = the wet weight of an individual at time t (day).

For comparison with previously published data, growth rates were converted to specific growth rates (% per d) with the following formula:

$$SGR = 100(e^G - 1). \qquad (2)$$

Growth rates for fish in the fed and fasted treatments were calculated from day 0 until the day the fish were sacrificed. Growth rates were calculated from day 0 until day 11 for the fasted portion of the refed treatment fish; for the fed portion of the refed treatment fish, growth rates were calculated from the first day of refeeding (day 11) until the day the fish were sacrificed. Because there is inherent variability in measuring the wet weight of fish, coupled with small changes in weight over short time intervals, growth rates from time intervals <4 days were not included in any of the statistical analyses.

Data analysis To examine the effect of the feeding treatment and sampling day on growth rate, RNA/DNA, RNA/pro, DNA/pro and IGF1, a 2-way multivariate analysis of covariance (MANCOVA) for unbalanced design was used with WW_{init} as the covariate. When interactions were significant, feeding treatment was nested in day, and follow-up comparisons were examined by using Tukey's HSD multiple range test. Linear growth rate models with all combinations of the 4 biochemical variables plus WW_{init} were constructed. Akaike's information criterion for small sample sizes (AICc; Wagenmakers and Farrell, 2004) was used to select the best candidate model from the 31 models tested. Because of high collinearity of RNA/DNA with the other 3 biochemical indices, all combinations of models without the RNA/DNA term were also investigated. To examine the response of the 4 biochemical indices and growth rate in individual fish to food withdrawal or introduction, paired initial and final data from individual fish from both the starved and refed fish were analyzed by using a repeated measure t-test.

Within each feeding group, a Dunnett 2-tailed t-test with WW_{init} as a covariate was used to detect changes in growth rate and the 4 biochemical variables compared with those in a control. Day 0 values were specified as the control for the biochemical variables for both fasted and fed treatments. The average growth rate of all fish from the time they were tagged until day 0 (50 days) was used as the control growth-rate value with the understanding that growth rates during this time would have been less than optimal. For the refed treatment, values for day 11 (day they were refed) were used as the control for all variables. An ANCOVA was used to test whether the slope of the relation of growth rate to the measured biochemical indices was significantly different between the fed and refed groups. All statistical analyses were carried out with SAS software, vers. 9.3 (Statistical Analysis Software Inst., Inc., Cary, NC) with a significance level set at $P \leq 0.05$.

Results

At the start of the experiment (day 0) ~78% of the fish exhibited frayed and ~12% exhibited eroded dorsal and pectoral fins. The frequency and severity of these conditions did not change throughout the experiment and there were no mortalities during the study. All fish appeared to be immature and sex was not a significant factor in any of the statistical analyses. On day 0, WW_{init} ranged from 43 to 132 g and FL from 18 to 23 cm. Initial size distributions (WW_{init}) between feeding treatments were not significantly different (fed mean=76 g, SD=12; fasted mean=75 g, SD=13; fasted then refed mean=80 g, SD=4).

Weight-based growth rates of the fish responded quickly to changes in food availability. Fasted fish lost weight beginning on day 7 and by day 11 their growth rates were statistically significantly less than the continually fed fish (Fig. 1A). Negative growth rates of the fasted fish remained constant throughout the experiment (Dunnett, P=0.747), whereas fed fish growth rates increased in relation to day 0 rates (Dunnett, P<0.0001). On day 19, fed fish had faster growth rates than refed fish, whereas the relation was reversed on day 23. Refed fish grew significantly faster than fasted fish beginning 4 days after refeeding (day 15). During the experiment we noted that the feeding intensity of the salmon visibly decreased when the total num-

[2] Caldarone, E. M., M. Wagner. J. St. Onge-Burns, and L. J. Buckley. 2001. Protocol and guide for estimating nucleic acids in larval fish using a fluorescence microplate reader. Northeast Fish. Sci. Cent. Ref. Doc. 01-11, 22 p. [Available at website]

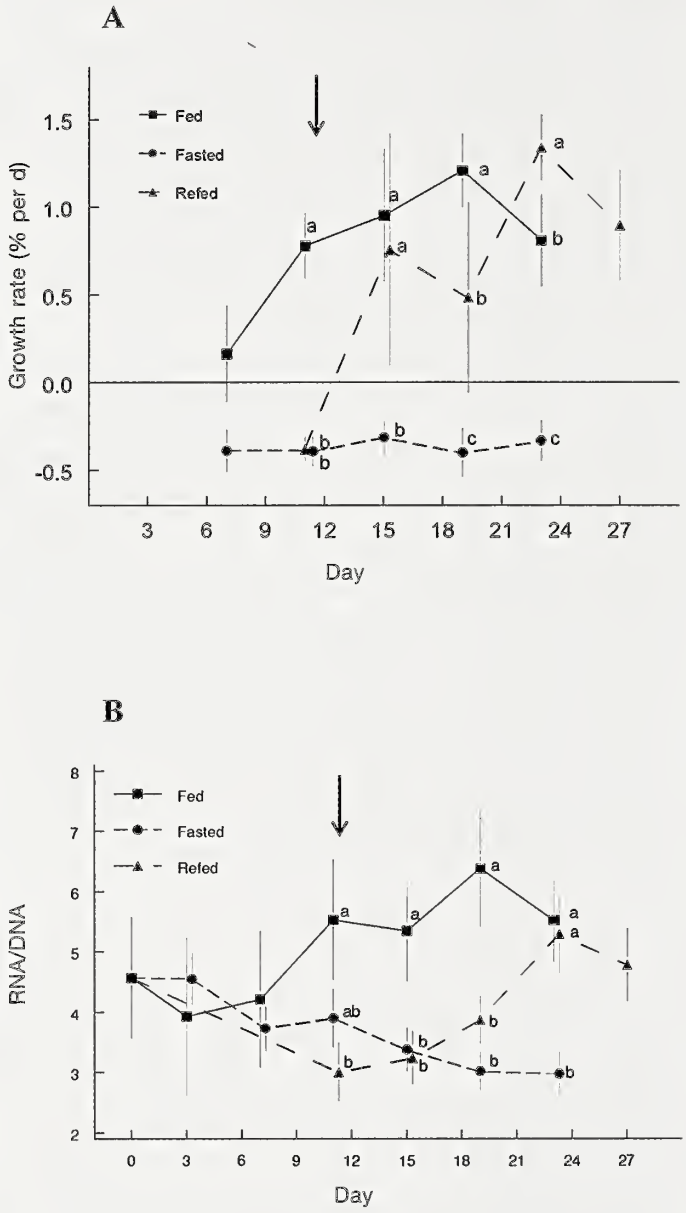

Figure 1

(**A**) Specific growth rates (% wet weight per d); and (**B**) RNA/DNA values of postsmolt Atlantic salmon (*Salmo salar*) reared in the laboratory at 12°C. Fish were either fed ad libitum, fasted, or refed (fed after 11 days of fasting). Values are mean values (±standard deviation [SD]) for each sampling day. Growth rates for fish in the fed and fasted treatments were calculated from day 0 until the day they were sacrificed. Growth rates for the refed treatment were calculated from the first day of refeeding (day 11) until the day fish were sacrificed. Within a sampling day, food treatments showing a common superscript, or without superscripts, do not differ significantly (Tukey's HSD multiple range tests). Where error bars would overlap, data are offset to facilitate viewing. The arrow indicates the day when food was introduced to the refed group. For fed and fasted fish, n=4 for each sampling day. For refed fish, n=22 for day 11, n=5 for days 15, 19, and 23, and n=7 for day 27.

ber of fish in the tanks fell below 8 individuals because of sampling. This observation was confirmed by the decrease in average growth rates for fish sampled on the last day of both the fed (day 23) and refed (day 27) treatments (Fig. 1A).

After 11 days, RNA/DNA values were significantly greater in fed fish than in the fasted portion of the refed fish (Fig. 1B), and from day 15 onward, significantly greater than values for fish in the fasted group. Twelve days after refeeding, RNA/DNA values of the refed group were greater than the fasted fish and equal to the continually fed fish (day 23, Fig. 1B). Mean RNA/DNA values in fed and refed fish increased in relation to their mean start values (Dunnett, P=0.011, P<0.0001 respectively), whereas mean RNA/DNA values for fasted fish decreased beginning 15 days after food was withheld (Dunnett, P=0.003). Repeated measurements from individuals in the fasted group exhibited an overall significant decrease in RNA/DNA from their start values (Student's paired t test P<0.0001, Fig. 2A). Repeated measurements of refed fish exhibited an overall significant increase from their individual start values (Student's paired t-test P<0.0001, Fig. 2B). RNA/DNA values were highly positively correlated with growth rates in the fed group, refed group, and the all-data-combined group, but not in the fasted group (Table 2).

Beginning on day 11, RNA/pro values were generally greater in the fed fish than in the fish in the fasted treatment (Fig. 3A). In fed fish, mean RNA/pro values did not change from mean initial values (Dunnett P=0.391), whereas fasted fish showed modest decreases with a significant Dunnett value (P=0.009), primarily driven by 1 fish on day 19 (Fig. 3A). Beginning 8 days after refeeding (day 19), mean RNA/pro values of refed fish increased from the mean start value (Dunnett P<0.0001). The same pattern was seen in paired data from individuals; repeated measurements from fasted fish exhibited an overall significant decrease from their start values (Student's paired t-test P=0.002), whereas values of refed fish increased (Student's paired t-test P<0.0001) (plots not shown). RNA/pro values were positively correlated with growth rates in the fed group, refed group, and the all-data-combined group, but not in the fasted group (Table 2).

The DNA/pro ratio of fasted and refed fish was higher (smaller cells) than in fed fish, and the main effect of feeding treatment on DNA/pro was statistically significant (Fig. 3B); but, because of high daily variability, coupled with a small sample size, most Tukey-Kramer post-hoc comparisons of feeding treatment within a sam-

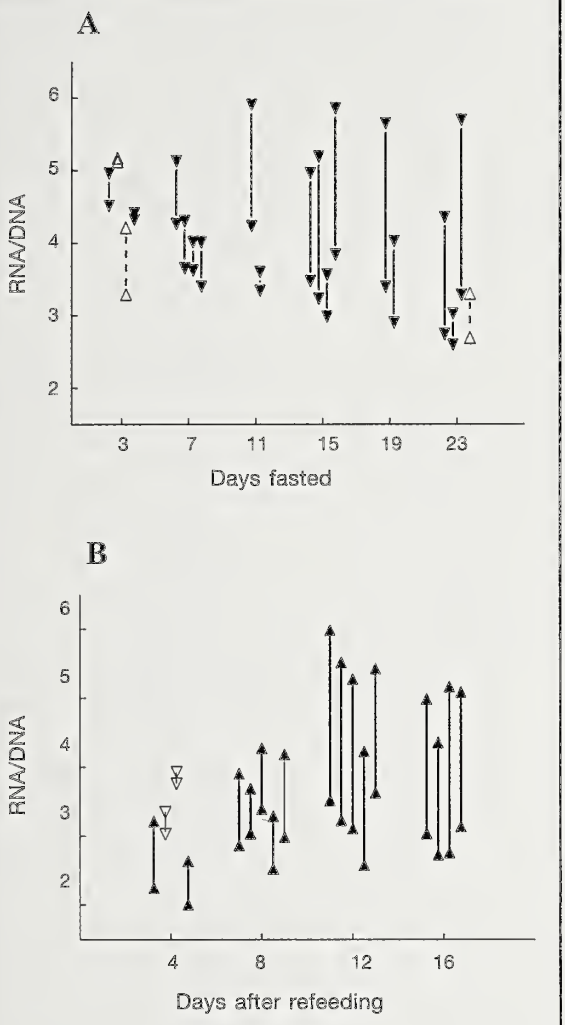

Figure 2

Each arrow represents changes in RNA/DNA values of individual laboratory-reared postsmolt Atlantic salmon (*Salmo salar*) that were either (**A**) fasted or (**B**) refed (fed after 11 days of fasting). Direction of the triangle is the direction of change in the values from (**A**) day 0 start values (when fish were fed) through the number of days (23 d) that fish were fasted; and (**B**) day 11 values (start of fasting) through number of days (16 days) that fish were refed after fasting. The open and closed triangles differentiate between the two different directions of change.

ple day were not statistically significant. Within each food treatment, DNA/pro did not change from mean initial values (Dunnett P=0.295, 0.090, 0.071 fasted, fed, refed, respectively). However, repeated measurements of individuals indicated that DNA/pro in individual fish increased during fasting (Student's repeated measure t-test P=0.033) (plot not shown). DNA/pro values were not correlated with growth rates in the 3 individual food treatment groups but had a significant, although

Table 2

Pearson product-moment correlations (r) between the instantaneous weight-based growth rate (per d) of postsmolt Atlantic salmon (*Salmo salar*) and the ratio of RNA:DNA (RNA/DNA, µg/µg), RNA and DNA on a protein basis (RNA/pro, DNA/pro, respectively, µg/mg), and circulating plasma insulin-like growth factor 1 (IGF1, ng/mL). Fish were either fed or fasted for 23 days, or refed (fed for 16 days after 11 days of fasting). For each feeding treatment, boldface type highlights the highest significant correlation with growth rate. *P<0.05, **P<0.005, ***P<0.0001. n=number of fish sampled.

Variable	Fed	Fasted	Refed	All data
n	19	19	17	55
RNA/DNA	**0.882*****	–0.295	**0.853*****	**0.832*****
RNA/pro	0.765***	–0.190	0.666**	0.727***
DNA/pro	–0.354	0.090	–0.238	–0.507***
IGF1	0.502*	–0.403	0.543*	0.661***

low, negative correlation when all three groups were combined (Table 2).

Within a sample day, IGF1 values between feeding treatments were not statistically significantly different (Fig. 3C). As with DNA/protein measurements, high variance (SD), coupled with a small sample size, yielded very low statistical power to detect differences between treatments. Beginning on day 15 and continuing until the conclusion of the experiment, mean IGF1 values in fed fish were significantly greater than day-0 mean values (Dunnett P<0.0001). Fasted fish showed no change in IGF1 with time, either on a daily mean (Dunnett P=0.722) or on an individual basis (Student's repeated measure t-test P=0.065, Fig. 4A). Mean IGF1 values of refed fish increased 12 days after food was introduced (day 23, Dunnett P<0.0001), and repeated measurements of individuals indicated that final IGF1 values in refed fish were greater than their start values (Student's repeated measure t-test P=0.0001, Fig. 4B). IGF1 values were positively and significantly correlated with growth rates in the fed group, refed group, and the all-data-combined group (Fig. 5, Table 2).

A plot of growth rate vs. RNA/DNA by food treatment revealed a difference in the relation of RNA/DNA to growth rate between the fed and refed groups (Fig. 6). ANCOVA results confirmed that the slopes of the regression lines of the two feeding treatments were the same but the intercept of the refed data was significantly greater. Slopes and intercepts of the regressions between the other 3 biochemical measures and growth rate did not differ between the fed and refed groups. Linear growth models containing all combinations of WW_{init}, RNA/pro, DNA/pro, RNA/DNA, and IGF1 were examined (31 models). On the basis of AICc values, the best candidate model for predicting growth rate in-

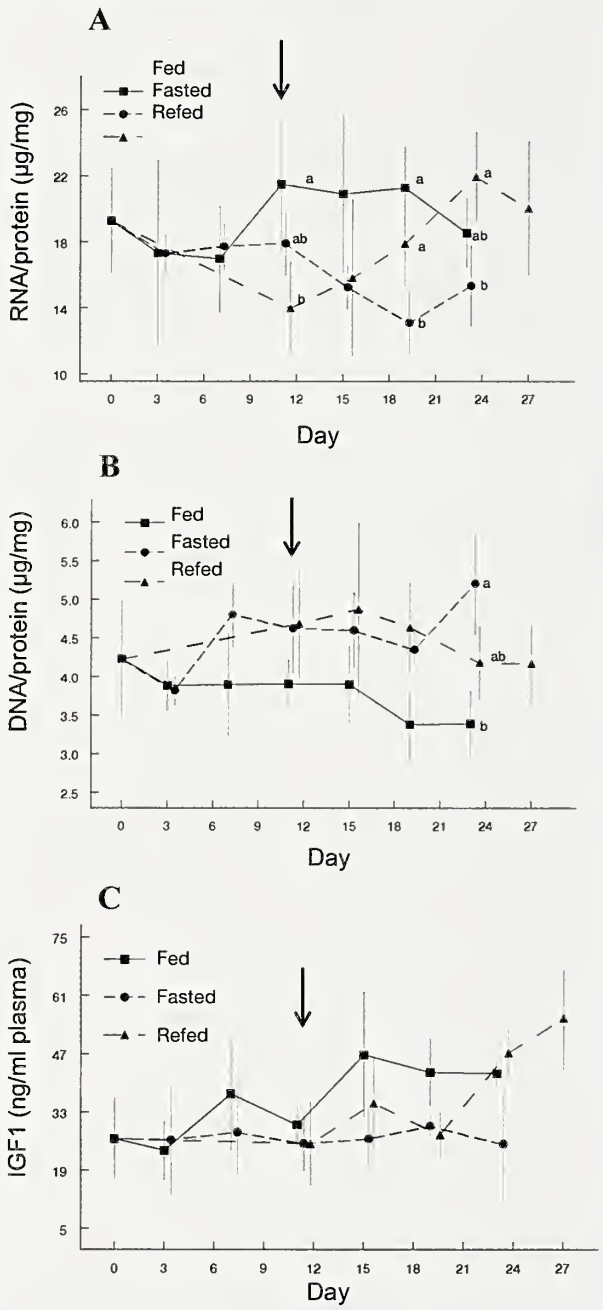

Figure 3

(**A**) RNA/protein (µg/mg); (**B**) DNA/protein (µg/mg) and (**C**) IGF1 (ng/mL plasma) values of postsmolt Atlantic salmon (*Salmo salar*) reared in the laboratory at 12°C. Values are mean values (±standard deviation [SD]) for each sampling day. Fish were either fed ad libitum, fasted, or refed (fed after 11 days of fasting). Within a sampling day, food treatments showing a common superscript, or without superscripts, do not differ significantly (Tukey's HSD multiple range tests). Where error bars would overlap, data are offset to facilitate viewing. The arrow indicates the day when food was introduced to the refed group. For fed and fasted fish, n=4 for each sampling day. For refed fish, n=22 for day 11, n=5 for days 15, 19, and 23 and n=7 for day 27.

cluded RNA/DNA and IGF1 (Table 3). Because RNA/DNA was highly correlated with the other biochemical terms, we also tested all combinations of the remaining 4 terms after eliminating RNA/DNA (15 models). The best candidate for a growth rate model from this grouping included RNA/pro, DNA/pro, and IGF1, and was essentially identical in predictive capability and mathematically equivalent to the model containing RNA/DNA and IGF1 (Table 3).

Summary

RNA/DNA ratios and recent growth rates of fed fish increased throughout the study and were highly correlated. Fed and fasted feeding treatments could be differentiated by RNA/DNA values after 11 days of fasting, and on an individual basis, significant decreases in RNA/DNA values were observed after 7 days of fasting. Growth rates and RNA/DNA values of previously fasted fish increased rapidly beginning 4 days after refeeding. The intercept from regressing growth rate on RNA/DNA was greater in refed fish than in continually fed fish, whereas the slopes were parallel. In the fasted group, the rate of weight loss remained fairly constant throughout the experiment and RNA/DNA values decreased.

In all 3 feeding treatments, RNA/pro values showed similar trends to those of RNA/DNA values; however, there was less statistical differentiation between the feeding treatments on most sampling days. Overall, fasted fish had significantly greater DNA/pro values (smaller cells) than fed fish, yet feeding treatments within a day could not be distinguished on this basis. Mean IGF1 values increased in fed fish but remained constant in fasted fish owing to inconsistent individual responses to fasting. Based on repeated measurements of individuals, IGF1 values responded rapidly (4 days) to refeeding. Owing to high daily variability, feeding treatments within a sampling day could not be distinguished with this index. A positive and significant relation was found between IGF1 and growth rate.

Of the 31 models tested, the best-fit growth rate model included RNA/DNA and IGF1 with a coefficient of determination (r^2) =0.73.

Discussion

The goal of our research and its companion study (Caldarone et al., 2012) was to identify physiological indices that could be obtained by nonlethal means and that would respond rapidly to short-term changes (4–23 days) in the nutritional state (feeding and fasting) of individual postsmolt salmon. The response time of an index allows investigators to match the index to environmental parameters on relevant temporal and spatial scales. Of the four indices we measured in this study, RNA/DNA was the most highly correlated with short-term growth rate. In sexually immature fish, an index that reflects protein production should be appro-

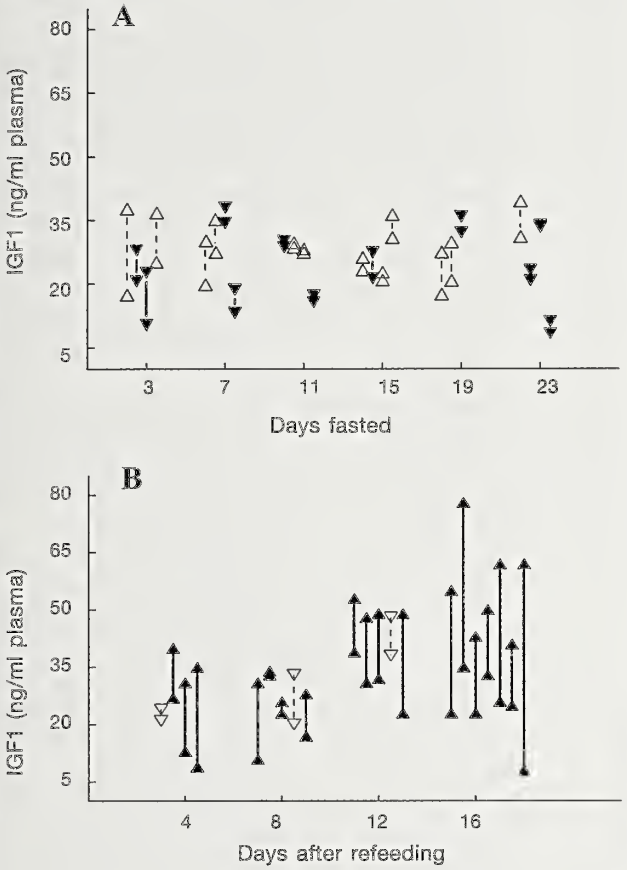

Figure 4

Each arrow represents changes in IGF1 values (ng/mL plasma) of individual laboratory-reared postsmolt Atlantic salmon (*Salmo salar*) that were either (**A**) fasted or (**B**) refed (fed after 11 days of fasting). Direction of the triangle is the direction of change in the values from (**A**) day 0 start values (when fish were fed) through the number of days (23 d) that fish were fasted; and (**B**) day 11 values (start of fasting) through number of days (16 days) that fish were refed after fasting. The open and closed triangles differentiate between the two different directions of change.

priate for estimating growth. At this stage, juvenile fish are directing their energy toward increasing their size to enable them to better escape predators and search for and capture prey (Shulman and Love, 1999). RNA based indices have consistently been shown to be well correlated with both weight-based and protein-based recent growth rates in multiple species of juvenile fish (Arndt et al., 1994; Peck et al., 2003; Stierhoff et al., 2009; Ciotti et al., 2010). RNA/DNA values of our fish responded quickly to changes in food availability. On the basis of repeated measurements of individuals, one-half of the refed fish sampled exhibited increases in RNA/DNA 4 days after food re-introduction, and RNA/DNA values in all refed fish increased by the 8th day. Other researchers have reported statistically significant increases in RNA/DNA and RNA concentration in fish within 1–4 days after being refed (Malloy and Targett, 1994; Stierhoff et al., 2009; Ciotti et al., 2010). The differing response times to refeeding is most likely linked to varying lengths of time fasted before food was re-introduced, to sizes of the fish, and to developmental stage or species. Our fish lost weight after 7 days of fasting and repeated measurements of individuals indicated that RNA/DNA values also decreased within this time frame. Decreases in RNA/DNA and RNA concentration have been observed after 1–14 days in a variety of juvenile fish (Loughna and Goldspink, 1984; Lowery and Somero, 1990; Arndt et al., 1996; Stierhoff et al., 2009; Ciotti et al., 2010). A differing response time of RNA/DNA to fasting is most likely due to temperature, species, developmental stage, and amount of fat stored (i.e., resistance to fasting). For example, Arndt et al.'s (1996) Atlantic salmon fry were much smaller than our postsmolts, averaged a weight loss rate 10× faster (–4.3% vs. –0.36%), and their RNA/DNA values decreased in approximately 1/2 the time compared with that of our postsmolts. But in all instances, response time of RNA/DNA to fasting has been observed over a time period of days to two weeks. This relatively rapid response of RNA/DNA values to short-term changes in food availability would allow researchers to investigate linkages between environmental variables and nutritional status of postsmolt Atlantic salmon on ecologically relevant scales.

The rate of protein accumulation is the difference between the rate of degradation and the rate of protein synthesis, and the rate of protein synthesis is dependent not only on RNA concentration but also its activity (rate of translation) and efficiency, among other factors (see review by Fraser and Rogers, 2007). Our fasted fish lost weight at a fairly constant rate throughout the experiment; however, a wide range of RNA/DNA values (4 to 2.5, Fig. 6) were associated with this negative growth rate and there was a noticeable trend toward lesser values as fasting days increased. These results indicate that, at least initially, the observed weight loss was either due to protein degradation rates increasing or translation rates decreasing (or both) before RNA concentrations decreased. An initial decrease in translation rates preceding a decrease in ribosomal number has been observed in fasting fish (Loughna and Goldspink, 1984; Lowery and Somero, 1990). During a previous study of Atlantic salmon postsmolt (MacLean et al., 2008), we observed a similar range of RNA/DNA values (4 to 2) associated with negative growth rates (Fig. 7). Because both studies were conducted at comparable temperatures and nucleic acids were analyzed with identical methodologies, RNA/DNA values from the two studies can be combined. On the basis of the data from both studies, we propose an RNA/DNA value of 3.0 as a conservative cutoff for distinguishing between positive and negative growth rates in juvenile

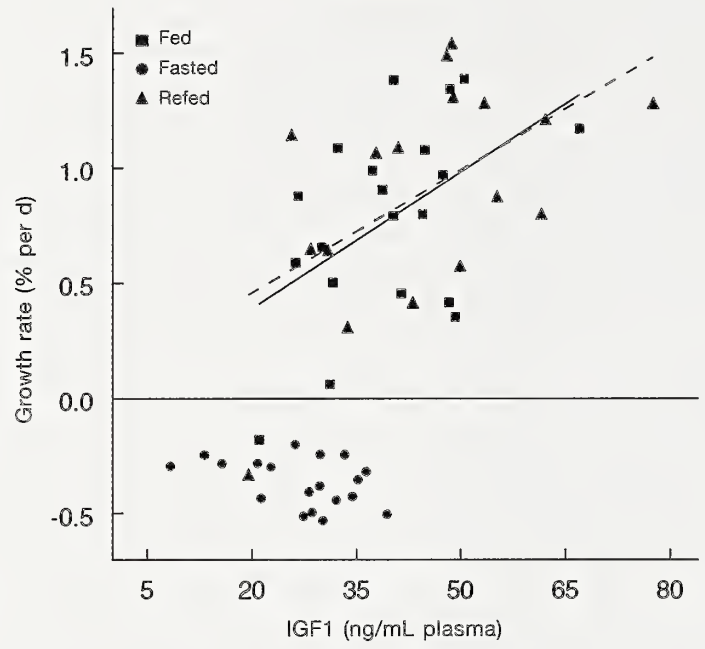

Figure 5

Growth rate (% wet weight per d) versus IGF1 for postsmolt Atlantic salmon (*Salmo salar*) reared in the laboratory at 12°C and sampled throughout a 27-day period. Fish were fed ad libitum, fasted, or refed (fed after 11 days of fasting). Regression lines represent fed (—) and refed (- -) fish.

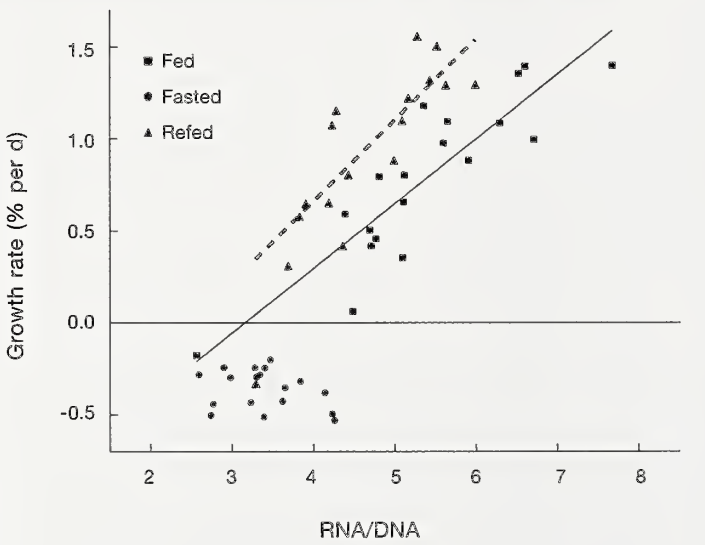

Figure 6

Specific growth rate (% wet weight per d) versus RNA/DNA for postsmolt Atlantic salmon (*Salmo salar*) reared in the laboratory at 12°C and sampled throughout a 27-day period. Fish were fed ad libitum, fasted, or refed (fed after 11 days of fasting). Regression lines represent fed (—) and refed (- -) fish.

Atlantic salmon residing at temperatures near 12°C.

Changes in RNA translation rates also may have influenced the relation of RNA/DNA to growth rate in the refed fish. Refed fish accumulated more protein per unit of RNA than their continually fed counterparts as evidenced by the significantly greater regression intercept (Fig. 6). This increase in protein accumulation could be due to an increase in translation rate or to a decrease in protein degradation rate (or to both). Researchers who have observed an increase in protein accumulation per unit of RNA have attributed it to a translation increase (McMillan and Houlihan, 1988, 1989; Miglavs and Jobling, 1989) although direct published evidence for choosing between the two pathways is scarce. Because traditional estimates of nucleic-acid–based growth-rates do not include a translation rate estimate, field estimates of RNA/DNA–based growth rates will not be exact. Nonetheless, by combining our refed with the fed and fasted data sets we obtained a significant regression between RNA/DNA and growth rate (r^2=0.692, P<0.0001) that can be used to coarsely estimate field growth rates at temperatures near 12°C. Because temperature affects protein degradation and translation rates (Buckley et al., 1999; McCarthy et al., 1999; Ciotti et al., 2010), a model incorporating an interaction term of temperature with RNA/DNA would need to be constructed before growth rates at different temperatures could be estimated.

RNA/pro In our study, RNA/pro values were less correlated with growth rate than the RNA/DNA values, although the relation of both indices to growth rate was similar, i.e., there was a high correlation with positive growth rates but a range of values associated with a constant negative growth rate. Unlike RNA/DNA, RNA/pro from both the fed and refed groups had the same relation to positive growth rates which could be advantageous for estimating field growth rates where the past feeding history of the animal is unknown. Repeated measurements of individuals indicated that RNA/pro responded quickly to food withdrawal (7 days) and reintroduction (4 days), but within any one-day values were variable, resulting in sampling days where the feeding groups could not be differentiated with this index. The positive and negative response of growth rate, RNA/DNA, and RNA/pro in individual fish to the positive and negative changes in food availability, respectively, and the high correlation

Table 3

Coefficients and Akaike's second-order information criterion for small sample sizes (AICc) for the top candidate regression models for growth rate of postsmolt Atlantic salmon (*Salmo salar*) reared at 12°C under 3 feeding regimens in order to generate a range of nutritional condition and growth rates. RNA/DNA (µg/µg); IGF1=circulating plasma insulin-like growth factor 1 (ng/mL); RNA/pro=RNA/protein (µg/mg); DNA/pro=DNA/protein (µg/mg); ΔAICc=difference in AICc values with respect to the best candidate model. For all models $P<0.0001$. r^2=coefficient of determination.

Dependent variable	n	Model	r^2	AICc	ΔAICc
All variables tested					
Growth rate (per d)	53	–0.0181+0.0040(RNA/DNA)+0.0001(IGF1)	0.733	–547.81	0
Growth rate (per d)	53	–0.0173+0.0048(RNA/DNA)	0.686	–542.39	5.42
RNA/DNA not included					
Growth rate (per d)	53	-0.0045+0.0011(RNA/pro)-0.0036(DNA/pro)+0.0001(IGF1)	0.738	–546.53	1.28
Growth rate (per d)	53	0.0001+0.0013(RNA/pro)-0.0045(DNA/pro)	0.712	–543.82	3.99

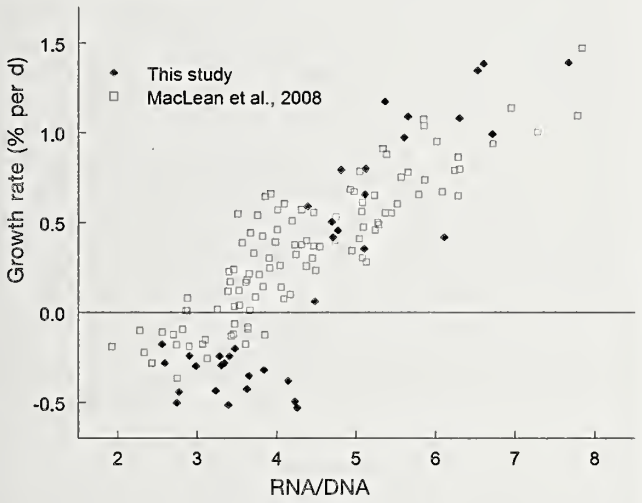

Figure 7

Specific growth rate (% wet weight per d) versus RNA/DNA for postsmolt Atlantic salmon (*Salmo salar*) reared in the laboratory. ♦ denotes data from fed and fasted fish held at 12° C and sampled throughout a 27-day period (present study). ❑ denotes data from the study of MacLean et al. (2008) in which postsmolts were sampled at the end of 30 days at a final water temperature of 12.8°C. In both experiments nucleic acid values were determined by the same method.

of RNA/DNA and RNA/pro to fed and refed growth rates are evidence that the relations between RNA indices and growth rate were not altered by repeated sampling of individual fish.

How best to standardize RNA values (RNA/DNA vs. RNA/pro) is not clear and may depend upon the developmental stage of the fish. Fish muscle is unique in that it increases in size throughout the life of a fish owing to both hyperplasia (increase in cell number) and hypertrophy (increase in cell size) (Weatherly et al., 1988; Higgins and Thorpe, 1990; Koumans et al., 1993; Mommsen, 2001). Hyperplastic muscle growth is accomplished by fusion of myosatellite cells, resulting in a brief initial increase in DNA per cell followed by a nearly constant amount of DNA per cell. In contrast, muscle growth through hypertrophy produces multiple nuclei per cell and often multiple copies of DNA per nucleus (polyploidy) resulting in a variable amount of DNA per cell (Jimenez and Kinsey, 2012). Higgins and Thorpe (1990) investigated muscle growth in Atlantic salmon and concluded that juvenile Atlantic salmon (<15 cm) increased muscle mass by hyperplasia, whereas hypertrophy was more important in autumn and winter when growth of the salmon was slow. Weatherly et al. (1988) concluded that in fish smaller than approximately 44% of their maximum size, most fish muscle growth was due to hyperplasia. Our fish were recent postsmolts, approximately 23% of their maximum size, and most likely increasing their muscle size predominantly through hyperplasia. In our study, RNA/DNA performed better than RNA/pro for indicating short-term growth. In general, RNA/DNA may be the better indicator of growth rate during larval and juvenile stages when a fish is growing rapidly by increasing cell numbers. Until the relation of RNA to DNA in polyploidy cells is better known, RNA/pro may be the preferred indicator of growth rate in older fish where growth by hypertrophy predominates. In adults, however, RNA-based indices may not be an appropriate index of condition or growth rate. In the adult stage, protein synthesis is directed more toward protein turnover rather than protein accretion. Additionally, fat retention or gonad development may be the driving force behind weight-specific growth. This increase in nonprotein mass would cause an uncoupling of the relation of RNA-mass to growth rate. Because the turnover rate of RNAs (mRNA, tRNA, rRNA) ranges from minutes to a few days (see Fraser and Rogers, 2007), RNA-based indices would be most useful for estimating recent growth rates and current nutritional state and would

not be an appropriate index to measure growth rates over long periods of time (months).

DNA/pro Some studies have reported an increase in DNA/pro (or its equivalent DNA/dry weight) during starvation, presumably due to muscle protein being used as an energy source while DNA content remained stable (Fukuda et al., 2001; Mathers et al., 1993; Malzahn et al., 2003). Our results are consistent with this observation with our fasted fish having significantly more DNA per unit of protein than both the fed and refed groups. However, DNA/pro was not strongly correlated with growth rate and feeding treatments within a day could not be distinguished on the basis of this index. Given the complex relation between DNA concentration and hyperplasia and hypertrophy, DNA/pro would not be a good potential physiological index of short-term changes in growth rate or nutritional state in juvenile salmon.

IGF1 IGF1 is an essential component in the endocrine system that regulates growth. Because of this attribute, experiments have been conducted to investigate the endocrine response of the coupled growth hormone and IGF1 systems (GH-IGF1) to nutritional state to help understand how that system regulates growth. Numerous studies have reported decreases in IGF1 in fish fasted for 4 or more weeks (Moriyama et al., 1994; Larsen et al., 2001; Picha et al., 2008) but few studies have investigated its use to assess the nutritional condition of fish over short time periods. Shimizu et al. (2009) reported a decline in IGF1 levels in coho salmon (*Oncorhynchus kisutch*) after 1 week of fasting and a statistically significant decrease after 3 weeks, whereas IGF1 levels in young Chinook salmon (*Oncorhynchus tshawytscha*) decreased significantly 6 days after fasting (Pierce et al., 2005). Based on repeated measurements of individuals in our study, IGF1 values in our fasting fish changed little throughout the 3 weeks. Different resistances to fasting may explain the different results. Of the aforementioned studies, Chinook salmon had low fat levels (3–5% by weight) and had the greatest rate of weight loss. Fat content of our Atlantic salmon was 7–8%; their body composition remained relatively stable throughout the experiment and there was only a small loss of fat in the fasted treatment (Caldarone et al., 2012). Based on repeated measurements of individuals, IGF1 levels in our fish responded rapidly to refeeding; values increased 4 days after the fish were refed. Immature rainbow trout (*Oncorhynchus mykiss*) that had been fasted for 4 weeks also exhibited increases in IGF1 levels 4 days after they were refed (Gabillard et al., 2006), whereas Atlantic salmon smolts after 15 days of fasting showed no change 7 days after being refed (Wilkinson et al., 2006). Further research is needed to determine factors affecting the response time of IGF1 to changes in food availability.

High variability in both the fasted and fed groups, coupled with a small sample size, hampered detection of statistically significant differences in IGF1 between our food treatments. Researchers have suggested that large differences in growth rate or a large sample size may be needed to use IGF1 levels to separate fish by nutritional condition (Beckman et al., 2004a, 2004b) (also see below with regard to serial sampling, acute stress, and IGF1 levels).

A significant linear relation has been observed between circulating plasma IGF1 levels and growth rate in a variety of salmonids (Pierce et al., 2001; Beckman et al., 2004a; Dyer et al., 2004). Beckman (2011) stated a number of caveats for the use of IGF1 as a growth index; in particular, do not compare fish in differing stages of maturation, be aware of issues which may be introduced by rapid changes in temperature, and be aware of potential difficulties which may be introduced by acute stress. Indeed in some studies, nonsignificant relations between IGF1 and growth have been reported (Silverstein et al., 1998; Andrews et al., 2011, in large but not small juvenile lingcod; Beckman et al., 2004b, in juvenile coho salmon soon after transfer to cool water, but not fish maintained in warm water nor fish acclimated to cool water). In our study the relation between IGF1 levels and growth rate was positive and significant but not highly correlative. It is possible that the IGF1 values were affected by our serial sampling protocol (multiple nonlethal blood draws). Pierce et al. (2001) compared IGF1 and growth relations between terminally and serially sampled juvenile coho salmon and found a large decrease in the correlation coefficient (r=0.78 vs r=0.51) between the two protocols. The correlation between IGF1 and growth in the present work (r=0.66) was more in line with Pierce's serially sampled values than with the more highly correlated responses found in studies with terminally sampled values (see Beckman, 2011).

The best candidate model for estimating growth rate did contain both IGF1 and RNA/DNA terms. These two indices reflect differing aspects of the physiology of growth. As part of the GH-IGF1 endocrine system, IGF1 levels reflect a specific stimulus for cellular growth, whereas RNA/DNA is a measure of a cell's capacity for growth. Thus the two measures together would reflect both upstream regulation of cellular growth and downstream response to that regulation.

Circulating levels of plasma IGF1 in fish are regulated by a suite of at least 6 different IGF binding proteins (Duan, 2002). These binding proteins themselves are differentially regulated by nutritional state as well as other factors, perhaps including stress (Kelley et al., 2001). The circulating level of IGF1 in the blood generally is determined by the most abundant binding protein (IGFBP2b), which itself is regulated by nutritional states (Shimizu et al., 2009; Kawaguchi et al., 2013). The establishment of methods to measure IGF binding proteins in fish blood is still on-going (Shimizu et al., 2011a, 2011b) and our understanding of the factors that regulate the abundance of different binding proteins and how they affect IGF1 levels is quite incomplete. We do not have the technical capacity to determine whether or not the current results (IGF1 and

fasting, IGF1 and growth, IGF1 and refeeding) were due to the induction of different suites of binding proteins and how these proteins may have affected circulating IGF1 levels differently from those of other studies. Shimizu et al. (2009) demonstrated a significant increase in 41kDa IGFBP of fasting fish in response to refeeding; perhaps the IGF1 increase we observed in our individual refed fish was modulated by changes in circulating IGFBP levels. The fact that IGF1 levels of fasted fish did increase in response to refeeding and that the overall relation of IGF1 to growth was positive and significant gives us confidence that IGF1 responds to changes in nutrition and growth. The use of IGF1 measures has been demonstrated in several ecological studies of juvenile salmonids where differences in IGF1 levels have been observed in fish reared in different areas (Bond et al., 2014; Daly et al., 2014; Ferriss et al., 2014). However, we suggest that the specific response of IGF1 and IGFBPs to fasting, feeding, and growth, in combination with acute or chronic stress, should be investigated.

Of the indices reported here (RNA/DNA, RNA/pro, DNA/pro, IGF1) and in Caldarone et al. (2012) (Fulton's K, BIA), RNA/DNA was the most suited for estimating recent growth rates and identifying the nutritional condition of our individual postsmolt Atlantic salmon exposed to short-term changes in food availability. Removing muscle samples with a biopsy punch for RNA/DNA analysis did not result in any mortalities and did not appear to inhibit growth of the fish, as evidenced by the rapid increase in growth rates of refed fish soon after a muscle sample was taken. The short response time of RNA/DNA (4–8 days) in individual fish to both positive and negative changes in food availability would allow researchers to investigate linkages between environmental variables and nutritional state on ecologically relevant scales. With the addition of a temperature calibration, estimates of growth rates in the field at a variety of temperatures could be calculated with RNA/DNA values

Acknowledgments

The authors would like to thank E. Baker, and K. Fredrick for assistance in aquarium setup and temperature control, M. Prezioso and J. St. Onge-Burns for help in rearing the salmon, K. Cooper for running the IGF1 analyses, and the University of Rhode Island Graduate School of Oceanography for the use of Blount Aquarium.

Literature cited

Andrews, K. S., B. R. Beckman, A. H. Beaudreau, D. A. Larsen, G. D. Williams, and P. S. Levin.
2011. Suitability of insulin-like growth factor 1 (IGF1) as a measure of relative growth rates in lingcod. Mar. Coast. Fish. 3:250–260.

Arndt, S. K. A., T. J. Benfey, and R. A. Cunjak.
1994. A comparison of RNA concentrations and ornithine decarboxylase activity in Atlantic salmon (*Salmo salar*) muscle tissue, with respect to specific growth rates and diel variations. Fish Physiol. Biochem. 13:463–471.
1996. Effect of temporary reductions in feeding on protein synthesis and energy storage of juvenile Atlantic salmon. J. Fish Biol. 49:257–276.

Beckman, B. R.
2011. Perspectives on concordant and discordant relations between insulin-like growth factor 1 (IGF1) and growth in fishes. Gen. Comp. Endocrinol. 170: 233–252.

Beckman, B. R., W. Fairgrieve, K. A. Cooper, C. V. W. Mahnken, and R. J. Beamish.
2004a. Evaluation of endocrine indices of growth in individual postsmolt coho salmon. Trans. Am. Fish. Soc. 133:1057–1067.

Beckman, B. R., M. Shimizu, B. A. Gadberry, P. J. Parkins, and K. A. Cooper.
2004b. The effect of temperature change on the relations among plasma IGF-I, 41-kDa IGFBP, and growth rate in postsmolt coho salmon. Aquaculture 241:601–619.

Bond, M. H., B. R. Beckman, L. Rohrbach, and T. P. Quinn.
2014. Differential growth in estuarine and freshwater habitats indicated by plasma IGF1 concentrations and otolith chemistry in Dolly Varden *Salvelinus malma*. J. Fish Biol. 85:1429–1445.

Buckley, L. J.
1979. Relationships between RNA–DNA ratio, prey density, and growth rate in Atlantic cod (*Gadus morhua*) larvae. J. Fish. Res. Board Can. 36:1497–1502.

Buckley, L., E. Caldarone, and T.-L. Ong.
1999. RNA–DNA ratio and other nucleic acid-based indicators for growth and condition of marine fishes. Hydrobiologia. 401:265–277.

Bulow, F. J.
1970. RNA–DNA ratios as indicators of recent growth rates of a fish. J. Fish. Res. Board Can. 27:2343–2349.

Caldarone, E. M.
2005. Estimating growth in haddock larvae *Melanogrammus aeglefinus* from RNA:DNA ratios and water temperature. Mar. Ecol. Prog. Ser. 293:241–252.

Caldarone, E. M., C. M. Clemmesen, E. Berdalet, T. J. Miller, A. Folkvord, G. J. Holt, M. P. Olivar, and I. M. Suthers.
2006. Intercalibration of four spectrofluorometric protocols for measuring RNA/DNA ratios in larval and juvenile fish. Limnol. Oceanogr. Methods 4:153–163.

Caldarone, E. M., S. A. MacLean, and B. Sharack.
2012. Evaluation of bioelectrical impedance analysis and Fulton's condition factor as nonlethal techniques for estimating short-term responses in postsmolt Atlantic salmon (*Salmo salar*) to food availability. Fish. Bull. 110:257–270.

Ciotti, B. J., T. E. Targett, R. D. Nash, R. S. Batty, M. T. Burrows, and A. J. Geffen.
2010. Development, validation and field application of an RNA-based growth index in juvenile plaice *Pleuronectes platessa*. J. Fish Biol. 77:2181–2209.

Daly, E. A., J. A. Scheurer, R. D. Brodeur, L. A., Weitkamp, B. R. Beckman, and J. A. Miller.
2014. Juvenile steelhead distribution, migration, feeding, and growth in the Columbia River estuary, plume, and coastal waters. Mar. Coast. Fish. 6:62–80.

Duan, C.
2002. Specifying the cellular responses to IGF signals: roles of IGF-binding proteins. J. Endocrinol. 175:41–54.
Dyer, A. R., C. G. Barlow, M. P. Bransden, C. G. Carter, B. D. Glencross, N. Richardson, P. M. Thomas, K. C. Williams, and J. F. Carragher.
2004. Correlation of plasma IGF-I concentrations and growth rate in aquacultured finfish: a tool for assessing the potential of new diets. Aquaculture. 236:583–592.
Federal Register.
2009. Endangered and threatened species; determination of endangered status for the Gulf of Maine distinct population segment of Atlantic salmon. Fed. Reg. 74:29344–29387.
Ferriss, B. E., M. Trudel, and B. R. Beckman.
2014. Regional and inter-annual trends in marine growth of juvenile salmon in coastal pelagic ecosystems of British Columbia, Canada. Mar. Ecol. Prog. Ser. 503:247–261.
Fraser, K. P. P., and A. D. Rogers.
2007. Protein metabolism in marine animals: the underlying mechanism of growth. Adv. Mar. Biol. 52:267–362.
Fukuda, M., H. Sako, T. Shigeta, and R. Shibata.
2001. Relationship between growth and biochemical indices in laboratory-reared juvenile Japanese flounder (*Paralichthys olivaceus*), and its application to wild fish. Mar. Biol. 138:47–55.
Gabillard, J-C., B. B. Kamangar, and N. Montserrat.
2006. Coordinated regulation of the GH/IGF system genes during refeeding in rainbow trout (*Oncorhynchus mykiss*). J. Endocrinol. 191:15–24.
Gwak, W. S., and M. Tanaka.
2001. Developmental change in RNA: DNA ratios of fed and starved laboratory-reared Japanese flounder larvae and juveniles, and its application to assessment of nutritional condition for wild fish. J. Fish Biol. 59:902–915.
Higgins, P. J., and J. E. Thorpe.
1990. Hyperplasia and hypertrophy in the growth of skeletal muscle in juvenile Atlantic salmon, *Salmo salar* L. J. Fish Biol. 37:505–519.
Jimenez, A. G., and S. T. Kinsey.
2012. Nuclear DNA content variation associated with muscle fiber hypertrophic growth in fishes. J. Comp. Physiol., B 182:531–540.
Kawaguchi, K., N. Kaneko, M. Fukuda, Y. Nakano, S. Kimura, A. Hara, and M. Shimizu.
2013. Responses of insulin-like growth factor (IGF)-I and two IGF-binding protein-1 subtypes to fasting and re-feeding, and their relationships with individual growth rates in yearling masu salmon (*Oncorhynchus masou*). Comp. Biochem. Physiol. A 165: 191–198.
Kelley, K. M., J. T. Haigwood, M. Perez, and M. M Galima.
2001. Serum insulin-like growth factor binding proteins (IGFBPs) as markers for anabolic/catabolic condition in fishes. Comp. Biochem. Physiol. B 129:229–236.
Koumans, J. T. M., H. A. Akster, G. H. R. Booms, and J. W. M. Osse.
1993. Growth of carp (*Cyprinus carpio*) white axial muscle; hyperplasia and hypertrophy in relation to the myonucleus/sarcoplasm ratio and the occurrence of different subclasses of myogenic cells. J. Fish Biol. 43:69–80.
Larsen, D. A., B. R. Beckman, and W. W. Dickhoff.
2001. The effect of low temperature and fasting during the winter on metabolic stores and endocrine physiology (insulin, insulin-like growth factor-I, and thyroxine) of coho salmon, *Oncorhynchus kisutch*. Gen. Comp. Endocrinol. 123:308–323.
Loughna, P. T., and G. Goldspink.
1984. The effects of starvation upon protein turnover in red and white myotomal muscle of rainbow trout, *Salmo gairdneri* Richardson. J. Fish Biol. 25:223–230.
Lowery, M. S., and G. N. Somero.
1990. Starvation effects on protein synthesis in red and white muscle of the barred sand bass, *Paralabrax nebulifer*. Physiol. Zool. 63:630–648.
MacLean, S. A., E. M. Caldarone, and J. M. St. Onge-Burns.
2008. Estimating recent growth rates of Atlantic salmon smolts using RNA-DNA ratios from nonlethally sampled tissues. Trans. Am. Fish. Soc. 137:1279–1284.
Malloy, K. D., and T. E. Targett.
1994. The use of RNA:DNA ratios to predict growth limitation of juvenile summer flounder (*Paralichthys dentatus*) from Delaware and North Carolina estuaries. Mar. Biol. 118:367–375.
Malzahn, A. M., C. Clemmesen, and H. Rosenthal.
2003. Temperature effects on growth and nucleic acids in laboratory-reared larval coregonid fish. Mar. Ecol. Prog. Ser. 259:285–293.
Mathers, E. M., D. F. Houlihan, I. D. McCarthy, and L. J. Burren.
1993. Rates of growth and protein synthesis correlated with nucleic acid content in fry of rainbow trout, *Oncorhynchus mykiss*: effects of age and temperature. J. Fish Biol. 43:245–263.
McCarthy, I. D., E. Moksness, D. A. Pavlov, and D. F. Houlihan.
1999. Effects of water temperature on protein synthesis and protein growth in juvenile Atlantic wolfish (*Anarhichas lupus*). Can. J. Fish. Aquat. Sci. 56:231–241.
McMillan, D. N., and D. F. Houlihan.
1988. The effect of refeeding on tissue protein synthesis in rainbow trout. Physiol. Zool. 61:429–441.
1989. Short-term responses of protein synthesis to refeeding in rainbow trout. Aquaculture 79:37–46.
Miglavs, I., and M. Jobling.
1989. Effects of feeding regime on food consumption, growth rates and tissue nucleic acids in juvenile Arctic charr, *Salvelinus alpinus*, with particular respect to compensatory growth. J. Fish Biol. 34:947–957.
Millward, D. J., P. J. Garlick, W. P. T. James, D. O. Nnanyelugo, and J. S. Ryatt.
1973. Relationship between protein synthesis and RNA content in skeletal muscle. Nature 241:204–205.
Mommsen, T. P.
2001. Paradigms of growth in fish. Comp. Biochem. Physiol. B 129:207–219.
Moriyama, S., P. Swanson, M. Nishii, A. Takahashi, H. Kawauchi, W.W. Dickhoff, and E. M. Plisetskaya.
1994. Development of a homologous radioimmunoassay for coho salmon insulin-like growth factor-I. Gen. Comp. Endocrinol. 96:149–161.
Peck, M. A., L. J. Buckley, E. M. Caldarone, and D. A. Bengtson.
2003. Effects of food consumption and temperature on growth rate and biochemical-based indicators of growth in early juvenile Atlantic cod *Gadus morhua* and haddock *Melanogrammus aeglefinus*. Mar. Ecol. Prog. Ser. 251:233–243.
Picha, M. E., M. J. Turano, B. R. Beckman, and R. J. Borski.
2008. Endocrine biomarkers of growth and applications to aquaculture: a minireview of growth hormone, insulin-like growth factor (IGF)-I, and IGF-binding proteins as

potential growth indicators in fish. N. Am. J. Aquacult. 70:196–211.

Pierce, A. L., B. R. Beckman, K. D. Shearer, D. A. Larsen, and W. W. Dickhoff.
2001. Effects of ration on somatotropic hormones and growth in coho salmon. Comp. Biochem. Physiol. B 128:255–264.

Pierce, A. L., M. Shimizu, B. R. Beckman, D. M. Baker, and W. W. Dickhoff.
2005. Time course of the GH/IGF axis response to fasting and increased ration in Chinook salmon (*Oncorhynchus tshawytscha*). Gen. Comp. Endocrinol. 140:192–202.

Ricker, W. E.
1979. Growth rates and models. *In* Fish physiology, vol. 8 (W. S. Hoar, D. J. Randall, and J. R. Brett, eds.), p. 677–743. Academic Press, New York.

Shimizu, M., K. A. Cooper, W. W. Dickhoff, and B. R. Beckman.
2009. Postprandial changes in plasma growth hormone, insulin, insulin-like growth factor (IGF)-I, and IGF-binding proteins in coho salmon fasted for varying periods. Am. J. Physiol. Regul. Integr. Comp. Physiol. 297: R352–R361.

Shimizu, M, K. Kishimoto, T. Yamaguchi, Y. Nakano, A. Hara, and W. W. Dickhoff.
2011a. Circulating salmon 28- and 22-kDa insulin-like growth factor binding proteins (IGFBPs) are co-orthologs of IGFBP-1. Gen. Comp. Endocrinol. 174:97–106.

Shimizu, M, S. Suzuki, M. Horikoshi, A. Hara, and W. W. Dickhoff.
2011b. Circulating salmon 41-kDa insulin-like growth factor binding protein (IGFBP) is not IGFBP-3 but an IGFBP-2 subtype. Gen. Comp. Endocrinol. 171:326–331.

Shulman, G. E., and R. M. Love.
1999. Molecular and metabolic aspects of life cycles. *In* The biochemical ecology of marine fishes. Advances in marine biology, vol. 36 (G. E. Shulman and R. M. Love, eds.), p. 89–137. Academic Press, San Diego, CA.

Silverstein, J. T., K. D. Shearer, W. W. Dickhoff, and K. M. Plisetskaya.
1998. Effects of growth and fatness on sexual development of Chinook salmon (*Oncorhynchus tshawytscha*) parr. Can. J. Fish. Aquat. Sci. 55:2376–2382.

Small, B. C., and B. C. Peterson.
2005. Establishment of a time-resolved fluoroimmunoassay for measuring plasma insulin-like growth factor I (IGF-I) in fish: effect of fasting on plasma concentrations and tissue mRNA expression of IGF-I and growth hormone (GH) in channel catfish (*Ictalurus punctatus*). Dom. Anim. Endocrinol. 28:202–215.

Stierhoff, K. L., T. E. Targett, and J. H. Power.
2009. Hypoxia-induced growth limitation of juvenile fishes in an estuarine nursery: assessment of small-scale temporal dynamics using RNA:DNA. Can. J. Fish. Aquat. Sci. 66:1033–1047.

Vasconcelos, R. P., P. Reis-Santos, V. Fonseca, M. Ruano, S. Tanner, M. J. Costa, and H. N. Cabral.
2009. Juvenile fish condition in estuarine nurseries along the Portuguese coast. Estuar. Coast. Shelf Sci. 82:128–138.

Wagenmakers, E.-J., and S. Farrell.
2004. AIC model selection using Akaike weights. Psychonomic Bull. Rev. 11:192–196.

Weatherley, A. H., H. S. Gill, and A. F. Lobo.
1988. Recruitment and maximal diameter of axial muscle fibres in teleosts and their relationship to somatic growth and ultimate size. J. Fish Biol. 33:851–859.

Wilkinson, R. J., M. Porter, H. Woolcott, R. Longland, and J. F. Carragher.
2006. Effects of aquaculture related stressors and nutritional restriction on circulating growth factors (GH, IGF-I and IGF-II) in Atlantic salmon and rainbow trout. Comp. Biochem. Physiol. A 145:214–224.

NOAA
National Marine
Fisheries Service

Fishery Bulletin
established 1881

Spencer F. Baird
First U.S. Commissioner
of Fisheries and founder
of *Fishery Bulletin*

Seasonal changes in abundance and compelling evidence of migration for 2 rockfish species (*Sebastes auriculatus* and *S. caurinus*) inhabiting a nearshore, temperate-water artificial reef

Larry L. LeClair (contact author)
Ocean Eveningsong
Jesse M. Schultz

Email for contact author: larry.leclair@dfw.wa.gov

Washington Department of Fish and Wildlife
600 Capitol Way North
Olympia, Washington 98501

Abstract—We used scuba over fixed-width strip transects to monitor seasonal abundances of brown rockfish (*Sebastes auriculatus*) and copper rockfish (*S. caurinus*) on a nearshore artificial reef in Puget Sound, Washington, over a 7-year period. Spring and fall abundances were intermediate and marked transitional phases between seasons of highest (summer) and lowest (winter) abundance for both species. Analyses of length classes indicated that the numbers of seasonal juvenile recruits were not sufficient to account for the marked differences in abundance between summer and winter. For both species, the proportion of large fish (≥20 cm in total length) to the total number observed in summer and winter was significantly greater during the winter. Late-stage gravid brown rockfish occurred in greatest abundance during the spring and late-stage gravid copper rockfish were observed only in the summer. We examined auxiliary data from a genetics study of brown rockfish that was conducted concurrently at the reef and interpreted the results, along with our survey findings, as providing compelling evidence of seasonal migrations on and off the reef.

Manuscript submitted 20 October 2015.
Manuscript accepted 19 April 2016.
Fish. Bull. 114:302–316 (2016).
Online publication date: 6 May 2016.
doi: 10.7755/FB.114.3.4

Understanding fish movement is paramount to the design and implementation of effective resource conservation and management strategies. Movement influences the dynamics, demographics, and genetics of populations; the structure and function of ecosystems; species interactions; modes of energy transfer; and biodiversity (Rothschild, 1986; Frank, 1992; Merz and Moyle, 2006; Clark et al., 2009; Condal et al., 2012). Known patterns of movement are often key considerations in the development of harvest management plans established to protect fish populations from overexploitation. For example, in the northeast Pacific Ocean, lingcod (*Ophiodon elongatus*) are widely believed to participate in seasonal nearshore–offshore spawning migrations (Jagielo, 1990, 1995), and in some regions (e.g., Puget Sound), recreational fisheries that target lingcod are managed to protect nearshore spawning fish (Palsson et al.[1]). Pacific halibut (*Hippoglossus stenolepis*) also undergo seasonal migrations (St-Pierre[2]), and establishment of the commercial fishery season by the International Pacific Halibut Commission is designed in large part to protect offshore spawning populations (Loher, 2011).

Fish movement also has crucial implications for the design of scientific sampling strategies and stock assessments, and movement poses both operational and conceptual challenges for the selection of appropriate temporal and spatial scales in ecological studies. Inferences about the ecological processes under investigation may be constrained or confounded when, as is often the case, scales of operational convenience, rather than ecological relevance, are incorporated into study designs. Failure to identify and integrate fish movement into study designs can lead to the selection of temporal or spatial scales of observation that are ill-fitted to the study objectives, particularly when movement occurs over multiple habitat types. Sampling strategies that

[1] Palsson, W. A., T. J. Northup, and M. W. Barker. 1998. Puget Sound Groundfish Management Plan, 48 p. Washington Dep. Fish Wildl., Olympia. [Available at website.]

[2] St-Pierre, G. 1984. Spawning locations and season for Pacific halibut. Int. Pac. Halibut Comm., Sci. Rep. 70, 46 p. [Available at website.]

focus on single habitat types are also subject to bias when based on untested assumptions about habitat use, extent of home range, and site fidelity, as reviewed by Pittman and McAlpine (2003). These authors assert that if information on movement is not available, the assumption of single habitat use should be considered carefully or rejected entirely. They advocate for an assumption of the use of multiple habitats because it allows for the consideration of broader-scale movement and potential linkages among habitat types. Movement patterns, whether over short (e.g., diel) or long (e.g., seasonal, annual) temporal scales, rank as one of the most important behavioral sources of bias in fish stock assessments (Gayanilo and Pauly, 1997; Sparre and Venema, 1998). Statistical methods for incorporating patterns of fish movement into stock assessments are advancing (Hilborn and Walters, 1992; Methot, 2011), and the integration of known fish behavior parameters, such as diel and seasonal movements, will likely lead to substantial improvements in the accuracy of stock assessment models (Fréon et al., 1993).

Although the potential conservation benefits of individual marine protected areas (MPAs) have been discussed for decades, there is currently a growing worldwide interest in establishing coordinated networks of MPAs that are ecologically joined over broad geographic regions, and this approach has been advocated for rockfishes in the northeast Pacific Ocean (Yoklavich, 1998; Parker et al., 2000). Further, understanding migrations and other movement patterns of adult rockfishes has been identified as critical for formulating effective recovery plans that may include MPAs for rockfishes in Puget Sound (Wyllie-Echeverria and Sato, 2005). The trend toward MPAs, however, is not without controversy—much of it centering on how to choose and configure MPA sites into mosaics that are adequately sized and placed to achieve prescribed conservation goals. The related and equally critical issue of how best to assess the performance of such networks once established is also a topic of considerable debate. The size and placement controversy owes much of its genesis to attempts at applying theories of island biogeography to the design of nature reserves (Diamond, 1975) and continues under what is widely known as the SLOSS (single large or several small) debate (Simberloff and Abele, 1982). Fundamental to the debate is the concept of source-sink dynamics (Pulliam, 1988) whereby, under optimal MPA performance conditions, increased regulatory protection is expected to result in a net export of individuals to unprotected habitat or to marginally suitable habitat within an MPA through larval advection, density-dependent displacements of later life history stages (spillover), or both. Many criteria for MPA design and site selection lack robust scientific justification and most established temperate-water MPAs are not subjected to systematic, or even periodic, performance evaluations relative to fishery enhancement, species recovery, biodiversity preservation, or other desired outcomes. Although the number of theoretical MPA performance models is proliferating (Willis et al., 2003), and presumably improving, these models rarely incorporate fish movement (but see Attwood and Bennett, 1995; Roberts and Sargant, 2002; Berezansky et al., 2011). Understanding the frequency, periodicity, and scale of fish movement will aid modelers and resource managers in choosing and scaling MPA sites, and in constructing MPA networks that adequately serve the ecological needs of species targeted for conservation.

In this study, we seasonally monitored the abundance of 2 demersal rockfish species, brown rockfish (*Sebastes auriculatus*) and copper rockfish (*S. caurinus*) over a 7-year period on an artificial reef in Puget Sound, Washington. Counts for each of the 2 species were obtained by using scuba-based underwater visual censuses (UVCs) conducted over fixed-width strip transects. Brown and copper rockfish belong to the subgenus *Pteropodus* and occur sympatrically in many regions of the northeast Pacific Ocean, including much of Puget Sound. They share similar life history attributes, habitat affinities, behavioral characteristics, and food preferences (Washington et al.[3]; Lea et al., 1999; Stout et al., 2001; Love et al., 2002) and, in Puget Sound there is evidence of hybridization between the species (Seeb, 1998; Schwenke, 2012). In Washington State, they are managed as "bottomfish" and brown rockfish stock status throughout Puget Sound is classified as "precautionary," whereas copper rockfish are classified as either precautionary (north Puget Sound) or "vulnerable" (south Puget Sound), as defined by Palsson et al.[4]

Although tagging studies involving brown or copper rockfish have occurred throughout much of the range of these species and have encompassed a variety of investigative objectives (Miller et al., 1967; Miller and Geibel, 1973; Dewees and Gotshall, 1974; Hallacher, 1977; Walton[5]; Laufle[6]; Gowan, 1983; Mathews and Barker, 1983; Hueckel et al.[7]; Matthews, 1985; Matthews et al., 1987; Hartmann, 1987; Matthews, 1990a; Matthews, 1990b; Lea et al., 1999; Eisenhardt, 2004; Lowe et al., 2009; Tolimieri et al., 2009; Reynolds et al., 2010; Longabach, 2010; Starr et al.[8]; Hannah and

[3] Washington, P. M., R. Gowan, and D. H. Ito. 1978. A biological report on eight species of rockfish (*Sebastes* spp.) from Puget Sound, Washington, 50 p. Northwest Alaska Fish. Cent. Proc. Rep. Northwest Alaska Fish. Cent., Natl. Mar. Fish. Serv., NOAA, Seattle. [Available at website.]

[4] Palsson, W. A., T.-S. Tsou, G. G. Bargmann, R. M. Buckley, J. E. West, M. L. Mills, Y. W. Cheng, and R. E. Pacunski. 2009. The biology and assessment of rockfishes in Puget Sound. Wash. Dep. Fish Wildl. FPT-09-04, 208 p. [Available at website.]

[5] Walton, J. M. 1979. Puget Sound artificial reef study. Wash. Dep. Fish., Tech. Rep. 50, 130 p.

[6] Laufle, J. C. 1982. Biological development and materials comparisons on a Puget Sound artificial reef. Wash. Dep. Fish. Tech. Rep. 72, 183 p.

[7] Hueckel, G. J., R. M. Buckley, and B. L. Benson. 1983. The biological and fishery development on concrete habitat enhancement structures off Gedney Island in Puget Sound, Washington. Wash. Dept. Fish. Tech. Rep. 78, 67 p.

[8] Starr, R. M., D. Wendt, K. T. Schmidt, R. Romero, J. Duryea, E. Loury, N. Yochum, R. Nakamura, L. Longabach, E.

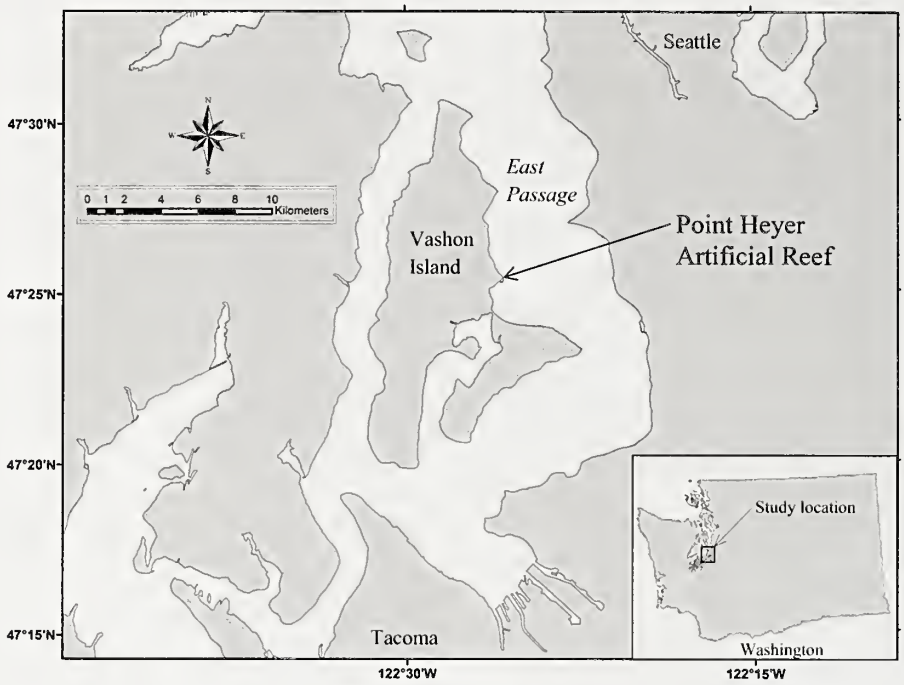

Figure 1

Location of Point Heyer Artificial Reef in central Puget Sound, Washington, where 2 rockfish species (brown rockfish [*Sebastes auriculatus*] and copper rockfish [*S. caurinus*]) were monitored over a 7-year period to determine seasonal changes in abundance and to find evidence of seasonal migrations.

Rankin, 2011; Hanan and Curry, 2012; Rankin et.al., 2013), long-term trends in seasonal abundance have not been specifically addressed, and drawing informed conclusions from these studies about potential seasonal changes in abundance or movement patterns is hampered by the temporal or spatial scales over which they were conducted, numbers of fish tagged, or insufficient information (e.g., mark and recapture dates). Collectively, the studies indicate that most adults of both species maintain high site fidelity, although some exceptions have been observed; that habitat type (e.g., high-relief, low-relief, natural, artificial) may influence site fidelity and movement behavior; and that some level of homing ability from beyond their putative home range is likely. Estimates of home range for brown and copper rockfish vary widely, from <10 m^2 over high relief habitat to 4656 m^2 over low relief habitat (Matthews 1990b; Tolimieri et al., 2009; Rankin et al., 2013).

The goal of our study was to determine whether there were patterned seasonal changes in abundance on the reef for either species, and if so, whether the observed patterns differed between species. In order to gain further insight into our monitoring results, we examined auxiliary data from a genetic study of brown rockfish that was conducted concurrently at our study site. These data, along with our findings, are discussed in the context of providing compelling evidence of rockfish migratory behavior. Migrations are well known for many temperate-water marine fishes (e.g., cods, herrings, and sharks) and are often associated with changes in seasonally variable resources, such as food supply or shelter, or with spawning or mating behaviors (Harden Jones, 1968; McCleave et al., 1984; McKeown, 1984; Smith, 1985).

Materials and methods

Point Heyer Artificial Reef (PHAR) is a high-relief, insular reef located along the eastern shore of Vashon Island in the hydrographically defined "main basin" (Ebbesmeyer et al. 1984) of central Puget Sound (Fig. 1). Puget Sound is a glacially formed saltwater estuary fjord characterized by mixed semidiurnal tides. It is connected to the Pacific Ocean through one, approximately east-west running strait (Strait of Juan de Fuca) that is bounded to the north by Canada's Vancouver Island, and by a north–south running inland waterway between Vancouver Island and the Canadian mainland. It consists of 5 sub-basins that are separated by shallow-water sills. The bathymetry of Puget Sound extends to depths of nearly 300 m (all depths reported herein are corrected to mean lower low water depths).

Nakada, D. Rasmussen, N. Hall, K. Green, and S. McMillan. 2010. Baseline surveys of nearshore fishes in and near central California marine protected areas 2007–2009. Final project report submitted to the Ocean Protection Council, 124 p. California Sea Grant College Program, La Jolla, CA. [Available at website.]

The reef was constructed in 1983 by the Washington Department of Fisheries (now the Washington Department of Fish and Wildlife) for the purpose of increasing the number of productive recreational fishing sites in the region (Buckley 1982). It covers an area of approximately 5400 m^2 and is constructed of various-size quarried boulders and cobble interspersed with long horizontally placed concrete beams. The near- and offshore margins of the reef lie at a depth of about 4 and 36 m, respectively. The surrounding seafloor consists primarily of unconsolidated sand, shell hash, and gravel, as well as widely dispersed small glacially deposited boulders. The reef is situated on a steeply sloping bottom that descends to depths of nearly 240 m over a distance of about 3 km to the approximate center of the passage that separates Vashon Island from the mainland (East Passage, Fig. 1). Large year-round patches of eelgrass (*Zostera spp.*) occur in the shallow water shoreward of the reef and dense growths of perennial nonfloating macroalgae (e.g., laminarians, ulvas, palmarials) form over the shallower portions of the reef during the summer and fall. Bull kelp (*Nereocystis leutkeana*), the predominant canopy-forming floating kelp in Puget Sound, does not grow on or near the reef. Twenty-two years had elapsed between the construction of the reef and the commencement of our study and we presume that sufficient time had passed for ecological succession to have occurred.

In 2005, 3 permanent straight-line 60-m transects (T-1, T-2, and T-3), each running due east–west (as per standard compass) and separated by a distance of at least 10 m, were established on the reef. The transects ran perpendicular to shore and were strategically placed in order to capture the dominant micro- and macrohabitat features of the reef (e.g., boulder, cobble, beams, sandy bottom, high and low relief, reef margins, crevice and overhang space). The nearshore ends were positioned in 4.5, 4.0, and 6.0 m and the offshore ends in 21.5, 21.0, and 20.5 m for T-1, T-2, and T-3, respectively. The offshore ends of each transect were semipermanently marked with a buoyed line of about 1 m in length fastened to a hollow-core cinder block of approximately 40×20×20 cm affixed to the seafloor with 2 steel bars. Coordinates (based on the North American Datum of 1983) for the offshore markers were as follows: T-1, 47.420040°N, 122.427145°W; T-2, 47.420082°N, 122.427182°W; T-3, 47.420579°N, 122.426947°W. Real-time coordinate-corrected positions were obtained by connecting a line between the transect marker to a surface buoy and registering the position with a GeoExplorer 6000 Centimeter Edition[9] GPS receiver (Trimble Navigation Ltd., Sunnyvale, CA).

The transects were divided into twelve, 5-m segments each and were surveyed by scuba divers swimming in tandem along the bottom from deep to shallow and pausing briefly at each segment marker. During surveys, divers counted fish in each segment on their respective sides of the transect centerline to a width of 2 m (total bottom coverage per transect=240 m^2) and as high into the water column as visibility permitted. Hand-held lights were used to search beneath overhangs, in crevices, and in other poorly lit areas. In order to ensure consistent effort among surveys, the slowest practical swimming speed was maintained over each transect as governed by the maximum allowable safe bottom-time using conventional scuba.

All species of fish that were conspicuous to the divers were recorded and enumerated. Highly cryptic species or species that remain very small into adulthood, though occasionally noted, were not targeted in the search effort. Careful written and hand-signal communication between divers reduced the risk of counting fish twice when they were swimming across transect from one survey lane to the other. Individual fish from the 3 most visually dominant taxonomic families (Sebastidae, Embitocidae, and Hexagrammidae) were recorded to species and their length (all fish lengths herein are reported as total length [TL] in centimeters) was estimated into length classes, which varied among species. The occurrence of apparent late-stage gravid brown and copper rockfish, evidenced by their prominently distended abdomens, was also noted. Cooper (2003) showed that bulging abdomens can be a reliable means for identifying late-stage gravid copper rockfish when they are viewed underwater.

In 2005, surveys were conducted on all 3 transects during the summer, but only on T-2 in the fall, and no surveys were conducted during the spring of 2005 or the winter of 2005–2006. Beginning in the spring of 2006, each transect was surveyed at least once during each season through summer of 2012. In most instances, multiple transects were not surveyed on the same day. The order in which transects were surveyed during any given season was randomly determined. No attempt was made to synchronize the surveys to the cycle of the tides; therefore the surveys occurred over a broad range of tidal conditions. Strong tidal currents are not generally encountered over the reef and current velocities rarely exceed 1.5 knots. The mean range of the tide at PHAR is approximately 2.4 m. Temperature data loggers (HOBO® Pro v2, Onset Computer Corporation, Bourne, MA) were deployed at the near- and offshore margins of the reef (4.5 m and 28 m, respectively) and they recorded water temperature every 4 hours for a period of one year beginning 8 December 2006.

In order to mitigate the potential effects of observer variation, only 5 divers were used throughout the entire course of the study and all surveys on the south side of the transect center-lines were conducted by the same diver. Four different divers conducted surveys on the north side of the transect center-lines; but nearly all (~96%) of those surveys were conducted by just 2 divers. All scuba divers had extensive experience in surveying rockfish on Puget Sound rocky reefs prior to

9 Mention of trade names or commercial companies is for identification purposes only and does not imply endorsement by the Washington Department of Fish and Wildlife or the National Marine Fisheries Service, NOAA.

Table 1

Number of surveys, by season and tide cycle, conducted over a 7-year period (from summer 2005 through summer 2012) at Point Heyer Artificial Reef, Puget Sound, Washington.

Transect	Flood tide	Ebb tide	Slack water before flood tide	Slack water before ebb tide	Total surveys by transect
Spring					
T-1	4	4	1	3	12
T-2	2	5	0	1	8
T-3	3	4	1	0	8
Summer					
T-1	0	6	1	0	7
T-2	2	6	0	0	8
T-3	3	7	0	0	10
Fall					
T-1	3	3	1	0	7
T-2	7	0	0	1	8
T-3	6	1	0	0	7
Winter					
T-1	2	3	0	1	6
T-2	2	4	0	0	6
T-3	1	5	0	0	6
Grand totals	35	48	4	6	93

participating in this study, and they periodically used hand-held graduated staffs to calibrate their visual estimates of fish length.

The genetic data were compiled from a study in which molecular markers had been used to estimate genotyping error rates from brown rockfish captured at PHAR (Hess et al. 2012). In that study, 718 brown rockfish ranging in length from 10 to 37 cm (M [mean]=22; SD [standard deviation]=7.1) were sampled and returned alive to their point of capture during all seasons between spring of 2004 and summer of 2009. The genetic data were used to identify individuals that were recaptured in multiple years.

Results

A total of 93 survey dives were conducted between 30 June 2005 and 18 September 2012. All surveys commenced between 1.5 and 7 hr after sunrise (M=4 hr, SD=1.2), and the mean survey time per transect was 28 minutes (SD=7.8). In no case was diver-estimated visibility less than twice the width of a survey lane. The numbers of surveys by tide cycle are presented in Table 1. The total numbers of brown and copper rockfish observed by length class summed over all 3 transects are presented in Figure 2. A list of all species recorded on transect over the course of the study (a subjective appraisal of how often the species were observed) and length classes for species from the 3 visually dominant taxonomic families are presented in the Supplementary Table [Online].

We fitted a generalized linear mixed model (GLMM) to the data by maximum likelihood by using the Laplace approximation and a Poisson link with the lme4 package, vers. 1.1-8 (Bates et al., 2015) and statistical software R, vers. 3.1.1 (R Core Team, 2014). For each of the 2 species, we ran a random effects only (null) model with count as the response variable, and year and transect as random effects. We then added season as the explanatory variable to produce a full model. We used ANOVA to compare the null and full models and for both species the results were significant (χ^2=386.64 and 214.09 [3 df] for brown and copper rockfish, respectively, P<0.001). The full model was selected over the null model by both Akaike information criteria (Akaike, 1974) and Bayesian information criteria (Schwarz 1978). The log-likelihood increased, and the deviance, which in linear models is equal to the residual sum of squares, decreased with the full model, further indicating that the full model provided a better fit to the data (Table 2). The GLMM back-transformed seasonal mean counts with 95% confidence intervals (confidence intervals were computed before back-transformation) are presented in Figure 3. We conducted a multiple means comparison of counts between seasons with Bonferroni corrected alpha (0.0042 from 0.05) to test the null hypothesis of no difference in mean counts between seasons. For both species, spring was not significantly different from

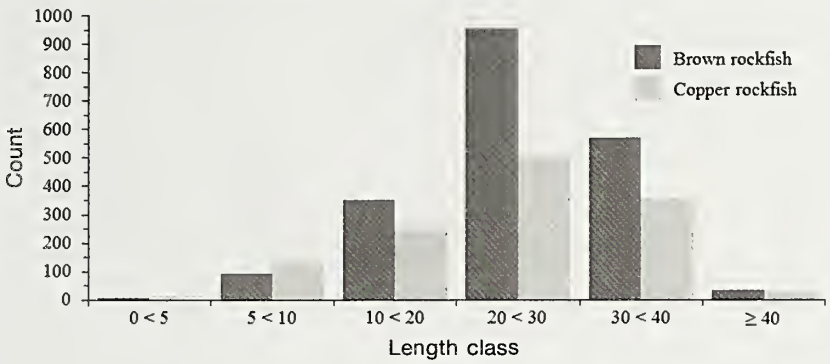

Figure 2

Total numbers (summed over 3 transects) by length class (total lengths in centimeters) of brown and copper rockfish (*Sebastes auriculatus* and *S. carinus*, respectively) observed during seasonal surveys at Point Heyer Artificial Reef, Puget Sound, Washington, from summer 2005 through summer 2012.

summer, fall, or winter; summer was significantly different from fall and winter; and fall was significantly different from winter.

For each species and for any given year, the summer fish density summed over all length classes was more than twice that for winter, and the densities did not vary greatly over time. To evaluate the potential impact of seasonal juvenile recruitment on overall seasonal abundances, we combined the 2 smallest length classes (<5 and 5<10 cm) and examined the relative proportion of these fish to the overall counts, by season, and summed over all surveys for both brown and copper rockfish. The number of juveniles encountered was greatest during the summer for both species, as was the relative proportion of juvenile copper rockfish to the total number of copper rockfish encountered (14%). Brown rockfish juveniles, however, represented the greatest proportion during the winter (9%) (Fig. 4). We used a two-tailed z-test for comparison of 2 proportions to determine whether juvenile rockfishes composed a significantly greater proportion of the total number of fish observed during either summer or winter. The proportion of juvenile brown rockfish was significantly greater in the winter (z=2.2, P<0.05), but the proportions did not differ significantly between summer and winter for copper rockfish (z=1.6, P>0.05) (satisfactory $n*p_i$ >5 and $n[1-p_i]$>5 sample-size tests where n=sample size and p=proportion).

To determine whether there were qualitative differences between brown and copper rockfish that occupied the reef in the summer and winter we divided them into 2 length classes, small (<20 cm) and large (≥20 cm). Summed over all surveys, the densities of both small and large fish were greatest during the summer, and large fish were more abundant than small fish year round (Fig. 5). For both species, the proportion of large fish to the total numbers observed was significantly greater in the winter (z=2.5 [brown rockfish] and 4.2

Table 2

Summary of analysis of variance (ANOVA) comparisons between generalized linear mixed model (GLMM) null models (fish count as the response variable, and year and transect as random effects) and full models (season added as explanatory variable) for seasonal counts of brown and copper rockfish at Point Heyer Artificial Reef, Puget Sound, WA.; AIC=Akaike information criteria; BIC=Bayesian information criteria; df =degrees of freedom.

Model	df	AIC	BIC	Log-likelihood	Deviance	χ^2	χ^2 df	P (>χ^2)
Brown rockfish Null model	3	1032.33	1039.93	–513.17	1026.33			
Brown full								
Full model	6	651.69	666.89	–319.85	639.69	386.64	3	<0.001
Copper rockfish Null model	3	1003.44	1011.04	–498.72	997.44			
Copper rockfish								
Full model	6	795.36	810.55	–391.68	783.36	214.09	3	<0.001

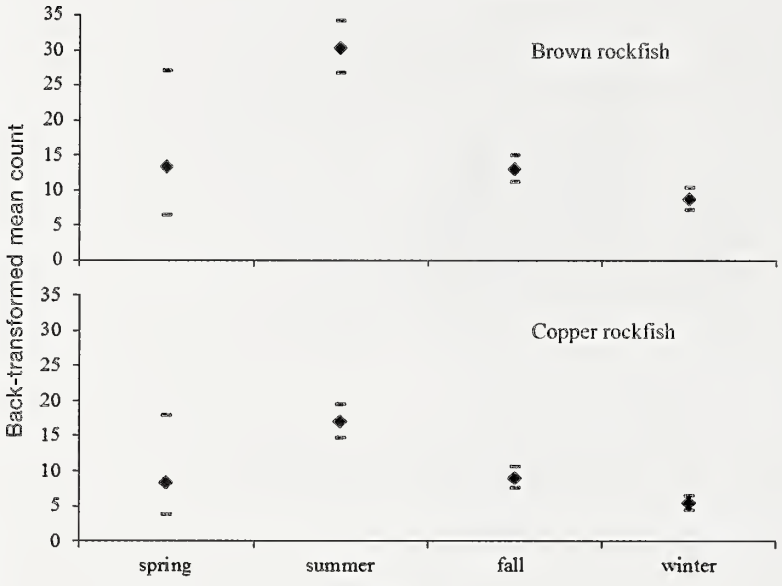

Figure 3

Backtransformed mean counts (summed over 3 transects and all years) and 95% confidence intervals for brown and copper rockfish (*Sebastes auriculatus* and *S. carinus*, respectively) observed at Point Heyer Artificial Reef , Puget Sound, WA, from summer 2005 through summer 2012.

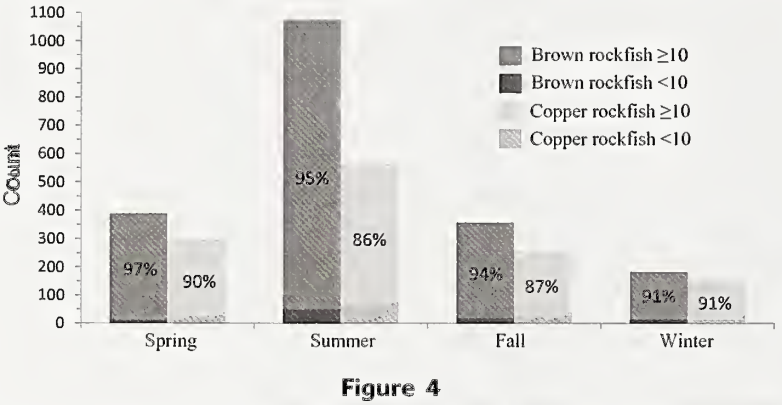

Figure 4

Counts and percent proportions (summed over 3 transects and all years) of brown and copper rockfish (*Sebastes auriculatus* and *S. carinus*, respectively) <10 and ≥10 centimeters (total length) observed at Point Heyer Artificial Reef, Puget Sound, WA, from summer 2005 through summer 2012.

[copper rockfish], $P<0.05$; two-tailed z-test for comparison of 2 proportions; satisfactory $n*p_i>5$ and $n[1-p_i]>5$ sample size tests) (Fig. 6).

Summed over all surveys, a total of 70 late-stage gravid brown and copper rockfish were observed, all of these in the spring and summer. Of the total number of brown rockfish ≥10 cm observed in the spring (N=377) and summer (N=998), 9% and 2%, respectively, were noted as late-stage gravid (we assume that no female rockfish reach maturity at <10 cm [Washington et al.[3]; Gowan, 1983]). Late-stage gravid copper rockfish were only observed during the summer, and of the total number of copper rockfish ≥10 cm observed (493), 3% were noted as late-stage gravid (Fig. 7). If we assume a population sex ratio of 1:1, the percentages double with respect to the total number of potential female spawners. In order to determine whether there were differences in time of spawning by length, we grouped the late-stage gravid brown rockfish into 2 length classes (10<30 and ≥30 cm) on the basis of 50% maturity at approximately 30 cm TL (Love et al., 2002). The proportion of late-stage gravid brown rockfish ≥30 cm to the total numbers of late-stage gravid fish observed in the spring and summer was significantly greater in the spring (z=2.4, $P<0.05$; z-test for comparison of 2 proportions; satisfactory $n*p_i>5$ and $n[1-p_i]>5$ sample-size tests).

Fifty-one (7%) of the 718 brown rockfish ≥10 cm sampled by Hess et al. (2012) were fish that had been recaptured (2 of these were recaptured twice) according to genotype matching. The number of days at liberty between first and final capture ranged from 1 to 1518 (M=615; SD=448.8). Thirty-one fish (4%) ranging in length from 17 to 35 cm (M=27; SD=4.1), including the 2 fish that were recaptured twice, were at liberty for more than one year between first and final capture. A total of 136 (19%) of the 718 samples were from late-stage gravid fish and 12 of those were captured twice in late-stage gravid condition in different years. The number of days at liberty between captures for these fish ranged from 328 to 1469 (M=635; SD=447.2). Overall, the lengths of the late-stage gravid brown rockfish sampled ranged from 21–35 cm (M=27; SD=3.28; includes only the length at time of first capture for fish that were captured twice).

Miniumum and maximum recorded temperatures during 2006–2007 at the near- and offshore margin of the reef ranged from 7.5° to 14.6°C and from 8.1° to 13.4°C, respectively. Mean daily temperature changes were at least twice as great in the spring and summer as they were in the fall and winter at both locations, and daily temperature flucuations tended to be slightly greater at the nearshore margin year-round (Table 3, Fig. 8). The mean monthly air temperatures during the 12-month water temperature recording period were all within 2% of the aver-

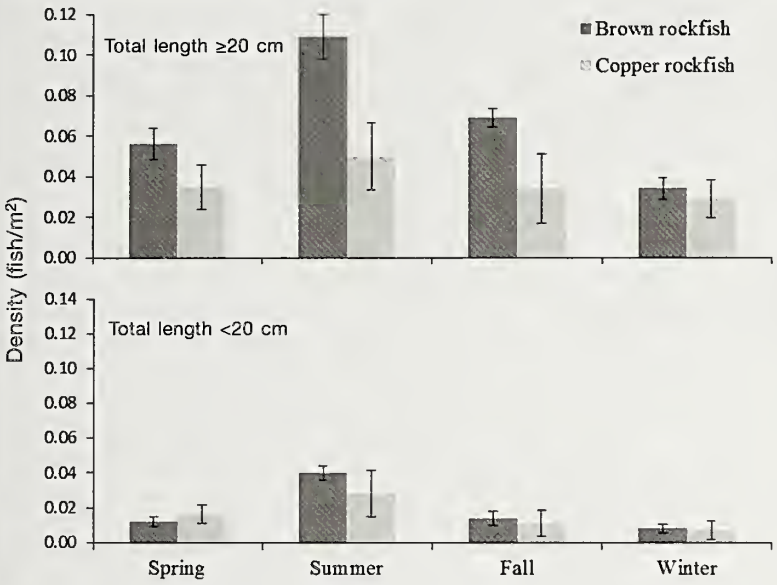

Figure 5

Mean densities and standard errors (summed over 3 transects and all years) for small (< 20 cm in total length [TL]) and large (≥ 20 cm TL) brown and copper rockfish (*Sebastes auriculatus* and *S. carinus*, respectively) observed at Point Heyer Artificial Reef , Puget Sound, WA, from summer 2005 through summer 2012.

age monthly air temperatures summed over a 12-year period beginning in 2000 and recorded at a weather observation station located less than 10 km from PHAR. Our water temperature data were therefore deemed to be an acceptable proxy for trends in seasonal temperature at PHAR during the study.

Discussion

The different sensory inputs that motivate animals to move and the variety of spatiotemporal scales over which movements may occur has led to some blurring among specialists over what constitutes migration (Dingle and Alistair Drake, 2007). The most broadly accepted definitions of fish migration include some element of to-and-fro movement during the life cycle of a fish, and some predictability of occurrence. Heape (1931) described migration as, "...that class of movement which impels migrants to return to the region from which they have migrated." Harden Jones (1984) defines fish migration as "...a coming and going with the seasons on a regular basis..." Migration is usually distinguished from emigration (a form of dispersal), whereby return to an area does not occur (Lidicker and Stenseth, 1992), or occurs only by chance. Adding confusion (or clarity, depending on one's perspective) to characterizing fish movement is the concept of home range (Burt 1943). According to McLoughlin and Ferguson (2000), home range is established once the cumulative area that is used ceases to increase over time (i.e., an asymptote is reached). However, and consistent with Burt (1943), it is generally accepted that home ranges comprise only those areas within which routine activities occur over finer temporal scales, and that they do not include infrequent spatially broad-scaled movements, migration corridors, or the movements of planktonic life history phases for which the total area used may not reach an asymptote over time.

We have shown that both brown and copper rockfish exhibited pronounced changes in abundance between summer and winter at PHAR, that the changes occurred with regularity over a broad time span, and that the observed patterns were similar for both species. Whether the seasonal changes in abundance reflect migratory behavior hinge on whether the same fishes return to repopulate the reef during the summer. If, for instance, fish populations disperse over broad geographic areas while overwintering in deeper water and return to shallower water without predilection toward

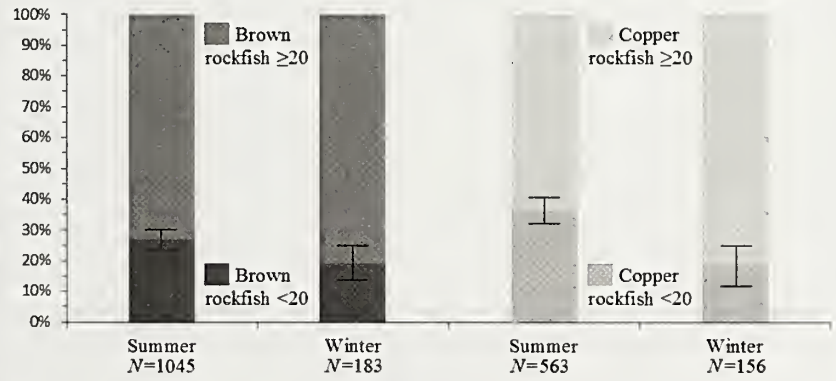

Figure 6

Relative proportions of large (≥20 cm in total length [TL]) and small (<20 cm TL) brown and copper rockfish (*Sebastes auriculatus* and *S. carinus*, respectively) to the total number (*N*) of fish observed for each species at Point Heyer Artificial Reef, Puget Sound, WA, during summer and winter from 2005 through 2012. Whiskers denote the 95% confidence intervals for the *z*-test comparisons of the 2 proportions.

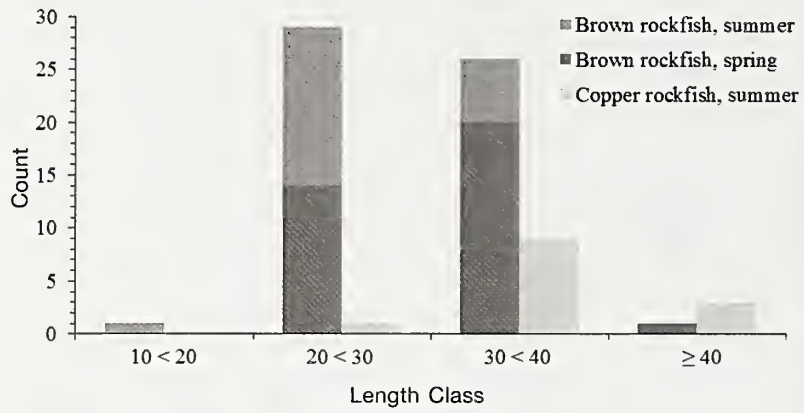

Figure 7

Total numbers (summed over 3 transects) of visually apparent late-stage gravid brown and copper rockfish (*Sebastes auriculatus* and *S. carinus*, respectively) by length class (total lengths in centimeters) observed during seasonal surveys at Point Heyer Artificial Reef, Puget Sound, WA, from summer 2005 through summer 2012. Note: Late-stage gravid copper rockfish were observed only during the summer, and late-stage gravid brown rockfish were observed only in the spring and summer.

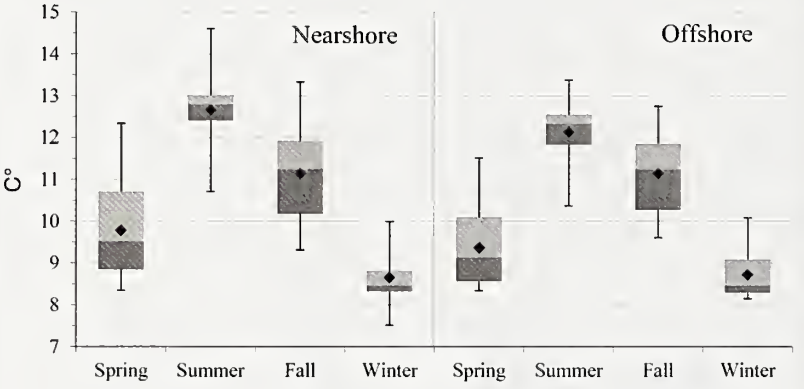

Figure 8

Temperatures at the near- and offshore reef margin, by season, at Point Heyer Artificial Reef, Puget Sound, WA, during 2006–2007. Whiskers indicate the minimum and maximum temperatures recorded, boxes capture the first and third quartiles, and the mean is denoted by a diamond shape.

their nearshore point of departure, then the behavior may be characterized as emigrative (Heape, 1931). Moreover, if emigrant populations lose their cohesiveness once they leave the reef, the seasonal return of itinerant individuals to the nearshore environment would result in an annual shuffling of members among geographically proximate, or possibly even distant, populations. Whether emigrants wander as groups or individuals, their return to the nearshore environment could serve to replenish local populations with harvest-size fishes, and may provide a buffer against localized overfishing provided they arrive from populations that are capable of sustaining a net export of individuals (i.e., source populations sensu stricto Pulliam, 1988). Conversely, local populations made up predominantly of seasonal migrants may be more vulnerable to depletion because replenishment would be less dependent on harvest-sized immigrants and more dependent on reproductive success and juvenile recruitment, both of which are known to be highly variable for rockfishes (Leaman and Beamish 1984; Ralston and Howard 1995; Ralston et al., 2013). We note here that the aforesaid statement lies in contrast to Mathews and Barker's (1983) view that local populations of "migratory" rockfishes would be less vulnerable to depletion; however, their opinion appears to have been formed around an implied working definition of migration that includes any type of movement beyond a narrowly defined geographic area, and without regard to whether the same fish are coming and going. This contrast in conclusions serves to underscore the importance of adequately defining the terms used to characterize fish movements.

We could not determine whether the brown rockfish recaptures identified by Hess et al. (2012) that were at liberty for more than one year remained on the reef year-round or left the reef in the winter and returned during the summer (i.e., migrated), although only one of the fish was recaptured in the winter. The recapture data indicate some degree of reef fidelity for some brown rockfish at PHAR. The relatively low abundance of brown rockfish on the reef during the winter, the year-round sampling effort, and the high rate of recapture in relation to effort lend substantial credence to the notion of seasonal movements by individuals on and off the reef over spatial scales that exceed reported maximum home ranges. Further, the 12 genetically identified brown rockfish that were encountered as late-stage gravid individuals in multiple years indicate that more than one spawning by the same fish occurred at the same location (assuming the fish carried their larvae through to parturition).

Diver effects on fish behavior can be a significant source of bias when producing estimates of standing stock or community structure by using noninstantaneous UVCs (i.e., strip transects) (see Bozec et al., 2011 and references therein). In this study, we assumed that bias due to diver effects remained constant over time

Table 3

Maximum and mean daily temperature (t) (°C) changes (Δt) by season recorded at the near- and offshore reef margins of Point Heyer Artificial Reef, Puget Sound, WA, during 2006–2007. SD=standard deviation.

	Spring		Summer		Fall		Winter	
Reef margin	24 hr max. Δt	Mean daily Δt (SD)	24 hr max. Δt	Mean daily Δt (SD)	24 hr max. Δt	Mean daily Δt (SD)	24 hr max. Δt	Mean daily Δt (SD)
Nearshore	2.2	0.7 (0.44)	2.1	0.8 (0.44)	1.1	0.3 (0.21)	1.1	0.2 (0.22)
Offshore	1.6	0.4 (0.31)	1.7	0.6 (0.32)	0.6	0.2 (0.14)	0.8	0.2 (0.19)

and thus was not a factor in assessing relative changes in abundance. Tides were also not judged to be a factor because the numbers of summer and winter surveys by tide cycle were not substantially different. Although rockfish are popular among Puget Sound anglers, recreational harvest was considered an unlikely source of bias, and commercial rockfish harvest is prohibited in central Puget Sound. From spring of 2005 through fall of 2006 the reef was closed to all rockfish retention. From fall of 2006 through spring of 2010, the rockfish season and retention rules were highly restrictive in Puget Sound, and PHAR attracted very few anglers. The minimal harvest that did occur took place during the summer, when rockfish abundance was highest. Since May of 2010, recreational rockfish retention throughout nearly all of Puget Sound, including PHAR and adjacent waters, has been prohibited. Effects from potential diel movements were also dismissed as a source of bias in estimating rockfish densities because all surveys were conducted approximately halfway between sunrise and mid-day.

Moulton (1977) observed a winter decrease in copper rockfish densities over the course of scuba surveys of nearshore rocky reefs in north Puget Sound. On the basis of seasonal density differences, over multiple depth strata, he concluded that over-wintering in deeper water beyond the survey range of his study was the most likely explanation. Richards (1987), observing a similar trend over rocky habitats, offered an alternative explanation. She postulated that reduced activity and more cryptic behavior by copper rockfish during winter months can lead to lower abundance estimates from scuba surveys over rocky habitat. This hypothesis is consistent with Patten's (1973) observation that copper rockfish on a small low-relief rocky reef in Puget Sound were more thigmotactic in the winter and spring. Similar behavior has been noted for dusky (*S. ciliates*) and yellowtail (*S. flavidus*) rockfish surveyed by scuba divers in southeast Alaska (Carlson and Barr, 1977). In reference to Richards' (1987) observation, Matthews (1990c) noted that winter decreases in brown and copper rockfish abundance had been observed in the nearshore environment of Puget Sound over sparsely vegetated low-relief reefs and sandy-bottom habitat, where hiding space is limited or nonexistent. The same author, however, also reported that brown and copper rockfish were more reclusive on high-relief reefs during the winter (Matthews, 1990a).

To ensure that our observed winter decreases in abundance were not due to fish moving into the interstices of the reef and beyond our vision, divers equipped with digging and prying tools searched for fish by excavating several off-transect boulder and cobble sites during the winter months. The excavations occasionally revealed rockfish that could have gone unnoticed with the use of our standard survey method, but the encounters were rare and we do not believe that they occurred with enough frequency to explain the marked decreases in abundance we observed during the winter. Also, several surveys, with roving divers covering distances of up to 2.5 km of the nearshore waters adjacent to and on either side of PHAR, were conducted during the winter in order to ascertain whether winter decreases in abundance might have been due to fish moving off the reef but remaining nearby within the same depth strata. No rockfish were encountered during any of these off-reef surveys. It was also possible that fish may have been crowding the deepest parts of the reef (beyond our maximum survey depth) during the winter. We conducted several winter dives along the deep offshore margin of the reef and found no evidence to indicate that fish remained, though at greater depths than those surveyed, on or near the reef during the winter.

For some fish species, seasonal changes in abundance may be attributed to an influx of juveniles that leads to higher counts during certain times of the year (Allen and Horn, 1975; Relini et al., 1994, Allen et al., 2002, Barreiros et al., 2004). In our study, although the proportion of juvenile brown rockfish was significantly greater in the summer, juveniles of both species (length <10 cm) accounted for a very small proportion of the overall counts by season. Young-of-the-year fish made up an even smaller proportion because the <10 cm length class would have included some fish that were greater than 1 year in age. We conclude that the seasonal changes in abundance that we observed were not due to juvenile recruitment. The higher overall number of copper than brown rockfish juveniles observed during the spring, summer, and fall is likely due to

the highly successful recruitment of juvenile copper rockfish observed in Puget Sound in 2006 (LeClair et al., 2007; Palsson et al., 2012). Although the numbers of juveniles did not influence the overall pattern of change in seasonal abundance for either species, juvenile recruits during one or more years may have been plentiful enough to account for the overall statistically significant greater proportion of small fish (< 20 cm) observed in the summer. Other potential explanations for the disproportion include seasonal mortality, predation, and movement.

Washington et al.[3] and Gowan (1983) reported female first-spawning lengths for both brown and copper rockfish in Puget Sound to be in excess of 20 cm (age 3–4 years) and our observations at PHAR are in general agreement, although a single late-stage gravid brown rockfish less than 20 cm was encountered in our study and we have observed late-stage gravid brown rockfish elsewhere in Puget Sound as small as 18 cm (determined by cannulation). All of the late-stage gravid brown rockfish sampled by Hess at al. (2012) were in excess of 20 cm. In our study, the percentages of late-stage gravid rockfish in relation to the number of potential female spawners are conservative because some fish ≥10 cm would not have reached maturity. The higher numbers of late-stage gravid brown rockfish encountered by Hess et al. (2012) than the numbers we observed reflect an intentional sampling bias toward gravid rockfish in their study.

We observed more late-stage gravid brown rockfish in the spring (N=35) than in the summer (N=22). The larger length classes comprised a statistically significant greater proportion of the spring observations, and this is consistent with Bobko and Berkeley (2004) and Love et al. (1990), who found that parturition occurs earlier for older black (*S. melanops*) and yellowtail rockfish. Cooper (2004) also found the same to be true for copper rockfish in Puget Sound. Because of sampling bias, we did not examine length-by-season for the late-stage gravid brown rockfish sampled by Hess et al. (2012). Nevertheless, the mean length of the late-stage gravid fish sampled in that study falls near the center of the length class that accounted for most of our observations of late-stage gravid brown rockfish. In Puget Sound, peak parturition is known to occur earlier in the year for copper rockfish than for brown rockfish (DeLacy et al.[10]; Washington et al.[3]). Curiously, we did not observe any late-stage gravid copper rockfish in the spring at PHAR. Of the 13 late-stage gravid copper rockfish observed, 10 were encountered during the final 2 years of the study and only 2 of those were in the largest length class. On the basis of length-frequency changes over time and a substantial increase in copper rockfish abundance over the study period after 2006, we surmise that most of the observed late-stage gravid copper rockfish belonged to the strong 2006 year class noted above. If so, they were just reaching maturity during the final years of the study and may have been spawning later in the season, as has been noted for black, yellowtail, and copper rockfish (see above).

Consistent with many habitat selection models, the results of Matthews (1990a, 1990b) indicated that the apparent homing ability of some rockfish species may enable them to embark on periodic exploratory excursions in response to unfavorable changes in habitat, allowing them to assess other environments but return to their point of departure if more suitable surroundings are not encountered. Matthews (1990c) further noted that the winter disappearance of canopy-forming bull kelp, with the structure and associated prey it provided, may have explained the seasonal exodus of brown and copper rockfish she observed on naturally formed low-relief reefs. Although bull kelp does not occur at PHAR, the seasonal presence of non-floating seaweeds may provide similar levels of refuge and prey. The study areas of Matthews (1990c) included a high-relief artificial reef (Boeing Creek Artificial Reef) also located in the main basin of Puget Sound. The reef is comparable in age, size, depth, and construction to PHAR; is subject to similar wave energy, current, and temperature regimes; and supports a similar ichthyofauna and flora that is devoid of canopy-forming kelp. However, the highest densities of >20 cm brown and copper rockfish recorded by Matthews at that site occurred during the fall and winter, not during the summer as observed in our study.

Resiliency to temperature fluctuations is not known for copper rockfish. However, Wilson et al. (1974) studied metabolic compensation in response to temperature in brown rockfish, and vermilion rockfish (*S. miniatus*). This latter species resides below the thermocline and is therefore not exposed to the same seasonal temperature fluctuations experienced by brown rockfish residing above the thermocline. Wilson et al. concluded that there are metabolic differences between the 2 species that correlate with differences in depth distribution, and that brown rockfish have a higher capacity to acclimate over a wider range of temperatures. Both brown and copper rockfish have a similar biological range, occurring from the subtropics to the subarctic (Horn et al., 2006) and are found in warmer inland seas, as well as colder oceanic waters (Love et al., 2002). The mean daily recorded temperature changes at PHAR were highest during the spring when both species began appearing on the reef, and during the summer when they appeared on the reef in their greatest abundance. Although we do not have temperature data beyond the offshore perimeter of the reef, water column data (available at website) in East Passage conducted by the Washington State Department of Ecology indicate that diurnal and seasonal temperature regimes become less labile with increasing depth. If, as noted by Neill and Gallaway 1989, fish move in response to the totality of

[10]DeLacy, A. C., C. R. Hitz, and R. L. Dryfoos. 1964. Maturation, gestation, and birth of rockfish (Sebastodes) from Washington and adjacent waters. Wash. Dep. Fish. Fish. Res. Pap. 2:51-67.

their environment and not to any single environmental factor in isolation (e.g., temperature), we consider it unlikely that either species moved on and off the reef in direct response to temperature alone, especially given that they would be leaving the relatively stable thermal environment of deeper water for the more broadly fluctuating temperatures encountered over the reef during the spring and summer.

We hypothesize on the basis of our survey findings and the evidence gleaned from Hess et al. (2012) that the observed changes in abundance of brown and copper rockfish at PHAR are the result of seasonal relocations of these species to different migratory destinations beyond their home ranges; most likely in response to reduced refuge space and prey density (e.g., due to reduced macroalgal cover and associated prey) during the winter months. Behaviors associated with spawning and mating may also play a crucial role in determining the seasonal movements and spatial distributions for these 2 rockfish species. The statistically significant greater proportion of large brown and copper rockfish present on the reef during the winter could be attributed to an overall suboptimal year-round habitat that is interspersed with enclaves of microhabitats suitable for year-round occupancy and that are held more successfully by larger territorial fishes.

The applicability of our hypothesis to brown and copper rockfish populations elsewhere in Puget Sound is unclear. If habitat quality is correlated with rockfish movement, behavioral variability among local populations is likely to be high and our observed seasonal changes in abundance would not be conserved across sites. If, as proposed by Matthews et al. (1987), there is a relationship between habitat quality and rockfish movement on and off reefs, determining the timing and magnitude of seasonal variability in rockfish abundance at different sites could prove to be a useful means for ranking the relative importance of those sites for rockfish conservation efforts. This research could be critical for establishing MPAs and for determining the spatial scales over which protection should be afforded.

Exploitation of aggregating behavior by fisheries, such as often occurs with cods, forage fish, and other species, may be detrimental to the recovery of declining rockfish stocks if the aggregations are composed of migrant adults. Fishery managers may wish to consider the potential for, and management implications of, local rockfish migratory behavior. Concentrating fisheries in the nearshore environment during times of year when migratory rockfish are present could result in the depletion of local populations, particularly if aggregations are linked to spawning, courtship, or mating behavior.

Generalized linear mixed-effects models, parameterized with spatially and temporally explicit habitat, prey availability, and movement data could aid researchers in identifying the key habitat attributes and environmental indicators that characterize essential habitat for these and other fish species.

Acknowledgments

We thank R. Buckley and T. Parra for assisting with data collection during the transect survey dives. Diver surface support was provided by P. Campbell, W. Dezan, R. Heikkila, L. Hiller, J. Hoback, W. Morris, B. Power, S. Reszczynski, J. Rohr, M. Ulrich, and T. Wilson. We are grateful to M. Hess for generously providing the genetic recapture data. Expert assistance with the statistical analyses and interpretation was provided by K. Fenske. We thank L. Hillier, D. Lowry, R. Pacunski, and 3 anonymous reviewers for providing helpful comments on an earlier draft.

Literature cited

Allen, L. G., and M. H. Horn.
1975. Abundance, diversity and seasonality of fishes in Colorado Lagoon, Alamitos Bay, California. Estuar. Coast. Mar. Sci. 3:371–380.

Allen, L. G., A. M. Findlay, and C. M. Phalen.
2002. Structure and standing stock of fish assemblages of San Diego Bay, California from 1994 to 1999. Bull. South. Calif. Acad. Sci. 101:49–85.

Attwood, C. G., and B. A. Bennett.
1995. Modelling the effect of marine reserves on the recreational shore-fishery of the South-Western Cape, South Africa. S. Afr. J. Mar. Sci. 16:227–240.

Barreiros, J. P., V. Figna, M. Hostim-Silva, and R. S. Santos.
2004. Seasonal changes in a sandy beach assemblage at Canto Grande, Santa Catarina, South Brazil. J. Coast. Res. 20:862–870.

Bates, D., M. Maechler, B. Bolker, and S. Walker.
2015. Fitting linear mixed-effects models using lme4. J. Stat. Softw. 67(1):1–48.

Berezansky, L., L. Idels, and M. Kipnis.
2011. Mathematical model of marine protected areas. IMA J. Appl. Math. 76:312–325.

Bobko, S. J., and S. A. Berkeley.
2004. Maturity, ovarian cycle, fecundity, and age-specific parturition of black rockfish (*Sebastes melanops*). Fish. Bull. 102:418–429.

Bozec, Y-M., M. Kulbicki, F. Laloë, G. Mou-Tham, and D. Gascuel.
2011. Factors affecting the detection distances of reef fish: implications for visual counts. Mar. Biol. 158:969–981.

Buckley, R. M.
1982. Marine habitat enhancement and urban recreational fishing in Washington. Mar. Fish. Rev. 44(6–7):28–37.

Buckley, R. M., and G. J. Hueckel.
1985. Biological processes and ecological development on an artificial reef in Puget Sound, Washington. Bull. Mar. Sci. 37:50–69.

Burt, W. H.
1943. Territoriality and home range: Concepts as applied to mammals. J. Mammal. 24:346–352.

Carlson, R. H., and L. Barr.
1977. Seasonal changes in spatial distribution and activity of two species of Pacific rockfishes, *Sebastes flavidus* and *S. ciliates*, in Lynn Canal, southeastern Alaska. Mar. Fish. Rev. 39(3):23–24.

Clark, R. D., S. Pittman, C. Caldrow, J. Christensen, B. Roque, R. S. Appeldoorn, and M. E. Monaco.
2009. Nocturnal fish movement and trophic flow across habitat boundaries in a coral reef ecosystem (SW Puerto Rico). Caribb. J. Sci. 45:282–303.

Condal, F., J. Aguzzi, F. Sardà, M. Nogueras, J. Cadena, C. Costa, J. Del Río, and A. Mànuel.
2012. Seasonal rhythm in a Mediterranean coastal fish community as monitored by a cabled observatory. Mar. Biol. 159:2809–2817.

Cooper, D.
2003. Possible differences in copper rockfish (*Sebastes caurinus*) fecundity and parturition with maternal size and age. Master's thesis, 64 p, Univ. Washington, Seattle, WA.
2004. Earlier parturition in older copper rockfish (*Sebastes caurinus*) in the San Juan Islands, Washington. *In* Proceedings of the 2003 Georgia Basin/Puget Sound research conference; Vancouver, Canada, 31 March–3 April 2003 (T. W. Droscher and D. A. Fraser, eds.), 5 p. [Available at website.]

Dewees, C. M., and D. W. Gotshall.
1974 An experimental artificial reef in Humboldt Bay, California. Calif. Fish Game 60:109–127.

Diamond, J. M.
1975. The island dilemma: lessons of modern biogeographic studies for the design of natural reserves. Biol. Conserv. 7:129–146.

Dingle, H., and V. Alistair Drake.
2007. What is migration? BioScience 57:113–121.

Ebbesmeyer, C. C., C. A. Coomes, J. M. Cox, J. M. Helseth, L. R. Hinchey, G. A. Cannon, and C. A. Barnes.
1984. Synthesis of current measurements in Puget Sound, Washington, vol. 3. Circulation in Puget Sound: an interpretation based on historical records of currents. NOAA Tech. Memo. NOS OMS 5, 73 p.

Eisenhardt, E.
2004. Acoustic telemetry of rocky reef fish home range to evaluate marine protected area size. *In* Proceedings of the 2003 Georgia Basin/Puget Sound Research Conference; Vancouver, Canada, 31 March–3 April 2003 (T. W. Droscher and D. A. Fraser, eds.), 18 p. [Available at website.]

Frank, K. T.
1992. Demographic consequences of age-specific dispersal in marine fish populations. Can. J. Fish. Aquat. Sci. 49:2222–2231.

Fréon, P., F. Gerlotto, and O. A. Misund.
1993. Consequences of fish behaviour for stock assessment. ICES Mar. Sci. Symp. 196:190–195.

Gayanilo, F. C., Jr., and D. Pauly (eds).
1997. FAO-ICLARM stock assessment tools (FiSAT): reference manual. FAO Comput. Inf. Ser. (Fish.) No. 8, 262 p. FAO, Rome.

Gowan, R. E.
1983. Population dynamics and exploitation rates of rockfish (*Sebastes* spp) in central Puget Sound, Washington. Ph.D. dissertation, 90 p. Univ. Washington, Seattle, WA.

Hallacher, L. E.
1977. Patterns of space and food use by inshore rockfishes (Scorpaenidae: *Sebastes*) of Carmel Bay, California. Ph.D. dissertation, 115 p. Univ. California Berkeley, Berkeley, CA.

Hanan, D. A., and B. E. Curry.
2012. Long-term movement patterns and habitat use of nearshore groundfish: tag-recapture in central and southern California waters. The Open Fish Science Journal 5:30–43.

Hannah, R. W., and P. S. Rankin.
2011. Site fidelity and movement of eight species of Pacific rockfish at a high-relief rocky reef on the Oregon coast. North Am. J. Fish. Manage. 31:483–494.

Harden Jones, F. R.
1968. Fish migration, 325 p. Edward Arnold, London.
1984. A view from the ocean. *In* Mechanisms of migration in fishes (J. D. McCleave, G. P. Arnold, J. J. Dodson, and W. H. Neill, eds.), p. 1–26. Plenum Press, New York.

Hartmann, A. R.
1987. Movement of scorpionfishes (Scorpaenidae: *Sebastes* and *Scorpaena*) in the southern California Bight. Calif. Fish Game 73:68–79.

Heape, W.
1931. Emigration, migration, and nomadism, 368 p. W. Heffer and Sons, Cambridge, UK.

Hess, M. A., J. G. Rhydderch, L. L. LeClair, R. M. Buckley, M. Kawase, and L. Hauser.
2012. Estimation of genotyping error rate from repeat genotyping, unintentional recaptures and known parent–offspring comparisons in 16 microsatellite loci for brown rockfish (*Sebastes auriculatus*). Mol. Ecol. Resour. 42:893–901.

Hilborn, R., and C. J. Walters (eds.).
1992. Quantitative fisheries stock assessment: choice, dynamics and uncertainty, 570 p. Chapman and Hall, New York.

Horn, M. H., L. G. Allen, and R. N. Lea.
2006. Biogeography. *In* The ecology of marine fishes: California and adjacent waters (L. G. Allen, D. J. Pondella II, and M. H. Horn, (eds.), p. 3–25. Univ. California Press, Berkeley, CA.

Jagielo, T. H.
1990. Movement of tagged lingcod *Ophiodon elongatus* at Neah Bay, Washington. Fish. Bull. 88:815–820.
1995. Abundance and survival of lingcod at Cape Flattery, Washington. Trans. Am. Fish. Soc. 124:170–183.

Lea, R. N., R. D. McAllister, and D. A. VenTresca.
1999. Biological aspects of nearshore rockfishes of the genus *Sebastes* from central California with notes on ecologically related sport fishes. Calif. Fish Game Fish Bull. 177, 109 p.

Leaman, B. M., and R. J. Beamish.
1984. Ecological and management implications of longevity in some Northeast Pacific groundfishes. Bull. Int. North Pac. Fish. Comm. 42:85–97.

LeClair, L. L., R. Buckley, W. Palsson, R. Pacunski, T. Parra, O. Eveningsong, J. Beam, and M. McCallum.
2007. A remarkable settlement of young-of-the-year rockfishes in Puget Sound and the Strait of Juan de Fuca in 2006 [abstract]. Proceedings of the 2007 Georgia Basin Puget Sound Research Conference; Vancouver, Canada, 26–29 March. [Available at website.]

Lidicker, W. Z., Jr., and N. C. Stenseth.
1992. To disperse or not to disperse: who does it and why? *In* Animal dispersal: small mammals as a model (N. C. Stenseth and W. Z. Lidicker, eds.), p. 21–36. Chapman and Hall, New York.

Loher, T.
2011. Analysis of match–mismatch between commercial fishing periods and spawning ecology of Pacific halibut (*Hippoglossus stenolepis*), based on winter surveys and behavioural data from electronic archival tags. ICES J. Mar. Sci. 68:2240–2251.
Longabach, L. J.
2010. Movement of selected nearshore temperate reef fishes along California's central coast. M.Sc. thesis, 69 p. Calif. Polytech. State Univ., San Luis Obispo, CA.
Love, M. S., P. Morris, M. McCrae, and R. Collins.
1990. Life history aspects of 19 rockfish species (Scorpaenidae: *Sebastes*) from the Southern California Bight. NOAA Tech. Rep. NMFS 87, 38 p.
Love, M. S., M. Yoklavich, and L. Thorsteinson.
2002. The rockfishes of the northeast Pacific, 414 p. Univ. California Press, Los Angeles, CA.
Lowe, C. G., K. M. Anthony, E. T. Jarvis, L. F. Bellquist, and M. S. Love.
2009. Site fidelity and movement patterns of groundfish associated with offshore petroleum platforms in the Santa Barbara Channel. Mar. Coast. Fish. 1:71–89.
Mathews, S. B., and M. W. Barker.
1983. Movements of rockfish (*Sebastes*) tagged in northern Puget Sound, Washington. Fish. Bull. 82:916–922.
Matthews, K. R.
1985. Species similarity and movement of fishes on natural and artificial reefs in Monterey, California. Bull. Mar. Sci. 37:252–270.
1990a. An experimental study of the habitat preferences and movement patterns of copper, quillback, and brown rockfishes (*Sebastes* spp.). Environ. Biol. Fish. 29:161–178.
1990b. A telemetric study of the home ranges and homing routes of copper and quillback rockfishes on shallow rocky reefs. Can. J. Zool. 68:2243–2250.
1990c. A comparative study of habitat use by young-of-the-year, subadult, and adult rockfishes on four habitat types in central Puget Sound. Fish. Bull. 88:223–239.
Matthews, K. R., B. S. Miller, and T. P. Quinn.
1987. Movement studies of nearshore demersal rockfishes in Puget Sound, Washington. *In* Proc. Int. Rockfish Symp.; Anchorage, AK, 20–22 October 1986, p. 63–72. Alaska Sea Grant Rep. 87-2, University of Alaska, Anchorage, AK.
McCleave, J. D., G. P. Arnold, J. J. Dodson, and W. H. Neill (eds.).
1984. Mechanisms of migration in fishes, 574 p. Plenum Press, New York.
McKeown, B. A.
1984. Fish migration, 224 p. Timber Press, Portland, OR.
McLoughlin, P. D., and S. H. Ferguson.
2000. A hierarchical pattern of limiting factors helps explain variation in home range size. Ecoscience 7:123–130.
Merz, J. E., and P. B. Moyle.
2006. Salmon, wildlife, and wine: marine-derived nutrients in human-dominated ecosystems of central California. Ecol. Appl. 16:999–1009.
Methot, R. D.
2011. User manual for Stock Synthesis, vers. 3.23b. NOAA Fisheries, Seattle, WA. [Available at website, accessed June 2012.]
Miller, D. J. and J. J. Geibel.
1973. Summary of blue rockfish and lingcod life histories; a reef ecology study; and giant kelp, *Macrocystis pyrifera*, experiments in Monterey Bay, California. Calif. Fish Game Fish Bull. 158, 137 p.
Miller, D. J., M. W. Odemar, and D. W. Gotshall.
1967. Life history and catch analysis of the blue rockfish (*Sebastodes mystinus*) off central California, 1961–1965. Calif. Fish Game, MRO Ref. No. 67-14, 130 p.
Moulton, L. L.
1977. An ecological analysis of fishes inhabiting the rocky nearshore regions of northern Puget Sound, Washington. Ph.D. diss., 145 p. Univ. Washington, Seattle, WA.
Neill, W. H. and B. J. Gallaway.
1989. "Noise" in the distributional responses of fish to environment: an exercise in deterministic modeling motivated by the Beaufort Sea experience. Biol. Pap. Univ. Alaska 24:123–130.
Parker, S. J., S. A. Berkley, J. T. Golden, D. R. Gunderson, J. Heifetz, M. A. Hixon, R. Larson, B. M. Leaman, M. S. Love, J. A. Musick, V. M. O'Connell, S. Ralston, H. J. Weeks, and M. M. Yoklavich.
2000. Management of Pacific rockfish. Fisheries 25:22–29.
Patten, B. G.
1973. Biological information on copper rockfish in Puget Sound, Washington. Trans. Am. Fish. Soc. 102:412–416.
Palsson, W.A., R. E. Pacunski, T. R. Parra, and J. Beam.
2012. Jackpot recruitment and conservative management effects on rockfish abundance inside and outside marine reserves in Puget Sound [abstract]. *In* Rockfish recovery in the Salish Sea; research and management priorities: a workshop; Seattle, 28–29 June 2011 (D. Tonnes, ed.), p. 73. Natl. Mar. Fish. Serv., Seattle, WA.
Pittman, S. J., and C. A. McAlpine.
2003. Movements of marine fish and decapods crustaceans: process, theory and application. Adv. Mar. Biol. 44:205–294.
Pulliam, H. R.
1988. Sources, sinks and population regulation. Am. Nat. 132:652–661.
R Core Team.
2014. R: a language and environment for statistical computing. R Foundation for Statistical Computing, Vienna, Austria. [Available at website.]
Ralston, S., K. M. Sakuma, and J. C. Field.
2013. Interannual variation in pelagic juvenile rockfish (*Sebastes* spp.) abundance—going with the flow. Fish. Oceanogr. 22:288–308.
Ralston, S., and D. F. Howard.
1995. On the development of year-class strength and cohort variability in two northern California rockfishes. Fish. Bull. 93:710–720.
Rankin, P. S., R. W. Hannah, and M. T. O. Blume.
2013. Effect of hypoxia on rockfish movements: implications for understanding the roles of temperature, toxins and site fidelity. Mar. Ecol. Prog. Ser. 492:223–234.
Relini, M., G. Torchia, and G. Relini.
1994. Seasonal variation of fish assemblages in the Loano Artificial Reef (Ligurian Sea Northwestern-Mediterranean). Bull. Mar. Sci. 55:401–417.
Reynolds, B. F., S. P. Powers, and M. A. Bishop.
2010. Application of acoustic telemetry to assess residency and movements of rockfish and lingcod at created and

natural habitats in Prince William Sound. PLoS ONE 5(8):e12130.

Richards, L .J.
1987. Copper rockfish (*Sebastes caurinus*) and quillback rockfish (*Sebastes maliger*) habitat in the Strait of Georgia, British Columbia. Can. J. Zool. 65:3188–3191.

Roberts, C. M., and H. Sargant.
2002. Fishery benefits of fully protected marine reserves: why habitat and behavior are important. Nat. Resour. Model. 15:487–507.

Rothschild, B. J.
1986. Dynamics of marine fish populations, 277 p. Harvard Univ. Press, Cambridge, MA.

Seeb, L. W.
1998. Gene flow and introgression within and among three species of rockfishes, *Sebastes auriculatus*, *S. Caurinus*, and *S. maliger*. J. Hered. 89:393–403.

Schwenke, P.
2012. History and extent of introgressive hybridization in Puget Sound rockfishes (*Sebastes auriculatus, S. caurinus, and S. maliger*). M.Sc. thesis, 77 p. Univ. Washington, Seattle, WA.

Simberloff, D., and L. G. Abele.
1982. Refuge design and island biogeographic theory: effects of fragmentation. Am. Nat. 120:41–50.

Smith, R. J. F.
1985. control of fish migration (Zoophysiology, vol. 17), 243 p. Springer-Verlag, Berlin.

Sparre, P., and S. C. Venema.
1998. Introduction to tropical fish stock assessment. Part 1. Manual. FAO Fish. Tech. Pap. 306/1, rev. 2, 407 p. FAO, Rome.

Stout, H. A., B. B. McCain, R. D. Vetter, T. L. Builder, W. H. Lenarz, L. L. Johnson, and R. D. Methot.
2001. Status review of copper rockfish (*Sebastes caurinus*), quillback rockfish (*S. maliger*), and brown rockfish (*S. auriculatus*) in Puget Sound, Washington. NOAA Tech. Memo. NOAA-NMFS-NWFSC TM-46, 158 p.

Tolimieri, N., K. Andrews, G. Williams, S. Katz, and P. S. Levin.
2009. Home range size and patterns of space use by lingcod, copper rockfish and quillback rockfish in relation to diel and tidal cycles. Mar. Ecol. Prog. Ser. 380:229–243.

Willis, T. J., R. B. Millar, R. C. Babcock, and N. Tolimieri.
2003. Burdens of evidence and the benefits of marine reserves: putting Descartes before des horse? Environ. Conserv. 30:97–103.

Wilson, F. R., G. Somero, and C. L. Prosser.
1974. Temperature-metabolism relations of two species of *Sebastes* from different thermal environments. Comp. Biochem. Physiol. B 47:485–491.

Wyllie-Echeverria, T., and M. Sato.
2005. Rockfish in San Juan County—recommendations for management and research. *In* Proceedings of the 2005 Puget Sound Georgia Basin Research Conference; Seattle, 29–31 March, 4 p. [Available at website.]

Yoklavich, M. M. (ed.).
1998. Marine harvest refugia for West Coast rockfish: a workshop. NOAA Tech. Memo. NOAA-TM-NMFS-SWFSC-255, 159 p.

NOAA
National Marine
Fisheries Service

Fishery Bulletin
established 1881

Spencer F. Baird
First U.S. Commissioner
of Fisheries and founder
of *Fishery Bulletin*

Feeding habits of 2 reef-associated fishes, red porgy (*Pagrus pagrus*) and gray triggerfish (*Balistes capriscus*), off the southeastern United States

Sarah F. Goldman (contact author)
Dawn M. Glasgow
Michelle M. Falk

Email address for contact author: sarahfgoldman@gmail.com

South Carolina Department of Natural Resources
P.O. Box 12559
Charleston, South Carolina 29422-2559

Abstract—The feeding habits of red porgy (*Pagrus pagrus*) and gray triggerfish (*Balistes capriscus*) were investigated by examining the gut contents of specimens collected during 2009–2011 from live bottom habitats off the southeastern United States. Red porgy had a diverse diet of 188 different taxa. Decapods, barnacles, and bivalves were their main prey. Canonical correlation analysis indicated that depth, season, and fish length were statistically significant factors determining the degree of variability in the diet of red porgy. Gray triggerfish also had a diverse diet, composed of 131 different prey taxa. Barnacles, gastropods, and decapods were their main prey. Of the 4 explanatory variables, latitude was highly significant, and season, depth, and length were statistically significant. Red porgy and gray triggerfish were observed to have a generalized feeding strategy of feeding opportunistically on a wide range of prey. This study contains fundamental trophic data on 2 important fishery species in the southeastern United States. Most importantly, it provides fisheries managers with some of the data necessary for the implementation of an ecosystem-based approach to fisheries management.

Manuscript submitted 23 April 2015.
Manuscript accepted 6 May 2016.
Fish. Bull. 114:317–329 (2016).
Online publication date: 26 May 2016.
doi: 10.7755/FB.114.3.5

There have been numerous calls and mandates to adopt an ecosystem-based approach to fisheries management (Link, 2002; Latour et al., 2003; NMFS, 2009). An ecosystem-based approach to fisheries management requires extensive knowledge of the dynamics of the ecosystem in question, the trophic ecology of individual species, and the food web as a whole (Byron and Link, 2010), as well as information on environmental and biological and economic factors. As fisheries managers move toward an ecosystem-based approach to management, the data inputs for ecosystem models, including diet information, must be acquired (Link et al., 2008; NMFS, 2009; SAFMC[1]). These models require long-term monitoring of the food web and information on species interactions—data that are lacking for most species in the southeastern United States (SAFMC[1]).

Red porgy (*Pagrus pagrus*) and gray triggerfish (*Balistes capriscus*) support commercial and recreational fisheries along the entire southeastern U.S. Atlantic continental shelf, often referred to as the South Atlantic Bight (SAB) (Bearden and McKenzie[2]; Manooch, 1977; Antoni et al., 2011), and both species are in the snapper grouper complex managed by the South Atlantic Fisheries Management Council. Much of the fishery-independent data used by managers for the snapper grouper complex are provided by the Marine Resources Monitoring, Assessment, and Prediction program, which is a cooperative, long-term, fishery-independent monitoring survey. A recent report on analysis of data from this survey program revealed that red porgy and gray triggerfish were the third and fifth most commonly caught species in chevron traps used in this survey, respectively (MARMAP[3]).

[1] SAFMC (South Atlantic Fishery Management Council). 2009. Fishery ecosystem plan of the South Atlantic region. Volume V: South Atlantic research programs and data needs, 177 p. SAFMC, North Charleston, SC. [Available at website.]

[2] Bearden, C. M., and M. D. McKenzie. 1969. An investigation of the offshore demersal fish resources of South Carolina. South Carolina Wildl. Resour. Dep., Tech. Rep. 2, 19 p. [Available at website.]

[3] MARMAP (Marine Resources Monitoring, Assessment, and Prediction). 2014. Semi-annual progress report. [Project report for the period 1 May–31 October 2014. Available from MARMAP, South Carolina Dep. Nat. Resour., 217 Fort Johnson Rd, Charleston, SC 29412.]

Previous studies regarding the trophic habits of red porgy and gray triggerfish in the SAB were limited in scope or are dated and, therefore, may not reflect possible recent dietary shifts that result from natural or anthropogenic disturbances. There has been, for example, only one published study on the feeding habits of red porgy in the southeast (Manooch, 1977). Although that study was very comprehensive and had a large sample size (n=779), it was completed more than 40 years ago. Additionally, we found a report from 1984 (SCWMRD[4]) on feeding of red porgy in the SAB in which diet by size class and calculated diet overlap were examined in relation with other common reef fishes. Information on the food habits of gray triggerfish is also limited, and the few studies that have been undertaken have focused on their feeding behavior on artificial reefs (Blitch, 2000; Kauppert, 2002) and on their interactions with sand dollars (Frazer et al., 1991; Kurz, 1995).

Ecological dynamics and processes can be influenced by changing environmental conditions and anthropogenic disturbances (Byron and Link, 2010), such as fishing. It is likely that intense fishing pressure has an impact on predator–prey relationships, and when these relationships are altered the food web can become unstable (Holling, 1973). Therefore, it is reasonable to postulate that intense fishing pressure over the last several decades not only has affected predatory fish species, such as red porgy and gray triggerfish, directly but has also altered other ecological interactions. An additional change in the trophic dynamics of fish species of the U.S. southeastern waters has been the accidental introduction of piscivorous lionfishes (*Pterois* spp.) (Whitfield et al., 2002; Meister et al., 2005) The scale of the ecological impact of lionfishes is uncertain as its range expands, but studies have indicated that lionfish predation has caused a reduction in prey communities and, therefore, a decrease of prey for native predators (Albins and Hixon, 2008; Morris and Akins, 2009).

This article provides descriptions of the current feeding habits of red porgy and gray triggerfish collected from natural, live bottom habitats in the SAB. This study is the first one on feeding habits of gray triggerfish on natural reefs off the Carolinas and Georgia. The primary objectives of this study were 1) to qualitatively and quantitatively describe the diet of red porgy and gray triggerfish; 2) to determine whether prey consumption differs significantly among seasons, depth zones, and latitudes; 3) to describe ontogenetic shifts in diet; 4) to determine the feeding strategy of each species; and 5) to provide data on diet to managers that use ecosystem-based models for fisheries management.

[4] SCWMRD (South Carolina Wildlife and Marine Resources Department). 1984. Final report: South Atlantic OCS Area Living Marine Resources Study, Phase III, vol. 1, 223 p. Prepared for Minerals Management Service, Washington, D.C., under contract 14-12-0001-29185. [Available from Mar. Resour. Library, South Carolina Dep. Nat. Resour., 217 Fort Johnson Rd., Charleston, SC 29412.]

Materials and methods

Collections

Red porgy and gray triggerfish were collected during seasonal cruises (May–October) from 2009 through 2011 in the SAB (Fig. 1) with hook-and-line fishing. The hooks were baited with cut squid (*Illex* sp.) and cut round scad (*Decapterus* sp.). Sampling was conducted during the day and night while the research vessel was anchored or drifted over hard-bottom reef habitat. Ten specimens of each species were targeted in each of 16 sampling zones. Each sampling zone consisted of 1 of 2 depth zones (20–50 m or >50 m) and 1 of 8 latitudinal zones (1° from 27°N through 34°N).

All specimens were weighed to the nearest gram, and total length (TL) was measured in millimeters. The digestive tract (gut) was excised from the esophagus to the anus and individually labeled. Intestines were included because both species consume prey with some anatomical features that are particularly resistant to digestion, and gray triggerfish lack a distinct stomach. Guts were fixed in 10% formalin for at least 14 days and then rinsed with freshwater. After rinsing, gut contents were scraped into individual jars containing 70% ethanol and stored for identification.

Identification of gut contents

Gut contents were sorted by taxa, enumerated, and weighed (wet weight to the nearest 0.001 g) with a Sartorius[5] balance, model BP211D (Sartorius AG, Goettingen, Germany). Prey items were identified to the lowest possible taxon. Multiple fragments of individual organisms were counted as single individuals, unless the number could be estimated by counting structures, such as eyes, claws. Colonial organisms (i.e., bryozoans and tunicates) were counted as one individual. Fishes were identified according to the identification guide of Carpenter (2002a, 2000b), decapods were identified by using Williams (1984), bivalves and gastropods were identified by using Abbott (1968), zooplankters were identified by using Johnson and Allen (2005) and Boltovsky (1999), echinoderms were identified by using Hendler et al. (1995), and isopods were identified by using Schultz (1969). Voucher specimens from the Southeastern Regional Taxonomic Laboratory of the South Carolina Department of Natural Resources were used to confirm some identifications.

Diet analyses

Description of general diet To quantify feeding habits, the relative contribution of food items to the total diet was determined by using 3 traditional indices: percent frequency of occurrence (%F), percent composition by number (%N), and percent composition by weight (%W).

[5] Mention of trade names or commercial companies is for identification purposes only and does not imply endorsement by the National Marine Fisheries Service, NOAA.

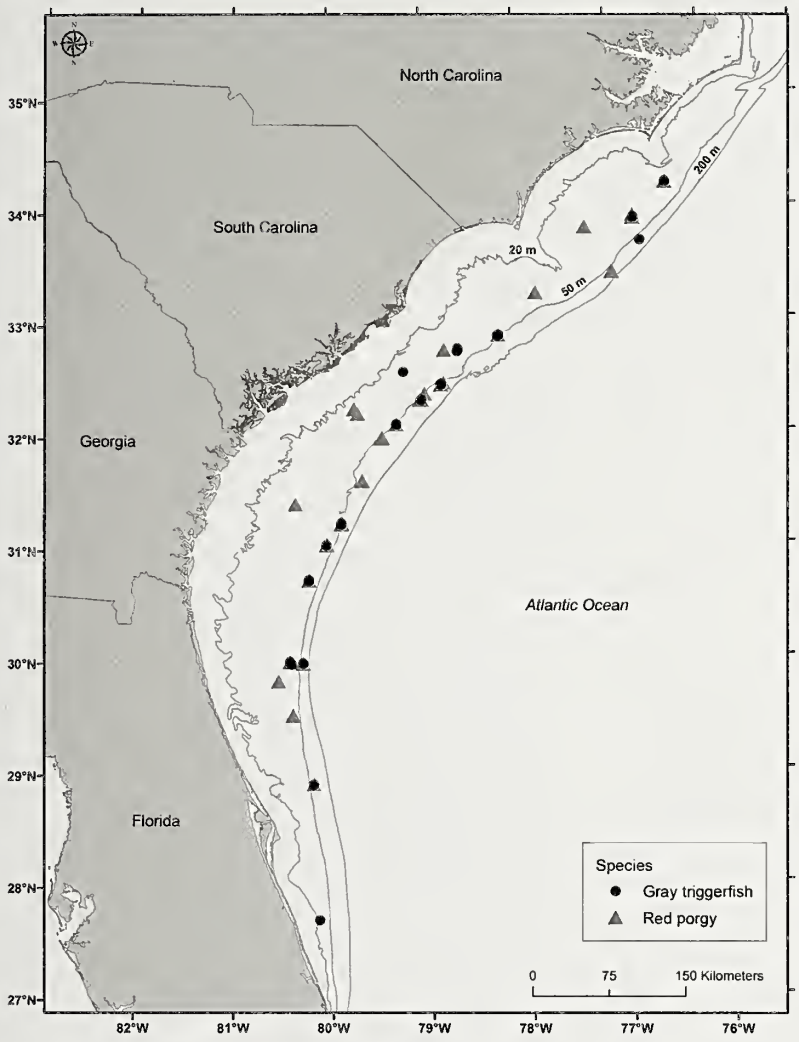

Figure 1

Map of catch locations off the southeastern United States, where specimens of red porgy (*Pagrus pagrus*) and gray triggerfish (*Balistes capriscus*) were collected for analysis of gut content in 2009–2011. Gray lines represent bathymetry (in meters).

Ontogenetic, temporal, and spatial changes in diet Prey were pooled on the basis of taxonomy (e.g., decapods and gastropods). Percent composition by weight was calculated for guts grouped by intervals of TL, season, depth (in meters), and latitude, and this metric was used for all analyses. For analytic purposes, prey types that contributed less than 1% by weight to the diet were excluded.

Canonical correspondence analysis (CCA; ter Braak, 1986), a multivariate direct gradient analysis technique, was used to determine the degree of variability in the diets of red porgy and gray triggerfish, explained by the canonical axes. The canonical axes are linear combinations of the 4 explanatory variables correlated to weighted averages of the prey within the cells of the response matrix (ter Braak, 1986; Garrison and Link, 2000). The CCA was performed with the community ecology package vegan, vers. 2.0-10 (Oksanen et al., 2013), an extension to the statistical software R, vers. 3.1.2 (R Core Team, 2014).

Each element in the response matrix was the mean percent weight of each prey taxon in a given length category, season, depth, and latitude combination. Prey data (%W) were log-transformed ($\ln[x+1]$) to normalize the data. The explanatory variables were coded as ordinal variables with the exception of season, which was coded as a categorical variable. The variance inflation factor was used to detect nearly collinear constraints (environmental variables), although it must be noted that these constraints are not a problem with the algorithm that is used in the CCA function of the vegan package to fit a constrained ordination (Oksanen et al., 2013). Any useless constraints would have been removed from the estimation, and no biplot scores or centroids would have been calculated (Oksanen et al., 2013). Permutation tests were used to determine the significant explanatory variables (ter Braak, 1986). A biplot of prey species and explanatory factors was constructed to examine the correlations between the explanatory variables (factors) and the canonical axes and to observe any dietary patterns associated with these factors. A descriptive analysis was generated for each of the significant factors identified by the CCA.

Hydrographic conditions were used to derive seasonal categories: spring: April through June; summer: July through September, and autumn: October through December. Latitudes were grouped into 3 categories: southern (27–29°N), middle (31–32°N), and northern (33–34°N). To examine the effect of fish length on the diets of red porgy and gray triggerfish, specimens were grouped into 50-mm-TL categories so that all members of a category displayed a reasonably consistent diet composition, and %W was calculated for each group. Groups with low sample sizes ($n \leq 3$) were trimmed to minimize outliers. Cluster analyses (Euclidean distance, average linkage method) were used to group these length classes into broader categories that represented relationships among the diet compositions.

Feeding strategies The feeding strategies of each species were analyzed according to the graphical method of Costello (1990), modified by Amundsen et al. (1996). Through the use of this method, prey-specific abundance was plotted against %F, making it possible to explore feeding strategies as well as shifts in niche use. Prey-specific abundance was defined as

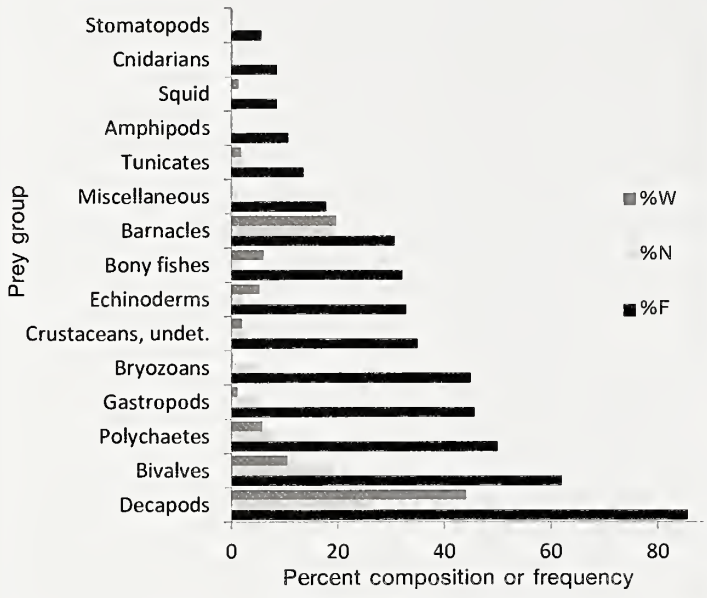

Figure 2

Percent frequency of occurrence (%F), percent composition by number (%N), and percent composition by weight (%W) of prey types present in the diet of 140 red porgy (*Pagrus pagrus*) captured in the South Atlantic Bight from 2009 through 2011. Prey items consumed by fewer than 5% of predators are not included. Miscellaneous=fish scales, foraminifera, eggs, macroalgae, and sediment.

$$P_i = (\Sigma S_i / \Sigma S_t)*100, \quad (1)$$

where S_i = the sum of prey i; and

S_t = the sum of all prey items found in only those predator guts that contained prey i. Percent composition by weight was the summed variable. On the graph that results from this method (Amundsen et al., 1996, fig. 3), the percent abundance, which increases along the diagonal from the lower left to the upper right corner, provides a measure of prey importance, with dominant prey on the top and rare or unimportant prey on the bottom. The vertical axis represents feeding strategy: specialization versus generalization. Prey points on the upper part of the graph represent prey on which predators have specialized, and prey positioned on the bottom half of the graph have been eaten occasionally or infrequently.

Results

Unidentified prey items were often encountered because both species bite or grind their food instead of consuming it whole. Fortunately, the majority of prey have parts that are resistant to digestion, making them easily identifiable on the basis of characteristic parts. For example, crab claws and legs, pieces of echinoderm test and spines, and pieces of barnacles were often seen in stomach contents. A full listing of prey items for both species is available in Suppl. Tables 1 and 2 [Online].

Red porgy

From 2009 through 2011, gut contents from 140 red porgy were collected. Lengths of red porgy ranged from 274 to 508 mm TL. Sample sizes were low at the extremes of our sampling range (i.e., 34°N and 27°N).

General diet description Red porgy had a diverse diet, composed of 188 different taxa that belong to 18 taxonomic groupings: decapods, bivalves, polychaetes, gastropods, bryozoans, unidentified crustaceans, echinoderms, bony fishes, barnacles, miscellaneous (e.g., fish scales and foraminifera), tunicates, amphipods, squid, cnidarians, stomatopods, isopods, ostracods, and protochordates. Decapods, barnacles, and bivalves were the main prey of red porgy, accounting for 44%, 20%, and 11% of the diet by weight, respectively (Fig. 2). The most frequently consumed decapods were parthenopid crabs (29%), portunid crabs (28%), calappid crabs (28%), and shrimps (28%). The most frequently consumed bivalve was the painted egg-cockle (*Laevicardium pictum*) (7%). Although polychaetes were consumed by 50% of red porgy, this taxon accounted for only 6% by weight and 8% by number. Other groups that were frequently consumed included gastropods (46%), bryozoans (45%), echinoderms (33%), and bony fishes (32%); however, these species contributed little by weight.

Ontogenetic, temporal and spatial changes in diet We determined that 6% of the total variability in the diet data was explained by the CCA. The first and second canonical axes accounted for 51% and 22%, respectively, of the constrained variation. Of the 4 environmental variables, depth and season were the most important ($P<0.001$), followed by length ($P<0.05$) (Fig. 3).

Although decapods were consumed in all seasons, fewer were consumed in the summer (29%) when barnacles were the primary food source (43%) (Fig. 4A). In the spring, red porgy consumed mostly decapods (50%) and bivalves (11%). In the autumn, decapods (53%) and polychaetes (20%) were the primary prey types.

Red porgy captured on the inner shelf (depths: 20.1–50.0 m) consumed a higher percentage of barnacles and bivalves than did their counterparts on the outer shelf, but decapods dominated diets of red porgy regardless of depth. Outer shelf red porgy also consumed bony fishes and polychaetes (Fig. 4B).

Decapods were the dominant prey at all latitudes, but fewer of them were consumed in the middle latitudes (31–32°N) (Fig. 4C). Red porgy captured at the middle latitudes (31–32°N) consumed barnacles (27%) and bivalves (11%) in addition to decapods. Barnacles

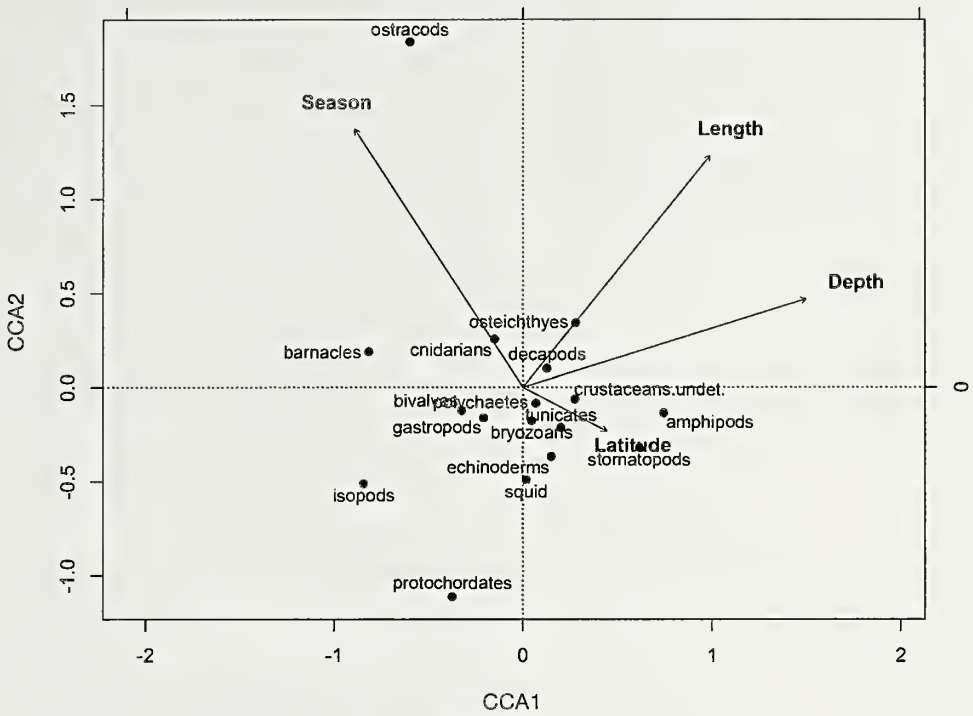

Figure 3

Biplot determined with canonical correspondence analysis (CCA) for the diet of red porgy (*Pagrus pagrus*) captured in the South Atlantic Bight from 2009 through 2011. Arrows represent significant explanatory factors, and dots represent prey types. The canonical axes represent linear combinations of the 4 explanatory variables (i.e., fish length, latitude of capture, season, and depth).

made up less than 1% of prey consumed at the northern latitudes (33–34°N).

The quantity of decapods in the diet of red porgy increased with increasing length (Fig. 4D), whereas smaller fish (<420 mm TL) consumed more barnacles and bivalves than their larger counterparts.

Feeding strategy According to the Amundsen graphical method, the feeding strategy of the red porgy population is generalized (points cluster lower on the *y*-axis of the graph) (Fig. 5), and therefore most prey types are eaten on occasion. Xanthid crabs were consumed by individual red porgy that were concentrating on this prey type as indicated by the point on the top left of the graph. The predator population had a broad niche width because most of the points are located along or below the diagonal from the upper left to the bottom right of the graph. A few prey items were eaten occasionally by most individuals, and these items are represented by the points on the bottom right of the graph (Fig. 5).

Gray triggerfish

Description of general diet Gut contents were collected from 82 gray triggerfish that ranged in size from 304 to 595 mm TL. Gray triggerfish had a diverse diet, composed of 131 different prey taxa that were combined into 19 broader taxonomic groups: gastropods, amphipods, decapods, unidentified crustaceans, polychaetes, bivalves, bryozoans, barnacles, bony fishes, echinoderms, tunicates, miscellaneous items (e.g., fish scales, foraminifera, and *Sargassum* spp.), stomatopods, isopods, cnidarians, ostracods, cephalopods, copepods, and unidentified mollusks. Barnacles, gastropods, and decapods were the main prey of gray triggerfish, accounting for 29%, 11%, and 11% of the diet by weight, respectively (Fig. 6). Although most gastropods were unidentified, 13 species were pelagic pteropods (group Thecosomata); cavolinid pteropods (40%) were the most frequently consumed pelagic pteropods. Unidentified shrimps were the most frequently consumed decapod (30%). Although amphipods were consumed by 63% of predators, this taxon accounted for only 0.5% of the diet by weight and 10% by number. Other species consumed frequently included unidentified crustaceans (59%), polychaetes (46%), bivalves (46%), and bryozoans (43%); however, these species contributed little by weight.

Ontogenetic, temporal, and spatial changes in diet We determined that 15% of the total variability in the diet data could be explained by the CCA. The first and second canonical axes accounted for 41% and 36% of the constrained variation, respectively. Latitude and season were the most important explanatory variables ($P<0.001$), followed by depth and length ($P<0.05$) (Fig. 7).

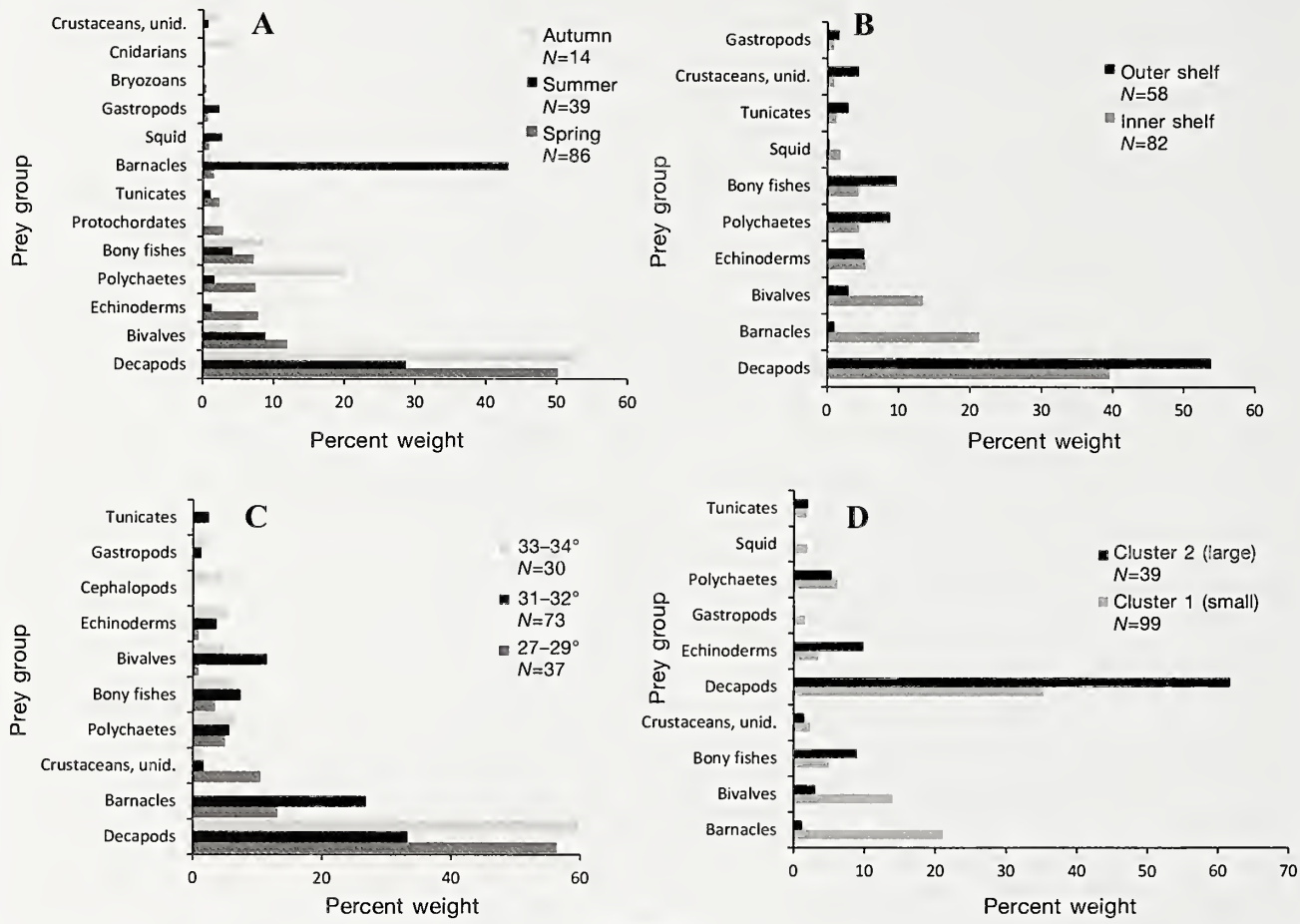

Figure 4

Diet composition by weight of red porgy (*Pagrus pagrus*) collected in the South Atlantic Bight from 2009 through 2011 presented by (**A**) season, (**B**) depth, (**C**) latitude, and (**D**) length. The number (*N*) of specimens collected in each season, at each depth zone, latitude range, or within each length cluster (small=321–420 mm in total length; large=421–520 mm TL) is given in the legends. unid=unidentified.

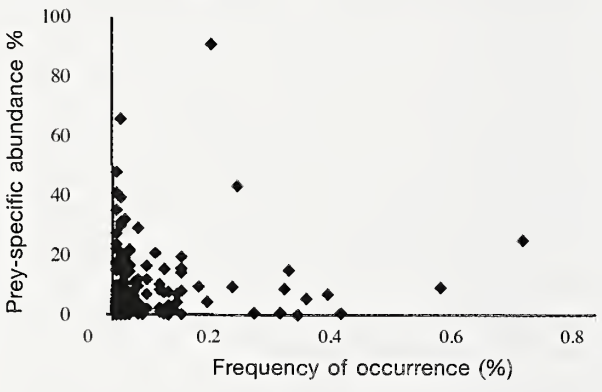

Figure 5

Graph of the feeding strategy of red porgy (*Pagrus pagrus*), captured during 2009–2011 in the South Atlantic Bight. The graph was developed in this study by using the Amundsen graphical method. Each dot represents a different prey species.

Barnacles (35%) and decapods (17%) were the primary prey for gray triggerfish captured in the spring (Fig. 8A). In the summer, the principal prey of gray triggerfish were barnacles (24%) and bivalves (23%), and, in the autumn, gray triggerfish consumed primarily gastropods (40%) and bony fishes (32%).

Gray triggerfish caught on the inner shelf consumed more barnacles, decapods, and polychaetes than did their outershelf counterparts, whereas, on the outershelf, they consumed more gastropods and bivalves (Fig. 8B).

Latitudinal differences in diet were substantial (Fig. 8C). Fish captured at the southern latitudes (27–29°N) preyed upon decapods (59%), and fish captured at the northern latitudes (33–34°N) consumed mostly barnacles (57%). Gray triggerfish caught in the central region (31–32°N) had a more diverse diet consisting of decapods, gastropods, barnacles, and bony fishes.

Small fish (<400 mm TL) consumed decapods and

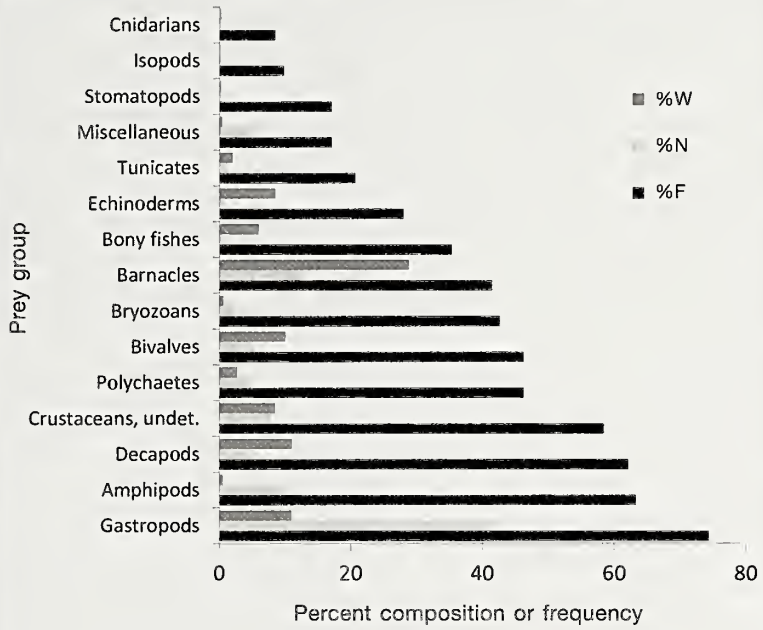

Figure 6

Percent frequency of occurrence (%F), percent composition by number (%N), and percent composition by weight (%W) of prey types present in the diet of 82 gray triggerfish (*Balistes capriscus*) captured in the South Atlantic Bight from 2009 through 2011. Prey items consumed by fewer than 5% of predators are not included.

relatively few bivalves. In contrast, large fish had a diet dominated by barnacles and bivalves. (Fig. 8D).

Feeding strategy On the basis of Amundsen graphical method, the feeding strategy of the gray triggerfish population is generalized (cluster of points lower on the *y*-axis of the graph) (Fig. 9); several prey items are eaten occasionally by most individuals. As with red porgy, the predator population has a broad niche width (points are all located below the diagonal from the upper left to the bottom right of the graph) (Fig. 9).

Discussion

Red porgy

Across the broad sampling range of this study, red porgy had a very diverse diet. Much of this diversity is likely a reflection of localized prey assemblages rather than a preference for specific prey items (Bearden and Mckenzie[2]; Manooch, 1977). Manooch (1977) and SCWMRD[4] reported findings similar to those of our study in that they found the red porgy to be a generalized predator. However, Manooch (1977) and SCWMRD[4] identified only 69 and 80 prey taxa, respectively, compared with the 188 taxa found in our study. In the case of the Manooch (1977) study, the difference in number of prey taxa may be attributed to the limited geographic range of his investigation; samples in that study came from only North and South Carolina, whereas samples from our study came from an area spanning from North Carolina to Florida.

It is also possible that the abundance of certain prey has shifted and, therefore, that red porgy have had to diversify their food resources. SCWMRD[4] found the preferred prey were decapods and fishes and that fishes made up the greatest volume of prey. We found fishes to be far less important prey (6%W). In contrast to Manooch (1977) and our study, SCWMRD[4] identified more nektonic and fewer benthic prey. In addition, SCWMRD[6] found very few mollusks in comparison with our study. The scientists at SCWMRD suggested that, because Manooch (1977) used stomach and intestine of red porgy and shelled organisms are slow to be digested, bivalves and gastropods would appear to be present more frequently than taxa such as small crustaceans and polychaetes. This suggestion could be one explana-

[6] SCWMRD (South Carolina Wildlife and Marine Resources Department). 1981. South Atlantic OCS Area Living Marine Resources Study, vol. 1, 297 p. Prepared for Bureau of Land Management, Washington, D.C, under contract AA551-CT9-27. [Available from Mar. Resour. Library, South Carolina Dep. Nat. Resour., 217 Fort Johnson Rd., Charleston, SC 29412.]

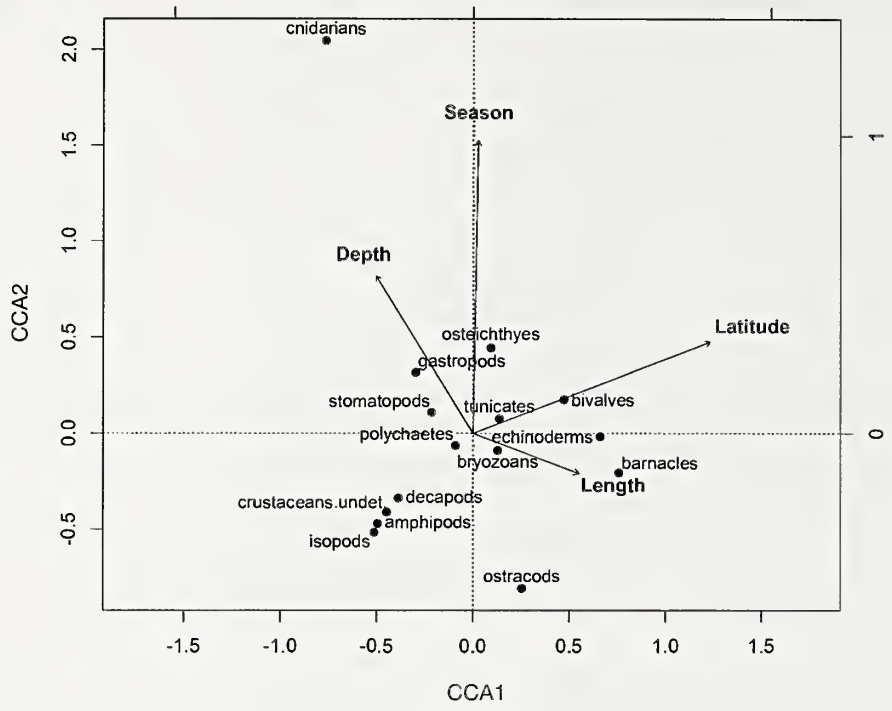

Figure 7

Biplot determined with canonical correspondence analysis (CCA) for the diet of gray triggerfish (*Balistes capriscus*) captured in the South Atlantic Bight from 2009 through 2011. Arrows represent significant explanatory factors, and dots represent different prey types. The canonical axes represent linear combinations of the 4 explanatory variables (i.e., fish length, latitude of capture, season, and depth [shown in bold type]).

tion for the frequently observed bivalves and gastropods in the diet of red porgy in our study.

Season was the second most significant explanatory factor in the CCA in our study, but Manooch (1977) found only slight seasonal variation in several groups of invertebrates. In our study, barnacles were the main food source in the summer, whereas, in the autumn and spring, red porgy depended more heavily on decapod prey. This seasonal shift in diet could have been the result of lower decapod availability during the summer and that in turn would have led to red porgy consuming more barnacles. In fact, Manooch (1977) found that several groups of invertebrates varied seasonally both in volume and frequency. Red porgy are not dependent on one type of food source; therefore this species has the advantage of being able to switch prey as necessary with fluctuating seasonal prey populations.

There were significant differences in prey among length classes. Small fish (<420 mm TL) generally consumed small prey (barnacles and bivalves), and large fish consumed larger prey (decapods). The SCWMRD[4] study found that red porgy consumed more fishes and fewer decapods as they grew—a finding that also contrasts with our results. However, that study included smaller fish (51–350 mm in standard length) than those collected in our study (274–508 mm TL), and that size difference is likely to be the main reason for the reported differences in prey types by fish length.

A generalized feeding strategy (Fig. 5) is not unexpected for a species that consumes such a great diversity of prey items. Manooch (1977) suggested that the tremendously diverse diet of red porgy probably reflects localized forage assemblages rather than a preference for a specific food and supports the idea of classifying red porgy as trophic generalists. He also noted that they have certain behavioral and morphological characteristics that make it easy to feed on a diversity of prey: swimming speed and strong molariform teeth that enable these fish to crush armored prey, such as sea urchins, crabs, and gastropods. This feeding strategy has a selective advantage because red porgy are not dependent on a small number of food types, and, therefore, are less likely to face competition.

Gray triggerfish

Gray triggerfish were found to have a very diverse diet of 131 prey taxa across a broad sampling range. Unlike the prey that we found, previous researchers found the most important prey of gray triggerfish to be bivalves, barnacles, and echinoderms (Vose, 1990; Vose and Nelson, 1994; Kauppert, 2002). However, fish living around

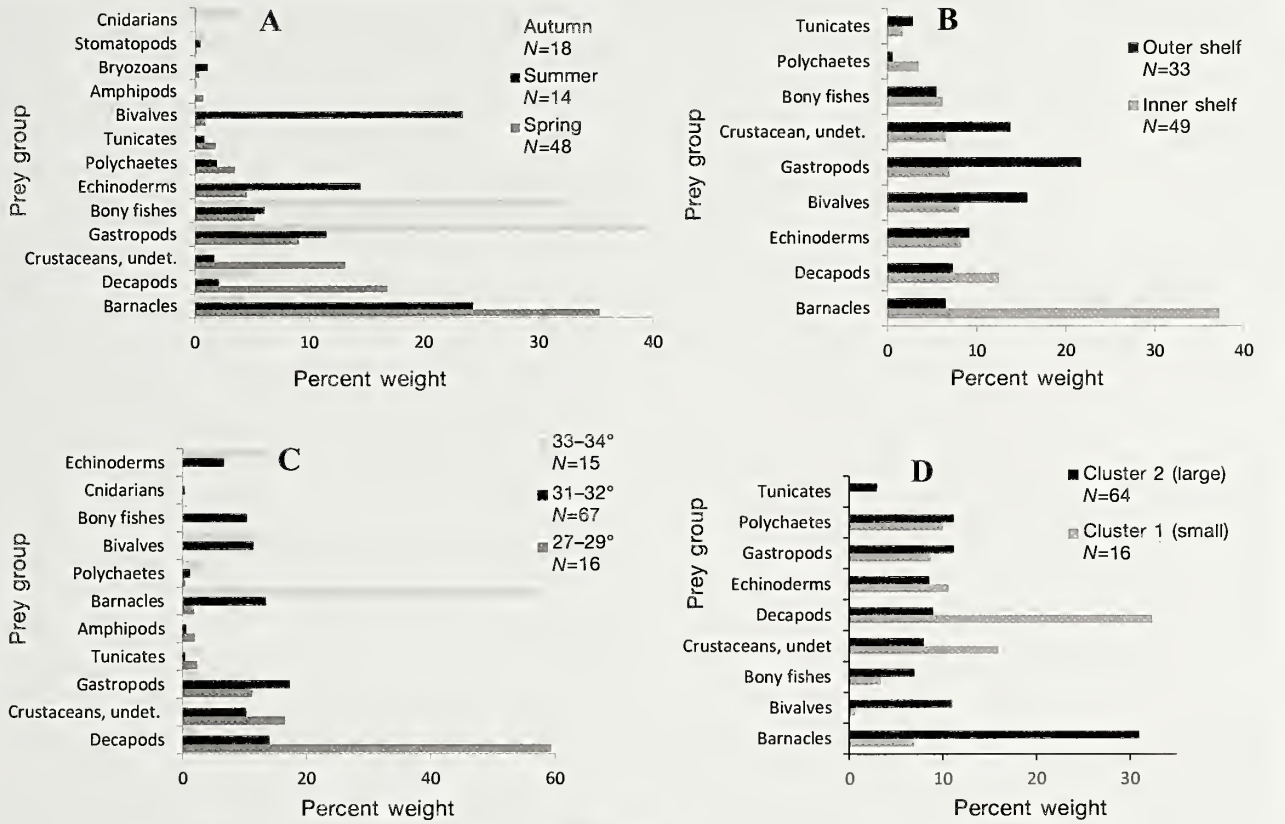

Figures 8

Diet composition by weight of gray triggerfish (*Balistes capriscus*) collected in the South Atlantic Bight from 2009 through 2011 presented by (**A**) season, (**B**) depth, (**C**) latitude, and (**D**) length. The number (*N*) of specimens in each season, depth group, latitude range, or length cluster (small=350–400 mm in total length; large=401–600 mm TL) is given in the legends.

artificial structures (as opposed to the natural reefs examined in our study) were examined in those previous studies, and other research focused on gray triggerfish interaction with sand dollars (Frazer et al., 1991; Kurz, 1995). Vose (1990) wrote that gray triggerfish are highly dependent on reef-associated prey and found diets of gray triggerfish to be quite different for natural and artificial reefs. On natural reefs, bivalves were a common food, whereas artificial reefs that were examined were dominated by fouling organisms such as barnacles. Of the previously published work, only one study on gray triggerfish collected from artificial reefs in the Gulf of Mexico had findings similar to those in our study: Blitch (2000) found pelagic mollusks and crustaceans to be the most important prey.

In our study, echinoderms were found in 28% of guts, but this finding may be an underrepresentation of their importance in the diet of gray triggerfish because the soft tissue of echinoderms may have been digested before a gray triggerfish was caught. Frazer et al. (1991) cautions that because gray triggerfish eat only soft tissue and not the hard test, echinoderms may be underrepresented in studies of stomach contents because of different digestion rates. We were able to identify sand dollars in guts only when gray triggerfish had eaten an entire organism with its test.

The diet of gray triggerfish was dominated by gastropods (primarily pelagic pteropods) in the autumn, a result that confirms Kauppert's (2002) observations that feeding habits of gray triggerfish in the autumn shifted to 60% nektonic and planktonic feeding, especially when compared with substrate feeding in the spring and summer. Some species of pteropods are reported to reproduce in the spring and summer (Rampal, 1975; Dadon and de Cidre, 1992) and could result in increases in pteropod numbers in the autumn months and consequently the seasonal shift in predation. Furthermore, seasonal migrations occur in some species of pteropods (Sardou et al., 1996). Results from Sardou et al. (1996) and Franqueville (1971) indicate that the pyramid clio (*Clio pyramidata*), a pteropod species commonly consumed by gray triggerfish in our study, becomes abundant at shallower depths in autumn. This occurrence offers a plausible explanation for the increased pteropod predation in the autumn.

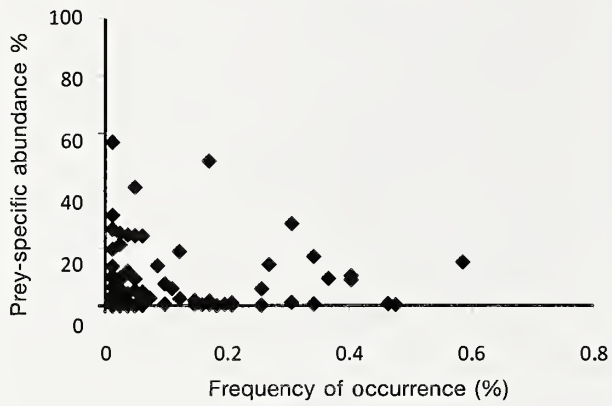

Figure 9

Graph of the feeding strategy for gray triggerfish (*Balistes capriscus*), captured from 2009 through 2011 in the South Atlantic Bight. The graph was developed by using the Amundsen graphical method. Each dot represents a different prey species.

Another reason for seasonal variation in diet could be the reproductive behavior of gray triggerfish. They spawn from April through September and peak spawning occurs from May through August (Kelly, 2014). During this time, they are found at deeper depths, and it is possible that their feeding behavior could change because they are nest guarders. Gray triggerfish caught on the outer shelf consumed more gastropods (primarily pteropods) than the gray triggerfish captured on the inner shelf. Pteropod distribution patterns remain poorly described (Bednaršek et al., 2012), but it has been reported that their distribution and migration vary seasonally (Dadon and de Cidre, 1992; Parra-Flores and Gasca, 2009).

Latitude was a highly significant explanatory factor in defining the diet for gray triggerfish, and there were changes in diet with fish length that might also have influenced our results. Small fish consumed more polychaetes and decapods, and large fish consumed more barnacles and bivalves (the opposite was true with red porgy). Decapod prey consumed by gray triggerfish were often smaller crab species or crustaceans in larval stages (i.e., crabs, shrimps, and lobsters). Gastropod consumption increased with predator size.

The percentages of explained variation found in this study are comparable to those in similar studies of diet composition (Jaworski and Ragnarsson, 2006; Latour et al., 2008). Although a relatively small proportion of the total variation is explained by the CCA, a small proportion is expected because the percentage-explained inertia (variance) for ecological data is typically low (<10%) (ter Braak and Verdonschot, 1995).

Some prey of gray triggerfish and red porgy have diel vertical migrations (at least 32 taxa) (Boltovskoy, 1973; Alldredge and King, 1980; Hopkins et al., 1994; Angel and Pugh, 2000). Pteropods, for example, exhibit diurnal vertical migrations along the depth range of 0–100 m. During the day, pteropods move to deeper waters but migrate to the surface at night (Angel and Pugh, 2000). They tend to concentrate in the upper layers during the night to feed and avoid predators (Hays, 2003). Gray triggerfish are rarely caught at night during cruises of the Marine Resources Monitoring, Assessment, and Prediction program (senior author, personal observ.), and they have been previously described as diurnal predators (Randall, 1968). It is possible that these fish are not caught on the bottom at night because this species migrates into the water column, following pelagic prey. Many fish species migrate in a diel pattern, both vertically (Narver, 1970; Blaxter, 1973; Begg, 1976) and horizontally (Baumann and Kitchell, 1974; Hobson, 1974; Bohl, 1979; Krumme, 2009), following prey migrations (Ahlbeck et al., 2012). Although gray triggerfish are highly reef associated, they also rely on migrating pelagic species as food sources. Other studies of reef fishes have reported trophic connections that are primarily dependent on these vertically migrating food webs (Weaver and Sedberry, 2001; Goldman and Sedberry, 2010).

Although competition between species was not a focus of our research, other studies have had results worth discussing in the context of our work. Johnson (1977) suggested that when %F exceeds 25% between 2 or more predators, competition is likely. In contrast, Pianka (1976) stated that competition for identical resources is only likely if resources are in short supply. Red porgy and gray triggerfish do share many of the same prey (e.g., decapods, gastropods, bivalves, bryozoans, echinoderms, polychaetes, and bony fishes), and, if food resources become scarce, then such scarcity could lead to competition. Possible causes for a short supply could be prey consumption by invasive lionfishes, ocean acidification, or other anthropogenic effects (e.g., fishing). In this study, we did not examine food availability, nor did we observe anything that indicated evidence of food scarcity.

Ocean acidification is of particular concern for gray triggerfish because a large part of its diet is composed of pelagic pteropods. Ocean acidification causes shell dissolution in pteropods and some benthic invertebrates that are $CaCO_3$-secreting organisms (Doney et al., 2009). Calcified structures provide protection from predators; therefore, pteropods would be adversely affected by the rising atmospheric CO_2 levels caused by human fossil fuel combustion and deforestation (Doney et al., 2009), and adverse effects on pteropods would, in turn, have serious effects on populations of gray triggerfish. This study is far more comprehensive than previous studies have been and covers a large geographic area, providing a baseline study that can be used to monitor potential dietary shifts that result from climate change.

The temporal and geographic differences in prey for red porgy and gray triggerfish highlight the need to incorporate information on fish food habits into ecosystem models. Many of the prey species consumed by fish

in our study are not well studied in the southeast, and their population statuses are not well known. Changes in their status could have unanticipated consequences for commercial fish species like red porgy and gray triggerfish. The most significant predator–prey interactions are those between red porgy and decapods and bivalves and those between gray triggerfish and gastropods. The information reported here complements the findings of previous studies and provides a critical link between the biology of red porgy and gray triggerfish and their role as predators in marine ecosystems. Although both species rely primarily on hard-bottom habitats for feeding, opportunistic prey switching allows both red porgy and gray triggerfish to adapt to ecological changes. This research and that of similar studies contribute to our understanding of the role of predators in changing ecosystems and provide fisheries managers with some of the data necessary for the implementation of an ecosystem-based approach to fisheries management in the southeastern United States.

Acknowledgments

For their help with identification of prey items, we thank D. Burgess, J. Cowan, D. Knott, C. Willis, and D. Wyanski. Thanks are extended to the staffs of the Marine Resources Monitoring Assessment and Prediction program and of the Southeast Fishery-independent Survey, NOAA Southeast Fisheries Science Center, and to the crews of the RV *Palmetto* and RV *Savannah*. G. Sedberry, W. Anderson, C. Barans, K. Spanik, and W. Bubley provided helpful comments on early drafts at the manuscript stage. This work was supported through funds provided by the Southeast Area Monitoring and Assessment Program—South Atlantic. This paper is contribution number 734 from the South Carolina Marine Resources Division.

Literature cited

Abbott, R. T.
1968. A guide to field identification: seashells of North America, 280 p. Western Publishing Company Inc., Racine, WI.

Aiken, K. A.
1983. The biology, ecology, and bionomics of the triggerfishes, Balistidae. *In* Caribbean coral reef fishery resources. ICLARM Stud. Rev.7 (J. L. Munro, ed.), p. 191–205. International Center for Living Aquatic Resources Management, Manila, Philippines.

Ahlbeck, I, S. Hansson, and O. Hjerne.
2012. Evaluating fish diet analysis methods by individual-based modeling. Can. J. Fish. Aquat. Sci. 69:1184–1201

Albins, M. A., and M. A. Hixon.
2008. Invasive Indo-Pacific lionfish *Pterois volitans* reduce recruitment of Atlantic coral-reef fishes. Mar. Ecol. Prog. Ser. 367:233–238.

Alldredge, A. L., and J. M. King.
1980. Effects of moonlight on the vertical migration patterns of demersal zooplankton. J. Exp. Mar. Biol. Ecol. 44:133–156.

Amundsen, P. A., H. M. Gabler, and F. J. Staldvik.
1996. A new approach to graphical analysis of feeding strategy from stomach contents data—modification of the Costello (1990) method. J. Fish Biol. 48:607–614.

Angel M. V. and P. R. Pugh.
2000. Quantification of diel vertical migration by micronektonic taxa in the northeast Atlantic. Hydrobiologia 440:161–179.

Antoni, L., N. Emerick, and E. Saillant.
2011. Genetic variation of gray triggerfish in the U.S. waters of the Gulf of Mexico and western Atlantic Ocean as inferred from motochondrial DNA sequences. North Am. J. Fish. Manage. 31:714–721.

Baumann, P. C., and J. F. Kitchell.
1974. Diel patterns of distribution and feeding of bluegill (Lepomis macrochirus) in Lake Wingra, Wisconsin. Trans. Am. Fish. Soc. 103:255–260.

Bednaršek, N., J. Možina, M. Vogt, C. O'Brien, and G. A. Tarling.
2012. The global distribution of pteropods and their contribution to carbonate and carbon biomass in the modern ocean. Earth Syst. Sci. Data 4:167–186.

Begg, G. W.
1976. The relationship between the diurnal movements of some of the zooplankton and the sardine Limnothrissa miodon in Lake Kariba, Rhodesia. Limnol. Oceanogr. 21:529–539.

Blaxter, J. H. S.
1973. Monitoring the vertical movements and light responses of herring and plaice larvae. J. Mar. Biol. Assoc. U.K. 53:635–647.

Blitch, K. M.
2000. The feeding habits of gray triggerfish, *Balistes capriscus* (GMELIN), from the northeast Gulf of Mexico. M.S. thesis, 85 p. Univ. Central Florida, Orlando, FL.

Bohl, E.
1979. Diel pattern of pelagic distribution and feeding in planktivorous fish. Oecologia 44:368–375.

Boltovskoy, E.
1973. Daily vertical migration and absolute abundance of living planktonic foraminifera. J. Foraminiferal Res. 3:89–94.

Boltovskoy, D. (ed).
1999. South Atlantic zooplankton, vols. 1 and 2, 1706 p. Backhuys Publs., Leiden, Netherlands.

Byron, C. J., and J. S. Link.
2010. Stability in feeding ecology of four demersal fish predators in the US Northeast Shelf Large Marine Ecosystem. Mar. Ecol. Prog. Ser. 406:239–250.

Carpenter, K. E. (ed.).
2002a. The living marine resources of the western central Atlantic. Volume 2: bony fishes part 1 (Acipenseridae to Grammatidae). FAO Species Identification Guide for Fishery Purposes and American Society of Ichthyologists and Herpetologist Special Publication No. 5, p. 601–1374. FAO, Rome.
2002b. The living marine resources of the western central Atlantic. Volume 3: bony fishes part 2 (Opistognathidae to Molidae), sea turtles and marine mammals. FAO Species Identification Guide for Fishery Purposes and

American Society of Ichthyologists and Herpetologist Special Publication No. 5, p. 1375–2127. FAO, Rome.

Costello, M. J.
1990. Predator feeding strategy and prey importance: a new graphical analysis. J. Fish Biol. 36:261–263.

Dadon, J. R., and L. L. de Cidre.
1992. The reproductive cycle of the Thecosomatous pteropod *Limacina retroversa* in the western South Atlantic. Mar. Biol. 114:439–442.

Doney, S. C., V. J. Fabry, R. A. Feely, and J. A. Kleypas.
2009. Ocean acidification: the other CO_2 problem. Annu. Rev. Mar. Sci. 1169–192.

Franqueville, C.
1971. Macroplancton profond (invertébrés) de la Méditerranée nord-occidentale. Téthys 3:11–56.

Frazer, T. K., W. J. Lindberg, and G. R. Stanton.
1991. Predation on sand dollars by gray triggerfish, *Balistes capriscus*, in the northeastern Gulf of Mexico. Bull. Mar. Sci. 48:159–164.

Garrison, L. P., and J. S. Link.
2000. Diets of five hake species in the northeast United States continental shelf ecosystem. Mar. Ecol. Prog. Ser. 204:243–255.

Goldman, S. F., and G. R. Sedberry.
2010. Feeding habits of some demersal fish on the Charleston Bump off the southeastern United States. ICES J. Mar. Sci. 68:390–398.

Hays, G. C.
2003. A review of the adaptive significance and ecosystem consequences of zooplankton diel vertical migrations. Hydrobiologia 503:163–170.

Hendler, G., J. E. Miller, D. L. Pawson, and P. M. Kier.
1995. Sea stars, sea urchins, and allies: echinoderms of Florida and the Caribbean, 390 p. Smithsonian Inst. Press, Washington, D.C.

Hobson, E. S.
1974. Feeding relationships of teleostean fishes on coral reefs in Kona, Hawaii. Fish. Bull. 72:915–1031.

Holling, C. S.
1973. Resilience and stability of ecological systems. Annu. Rev. Ecol. Syst. 4:1–23.

Hopkins, T. L., M. E. Flock, J. V. Gartner Jr., and J. J. Torres.
1994. Structure and trophic ecology of a low latitude midwater decapod and mysid assemblage. Mar. Ecol. Prog. Ser. 109:143–156.

Jaworski, A., and S. A. Ragnarsson.
2006. Feeding habits of demersal fish in Icelandic waters: a multivariate approach. ICES J. Mar. Sci. 63:1682–1694.

Johnson, F. H.
1977. Responses of walleye (*Stizostedion vitreum vitreum*) and yellow perch (*Perca flavescens*) populations to removal of white sucker (*Catostomus commersoni*) from a Minnesota lake, 1966. J. Fish. Res. Board Can. 34:1633–1642.

Johnson, W. S., and D. M. Allen.
2005. Zooplankton of the Atlantic and Gulf Coasts: a guide to their identification and ecology, 379 p. Johns Hopkins Univ. Press, Baltimore, MD.

Kauppert, P. A.
2002. Feeding habits and trophic relationships of an assemblage of fishes associated with a newly established artificial reef off South Carolina. M.S. thesis, 123 p. College of Charleston, Charleston, SC.

Kelly, A. M.
2014. Age, growth, and reproduction of gray triggerfish *Balistes capriscus* off the southeastern U.S. Atlantic coast. M.S. thesis, 54 p. College of Charleston, Charleston, SC.

Krumme, U.
2009. Diel and tidal movements by fish and decapods linking tropical coastal ecosystems. *In* Ecological connectivity among tropical coastal ecosystems (I. Nagelkerken, p. 271–324. Springer, Dordrecht, Netherlands.

Kurz, R. C.
1995. Predator–prey interactions between gray triggerfish (*Balistes capriscus* Gmelin) and a guild of sand dollars around artificial reefs in the northeastern Gulf of Mexico. Bull. Mar. Sci. 56:150–160.

Latour, R. J., M. J. Brush, and C. F. Bonzek.
2003. Toward ecosystem-based fisheries management: strategies for multispecies modeling and associated data requirements. Fisheries 28(9):10–22.

Latour, R. J., J. Gartland, C. F. Bonzek, and R. A. Johnson.
2008. The trophic dynamics of summer flounder (*Paralichthys dentatus*) in Chesapeake Bay. Fish. Bull. 106: 47–57.

Link, J. S.
2002. What does ecosystem-based fisheries management mean? Fisheries 27(4):18–21.

Link, J. S., J. Burnett, P. Kostovick, and J. Galbraith.
2008. Value-added sampling for fishery independent surveys: don't stop after you're done counting and measuring. Fish. Res. 93:229–233.

Manooch, C. S., III.
1977. Foods of the red porgy, *Pagrus pagrus* Linnaeus (Pisces: Sparidae), from North Carolina and South Carolina. Bull. Mar. Sci. 27:776–787.

Meister, H. S., D. M. Wyanski, J. K. Loefer, S. W. Ross, A. M. Quattrini, and K. J. Sulak.
2005. Further evidence for the invasion and establishment of *Pterois volitans* (Teleostei: Scorpaenidae) along the Atlantic coast of the United States. Southeast. Nat. 4:193–206.

Morris, J. A., Jr., and J. L. Akins.
2009. Feeding ecology of invasive lionfish (*Pterois volitans*) in the Bahamian archipelago. Environ. Biol. Fish. 86(3): 389–398.

Narver, D. W.
1970. Diel vertical movements and feeding of underyearling sockeye salmon and the limnetic zooplankton in Babine Lake, British Columbia. J. Fish. Res. Board Can. 27:281–316.

NMFS (National Marine Fisheries Service).
2009. Report to Congress: the state of science to support an ecosystem approach to regional fishery management. NOAA Tech. Memo. NMFS-F/SPO-96, 24 p.

Oksanen, J., F. G. Blanchet, R. Kindt, M. J. Oksanen,, and M. A. S. S. Suggests.
2013. vegan: community ecology package. R package, vers. 2.0-10. [Available at website.]

Parra-Flores, A., and R. Gasca.
2009. Distribution of pteropods (Mollusca: Gastropoda: Thecosomata) in surface waters (0–100 m) of the Western Caribbean Sea (winter, 2007). Rev. Biol. Mar. Oceanogr. 44:647–662.

Pianka, E. R.
1976. Competition and niche theory. *In* Theoretical ecol-

ogy: principles and applications (R. M. May, ed.), p. 114–141. Saunders, Philadelphia, PA.

R Core Team.
2014. R: a language and environment for statistical computing. R Foundation for Statistical Computing, Vienna, Austria. [Available from website, accessed December 2014.]

Rampal, J.
1975. Les thécosomes (mollusques pélagiques): systématique et évolution, écologie et biogéographie Méditerranéennes. Thesis, 485 p. Univ. Provence, Aix-Marseille, France.

Randall, J. E.
1968. Caribbean reef fishes, 318 p. T. F. H. Publications, Jersey City, NJ.

Sardou, J., M. Etienne, and V. Andersen.
1996. Seasonal abundance and vertical distributions of macroplankton and micronekton in the northwestern Mediterranean Sea. Oceanol. Acta 19:645–656.

Schultz, G. A.
1969. How to know the marine isopod crustaceans, 359 p. W.C. Brown Co., Dubuque, IA.

ter Braak, C. J. F.
1986. Canonical correspondence analysis: a new eigenvector technique for multivariate direct gradient analysis. Ecology 67:1167–1179.

ter Braak, C. J. F., and P. F. M. Verdonschot
1995. Canonical correspondence analysis and related multivariate methods in aquatic ecology. Aquat. Sci. 57: 255–289.

Vose, F. E.
1990. Ecology of fishes on artificial and rock outcrop reefs off the central east coast of Florida. Ph.D. diss., 140 p. Florida Inst. Tech., Melbourne, FL.

Vose, F. E., and W. G. Nelson.
1994. Gray triggerfish (*Balistes capriscus* Gmelin) feeding from artificial and natural substrate in shallow Atlantic waters of Florida. Bull. Mar. Sci. 55:1316–1323.

Weaver, D. C., and G. R. Sedberry
2001. Trophic subsidies at the Charleston Bump: food web structure of reef fishes on the continental slope of the southeastern United States. Am. Fish. Soc. Symp. 25:137–152.

Whitfield P. E., T. Gardner, S. P. Vives, M. R. Gilligan, W. R. Courtenay Jr., G. C. Ray, and J. A. Hare.
2002. Biological invasion of the Indo-Pacific lionfish *Pterois volitans* along the Atlantic coast of North America. Mar. Ecol. Prog. Ser. 235:289–297.

Williams, A. B.
1984. Shrimps, lobsters, and crabs of the Atlantic Coast of the eastern United States, Maine to Florida, 550 p. Smithsonian Inst. Press, Washington, DC.

NOAA
National Marine
Fisheries Service

Fishery Bulletin
established 1881

Spencer F. Baird
First U.S. Commissioner
of Fisheries and founder
of *Fishery Bulletin*

Predicting potential fishing zones for Pacific saury (*Cololabis saira*) with maximum entropy models and remotely sensed data

Achmad F. Syah (contact author)[1,2]
Sei-Ichi Saitoh[1,3]
Irene D. Alabia[3]
Toru Hirawake[1]

Email address for contact author: fachrudinsyah@gmail.com

[1] Laboratory of Marine Environment and Resource Sensing
Faculty of Fisheries Sciences
Hokkaido University
3-1-1 Minato-cho
Hakodate 041-8611, Japan

[2] Department of Marine Science
University of Trunojoyo Madura
Jalan Raya Telang
P.O. Box 2 Kamal
Bangkalan-Madura, Indonesia

[3] Arctic Research Center
Hokkaido University
N21-W11 Kita-ku
Sapporo 001-002, Japan

Abstract—Fishing locations for Pacific saury (*Cololabis saira*) obtained from images of the Operational Linescan System (OLS) of the U.S. Defense Meteorological Satellite Program, together with maximum entropy models and satellite-based oceanographic data of chlorophyll-*a* concentration (chl-*a*), sea-surface temperature (SST), eddy kinetic energy (EKE), and sea-surface height anomaly (SSHA), were used to evaluate the effects of oceanographic conditions on the formation of potential fishing zones (PFZ) for Pacific saury and to explore the spatial variability of these features in the western North Pacific. Actual fishing regions were identified as the bright areas created by a 2-level slicing method for OLS images collected August–December during 2005–2013. The results from a Maxent model revealed its potential for predicting the spatial distribution of Pacific saury and highlight the use of multispectral satellite images for describing PFZs. In all monthly models, the spatial PFZ patterns were explained predominantly by SST (14–16°C) and indicated that SST is the most influential factor in the geographic distribution of Pacific saury. Also related to PFZ formation were EKE and SSHA, possibly through their effects on the feeding grounds conditions. Concentration of chl-*a* had the least effect among other environmental factors in defining PFZs, especially during the end of the fishing season.

Manuscript submitted 20 July 2015.
Manuscript accepted 12 May 2016.
Fish. Bull.:330–342 (2016).
Online publication date: 2 June 2016.
doi: 10.7755/FB.114.3.6

The Pacific saury (*Cololabis saira*) is widely distributed in the western North Pacific from subarctic to subtropical waters and is one of the commercially important pelagic species in Japan, Russia, Korea, and Taiwan. The total landings of this species in these countries increased from 171,692 metric tons (t) in 1998 to 449,738 t in 2011. Over the last half century, annual catches of Pacific saury in Japan, for example, have averaged around 257,800 t (Tian et al., 2003) and have fluctuated greatly from 52,207 t in 1969 to 207,770 t in 2011 (Fisheries Agency and Fisheries Research Agency of Japan, 2012).

The number, size, and location of fishing grounds for Pacific saury are largely affected by oceanographic conditions (Yasuda and Watanabe, 1994; Kosaka, 2000; Tian et al., 2002), and the significant effect of environmental factors on abundance of Pacific saury was evident in the unexpected drop in both the catch and catch per unit of effort in 1998, following a period of high abundance (Tian et al., 2003). The distribution and migratory patterns of Pacific saury have been associated with chlorophyll-*a* (chl-*a*) concentration and sea-surface temperature (SST) (Watanabe et al., 2006; Mukai et al., 2007; Tseng et al., 2013). Moreover, sea-surface height indicates water mass movements and, by extension, the flow of heat and nutrients, which will subsequently influence productivity (Ayers and Lozier, 2010). Sea-surface height can also be used to infer physical oceanographic features, such as eddies, fronts, and convergences (Polovina and Howell, 2005). Therefore, understanding the relationship between oceanographic

factors and the migration and distribution of species is essential for fisheries management.

Most studies of Pacific saury have concentrated on distribution and migration and have used in situ or logbook data (Huang et al., 2007; Tseng et al., 2013), and models have been developed to investigate growth and abundance (Tian et al., 2004; Ito et al., 2004, 2007; Mukaietal., 2007). In contrast, Watanabe et al. (2006) proposed a spatial and temporal migration model for stock size that was dependent on SST. However, integrated high-resolution nighttime satellite images, such as those available in the time-series data from the Operational Linescan System (OLS) of the Defense Meteorological Satellite Program, U.S. Department of Defense, together with habitat and environmental modeling, have not been used to predict the potential fishing zones for Pacific saury.

In Japan, fishing vessels operate at night and use stick-held dip nets, locally known as *bouke ami*, which are equipped with lights to attract fishes (Fukushima, 1979). These fishing vessels, equipped with lights, as are vessels that fish for Pacific saury, can be identified by the OLS sensor, which also enables the detection of moonlight-illuminated clouds and lights from cities, towns, industrial sites, gas flares, and ephemeral events, such as fires and lightning-illuminated clouds (Elvidge et al., 1997). In addition, OLS nighttime images can be used to estimate fishing vessel numbers and fishing areas for squid (Kiyofuji and Saitoh, 2004; Kiyofuji et al., 2004). The relationship between the number of lit pixels in OLS nighttime images and the number of fishing vessels also has been analyzed for the fishery of *Illex argentinus* (Waluda et al., 2002). The brightly lit areas seen in nighttime images of the western North Pacific are the result of vessels fishing for Pacific saury or squid (Semedi et al., 2002; Saitoh et al., 2010; Mugo et al., 2014).

Predictive habitat modeling has become an increasingly useful tool for marine ecologists and conservation scientists in order to estimate the patterns of species distribution and to subsequently develop conservation strategies (Johnson and Gillingham, 2005; Tsoar et al., 2007; Ready et al., 2010). The maximum entropy method (Phillips et al., 2006) involves one of the most widely used machine-learning algorithms for inferring species distributions. In recent studies, the method of maximum entropy has been applied to both terrestrial (Peterson et al., 2007) and marine ecosystems (Ready et al., 2010; Edrén et al., 2010; Alabia et al., 2015). In this study, we used a maximum entropy approach with multi sensor satellite datasets and OLS-derived species occurrences to create an accurate prediction model and investigate the potential fishing zones for Pacific saury in the western North Pacific. The objectives of this study were to evaluate the effects of oceanographic factors on the formation of potential fishing zones for Pacific saury and to examine the variability in spatial patterns of potential fishing zones in relation to the prevailing oceanographic conditions in the western North Pacific.

Materials and methods

Study area

This study was conducted in the western North Pacific, extending from 140° to 155°E and from 34° to 46°N (Fig. 1). In this study area, located between the subarctic and subtropical domains of the North Pacific, the confluence of the warm Kuroshio Current and the cold Oyashio Current forms the Kuroshio–Oyashio transition zone (Roden, 1991), also called the subarctic–subtropical transition zone. The Kuroshio Current is characterized by warm, low-density, nutrient-poor, and high-salinity surface waters (Yatsu et al., 2013), whereas the Oyashio Current is characterized by low-salinity, low-temperature, and nutrient-rich waters (Sakurai, 2007). The Kuroshio–Oyashio transition zone is characterized by the mixing of various water masses and complex physical oceanographic structures (Roden, 1991). Moreover, 3 major oceanic fronts exist in this region: the Polar Front, Subarctic Front, and Kuroshio Extension Front (Science Council of Japan[1]). The characteristic patterns of these oceanic fronts also have been well documented in earlier studies (Kitano, 1972; Roden et al., 1982; Belkin and Mikhailichenko, 1986; Miyake, 1989; Belkin et al., 1992, 2002; Yoshida, 1993; Onishi, 2001; Murase et al., 2014; Shotwell et al., 2014).

Satellite nighttime images

Daily cloud-free OLS nighttime images were downloaded from the Satellite Image Database System of the Agriculture, Forestry and Fisheries Research Information Center of the Japan Ministry of Agriculture, Forestry and Fisheries [the system is no longer operating]. The images were then used to determine the location of the vessels that fish for Pacific saury in the western North Pacific. A TeraScan[2] system, vers. 4.0 (Seaspace Corp., Poway, CA) was used to analyze the images and to process the nighttime lights into digital numbers (DNs), in a range of 0–63, that represent the visible pixels in relative values. We selected 1264 single pass images collected from August through December during 2005–2013 (9 years) by 6 Defense Meteorological Satellite Program satellites (F13, F14, F15, F16, F17, and F18) (Table 1). The period from August through December was chosen for analysis because it corresponds with the fishing season of Pacific saury. To construct the habitat suitability model, the daily images were reprocessed with a 1-km resolution and then compiled in a monthly database. The location of the vessels was assumed to represent the location of Pacific saury.

[1] Science Council of Japan. 1960. The results of the Japanese oceanographic project for the International Geophysical Year 1957/8, 145 p. National Committee for the International Geophysical Year, Science Council of Japan, Tokyo.

[2] Mention of trades names or commercial companies is for identification purposes only and does not imply endorsement by the National Marine Fisheries Service, NOAA.

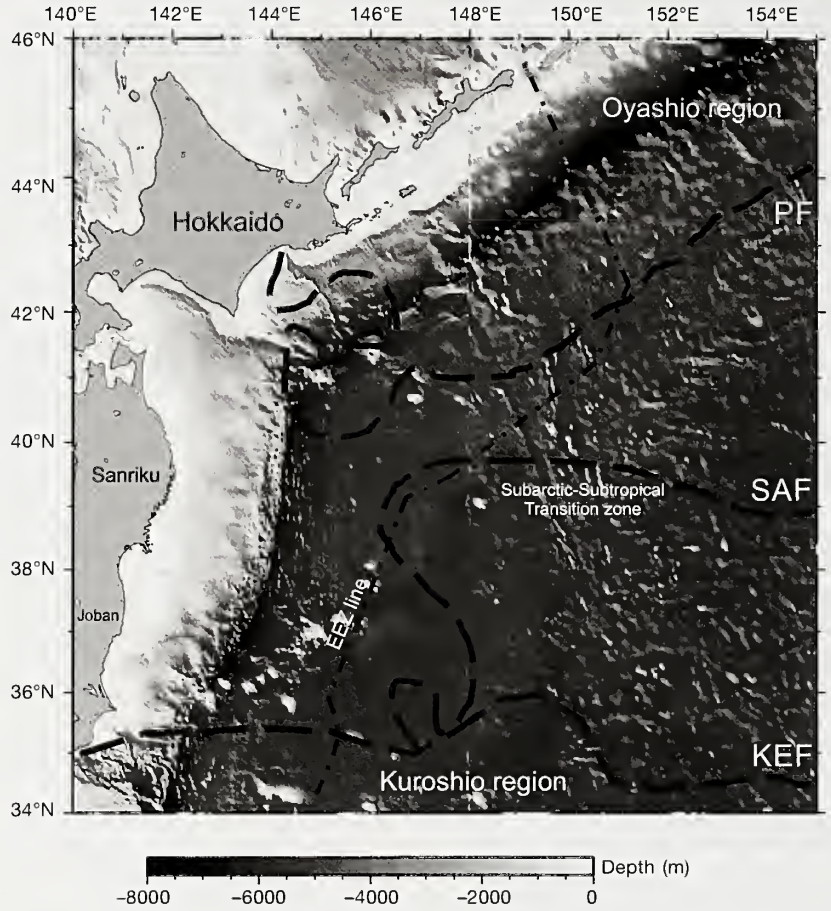

Figure 1

Map of the study area in the western North Pacific with the hydrographic and topographic features of the ocean basin. The line with dashes and dots represents the boundary of the EEZ of Japan. The lines with dashes correspond to the 3 major oceanic fronts—the Polar Front (PF), Subartic Front (SAF), and Kuroshio Extension Front (KEF). The subarctic–subtropical transition zone is also shown. Redrawn after Murase et al. (2014).

Detection of fishing vessel

We examined the histograms of DNs in our analyses of OLS images for each month in order to identify the fishing areas. Several peaks in DNs were recorded over the examined 5-month periods (Fig. 2). To extract the areas with fishing-vessel lights, DN thresholds for identifying Pacific saury fishing vessels were calculated for each month because of the monthly differences in DN frequency distribution. A 2-level slicing method was used to extract the bright areas thought to be caused by the fishing fleet. This method is used to find a statistical optimum threshold from the DN frequency distribution (Takagi and Shimoda, 1991).

The thresholds, k, were determined through the use of the following method proposed by Kiyofuji and Saitoh (2004), and the variance, $\sigma^2(k)$, was calculated with the equations proposed by Takagi and Shimoda (1991):

$$\sigma^2(k)=\omega_0(\mu_0-\mu_T)^2 + \omega_1 (\mu_1-\mu_T)^2, \quad (1)$$

where n_i = the number of pixels at i levels;
N = the total number of pixels;
P_i = n_i/N;
ω_0 = $\sum_{i=1}^{k} Pi$ and ω_1 = $\sum_{i=k+1}^{l} Pi$;
μ_0 = $\sum_{i=1}^{k} iPi \,/\, \omega_0$ and μ_1 = $\sum_{i=k+1}^{l} iPi \,/\, \omega_1$;
μ_T = $\sum_{i=1}^{l} iPi$.

With these methods, 5 thresholds were identified (Table 2). Class 1, 2, 3, and 4 thresholds indicate ocean water or cloud coverage, and the class 5 threshold indicates bright areas resulting from fishing vessel lights. Therefore, class 5 threshold values were applied to extract the bright areas that represented fishing vessel lights.

Lights from vessels that fish for Pacific saury and those that fish for squid are contained in OLS images. These lights are difficult to distinguish from each other; therefore, it is necessary to generate OLS images with less contamination from the lights of vessels fishing for

Table 1

Number of images from the Operational Linescan System of the U.S. Defense Meteorological Satellite Program for the period 2005–2013, by month and year, that were used in this study to predict fishing locations of Pacific saury (*Cololabis saira*) in the western North Pacific.

Month	2005	2006	2007	2008	2009	2010	2011	2012	2013
August	37	24	14	0	0	15	15	12	4
September	44	43	9	2	7	27	17	29	17
October	67	70	55	3	11	47	36	33	31
November	72	53	69	16	16	43	34	27	36
December	51	31	21	1	10	30	43	22	20

squid. In this study, we used SST to distinguish between the lights of the vessels that fish for Pacific saury and those of other fishing vessels because Pacific saury prefers colder areas for their migration routes (Saitoh et al., 1986) and this approach was used earlier by Mugo et al. (2014).

Because Pacific saury are distributed below the upper SST limit (Table 3), we split the nighttime light images into 2 categories. All lights that occurred above the upper SST limit were categorized as lights related to squid fishing, and all lights that occurred below this limit were assumed to be from vessels fishing for Pacific saury. Consequently, only the locations of lights that indicated fishing for Pacific saury were used for our habitat modeling procedures.

Environmental data

We used satellite-derived data—chl-*a*, SST, eddy kinetic energy (EKE), and sea-surface height anomaly (SSHA)—from 2005 through 2013 as environmental factors in the maximum entropy models. Daily chl-*a* and SST values were derived from satellite images from the Moderate Resolution Imaging Spectroradiometer (MODIS)-Aqua mission and were downloaded from NASA Goddard Space Flight Center [website]. These data were processed with the SeaDAS package, vers. 6.4 (NASA Goddard Space Flight Center, Greenbelt, MD) and reprocessed to create maps with a 1-km resolution.

Daily SSHA and geostrophic velocities (u, v) from the Topex/Poseidon and ERS-1/2 altimeters were

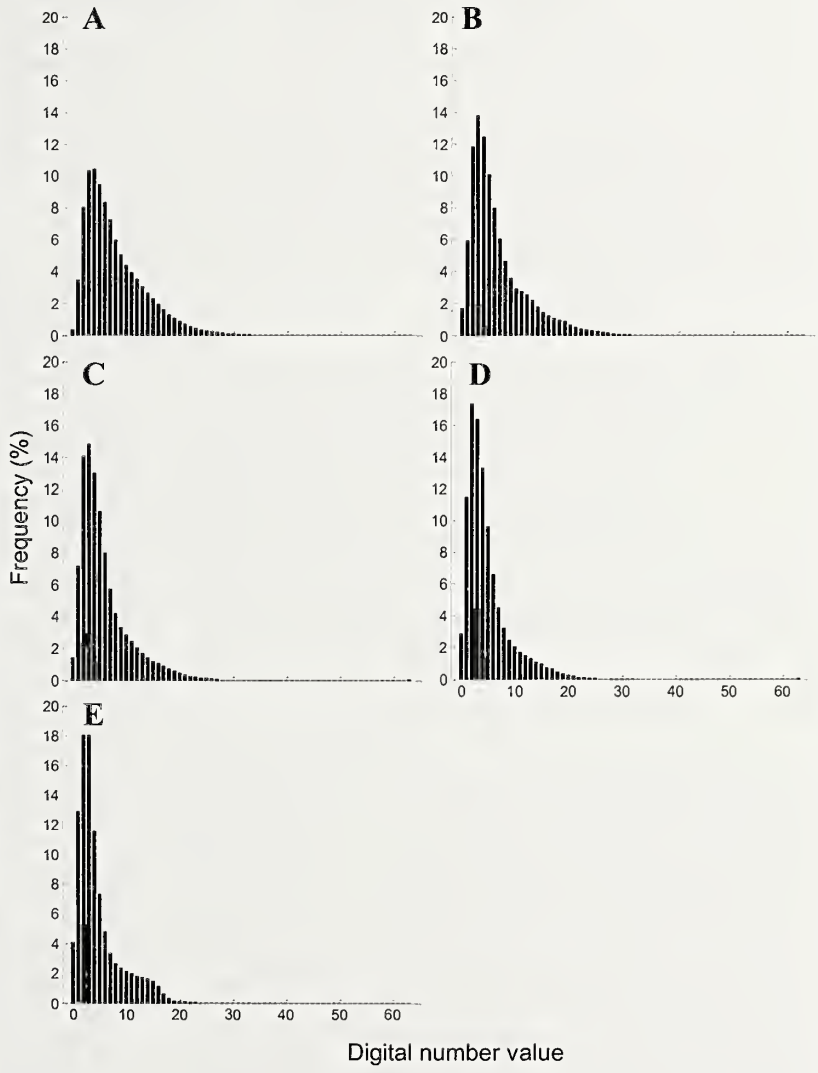

Figure 2

Histograms of the relative frequency of visible pixels derived from monthly composite images obtained from the western North Pacific from the Operational Linescan System of the U.S. Defense Meteorological Satellite Program for (**A**) August, (**B**) September, (**C**) October, (**D**) November, and (**E**) December for the period 2005–2013

Table 2

Thresholds for digital numbers (in pixels) for satellite images from the Operational Linescan System of the U.S. Defense Meteorological Satellite Program for the period 2005–2013. Thresholds were calculated from the histogram in Figure 2. Pixels within the class 5 range represent fishing vessel lights. Classes 1–4 represent reflected light from ocean water or light from cloud cover.

Month	Class 1	Class 2	Class 3	Class 4	Class 5
August	10	17	23	30	40
September	9	16	22	28	38
October	8	14	19	27	38
November	8	13	19	28	38
December	7	12	18	27	38

Table 3

Mean monthly sea-surface temperature (SST) values (°C) and standard deviations (SD), used to distinguish the light of vessels fishing for Pacific saury (*Cololabis saira*) from the lights of fishing fleets fishing for other fish. All lights occurring below the upper SST limit were categorized as locations of vessels targeting Pacific saury.

Month	Mean	SD	Upper SST limit
August	20.79	2.69	23.48
September	18.89	2.47	21.36
October	15.90	2.58	18.48
November	14.56	2.88	17.44
December	13.60	2.89	16.49

produced and distributed by Archiving Validation and Interpretation of Satellite Oceanographic Data (AVISO; website) at a spatial resolution of 0.33°×0.33°. The surface geostrophic velocities were used to compute for EKE by using the following equation (Steele et al., 2010):

$$EKE = \frac{1}{2}(u'^2 + v'^2), \quad (2)$$

where u' and v' = the zonal and meridional components of geostrophic currents, respectively.

With the grid function of the software package Generic Mapping Tools, vers. GMT 4.5.7 (website),we were able to calculate the monthly averages for each environmental variable from daily data sets, resampled to 1-km resolution and converted to Esri ASCII grid format(Esri, Redlands, CA) or to comma-separated values (CSV) format, as required by the software program Maxent (website).

Construction of a maximum entropy model

To develop a model with a maximum entropy approach, we used the software program Maxent, vers. 3.3.3k. Phillips et al. (2006) provided detailed information on the mode of operating this software. We constructed models using default values for regulation parameter (1), maximum iteration (500), and automatic feature class selection. We used a cross-validation procedure to evaluate the performance of the models. For background points, we generated pseudo-absences (10:1 ratio of pseudo-absence to presence) following Barbet-Massin et al., (2012) on the basis of random spatial sampling within the study area (excluding points of presence of Pacific saury). We used the *density.tools. RandomSample* command line in Maxent to generate the random pseudo-absences. For each monthly model, the data were randomly split into 2 categories: one category for training data (70%) and one for test data (30%). The test points were then used to calculate the area under the curve (AUC) of the receiver operating characteristic (ROC) (Phillips et al., 2006).

Evaluation and validation of the model

We used the AUC metric of the ROC curve to evaluate model fit (Elith et al., 2006; Phillips et al., 2006). The relative contribution of individual environmental variables within the maximum entropy model was examined by using the heuristic estimates of variable importance based on the increase in the model gain, which is associated with each environmental factor and its corresponding model feature. Response curves generated for each factor were examined to derive the favorable environmental ranges for potential fishing zones.

Independent sets of monthly OLS data from 2011 through 2013 were used to validate the models. The base models were used to create habitat suitability indices (HSIs) that assimilated similar environmental layers for the corresponding period from 2011 through 2013. Spatial HSI maps were generated and overlain with information on OLS data from the period 2011–2013.

Results

Spatiotemporal distribution of fishing locations, and environmental data

Figure 3 shows the variation in the distribution of fishing vessel lights from August through December during 2005–2013. Vessels started to appear off the Kuril Islands and east of Hokkaido in August (Fig. 3A). At the same time, fishing also occurred around the Sanriku coast of Japan and an offshore area between 150°E and 41°N that extended northeast to155°E and 43°N.

During September (Fig. 3B), fishing vessels were distributed mostly north of 42°N, especially off east-

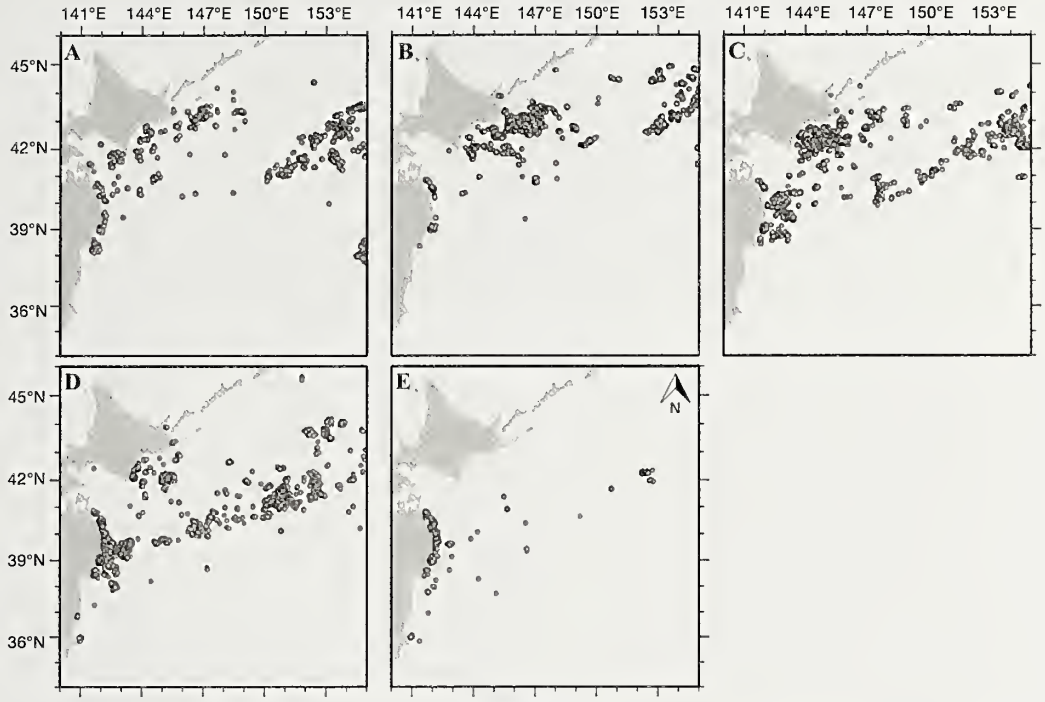

Figure 3

Spatial distribution of fishing locations for Pacific saury (*Cololabis saira*) in the western North Pacific pooled during (**A**) August, (**B**) September, (**C**) October, (**D**) November, and (**E**) December for the period 2005–2013.

ern Hokkaido, whereas the number of vessels off the Sanriku coast decreased. In October (Fig. 3C), fishing vessels were widely distributed in Hokkaido and Sanriku waters. The distribution of fishing vessels moved slightly to the south and approached the shores of southeastern Hokkaido and Sanriku (38–41°N). During this same month, the offshore fishing locations (148°E and 48°N) also increased and extended northeast to 154°E and 43°N.

During November (Fig. 3D), fishing vessels moved southward. The number of fishing vessels in eastern Hokkaido waters decreased, but the number of fishing vessels around the Sanriku coast increased (38–41°N) and moved northeast to 155°E and 43°N. A small number of fishing vessels also appeared off the Joban coast. In December (Fig. 3E), fishing vessels appeared mostly along the Sanriku coast and were distributed in nearshore waters between 38°N and 40°N; however, a small number of fishing vessels still remained offshore and along the Joban coast.

The monthly averaged time series of environmental data for the period 2005–2013 are shown in Figure 4. Mean SST values indicated a decreasing trend of temperature on the fishing locations from August through December (Fig. 4A). Mean chl-*a* concentrations (Fig. 4B) increased in September but declined in December. The mean chl-*a* concentration was highest in September (0.93 mg/m^3), when most vessels were concentrated off the eastern coast of Hokkaido and near the southern Kuril Islands. Mean EKE and SSHA values (Fig. 4, C–D) increased in trends that corresponded with the southward shift of fishing vessels, especially from September until November.

Model performance and potential fish habitat

All monthly maximum entropy models significantly fitted better than they were fitted by chance as supported by the modest values of the performance metric (AUC>0.5; Table 4). This outcome indicates the high predictive success of these models (Elith et al., 2006; Phillips et al., 2006). The relative contribution of each environmental variable to model prediction is shown in Table 5. Model results indicate that the 2 most important factors in August and October were SST and EKE, and in September the most important factors were SST and chl-*a*. In November and December, the 2 highest contributions to model gain were SST and SSHA.

Figure 5 provides the model-derived preferred ranges for each environmental variable. The plots in this figure show the performance and contribution of the various environmental data to model fit. High probabilities of occurrence of Pacific saury were observed in varied ranges for each month. In general, occurrence of Pacific saury had the highest probabilities in cool (14–16°C) waters with chl-*a* concentrations of 0.5–2.0 mg/m^3. In addition, there were high probabilities of occurrence of Pacific saury at low to moderate EKE and positive SSHA values.

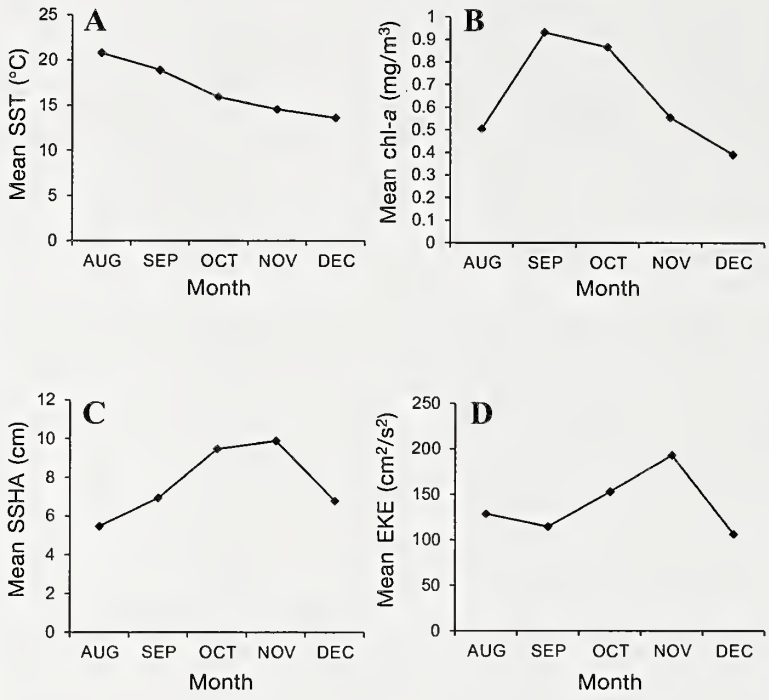

Figure 4

Monthly mean time series of (**A**) sea-surface temperature (SST), (**B**) chlorophyll-*a* (chl-*a*), (**C**) sea-surface height anomaly (SSHA), and (**D**) eddy kinetic energy (EKE) in the western North Pacific from August through December for the period 2005–2013.

Table 4

Summary statistics derived from the monthly models for the period 2005–2010. The base models were calibrated with 70% of Pacific saury occurrence data, and values for the area under the curve (AUC) were calculated from the remaining 30% of the occurrence data. The total number of fishing locations (*N*) is given for each month. All the models fitted significantly better than if they were fitted by chance (AUC>0.5).

Month	AUC	*N*
August	0.907	8074
September	0.910	7411
October	0.912	10,062
November	0.886	5162
December	0.949	429

Table 5

Heuristic estimates of the relative percent contribution of environmental variables to models derived by using a maximum entropy approach. The 2 most important variables for each monthly model are presented in bold. SST=sea surface temperature; chl-*a*=chlorophyll-*a*; EKE=eddy kinetic energy; SSHA=sea-surface height anomaly.

	Environmental predictors			
Model	SST	Chl-*a*	EKE	SSHA
August	**55.6**	7.1	**28.1**	9.2
September	**56.8**	**21.6**	14.4	7.2
October	**72.2**	5.9	**13.6**	8.3
November	**73.2**	2.9	9.4	**14.5**
December	**57.6**	0.8	6.2	**35.4**

Prediction and validation of occurrence

Maps of predicted HSI for August–December (2011–2013) are shown in Figure 6. In August, the predicted probability of occurrence of Pacific saury covered the entire Oyashio region, but it did so with a small value of HSI (Fig. 6, A–C). In September, high probability areas (HIS ≥0.6) increased, especially east of Hokkaido and the Kuril Islands. The presence of fishing locations derived from OLS images also increased east of Hokkaido during this period (Fig. 6, D–F). In October, the known peak of the fishing season, a high

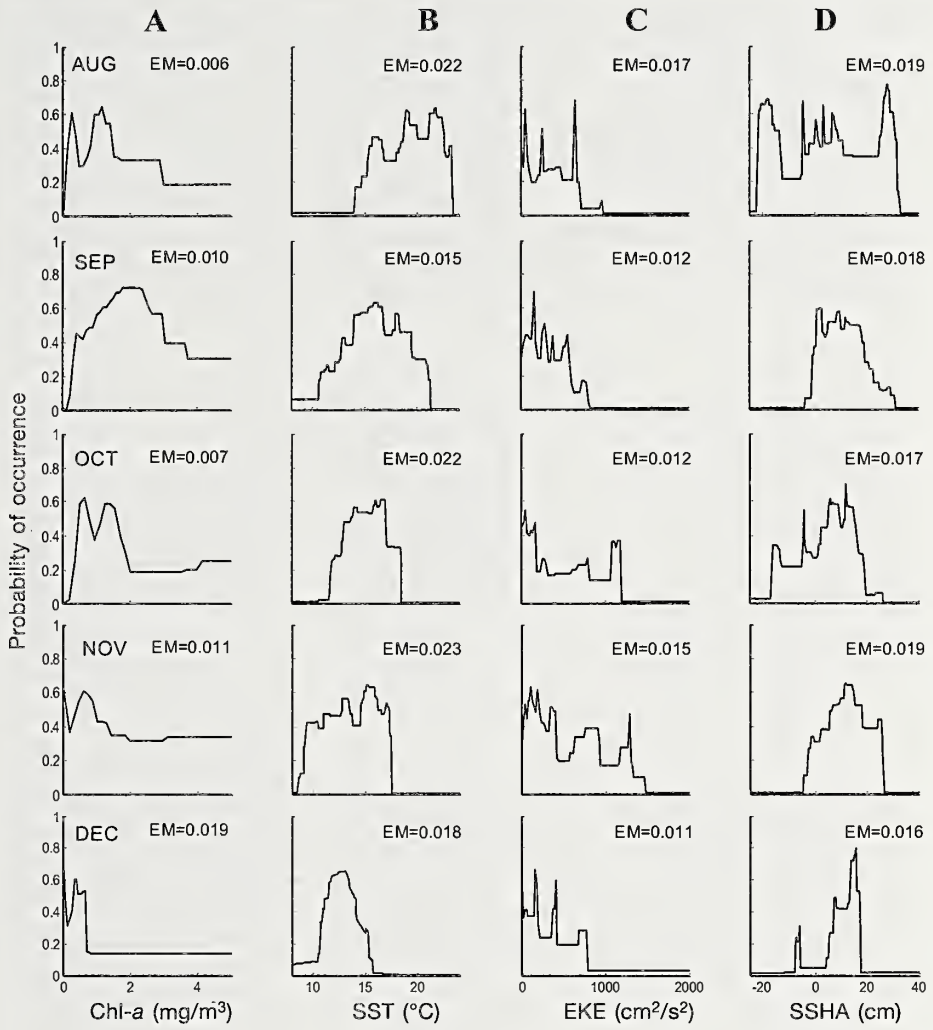

Figure 5

Response curves from the monthly base model for (**A**) chlorophyll-*a* (chl-*a*), (**B**) sea surface temperature (SST), (**C**) eddy kinetic energy (EKE), and (**D**) sea-surface height anomaly (SSHA) in the western North Pacific. The error margin (EM) for each plot is provided.

probability of occurrence of Pacific saury remained for east and southeast of Hokkaido and south of the Kuril Islands. During the same month, the results from the predicted HSI indicated the Kuroshio–Oyashio transition zone at 40°N, and a correspondingly high probability of occurrence of Pacific saury (Fig. 6, G–I). In November, the high predicted HSI in the transition zone (38–42°N and 142–155°E) increased, especially off the Sanriku (39–41°N) and Joban (38–39°N) coasts (Fig. 6, J–L). At the end of the fishing season in December, the predicted probability of occurrence dramatically decreased in the offshore areas but remained high off the Sanriku and Joban coasts (Fig. 6, M–O). In general, the distribution of Pacific saury based on the HSI showed moderate spatial correlation with actual fishing locations derived from OLS images, although it did so with relatively low HSI values, particularly in August.

Discussion

We used fishing locations for Pacific saury and oceanographic variables with maximum entropy models to predict the potential fishing zones for Pacific saury in western North Pacific waters. Analyses of OLS nighttime images allowed us to locate fishing vessel lights across space and time, and we assumed that Pacific saury were caught in areas where fishing vessels were identified. On the basis of the derived fishing vessel locations, we were able to estimate the spatial and temporal distribution of potential fishing zones for Pacific saury.

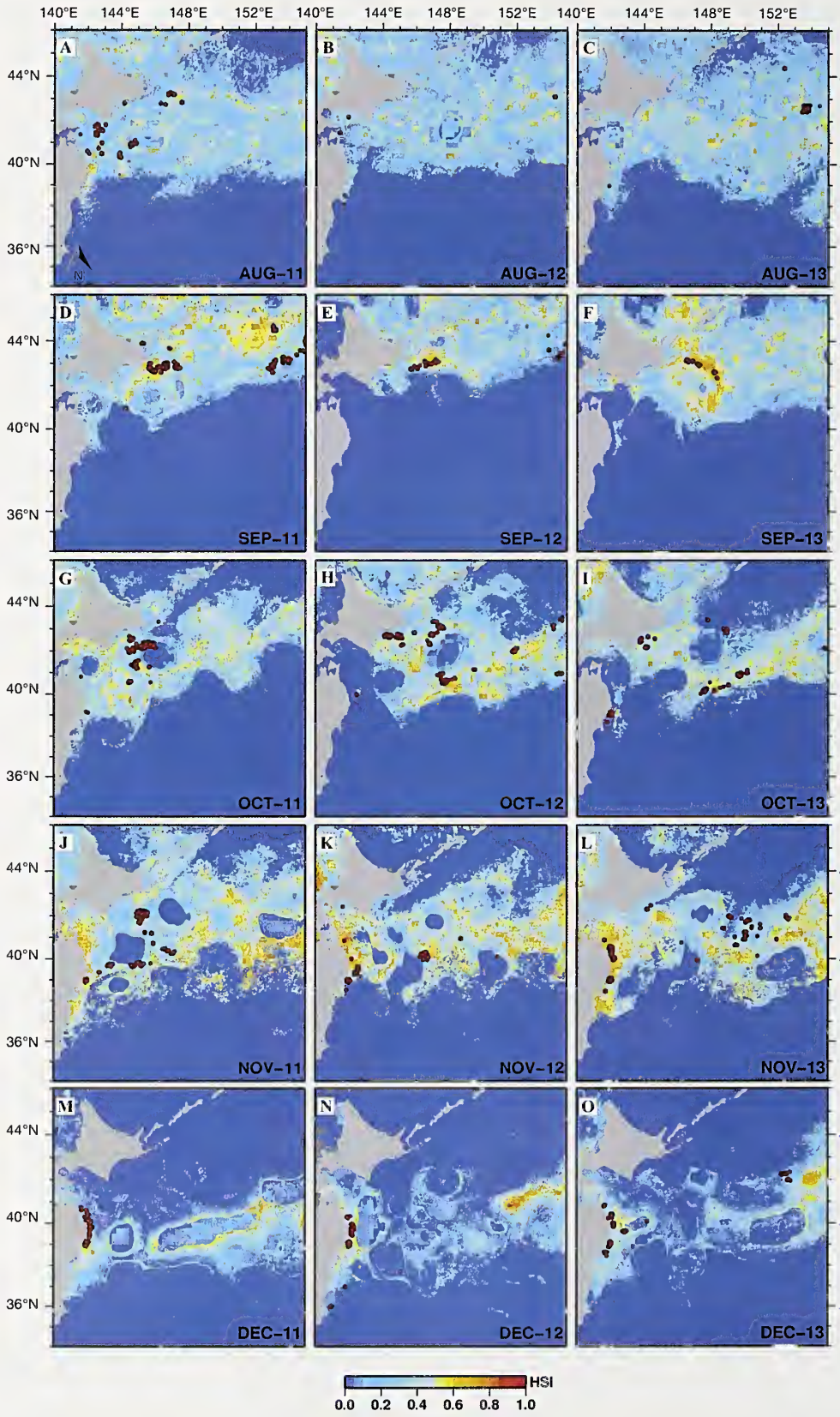

Figure 6

The spatial distribution of fishing locations (red dots) for Pacific saury (*Cololabis saira*) in the western North Pacific derived from analyses of images from the Operational Linescan System of the U.S. Defense Meteorological Satellite Program for the period August–December during 2011–2013, overlain on maps of habitat suitability predicted with base models. The suitability is depicted as an Habitat Suitability Index (HSI) score ranging from 0 to 1, representing "poor" to "good" habitat quality, respectively.

At the beginning of the fishing season, fishing locations derived from OLS images showed that most of the vessels that fished for Pacific saury appeared east of Hokkaido and south of the Kuril Islands (Fig. 3, A and B). In the middle of the fishing season (October to November) (Fig. 3, C and D), vessels that fish for Pacific saury moved slightly to the south and appeared mostly around the eastern coasts of Hokkaido and Sanriku—a finding that potentially resulted from the southward extension of Oyashio fronts (Watanabe et al., 2006; Tseng et al., 2011). At the end of the fishing season, vessels that fish for Pacific saury were concentrated along the Sanriku coast (Fig. 3E).

Images from the OLS also showed that some of the fishing vessels appeared outside the EEZ, possibly because Pacific saury is an oceanic spawner, unlike other small pelagic fishes, such as the Japanese sardine (*Sardinops melanostictus*) and the Japanese anchovy (*Engraulis japonicus*), that generally spawn in the coastal and near shore waters of Japan (Zenitani et al., 1995). The low capture of fish west of 150°E from June through July before the fishing season indicates that Pacific saury caught by Japanese fishing vessels were located far from the northeastern coasts of Japan (Tohoku National Fisheries Research Institute[3]).

The predicted distribution of Pacific saury in the western North Pacific revealed areas of high probability of occurrence off Hokkaido and the Kuril Islands (Fig. 6, A–F), areas that gradually moved south toward the Sanriku and Joban coasts by the end of the fishing season (Fig. 6, M–O). These patterns coincided with the north–south migration of Pacific saury that marks the start and end of the fishing season. Results from a maximum entropy approach further indicate that the highest probability of presence occurred along the Kuroshio–Oyashio transition zone in November (Fig. 6, J–L).

The occurrence of large-size Pacific saury (>29.0 cm in knob length) off the southern Kuril Islands during their spawning migration indicates that a high proportion of large-size Pacific saury moved from the high seas to coastal waters at the beginning of their migration toward the southwest—movement that was then followed by a similar migration of medium-size Pacific saury (24.0–29.0 cm in knob length). Therefore, abundance of Pacific saury off the coastal waters in our study is higher than the abundance observed in regions in the high seas (Huang, 2010). In addition, the high density of Pacific saury off Hokkaido and the Kuril Islands was probably related to the southward movement of the Oyashio Current (Tseng et al., 2011). The high presence of Pacific saury at the coasts also could be a result of a westward current intensification, which can result in the formation of oceanic fronts (Huang, 2010). These frontal features have been known as the preferred migratory routes of Pacific saury and other marine species (Saitoh et al., 1986; Zainuddin et al., 2008).

Although oceanographic conditions are likely to affect species distribution, other factors, such as prey density, are equally important. In the Kuroshio–Oyashio transition zone, Oyashio intrusions transport organic matter, thereby supporting the production of copepods, which are the primary prey of Pacific saury (Odate, 1994; Shimizu et al., 2009). This salient physical process could potentially explain the existence of habitat areas of Pacific saury in the transition zone, areas that were identified with maximum entropy models and that consequently highlight the importance of this region as migratory and feeding corridors for Pacific saury.

The variability of the performance of the maximum entropy model was very low across the monthly base models, where AUCs higher than 0.9 indicate that models had excellent agreement with the test data (Table 4). As pointed out earlier, productivity and fish distribution are influenced by changes in the environment evident from the variations in temperature, currents, salinity, and wind fields (Southward et al., 1988; Alheit and Hagen, 1997). In our study, SST (among the set of oceanographic variables examined) showed the highest contribution to all monthly base models (Table 5), indicating the sensitivity of Pacific saury to temperature changes. For instance, increasing SST will directly reduce juvenile growth and prevent, or delay, the southern migration of Pacific saury in winter (Ito et al., 2013). Moreover, changes in winter SSTs in the Kuroshio–Oyashio transition zone and in the Kuroshio and Oyashio regions also affected the abundance of the large-size (winter cohort) and medium-size (spring cohort) groups of Pacific saury (Tian et al., 2003).

To our knowledge, this study was the first attempt to use both EKE and SSHA to describe potential fishing habitat of Pacific saury in relation to mesoscale oceanography variability. Our results indicate that fishing activities occurred in areas with low to moderate EKE (Fig. 5), reflecting the likely association of this species with eddies. Meandering eddies likely trap prey of Pacific saury, creating good feeding opportunities through local enhancement of chl-*a* and zooplankton abundance and through the aggregation of prey organisms (Owen, 1981; Zhang et al., 2001). The importance of forage availability for Pacific saury is further reflected in the higher contribution of chl-*a* concentration to the base model in September (Table 5). Together with SST, chl-*a* has been found to influence Pacific saury growth, recruitment, distribution, and migratory patterns (Ito et al., 2004; Oozeki et al., 2004; Yasuda and Watanabe, 2007). However, from November through December, the distribution of Pacific saury likely is not limited by food availability because of a general increase in ocean mixing and a decrease in water column stratification during this period. These oceanographic conditions consequently enhance the chl-*a* concentration in the mixed-water region (Mugo et al., 2014).

[3] Tohoku National Fisheries Research Institute. 2010. The 58th Annual Report of the Research Meeting on Saury Resources, 250 p. Tohoku Natl. Fisheries Res. Inst., Hachinohe, Japan. [In Japanese.]

Finally, OLS nighttime images were found to be useful for investigating the distribution of the lights of fishing vessels—an outcome that supports the results of earlier studies (Semedi et al., 2002; Saitoh et al., 2010). However, cloud contamination significantly limited the use of OLS images and reduced the density of proxy fishing locations; therefore, logbook data are needed to confirm the validity of fish occurrences in the future. The integration of these empirical data with multi sensor remote sensing information within a modeling platform could offer a powerful and innovative way to identify the potential fishing zones for Pacific saury and could be used to support fisheries management decisions.

Acknowledgments

This work was supported by the Directorate General of Higher Education of the Republic of Indonesia. We thank the 3 anonymous reviewers for their valuable comments. We also recognize the use of OLS images downloaded from the Satellite Image Database System of the Ministry of Agriculture, Forestry and Fisheries, SST and chl-*a* data from NASA's Goddard Space Flight Center, and SSHA and geostrophic velocity data from the AVISO website.

Literature cited

Alabia, I. D., S. Saitoh, R. Mugo, H. Igarashi, Y. Ishikawa, N. Usui, M. Kamachi, T. Awaji, and M. Seito.
2015. Seasonal potential fishing ground prediction of neon flying squid (*Ommastrephes bartramii*) in the western and central North Pacific. Fish. Oceanogr. 24:190–203.

Alheit, J., and E. Hagen.
1997. Long-term climate forcing of European herring and sardine populations. Fish. Oceanogr. 6:130–139.

Ayers, J. M., and M. S. Lozier.
2010. Physical controls on the seasonal migration of the North Pacific transition zone chlorophyll front. J. Geophys. Res. 115:C05001.

Barbet–Massin, M., F. Jiguet, C. H. Albert, and W. Thuiller.
2012. Selecting pseudo-absences for species distribution models: how, where and how many? Methods Ecol. Evol. 3:327–338.

Belkin, I. M., and Y. G. Mikhailichenko.
1986. Thermohaline structure of the Northwest Pacific Frontal Zone near 160° E. Oceanology [English translation.] 26:47–49.

Belkin, I. M., V. A. Bubnov, and S. E. Navrotskaya.
1992. Ocean fronts of "Megapolygon-87." *In* The Megapolygon experiment (Y. A. Ivanov, ed.), p. 96–111. Nauka, Moscow. [In Russian.]

Belkin, I., R. Krishfield, and S. Honjo.
2002. Decadal variability of the North Pacific Polar Front: subsurface warming versus surface cooling. Geophys. Res. Lett. 29:65-1–65-4.

Edrén, S. M. C., M. S. Wisz, J. Teilmann, R. Dietz, and J. Söderkvist.
2010. Modelling spatial patterns in harbour porpoise satellite telemetry data using maximum entropy. Ecography 33:698–708.

Elith, J., C. H. Graham, R. P. Anderson, M. Dudik, S. Ferrier, A. Guisan, R. J. Hijmans, F. Huettmann, J. R. Leathwick, A. Lehmann, et al.
2006. Novel methods improve prediction of species' distributions from occurrence data. Ecography 29:129–151.

Elvidge, C. D., K. E. Baugh, E. A. Kihn, H.W. Kroehl, and E.R. Davis.
1997. Mapping city lights with nighttime data from the DMSP Operational Linescan System. Photogramm. Eng. Remote Sens. 63:727–734.

Fisheries Agency and Fisheries Research Agency of Japan.
2012. Marine fisheries stock assessment and evaluation for Japanese waters (fiscal years 2011/2012), 1743 p. Fisheries Agency and Fisheries Research Agency of Japan, Tokyo. [In Japanese.]

Fukushima, S.
1979. Synoptic analysis of migration and fishingconditions of saury in northwest Pacific Ocean. Bull. Tohoku Reg. Fish Res. Lab. 41:1–70. [In Japanese.]

Huang, W.-B.
2010. Comparisons of monthly and geographical variations in abundance and size composition of Pacific saury between the high-seas and coastal fishing grounds in the northwestern Pacific. Fish. Sci. 76:21–31.

Huang, W.-B., N. C. H. Lo, T.-S. Chiu, and C.-S. Chen.
2007. Geographical distribution and abundance of Pacific saury, *Cololabis saira* (Brevoort) (Scomberesocidae), fishing stocks in the northwestern Pacific in relation to sea temperature. Zool. Stud. 46:705–716.

Ito, S., H. Sugisaki, A. Tsuda, O. Yamamura, and K. Okuda.
2004. Contributions of the VENFISH program: mesozooplankton, Pacific saury (*Cololabis saira*) and walleye pollock (*Theragra chalcogramma*) in the northwestern Pacific. Fish. Oceanogr. 13 (suppl. S1):1–9.

Ito, S.-I., B. A. Megrey, M. J. Kishi, D. Mukai, Y. Kurita, Y. Ueno, and Y. Yamanaka.
2007. On the interannual variability of the growth of Pacific saury (*Cololabis saira*): a simple 3-box model using NEMURO.FISH. Ecol. Model. 202:174–183.

Ito, S.-I., T. Okunishi, M. J. Kishi, and M. Wang.
2013. Modelling ecological responses of Pacific saury (*Cololabis saira*) to future climate change and its uncertainty. ICES J. Mar. Sci. 70:980–990.

Johnson, C. J., and M. P. Gillingham.
2005. An evaluation of mapped species distribution models used for conservation planning. Environ. Conserv. 32:117–128.

Kitano, K.
1972. On the polar frontal zone of the northern North Pacific Ocean. *In* Biological oceanography of the northern North Pacific Ocean (A.Y. Takenouti, ed.), p. 73–82. Idemitsu Shoten, Tokyo.

Kiyofuji, H., and S. Saitoh.
2004. Use of nighttime visible images to detect Japanese common squid *Todarodes pacificus* fishing areas and potential migration routes in the Sea of Japan. Mar. Ecol. Prog. Ser. 276:173–186.

Kiyofuji. H., K. Kumagai, S. Saitoh, Y. Arai, and K. Sakai.
2004. Spatial relationship between Japanese common squid (*Todarodes pacificus*) fishing grounds and fishing ports: an analysis using remote sensing and geographical information systems. *In* GIS/spatial analyses in fishery and aquatic sciences, vol. 2 (T. Nishida, P. J. Kaiola, and

C. E. Hollingworth, eds.), p 341–354. Fishery-Aquatic GIS Research Group, Saitama, Japan.

Kosaka, S.
2000. Life history of Pacific saury, *Cololabis saira,* in the Northwest Pacific and consideration of resource fluctuation based on it. Bull. Tohoku Natl. Fish. Res. Inst. 63:1–96. [In Japanese with English abstract.]

Miyake, H.
1989. Water mass structure and the salinity minimum waters in the western subarctic boundary region of North Pacific. Umi to Sora 65:107–118. [In Japanese.]

Mugo, R. M., S. Saitoh, F. Takahashi, A. Nihira, and T. Kuroyama.
2014. Evaluating the role of fronts in habitat overlaps between cold and warm water species in the western North Pacific: a proof of concept. Deep-Sea Res., II 107:29–39.

Mukai, D., M. J. Kishi, S. Ito, and Y. Kurita.
2007. The importance of spawning season on the growth of Pacific saury: a model-based study using NEMURO. FISH. Ecol. Model. 202:165–173.

Murase, H., T. Hakamada, K. Matsuoka, S. Nishiwaki, D. Inagake, M. Okazaki, N. Tojo, and T. Kitakado.
2014. Distribution of sei whales (*Balaenoptera borealis*) in the subarctic–subtropical transition area of the western North Pacific in relation to oceanic fronts. Deep-Sea Res., II 107:22–28.

Odate, K.
1994. Zooplankton biomass and its long-term variation in the western North Pacific Ocean, Tohoku sea area, Japan. Bull. Tohoku Natl. Fish Res. Inst. 56:115–163. [In Japanese with English abstract.]

Onishi, H.
2001. Spatial and temporal variability in a vertical section across the Alaskan Stream and Subarctic Current. J. Oceanogr. 57:79–91.

Oozeki, Y., Y. Watanabe, and D. Kitagawa.
2004. Environmental factors affecting larval growth of Pacific saury, *Cololabis saira*, in the northwestern Pacific Ocean. Fish. Oceanogr. 13(suppl. S1):44–53.

Owen, R.W.
1981. Fronts and eddies in the sea: mechanisms, interactions and biological effects. *In* Analysis of marine ecosystems (A. R. Longhurst, ed.),p. 197–233. Academic Press, New York.

Peterson, A.T., M. Papes, and M. Eaton.
2007. Transferability and model evaluation in ecological niche modeling: a comparison of GARP and Maxent. Ecography 30:550–560.

Polovina, J. J., and E. A. Howell.
2005. Ecosystem indicators derived from satellite remotely sensed oceanographic data for the North Pacific. ICES J. Mar. Sci. 62:319–327.

Phillips, S. J., R. P. Anderson, and R. E. Schapire.
2006. Maximum entropy modeling of species geographic distributions. Ecol. Model. 190:231–259.

Ready, J., K. Kaschner, A. B. South, P. D. Eastwood, T. Rees, J. Rius, E. Agbayani, S. Kullander, and R. Froese.
2010. Predicting the distributions of marine organisms at the global scale. Ecol. Model. 221:467–478.

Roden, G. I.
1991. Subarctic-subtropical transitional zone of the North Pacific: large-scale aspects and mesoscale structure. *In* Biology, oceanography, and fisheries of the North Pacific transitional zone and subarctic frontal zone. NOAA Tech. Rep. NMFS 105 (J. A. Wetherall, ed.), p. 1–38.

Roden, G. I., B. A. Taft, and C. C. Ebbesmeyer.
1982. Oceanographic aspects of the Emperor Seamounts region. J. Geophys. Res., C 87:9537–9552.

Saitoh, S.,-I. A. Fukaya, K. Saitoh, B. Semedi, R. Mugo, S. Matsumura, and F. Takahashi.
2010. Estimation of number of Pacific saury fishing vessels using night-time visible images. Int. Arch. Photogramm. Remote Sens. Spatial Inf. Sci. 38:1013–1016.

Saitoh, S., S. Kosaka, and J. Iisaka.
1986. Satellite infrared observations of Kuroshio warm-core rings and their application to study of Pacific saury migration. Deep-Sea Res., A33:1601–1615.

Sakurai, Y.
2007. An overview of the Oyashio ecosystem. Deep-Sea Res., II 54:2526–2542.

Semedi, B., S.-I. Saitoh, K. Saitoh, and K. Yoneta.
2002. Application of multi-sensor satellite remote sensing for determining distribution and movement of Pacific saury, *Cololabis saira*. Fish. Sci. 68:1781–1784.

Shimizu, Y., K. Takahashi, S.-I. Ito, S. Kakehi, H. Tatebe, I. Yasuda, A. Kusaka, and T. Nakayama.
2009. Transport of subarctic large copepods from the Oyashio area to the mixed water region by the coastal Oyashio intrusion. Fish. Oceanogr. 18:312– 327.

Shotwell, S. K., D. H. Hanselman, and I. M. Belkin.
2014. Toward biophysical synergy: investigating advection along the Polar Front to identify factors influencing Alaska sablefish recruitment. Deep-Sea Res., II 107:40–53.

Southward, A. J., G. T. Boalch, and L. Maddock.
1988. Fluctuations in the herring and pilchard fisheries of Devon and Cornwall linked to change in climate since the 16th century. J. Mar. Biol. Assoc. U.K. 68:423–445.

Steele, J. H., S. A. Thorpe, and K. K. Turekian (eds.).
2010. Elements of physical oceanography: a derivative of the Encyclopedia of Ocean Science, 660 p. Academic Press, London.

Takagi, M., and H. Shimoda.
1991. Handbook of image analysis, 2032 p. Univ. Tokyo Press, Tokyo. [In Japanese.]

Tian, Y., T. Akamine, and M. Suda.
2002. Long-term variability in the abundance of Pacific saury in the northwestern Pacific Ocean and climate changes during the last century. Bull. Jpn. Soc. Fish. Oceanogr. 66:16–25. [In Japanese with English abstract.]
2003. Variations in the abundance of Pacific saury (*Cololabis saira*) from the northwestern Pacific in relation to oceanic-climate changes. Fish. Res. 60:439–454.
2004. Modeling the influence of oceanic-climatic changes on the dynamics of Pacific saury in the northwestern Pacific using a life-cycle model. Fish. Oceanogr. 13:125–137.

Tohoku National Fisheries Research Institute.
2010. The 58thAnnual Report of the ResearchMeeting on Saury Resources. Tohoku National Fisheries Research Institute, Hachinohe, Japan. [In Japanese.]

Tseng, C.-T., C.-L. Sun, S.-Z. Yeh, S.-C. Chen, W.-C. Su, and D. C. Liu.
2011. Influence of climate-driven sea surface temperature increase on potential habitats of the Pacific saury (Cololabis saira). ICES J. Mar. Sci. 68:1105–1113.

Tseng, C.-T., N.-J. Su, C.-L. Sun, A. E. Punt, S.-Z. Yeh, D.-C. Liu, and W.-C. Su.
2013 Spatial and temporal variability of the Pacific saury (*Cololabis saira*) distribution in the northwestern Pacific Ocean. ICES J. Mar. Sci. 70:991–999.

Tsoar, A., O. Allouche, O. Steinitz, D. Rotem, and R. Kadmon.
2007. A comparative evaluation of presence only methods for modelling species distribution. Diversity Distrib. 13:397–405.

Waluda, C. M., P. N. Trathan, C. D. Elvidge, V. R. Hobson, and P. G. Rodhouse.
2002. Throwing light on straddling stocks of *Illex argentinus*: assessing fishing intensity with satellite imagery. Can. J. Fish. Aquat. Sci. 59:592–596.

Watanabe, K., E. Tanaka, S. Yamada, and T. Kitakado.
2006. Spatial and temporal migration modeling for stock of Pacific saury, *Cololabis saira* (Brevoort), incorporating effect of sea surface temperature. Fish. Sci. 72:1153–1165.

Yasuda, I., and Y. Watanabe.
1994. On the relationship between the Oyashio front and saury fishing grounds in the north-western Pacific: a forecasting method for fishing ground locations. Fish. Oceanogr. 3:172–181.
2007. Chlorophyll *a* variation in the Kuroshio Extension revealed with a mixed-layer tracking float: implication on the long-term change of Pacific saury (*Cololabis saira*). Fish. Oceanogr. 16:482–488.

Yatsu, A., S. Chiba, Y. Yamanaka, S.-I. Ito, Y. Shimizu, M. Kaeriyama, and Y. Watanabe.
2013. Climate forcing and the Kuroshio/Oyashio ecosystem. ICES J. Mar. Sci. 70:922–933.

Yoshida, T.
1993. Oceanographic structure of the upper layer in the western North Pacific subarctic region and its variation. PICES Sci. Rep. 1:38–41.

Zainuddin, M., K. Saitoh, and S.-I. Saitoh.
2008. Albacore (*Thunnus alalunga*) fishing ground in relation to oceanographic conditions in the western North Pacific Ocean using remotely sensed satellite data. Fish. Oceanogr. 17:61–73.

Zenitani, H., M. Ishida, Y. Konishi, T. Goto, Y. Watanabe, and R. Kimura.
1995. Distributions of eggs and larvae of Japanese sardine, Japanese anchovy, mackerels, round herring, Japanese horse mackerel, and Japanese common squid in the waters around Japan, 1991 through 1993. Natl. Res. Inst., Fish. Agency Jap., Res. Manage. Res. Rep. Ser. A-1, 368 p.

Zhang, J.-Z., R. Wanninkhof, and K. Lee.
2001. Enhanced new production observed from the diurnal cycle of nitrate in an oligotrophic anticyclonic eddy. Geophys. Res. Lett. 28:1579–1582.

NOAA
National Marine
Fisheries Service

Fishery Bulletin
established 1881

Spencer F. Baird
First U.S. Commissioner
of Fisheries and founder
of *Fishery Bulletin*

Depth and temperature distribution, morphometrics, and sex ratios of red deepsea crab (*Chaceon quinquedens*) at 4 sampling sites in the Mid-Atlantic Bight

Bradley G. Stevens (contact author)[1]
Vincent Guida[2]

Email address for contact author: bgstevens@umes.edu

[1] Department of Natural Sciences
University of Maryland Eastern Shore
Carver Hall
Princess Anne, Maryland 21853

[2] Northeast Fisheries Science Center
National Marine Fisheries Service, NOAA
James J. Howard Marine Sciences Laboratory
74 Magruder Road, Sandy Hook
Highlands, New Jersey 07732

Abstract—The red deepsea crab (*Chaceon quinquedens*) supports a small fishery of <2000 metric tons annually along the U.S. East Coast, but little is known about the life history of this crab. We sampled red deepsea crab from 4 sites and 3 depth strata (250–450 m, 450–700 m, and 700–850 m) in the Mid-Atlantic Bight in January 2011 and 2012 and in July 2013. Crab size decreased with depth, whereas shell age indices increased with depth. Crab occurred at temperatures from 4.6°C to 10.6°C (mean: 6.37°C) and there was little difference between sexes. Size at 50% maturity (SM_{50}) could not be determined with chela or abdomen allometry, but SM_{50} was estimated at 61.6 mm in carapace length for females on the basis of gonopore condition. Sex ratios (M:F) involving female crab above the SM_{50} were <0.5, indicating that large males are depleted in comparison with female abundance. The proportion of ovigerous females was 33% in January 2012 and <6% in July 2013, proportions that support the hypothesis of a biennial (or longer) reproductive cycle. Red deepsea crab probably recruit to deep water (>1000 m), move upslope during adolescence, and become mature in the shallowest strata, before undergoing an ontogenetic migration back to intermediate depths.

Manuscript submitted 29 May 2015.
Manuscript accepted 2 May 2016.
Fish. Bull. 114:343–359 (2016).
Online publication date: 2 June 2016.
doi: 10.7755/FB.114.3.7

The red deepsea crab (*Chaceon quinquedens*) ranges from the Gulf of Maine to the Gulf of Mexico, at depths from 200 to 1800 m, and temperatures of 5–8°C (Haefner and Musick, 1974; Wigley et al., 1975; Serchuk[1]; Steimle et al., 2001; Wahle et al., 2008; NEFSC[2]). Stocks along the Atlantic coast are considered a single population and distinct from the stock in the Gulf of Mexico. Red deepsea crab support a small but valuable fishery in federally managed waters along the continental slope of southern New England and the Mid-Atlantic, a fishery that has been managed since 2002 by the New England Fishery Management Council (Wigley et al., 1975; Wahle et al., 2008). In recent years, 4 vessels have fished for red deepsea crab and have averaged annual landings of 1360 metric tons (t) over the time period 2002–2013, but landings have declined from 1600 to 930 t during that period (Chute[3]). Red deepsea crab are a data-poor fishery stock. Very little is known about their biology, abundance, growth, age, or reproduction, and, as a result, management consists primarily of controls on total allowable catch, currently set at 2688 t. Because of inadequate information on biomass, the New England Fishery Management Council Scientific and Statistical Committee has not set a fishing-induced mortality rate or determined whether the stock is in a status of overfished or overfishing (Chute et al.[4]).

[1] Serchuk, F. M. 1977. Assessment of red crab (*Geryon quinquedens*) populations in the northwest Atlantic. Natl. Mar. Fish. Serv., Northeast Fish. Sci. Cent. Lab. Ref. 77-23, 15 p. [Available at website.]

[2] NEFSC (Northeast Fisheries Science Center). 2009. The Northeast Data Poor Stocks Working Group report, December 8–12, 2008 meeting. Part A. Skate species complex, deep sea red crab, Atlantic wolffish, scup, and black sea bass. NOAA, Natl. Mar. Fish. Serv., Northeast Fish. Sci. Cent. Ref. Doc. 09-02, 496 p. [Available at website.]

[3] Chute, A. 2014. Personal commun. Northeast Fish. Sci. Cent., Natl. Mar. Fish. Serv., NOAA, Woods Hole, MA 02543.

[4] Chute, A., L. Jacobson, P. Rago, and A.

Because of their extended depth range, few red deepsea crab are captured during semiannual assessment surveys conducted by the National Marine Fisheries Service. Red deepsea crab have been studied during several previous surveys. McRae (1961) found significant concentrations of crab southeast of Ocean City, Maryland, but concluded that they were too sparse to support a commercial fishery. In two surveys, abundance of populations of red deepsea crab was estimated by using towed camera systems. The first survey (Wigley et al., 1975) was conducted in 1974 before the onset of commercial fishing. The second, conducted during 2003–2005 (Wahle et al., 2008), showed a 250% increase in overall biomass (mostly due to juveniles), after a decade of targeted harvesting of males, but a 42% decline in the biomass of large males at depths of 350–500 m where fishing occurs, as well as a decline in body condition indices (carapace length [CL]: weight ratios) (Weinberg and Keith, 2003). In addition, the size of landed crabs has declined from 114 mm in carapace width (CW) in 1974 to <90 mm CW by 2008 (Chute et al.[4]).

There is scant information on biological parameters of red deepsea crab, such as size at maturity, fecundity, or timing of reproduction. Fecundity increases with body size (Hines, 1988). Size at maturity for female red deepsea crab has been estimated by Haefner (1977, 1978) to be between 65–75 mm CL, but a large portion of his samples were barren, indicative of biennial spawning. Size at 50% maturity has been estimated with ratios of chela width (ChW) to CW for the congener *C. affinis* from the Canary Islands (males: 129 mm CW; females: 99 mm CW) (Fernández-Vergaz et al., 2000), by gonad condition for *C. affinis* in the northeast Atlantic (males: 94 mm CW; females: 109 mm CW) (Robinson, 2008), and for male *C. maritae* in South Africa (93 mm CW) by using growth increment analysis (Melville-Smith, 1989). Spawning of *C. affinis* in the Canary Islands occurs from October to May, but ovigerous females were found only in March and April (López Abellán et al., 2002) and from October to March in the Azores (Pinho et al., 2001). In the Gulf of Mexico, male golden deepsea crab (*C. fenneri*) produce sperm in late winter and mate with females during March–April, but females do not extrude eggs until the following fall (Hinsch, 1988a, 1988b). Life history characteristics of other geryonid crab species were reviewed and compared by Hastie (Hastie, 1995).

Maturity of female crabs can be inferred from the presence of eggs, gonopore condition, or ovary development, but maturity of male crabs is difficult to determine. Male crabs may carry spermatophores, indicative of physiological maturity, at sizes well below that at which they can mate. Many genera (e.g., *Chionoecetes, Lithodes, Cancer*) exhibit allometric growth of the chelae at the pubertal molt, after which they are classified as morphometrically mature and are distinguishable by an increase in the slope and intercept of the ratio of chela height (ChH) to CW (ChH:CW) (Somerton, 1980; Somerton and MacIntosh, 1983; Comeau and Conan, 1992; Stevens, et al., 1993; Corgos and Freire, 2006).

Lack of biological, survey, and fishery information for the red deepsea crab causes major uncertainties about the status of its stock and possible management approaches. Up to 85% of the catch of this species consists of females and undersize crab that are discarded and that result in a possible mortality of about 5% (Tallack, 2007). At present, it is not possible to calculate biological reference points (e.g., biomass or fishing-induced mortality at maximum sustainable yield [B_{MSY}, F_{MSY}, respectively]) because of a lack of information on growth, longevity, and mortality (NEFSC[5]). For the same reasons, it is not possible to predict future stock status, biomass, or response to changes in climate or fishing mortality. Although landings of red deepsea crab have stabilized at intermediate levels in recent years, the landed size has declined from 114 mm CW in 1974 to 105 mm CW in 2005, and there is concern about sperm limitation because of reductions in biomass of large males.

At a minimum, effective management requires information on growth, mortality, and size at maturity. In particular, it is necessary to know the frequency of molt and reproduction in females, the presence or absence of terminal molt and multiple fertilizations, and the status of sperm storage and fecundity. The NOAA Red Crab Working Group has made a variety of high-priority research recommendations for understanding the life history of red deepsea crab, including a better understanding of the reproductive cycle, maturity schedule, and fecundity of female red deepsea crab; of the potential reproductive consequences of removing large males from the population; and of the growth rate and molt cycle of red deepsea crab (Miller et al.[6]).

We began studies of the red deepsea crab in 2011 to provide data on reproduction and life history for this species. Data were collected aboard NOAA research vessels during 3 cruises jointly sponsored by the NOAA Northeast Fishery Science Center and the Living Marine Resources Cooperative Science Center at the University of Maryland Eastern Shore. The objectives for these cruises were to sample the continental shelf fauna during winter (in 2011 and 2012) and

MacCall. 2009. Deep sea red crab. *In* Northeast Data Poor Stocks Working Group report, December 8–12, 2008 meeting. Part A. Skate species complex, deep sea red crab, Atlantic wolffish, scup, and black sea bass. NOAA, Natl. Mar. Fish. Serv., Northeast Fish. Sci. Cent. Ref. Doc. 09-02, p. 181–214. [Available at website.]

[5] NEFSC (Northeast Fisheries Science Center). 2006. 43rd Northeast Regional Stock Assessment Workshop (43rd SAW): 43rd SAW assessment summary report. NOAA, Natl. Mar. Fish. Serv., Northeast Fish. Sci. Cent. Ref. Doc.. 06-14, 54 p. [Available at website.]

[6] Miller, T., R. Muller, B. O'Boyle, and A. Rosenberg. 2009. Report by the Peer Review Panel for the Northeast Data Poor Stocks Working Group, 38 p. NOAA, Natl. Mar. Fish. Serv., Northeast Fish.s Sci. Cent., Woods Hole, MA. [Available at website.]

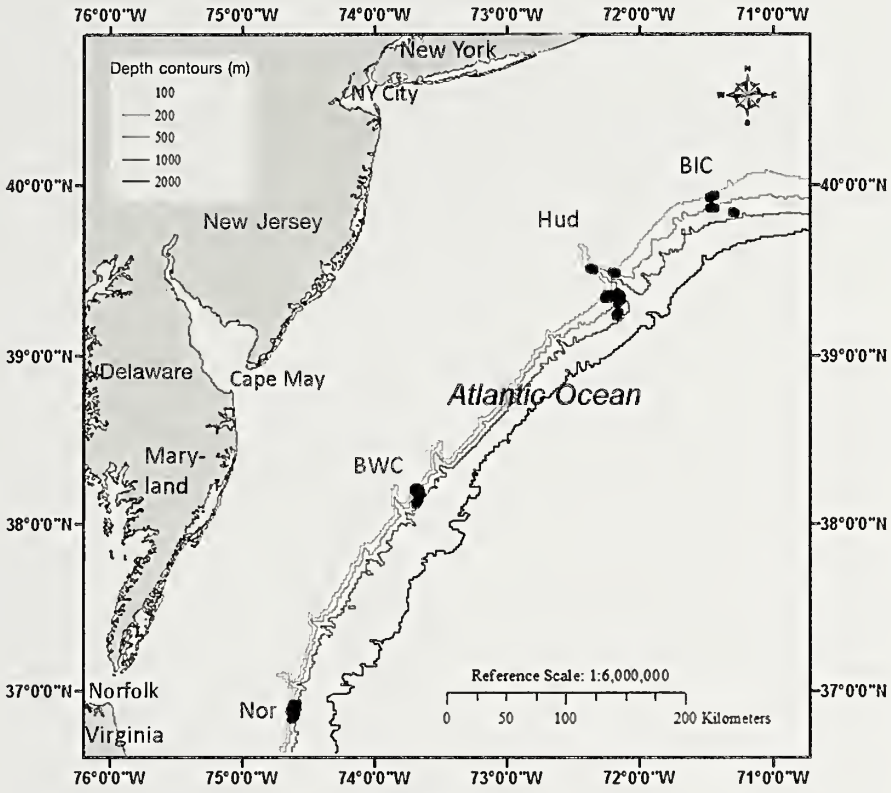

Figure. 1

Locations of sampling sites for red deepsea crab (*Chaceon quinquedens*) during cruises aboard the NOAA Ship *Delaware II* in the Mid-Atlantic Bight in 2011 and 2012 and aboard the NOAA Ship *Gordon Gunter* in 2013. The sites were Block Island Canyon (BIC), Hudson Canyon (Hud), Baltimore and Washington Canyons (BWC), and Norfolk Canyon (Nor).

to collect samples of red deepsea crab. Specific goals for research of red deepsea crab were to determine 1) the distribution of crab by sex, size, shell condition, depth, and temperature, 2) to obtain morphometric data for determination of sexual maturity, and 3) to collect specimens for studies of reproductive biology. This article presents information on distribution and morphometry of red deepsea crab collected during the 3 NOAA cruises.

Materials and methods

Sampling locations

Two research cruises were conducted aboard the NOAA Ship *Delaware II* (10–21 January 2011 and 21–30 January 2012) and one cruise was completed aboard the NOAA Ship *Gordon Gunter* (5–8 July 2013). Red deepsea crab were sampled in 4 general areas within the Mid-Atlantic Bight (defined as coastal waters along the U.S. Atlantic coast from Cape Cod to Cape Hatteras), and stations were selected to cover a range of latitudes and depths: near Block Island Canyon (BIC), at the mouth of Hudson Canyon (Hud), on the continental slope between Baltimore and Washington Canyons (BWC), and on the slope near Norfolk Canyon (Nor; Fig. 1). Actual locations within each site where trawl nets were hauled were chosen for their relatively flat contours within specified depth ranges (see below) after reconnaissance with multibeam sonar. Goals of the cruise in 2011 were primarily focused on sampling fish; red deepsea crab were caught incidentally in the deeper (>300 m) tows, and sampling of crab was mostly opportunistic. In 2012 and 2013, stations were specifically defined to capture red deepsea crab, and tows were made in 3 depth strata defined as shallow (250–450 m), middle slope (450–700 m), and deep (700–850 m) (Table 1). One attempt to tow a trawl net at a depth of 1000 m failed when the net was snagged and both trawl warps were broken, resulting in loss of a trawl net. Because of inclement weather and technical delays, site BIC was sampled only in 2012, and site BWC was not sampled in 2011.

Water temperature and depth profiles were recorded with a conductivity, temperature, and depth profiler before each trawl tow at each site and depth stratum. In 2011, a Yankee 36 otter trawl with an 18.3-m headrope,

Table 1

Data collected from trawl tows and expanded catch data from surveys of red deepsea crab (*Chaecon quinquedens*) conducted in the mid-Atlantic Bight during 3 cruises (2011–2013): depth stratum of trawl (Strat; 1=shallow [250–450 m], 2=middle slope [450–700 m], and 3=deep [700–850 m]); bottom temperature (Btemp, °C); swept area (Area, m^2); number of male crab caught (Males), number of female crab caught (Females); total number of crab caught (Total); density of male crab (Mdens, individuals/ha); density of female crab (Fdens, individuals/ha), total density of crab (Tdens, individuals/ha); expansion factor for subsampled tows (ExpFac); mean weight of male crab (Mwt, kg); and mean weight of female crab (Fwt, kg). Stations were located at 4 sites: Block Island Canyon (BIC), Hudson Canyon (Hud), Baltimore and Washington Canyons (BWC), and Norfolk Canyon (Nor).

Station	Year	Date	Strat	Depth (m)	Btemp	Area	Males	Females	Total	Mdens	Fdens	Tdens	ExpFac	Mwt	Fwt
Hud-1	2011	1/15/2011	1	403.7	7.8	30,512	170	307	477	55.7	100.7	156.3	3.613	0.236	0.265
Hud-2	2011	1/15/2011	2	499.4	6.4	33,057	480	655	1134	145.1	198.0	343.1	5.643	0.357	0.206
Hud-2	2011	1/15/2011	2	558.5	7.3	31,866	1017	1645	2662	319.2	516.1	835.3	10.820	0.213	0.156
Hud-3	2011	1/14/2011	2	631.7	5.5	31,413	725	1755	2480	230.7	558.8	789.5	10.206	0.289	0.130
Nor-1	2011	1/18/2011	1	363.4	9.0	29,312	20	177	197	6.8	60.2	67.0	2.487	0.360	0.350
Nor-3	2011	1/17/2011	2	580.8	5.1	26,645	388	509	897	145.7	190.9	336.6	6.693	0.263	0.284
BIC-1	2012	1/19/2012	1	246.9	10.2	47,921	0	0	0	0.0	0.0	0.0	0		
BIC-2	2012	1/19/2012	2	483.6	6.1	41,463	103	211	315	25.0	51.0	75.9	4.312		
BIC-3	2012	1/19/2012	3	731.5	4.6	30,482	214	62	276	70.1	20.3	90.4	3.444		
Hud-1	2012	1/21/2012	1	294.0	11.5	42,011	0	0	0	0.0	0.0	0.0	0		
Hud-2	2012	1/26/2012	1	298.3	8.8	32,071	277	92	369	86.3	28.8	115.1	5.127		
Hud-3	2012	1/26/2012	2	644.2	6.9	34,345	125	200	326	36.5	58.3	94.8	2.022	0.278	0.20
BWC-1	2012	1/25/2012	1	134.8	14.2	30,847	0	5	5	0.0	1.6	1.6	1		
BWC-2	2012	1/25/2012	2	571.4	5.6	25,973	520	2092	2612	200.2	805.3	1005.5	11.556	0.386	0.190
BWC-3	2012	1/25/2012	3	760.5	5.1	27,007	100	51	151	37.0	18.9	55.9	1		
Nor-1	2012	1/23/2012	1	321.4	9.2	37,555	0	0	0	0.0	0.0	0.0	0		
Nor-2	2012	1/23/2012	2	521.9	6.8	42,703	377	882	1259	88.3	206.5	294.7	6.389		
Nor-3	2012	1/22/2012	3	773.7	4.8	25,800	90	64	154	34.8	24.8	59.6	1.830		
Hud-1	2013	7/7/2013	1	263.6	8.1	34,124	0	0	0	0.0	0.0	0.0	0		
Hud-2	2013	7/7/2013	2	569.2	5.7	42,385	0	0	0	0.0	0.0	0.0	0		
Hud-3	2013	7/7/2013	3	792.5	4.8	32,560	113	26	139	34.7	8.0	42.7	1	0.27	0.326
BWC-1	2013	7/8/2013	1	288.7	11.2	34,070	1	10	11	0.3	2.9	3.2	1	0.306	0.221
BWC-2	2013	7/8/2013	2	500.8	6.5	33,171	387	1391	1778	116.7	419.4	536.1	5.610	0.306	0.221
Nor-1	2013	7/5/2013	1	236.5	12.2	37,488	0	0	0	0.0	0.0	0.0	0		
Nor-2	2013	7/5/2013	1	414.4	8.1	31,094	151	416	567	40.4	110.8	151.2	3.883	0.401	0.332
Nor-3	2013	7/5/2013	3	750.0[a]	7.1	33,694	336	78	414	99.8	23.1	122.9	2.101	0.211	0.185

[a] Conductivity, temperature, and depth sensor failed; depth estimated from chart.

a codend that had a 1-cm mesh liner, and deepwater headrope floats ("rock hoppers") was deployed from the stern trawl A-frame by using both trawl winches and 2.5-cm trawl wires. In 2012 and 2013, a similarly size 4-seam otter trawl net (with 6.0-cm body mesh and 2.5-cm codend liner) was used. In all years, a 30-min tow was made at ~1.5 m/s (3 kt) along a specified depth contour at each site and stratum. Distance towed was determined from GPS coordinates, and area towed was estimated as the distance multiplied by average net width (13.0 m). Tows were made during all hours of day or night. Time constraints prevented measuring all crab in tows with larger catches (catch for 6 of the tows exceeded 1000 crab); as a result, a goal of 150–200 crab per catch was set. All catches that consisted of up to 3 baskets or a total of 60 kg of red deepsea crab (approximately 150 crabs) were sampled completely, whereas, for larger catches, a subsample of 2–3 baskets that composed from 10% to 50% of the catch was taken. The subsample was sorted by sex, after which males and females were weighed separately to determine the proportion of their biomass in the whole catch. A sampling factor for each tow was recorded along with each crab for later data expansion.

For each crab in a subsampled tow, the sex and shell condition were recorded. Shell condition includes coloration and abrasions of the carapace, sternum, and dactyls, and therefore provides a crude but integrated index of time since molt. Shells were classified into 4 standard categories, defined by the National Marine Fisheries Service for brachyuran crabs (see Jadamec et al., 1999), that represented relative time since molting, determined by radiometric aging (Nevissi et al., 1996). We have adapted the following cat-

egories for red deepsea crab: 1) new-shell crab were relatively soft, clean, and brightly colored, had sharp dactyls, and indicated that the crab had molted (probably) within the last 1–2 months; 2) hard-shell crab had harder shells with some discoloration and scratches but were still glossy and may have molted within the last 6–12 months; 3) old-shell crab had lost their glossy, reflective sheen, had numerous dark patches, scratches, and dull dactyls, and probably had not molted for 2 or more years; 4) very-old-shell crab were much darker and discolored, indicating these crab had not molted for 4–6 years.

Electronic calipers were used to measure different dimensions of the crab. We used CL instead of CW as our standard dimension of size, measured from the rear margin of the right eyesocket to the rear midline of the carapace. Carapace length is a more accurate measurement because spines are usually included in CW, and spines can wear down over time. In addition, we redefined the width measurement between spine tips as spine width (SW), as opposed to CW, which is often measured across the carapace in front of the spines. For comparative purposes, we also recorded SW for 48% and CW for 12% of the measured crab to allow for conversions between them. Time constraints prevented taking all measurements on all crabs, but additional measurements were taken for a subset of the sampled crabs that were systematically selected to fill out size categories for reproductive studies. Additional measurements included chela propodus length (ChL), ChH (males only), abdomen width (AW) at the widest point (females only), and presence and condition of eggs (females).

Haefner (1977) reported that abrasion and discoloration (blackening) around the gonopores (which he termed "vulvae") of female red deepsea crab were indications of previous mating, and he demonstrated that 87% of 67 female red deepsea crab with open, discolored gonopores contained sperm, whereas none of the 38 crabs with immature (closed) gonopores contained sperm. Therefore, in 2012 and 2013, in our surveys maturity of females was estimated on the basis of gonopore condition; females with closed and unabraded gonopores were classified as immature, whereas those with open or discolored gonopores (or external eggs) were considered mature.

Data analysis

For subsampled tows, the average weight of crab was calculated separately for males and females, and the proportion of each sex by weight was determined. Total catch for each sex (C_{sex}) was calculated by multiplying the total catch weight (W_t) by the weight proportion (P_{sex}) and dividing the result by mean weight (MW_{sex}) of each sex in the subsample:

$$C_{sex} = W_t \cdot P_{sex} \cdot MW_{sex}^{-1} .$$

Density of crab was calculated as the catch (total number) of each sex divided by the area towed and expressed as the mean number of crab·per hectare, for comparison with results reported by Wahle et al. (2008).

Because replicate tows were not made at each station, density of each sex was compared separately between years, sites, and depth strata by using single-factor analysis of variance (ANOVA), and P-values <0.05 were considered significant. If factor effects were significant, pairwise comparisons were made with the Bonferroni correction. Likewise, differences in mean size (CL) were compared between sexes, sites, and depth strata with a weighted ANOVA, where the sampling factors were used as weights to account for unequal subsampling. Weighting had little impact on post-hoc pairwise comparisons; therefore, post-hoc comparisons were unweighted. Proportions of male and female crab within 0.5°C categories were also compared by using ANOVA and a Kruskal-Wallis test.

Sex ratios were calculated after summing the catch of crab in bins of 5 mm CL. Comparisons were made between sites (with depths as replicates) because sites were geographically separated. Red deepsea crab may make seasonal vertical migrations for reproduction, and crab at different depths would comingle; therefore, they were considered to represent a single local mating pool. In most brachyuran species, males are larger than females, and assortative mating is common: females pair with males up to 40% larger, as reported for snow crab (*Chionoecetes opilio*; Sainte-Marie et al., 1999) and southern Tanner crab (*C. bairdi*; Stevens et al., 1993). Male red deepsea crabs in 10 mating pairs observed by Wahle et al. (2008) were 50% larger than their female partners, and males in 3 mating pairs observed in another study were 28% larger than their female counterparts (Elner et al., 1987). Therefore, in our study, sex ratios were calculated between numbers of crab in offset size categories. Given that the mean size of females was about 75 mm CL, the number of females in each 5-mm bin was compared with the number of males in bins that were 20 mm larger (e.g., number of females in the bin of 50–55 mm CL was compared with that of males in the bin of 70–75 mm CL).

Relationships between morphometric characters, such as CL, ChL, ChH, and AW were determined for selected crabs by using analysis of covariance, with sex as a categorical factor. Data were linear and therefore were not transformed, but the slopes of the log-transformed relationships were calculated to determine the allometry coefficient. The size at 50% maturity (SM_{50}) for females was calculated by using logistic regression with maturity (0, 1; determined on the basis of gonopore condition) as the dependent variable, and CL as the independent variable. Standard error (SE) of SM_{50} was calculated with a bootstrap analysis with 1000 repetitions. Shell conditions and proportion of mature crab with eggs were determined and plotted. All data analysis was conducted with R, vers. 3.0.2 (R Core Team, 2013). Most mean values are presented with standard deviations (SDs), and a few are noted with SEs.

Table 2

Mean temperatures (°C), with standard deviations (SD) and results of analysis of variance between years, from surveys of red deepsea crab (*Chaecon quinquedens*) conducted in the Mid-Atlantic Bight in 2011, 2012, and 2013. Results are averaged across all trawl tows made at each site ($Temp_s$), weighted by numbers of crabs caught ($Temp_c$), and for females with eggs ($Temp_e$). Also shown are results of analysis of variance between years, including *F*-value (*F*), probability (*P*), and degrees of freedom (df).

Year and results of variance	Tows	$Temp_s$	$Temp_c$	$Temp_e$
Jan 2011	6	6.9 (SD 1.5)	6.41 (SD 0.96)	6.05 (SD 0.76)
Jan 2012	12	7.8 (SD 3.0)	6.07 (SD 1.10)	6.27 (SD 0.62)
Jul 2013	8	8.0 (SD 2.6)	6.71 (SD 1.11)	7.68 (SD 0.72)
Total	26	7.8 (SD 2.5)	6.37 (SD 1.09)	6.25 (SD 0.82)
F		0.361	44.48	26.08
P		0.701	<0.001	<0.001
df		2, 23	2, 2813	2, 330

Results

Catch and density

During cruises of NOAA research vessels in 2011, 2012, and 2013, 26 deepwater tows were completed for research of red deepsea crab (Table 1). One site (BIC) was sampled only in 2012, whereas others were omitted in some years (e.g., BWC in 2011), and not all depths were sampled each year because of time constraints. Mean bottom temperatures at all sampled stations did not differ significantly between years despite sampling in January of 2011 and 2012 and in July of 2013 (Table 2). Temperatures weighted by number of crab captured differed significantly among years, but the greatest difference was <0.7°C. Temperatures at which ovigerous females occurred also differed significantly among years and temperatures were warmer in July 2013 than in January of either 2011 or 2012. Although differences between stations were minimal, crab concentrated at specific depths in each season, and, as a result, crab-weighted temperatures showed greater differences because of changes in crab distribution.

During the 3 cruises combined, 5594 male and 10,627 female crab were captured for a total of 16,221 crab, of which 2815 crab (17.4%) were measured, including 1191 males (21.3% of males) and 1624 females (15.3% of females). Highest mean densities occurred in the middle slope depth stratum (450–700 m; Table 3) for both males (131 individuals/ha) and females (300 individuals/ha), but differences between sites were not significant (Table 3). However, mean densities of male crab were significantly greater in 2011 than in 2012 or 2013; a similar but nonsignificant decline occurred for females. This difference remained even after removal of site BIC (only sampled in 2012) and was mostly due to samples at sites Hud and Nor. Estimates of biomass density were calculated with mean weights from 13 subsampled tows and ranged from 0 to 241 kg/ha, with a mean of 49.7 kg/ha (SD 69.6). Biomass averaged across years was lowest at site BIC (14.7 kg/ha [SD 13.1]) and highest at site BWC (77.4 kg/ha [SD 106.4]) (Table 4).

Table 3

Mean density (individuals/ha), with standard deviations (SDs), of red deepsea crab (*Chaecon quinquedens*) averaged across depth strata, years, and sites sampled in the Mid-Atlantic Bight during 2011–2013. Analysis of variance results include *F*-value (*F*), probability (*P*), and degrees of freedom (df). Superscript letters indicate similar groups (within columns) where $P<0.05$. Sampling occurred at 3 depth strata, shallow (250–450 m), middle slope (450–700 m), and deep (700–850 m), at 4 sites, Block Island Canyon (BIC), Hudson Canyon (Hud), Baltimore and Washington Canyons (BWC), and Norfolk Canyon (Nor).

Stratum	Male	Female	Year	Male	Female	Site	Male	Female
Shallow	18^b (SD 30.7)	30^b (SD 47.7)	2011	151^a (SD 114)	271 (SD 214)	BIC	32 (SD 35.6)	24 (SD 25.6)
Middle	131^a (SD 100)	300^a (SD 263)	2012	48^b (SD 57.9)	101 (SD 229)	BWC	71 (SD 86.6)	250 (SD 358)
Deep	55^b (SD 29.0)	19^b (SD 6.6)	2013	37^b (SD 47.6)	73 (SD 147)	Hud	81 (SD 98.2)	125 (SD 193)
						Nor	55 (SD 61.4)	96 (SD 95.9)
Analysis of variance								
F	2.559	0.47		7.263	2.97		0.319	0.817
P	0.123	0.5		0.013	0.09		0.811	0.498
df	2, 23	2, 23		1, 24	1, 24		3, 22	3, 22

Table 4

Total biomass density (kg/ha) of red deepsea crab (*Chaecon quinquedens*) at each site and depth stratum sampled in the Mid-Atlantic Bight during 2011–2013, and summaries across sites and depth strata are provided. Sampling occurred at 3 depth strata, shallow (250–450 m), middle slope (450–700 m), and deep (700–850 m), at 4 sites, Block Island Canyon (BIC), Hudson Canyon (Hud), Baltimore and Washington Canyons (BWC), and Norfolk Canyon (Nor).

		Depth stratum			
Year	Site	Shallow	Middle	Deep	Mean
2011	Hud	39.8	126.8		105.1
2011	Nor	0	92.5		92.5
2012	BIC	0	18.9	25.2	14.7
2012	Hud	16.0	21.6		17.9
2012	BWC	0.0	241.4	17.9	86.4
2012	Nor	0.0	72.8	15.9	29.5
2013	Hud	0.0	0.0	9.7	3.2
2013	BWC	1.0	128.4		64.2
2013	Nor	32.0		25.3	29.8
Mean		13.6	95.6	18.8	47.4

Size of crab

Carapace length was measured on all sampled crabs except for 133 crab from site BIC in 2012; for those crab, CL was calculated from the regression of CL on SW and used in all further analyses. The mean size of male crab captured (79.4 mm CL [SD 14.7], range: 31.6–126.5 mm CL) was significantly greater (t=11.62, df=1974, P<0.0001) than that of female crab (73.7 mm CL [SD 10.1], range: 26.5–103.6 mm CL). Mean size of males differed between years (weighted F, Table 5) and was lower in July 2013 (73.9 mm CL [SD 17.5]) than in January 2011 (80.5 mm CL [SD 10.6]) or 2012 (83.2 mm CL [SD 13.6]). Mean size of females also differed between years (weighted F, Table 5), but pairwise comparisons among years were not significant. Lack of sampling at some sites and depths prevented making annual comparisons among all samples; therefore, further comparisons were made by combining data across years. Mean weights determined from 13 subsampled tows (for which sexes were weighed in aggregate) were 294 g (SD 68) for males and 227 g (SD 71) for females.

Length-frequency distribution of males showed a mode in the range of 80–90 mm CL, and a distinct drop in abundance at sizes >90 mm CL (Fig. 2). Hard-shell crab predominated below 70 mm CL, old-shell crabs were more abundant from 75 to 100 mm CL, and most crabs >100 mm CL were classified as very-old-shell. Female crab exhibited a mode at 70–75 mm CL. Hard-shell females predominated below 60 mm CL, and old-shell females were more abundant in all size groups above 60 mm CL.

Morphometrics

Sex did not affect the relationship between CL and SW; therefore, a combined regression equation was derived for both sexes (Tables 5 and 6; Fig. 3A). The inverse relationship was also determined and used to predict CL for 133 crab that were missing CL measurements. The relationship between ChL and CL differed between sexes with a significant interaction (Table 5); males had longer chelae at sizes >50 mm CL, but females had longer chelae below 50 mm CL (Fig. 3B). Males had an allometry coefficient (the log-transformed slope) of 1.09, indicating isometric growth, whereas females had an allometry coefficient of 0.862, implying slight negative allometry. Among male crab, the relationship between ChH and CL had an allometry coefficient of 1.16, indicating slightly positive allometry (Table 6, Fig. 3C), and the relationship between ChH and ChL had an allometry coefficient of 1.06 (Fig. 3D). Neither the relationship between ChL and CL nor the relationship between ChH and ChL revealed any apparent inflections in the growth pattern that could be used to determine maturity. The relationship between female AW and CL was significant but did not differ with maturity status (Table 5). Nonetheless, there was a significant interaction effect; therefore, combined and separate equations for immature and mature females are presented in Table 6.

Distribution by depth, temperature, crab size, and shell condition

Females were more abundant than males at depths from 400 to 650 m, but males predominated at greater depths (Fig. 4). Weighted ANOVA showed that size varied with both depth and sex, and a significant interaction occurred (Table 5). Mean CL of male crab decreased with depth: 83.1 mm CL (SD 13.7), 79.7 mm CL (SD 11.6), and 78.2 mm CL (SD 17.9) in the shallow, middle slope, and deep strata, respectively (Fig. 5A). Mean CL for males differed significantly between the shallow and deep strata (pairwise t-test, P<0.05 with Bonferroni correction), but the values for neither strata differed from the middle slope stratum. Mean CL of females also decreased with depth to a greater degree than it did for males (Table 5, Fig. 5B): 80.6 mm CL (SD 10.1), 73.8 mm CL (SD 9.1), and 67.0 mm CL (SD 12.8) in the shallow, middle slope, and deep strata, respectively, and all differed significantly (P<0.05). Mean CL of male crab did not differ between sites (Table 5, Fig. 6C), whereas mean CL of female crab was significantly greater at site Nor than at all other sites (P<0.05; Fig. 6D).

Mean shell condition for males was significantly less in stratum 1 (2.2) than in stratum 2 (2.6) or stratum 3 (2.5), but the latter 2 strata did not differ significantly (Fig. 6A). Mean shell condition for females was significantly greater in stratum 2 (2.8) than in either stratum 1 or 3 (both 2.4), but strata 1 and 3 did not differ significantly (Fig. 6B). New-shell male crab were most

Table 5

Analysis of variance results for comparisons among carapace length (CL), year, sex, shell width (SW), chela propodus length (ChL), site, depth or stratum, shell condition, bottom temperature (Btemp), abdomen width (AW), and maturity (females only) of red deepsea crab (*Chaecon quinquedens*) captured from the Mid-Atlantic Bight during 2011–2013. Other abbreviations: df=degrees of freedom, SS=Sum of squares, MS=Mean square, *F*=F-value, *P*=P-value.

Response	Predictor	df	SS	MS	*F*	*P*
CL (males)	Year	1	5233	5233	6.67	0.01
	Residual	1189	932,745	784		
CL (females)	Year	1	19,286	19,286	33.88	<0.001
	Residual	1622	923,249	569		
SW	CL	1	427,647	427,647	52,382	<0.001
	Sex	1	0	0	0.020	0.887
	Residual	1313	10,719			
ChL	CL	1	76,716	76,716	13,008	<0.001
	Sex	1	3505	3505	594	<0.001
	CL × sex	1	1555	1555	263	<0.001
	Residual	321	1893	6		
AW (females)	CL	1	19,761	19,761	5310	<0.001
	Maturity	1	8.1	8.1	2.17	0.143
	CL × maturity	1	20.2	20.2	5.43	0.021
	Residual	179	666.2	3.7		
CL	Depth	1	90,540	90,540	144	<0.0001
	Sex	1	140,428	140,428	224	<0.0001
	Sex × depth	1	24,764	24,764	39.4	<0.0001
	Residual	2811	1,765,210	628		
CL (male)	Depth	1	7915	7915	10.1	0.002
	Residual	1189	930,063	782		
CL (female)	Depth	2	35,721	17,861	31.9	<0.001
	Residual	1621	906,814	559		
CL (male)	Site	3	3644	1215	1.54	0.202
	Residual	1187	934,334	787		
CL (female)	Site	3	57,588	19,196	35.14	<0.001
	Residual	1620	884,947	546		
Shell (male)	Stratum	2	82.2	41.1	25.5	<0.001
	Residual	1188	1911	1.61		
Shell (female)	Stratum	2	103	51.6	33.2	<0.001
	Residual	1621	2518	1.55		
Btemp	Sex	1	31.4	31.4	6.02	0.014
	Residual	2813	14,683	5.22		
Btemp (female)	Eggs	1	362	362	75.4	<0.001
	Residual	1406	6759	4.81		

abundant in the shallow stratum (<450 m), whereas new-shell females were most abundant in the deep stratum (>700 m). Hard-shell male crab predominated in the shallow and deep strata, whereas old-shell crab predominated in the middle slope stratum. Hard-shell female crab predominated in the shallow strata, whereas old-shell females predominated in the middle slope and deep strata.

Bottom temperatures at which crabs were captured ranged from 4.6°C to 10.6°C, but mean temperatures differed by sex (Table 5). The mean temperatures at which crab were captured were 6.27°C (SD 1.18) for males (n=1191) and 6.45°C (SD 1.01) for females (n=1624). Because these data were not normally distributed, a Kruskal-Wallis analysis was conducted and also indicated significant differences (χ^2=20.12, P<0.0001). Ovigerous females occurred at slightly colder temperatures (6.25°C [SD 0.82]) than those temperatures at which females without eggs were found (6.59°C [SD 1.05]; Kruskal-Wallis test (χ^2=26.69, P<0.0001). Only 11 crabs were caught at temperatures above 9.0°C; these crab were captured in one sample at a temperature of 11.2°C and

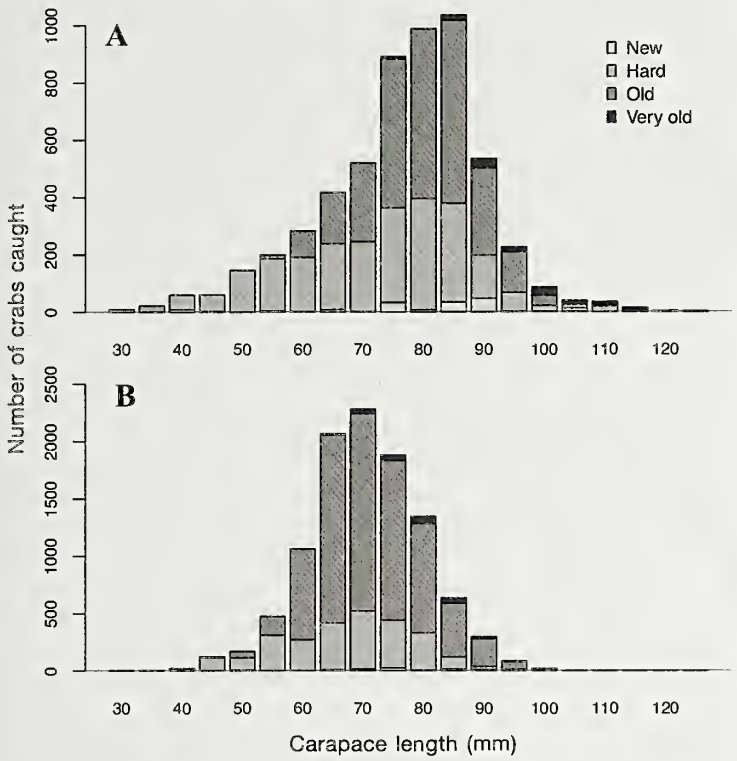

Figure 2

Length-frequency distributions and shell conditions of (**A**) male and (**B**) female red deepsea crab (*Chaceon quinquedens*) captured during cruises in the Mid-Atlantic Bight in 2011–2013. Note that vertical scales differ between sexes.

depth of 288 m. There was no relationship between temperature and size (CL) of male crab (F=0.833, coefficient of determination [r^2]= −0.0001, P=0.362, df=1189), but size of female crab increased with temperature (F=31.3, r^2=0.018, P<0.001, df=1622).

Sex ratios (M:F) varied greatly both among sizes and between sampling sites. For pairs in the smallest size group for their sex (females: 55–60 mm CL; males: 75–80 mm CL) and in which females carried eggs, sex ratios ranged from 2.1 to 3.6; however, for the interval in which female sexual maturity occurs (60–65 mm CL), ratios exceeded 1.0 only at sites BIC and Nor (Fig. 7). For females between 70 and 80 mm CL, only site BIC had a sex ratio >0.5, and ratios at all other sites were <0.4. For females >80 mm CL, there were no sites or size categories where sex ratios exceeded 0.1. At female sizes above 60 mm CL, crab at sites BIC and Nor generally had higher sex ratios than crab at sites Hud or BWC.

Female maturity and ovigerity

The smallest female with external eggs was 58.5 mm CL. Logistic regression of maturity, based on gonopore condition, showed that the SM_{50} was 61.6 mm CL (SE 0.1), equivalent to 78.2 mm SW (Fig. 8). In January 2012, 33.3% of mature female crab were ovigerous, and the maximum proportion exceeded 50% only in the size group of 95–100 mm CL (Fig. 9). In contrast, in July 2013, only 5.9% of mature female crab were ovigerous, and the maximum proportion was 17.9% in the size group of 80–85 mm CL. Analysis of egg samples taken in July 2013 indicated that 80% of eggs were at stage 6 (prehatching or hatching stage), whereas 20% of eggs were at stage 1 (early cell division).

Discussion

Our results add significantly to previous studies of red deepsea crab. Wigley et al. (1975) sampled extensively off the southern New England shelf but included only 2 stations off the Maryland coast, and all sites sampled by Wahle et al. (2008) were north of Delaware Bay (at approximately 38°40′N). We sampled 2 sites (BWC and Nor) that were farther south and that represent locations that are targeted heavily by the current commercial fishery. In addition, we captured about 10 times more crabs than Wigley et al. (1975) and twice as many as Wahle et al. (2008), and we sampled twice as many females as Haefner (1977). Our report is the first to conduct detailed analysis of morphometrics of the red deepsea crab and the first to provide detailed information on distribution by temperature and shell condition.

Catch and density

Tows made during our cruises were not optimized for estimating abundance of red deepsea crab because the net was not outfitted with mensuration gear to measure the net width or bottom contact. As a result, area towed was estimated on the basis of the operator's (subjective) estimate of contact time, distance towed, and average net width. Furthermore, differences in vessel characteristics, operational protocols, and net efficiency make any direct comparisons with previous surveys questionable. The trawl nets we used had a belly mesh of 6 cm and smaller mesh codend liners than those in nets with 3.8-cm mesh used by Wigley et al (1975) and Wahle et al (2008), but all trawl nets caught a similar size range of crab and few crab <50 mm SW. Nonetheless, because there are no other estimates of density of red deepsea crab, our data can be compared with previous estimates in a relative context.

Two of our sites (Hud and BWC) overlap with the area defined as "geographic zone A" by Wigley et al. (1975) (referred to as "sectors" by Wahle et al [2008]). Therefore, we estimated biomass density of red deepsea crab separately within each depth stratum over those 2

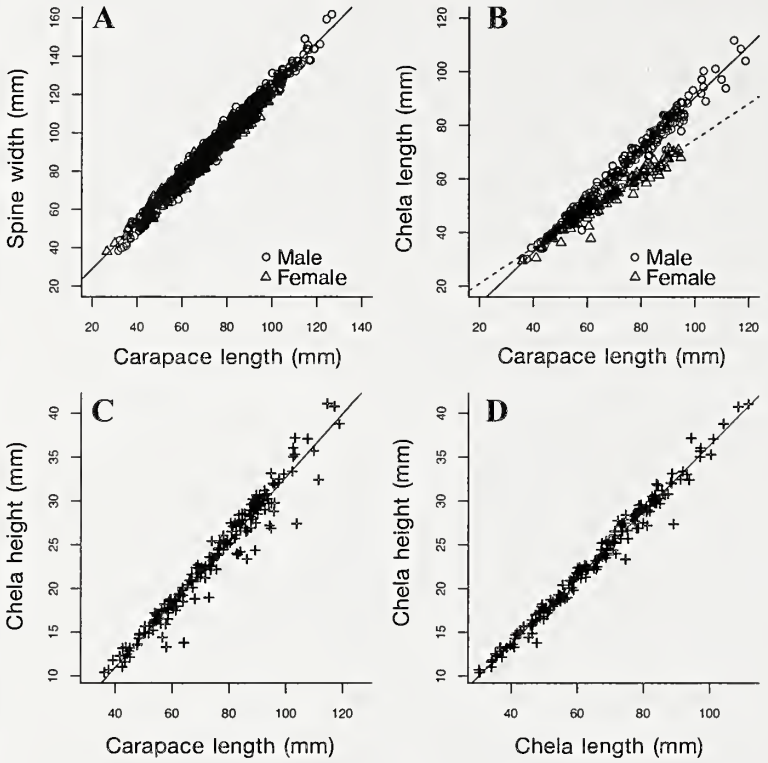

Figure 3

Morphometric relationships for a subsample of 185 male and 138 female red deepsea crab (*Chaceon quinquedens*) captured in the Mid-Atlantic Bight during 2011–2013: (**A**) carapace width with spines (spine width) versus carapace length, (**B**) chela length versus carapace length, (**C**) male chela height versus carapace length, and (**D**) male chela height versus chela propodus length.

sites (12.6, 107.5, and 13.8 kg/ha, respectively), and we multiplied those values by area estimates for similar depth strata within the same geographic sector from Wahle et al. (2008) to provide a depth-stratified estimated biomass of 9143 t for sector A. This value was lower than the approximately 30,000 t estimated by Wahle (2008) during 2003–2005, but it is almost identical to the 9000 t estimated by Wigley et al. (1975) 20 years earlier. We could not separate biomass by sex or size because crab were usually weighed in aggregate. During the survey by Wahle et al. (2008), the highest biomass densities occurred in sectors C and D along the edge of the southern New England shelf, whereas most of our tows were made in sectors A and B, which had the lowest biomass in both the 1974 and 2003–2005 surveys. Mean biomass density over all our stations (42.8 kg/ha) was in the same range (7–80 kg/ha) as levels observed for *C. maritae* off Namibia (Hastie, 1995), but it was much greater than the 1.9 kg/ha calculated for the golden deepsea crab off the coast of South Carolina (Wenner and Barans, 1990) that were surveyed with an occupied submersible.

Size of crabs

Selectivity of commercial crab traps ranges from 0% at 80 mm CW to 100% at 120 mm CW (Wahle et al., 2008),

Table 6

Morphometric relationships for male and female red deepsea crab (*Chaecon quinquedens*) captured from the mid-Atlantic Bight during 2011–2013. Response and predictor variables are, abdomen width (AW), chela propodus length (ChL), carapace length (CL), spine width (SW). Fem(i or m) refers to immature or mature females. Other abbreviations: intercept (Int), coefficient of determination (r^2), degrees of freedom (df), and allometry coefficient (AC; slope of log-transformed relationship).

Sex	Response	Predictor	Int	Slope	r^2	df	AC
Both	SW	CL	5.45	1.180	0.976	1313	0.94
Both	CL	SW	−2.65	0.826	0.976	1313	1.03
Male	ChL	CL	−5.78	0.962	0.977	184	1.09
Fem	ChL	CL	7.55	0.671	0.952	137	0.86
Fem(i)	AW	CL	−13.0	0.735	0.967	105	1.40
Fem(m)	AW	CL	−8.38	0.677	0.937	74	1.19
Fem(all)	AW	CL	−12.26	0.725	0.966	182	
Male	ChH	CL	−3.52	0.362	0.954	184	1.16
Male	ChH	ChL	−1.44	0.378	0.983	184	1.06

equivalent to a range of 63.4–96.5 mm CL, and the median size of crab captured by traps was 92.5 mm CW, or 73.8 mm CL. Therefore, abundance of males declines abruptly above 90 mm CL, which approximately corresponds with the minimum size captured by the fishing industry. Width frequencies of crab captured by Wahle et al. (2008) during 2003–2005 showed a mode in the range of 65–75 mm CW (equivalent to 51–59 mm CL) for males and in the range of 95–105 mm CW (76–84 mm CL) for females. In contrast, male red deepsea crab captured during our study were larger, with a mode in the range of 80–90 mm CL, whereas females were slightly smaller, with a mode at 70–75 mm CL.

Differences in mean size of male and female red deepsea crab (79.4 and 73.7 mm CL, respectively, equivalent to 99.1 and 92.4

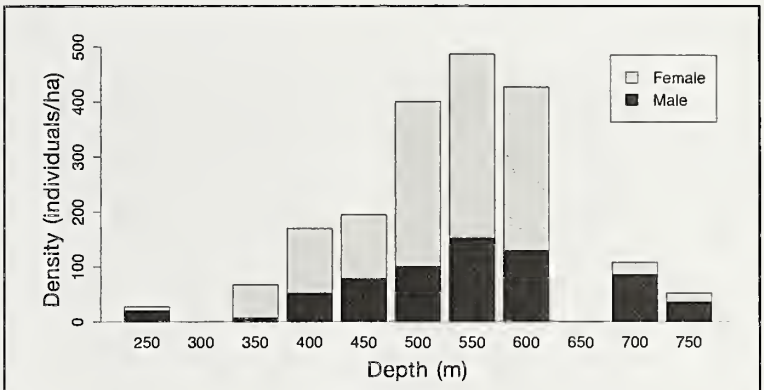

Figure 4

Depth distribution of male and female red deepsea crab (*Chaceon quinquedens*) captured during 2011–2013 in the Mid-Atlantic Bight, expressed as density or number of crab per hectare (ha). Minimum depths are shown for each 50-m depth bin.

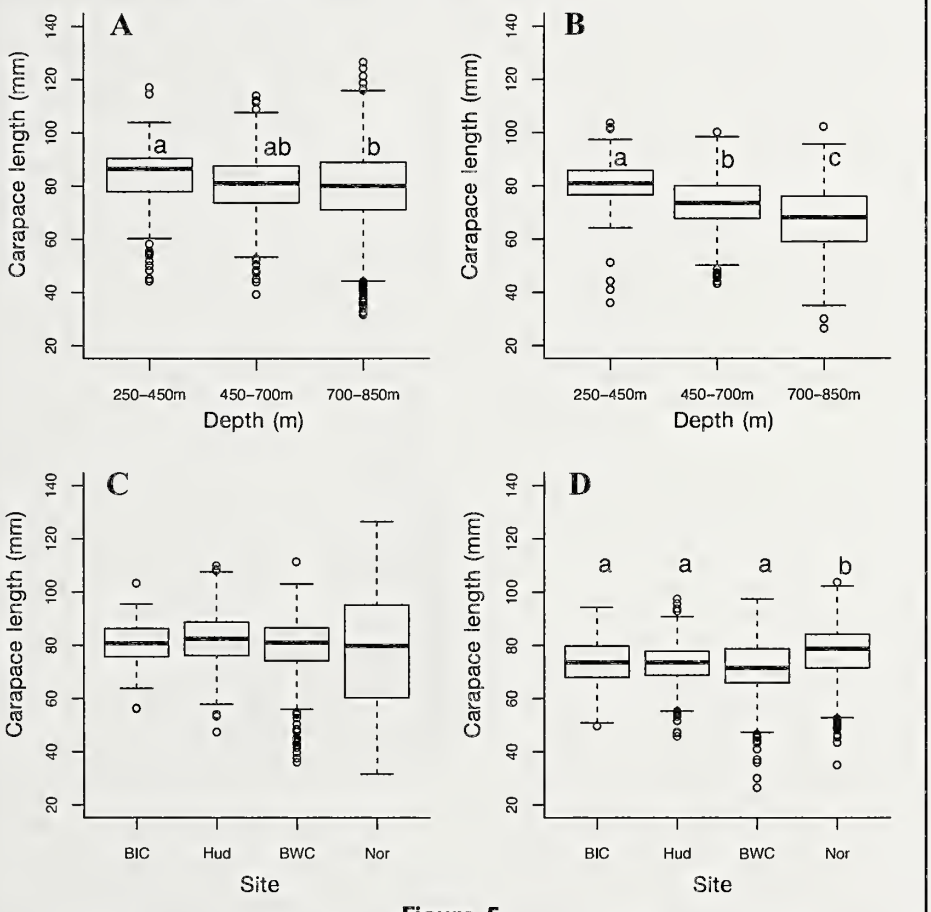

Figure 5

Mean size of red deepsea crab (*Chaceon quinquedens*) sampled during 2011–2013 at 3 depth strata (years and sites combined) for (**A**) males and (**B**) females and at 4 sites (years and depth strata combined) for (**C**) males and (**D**) females. Letters indicate similar groups within frames. The 4 sites in the Mid-Atlantic Bight were Block Island Canyon (BIC), Hudson Canyon (Hud), Baltimore and Washington Canyons (BWC), and Norfolk Canyon (Nor)

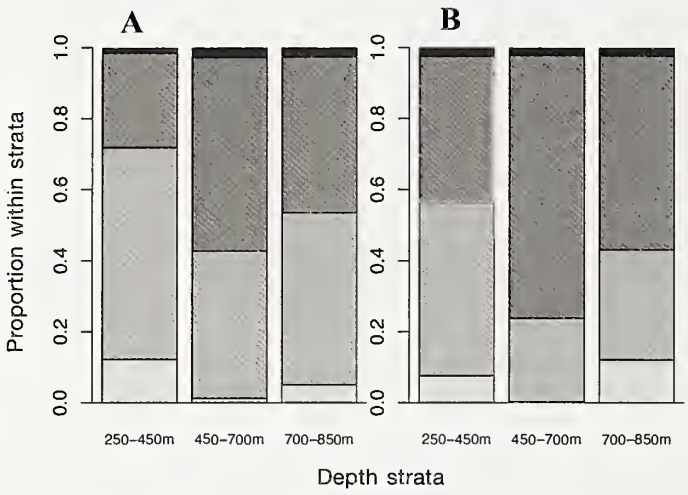

Figure 6

Proportion of (**A**) male and (**B**) female red deepsea crab (*Chaceon quinquedens*) in each of 4 categories of shell condition at 3 depth strata sampled in the Mid-Atlantic Bight during 2011–2013 (years and sites combined). Shell conditions are new (light gray), hard (medium gray), old (dark gray), and very old (black).

mm SW) have been previously noted (McRae, 1961; Haefner, 1978; Weinberg and Keith, 2003). According to McRae (1961), mean weights for a "random sample" of crabs were 794 g for males, and 312 g for non-ovigerous females, equivalent to sizes of 116.4 mm CL and 88.4 mm CL, respectively, or 144.2 and 110.2 mm SW (converted with the equation for CW from Weinberg and Keith, 2003). The source of this sample was not described, but presumably it was near our sampling area. Therefore, either mean size of red deepsea crab has declined significantly since McRae's study in 1960, or his random sample was biased toward large crab. The mean size of male crab reported by McRae (1961) was 31% larger than the mean size of females. This difference is similar to the mean size differential of 27.9% reported by Elner et al. (1987) for 3 pairs of crab (involving 2 males and 2 females) observed mating in captivity, but it is smaller than the differential of 50% between 10 mating pairs observed by Wahle et al. (2008) during tows with video cameras. Although sample sizes for the latter 2 studies were small, they indicate that the relative size of male and female crabs observed by McRae (1961) offered adequate opportunities for mating.

Sex ratios are commonly used to determine whether fishing has affected a crab population, but they are usually calculated over large geographic areas. However, functional maturity (i.e., the ability of male crabs to mate in competitive, natural environments) is dependent on both size (Paul, 1984) and shell condition (Stevens, et al., 1993) because harder shells are necessary to grasp females and defend them from other males. As a result, the effective sex ratio of mating-capable partners may vary greatly over small geographic areas. For this reason we calculated effective sex ratio only within sampling sites, where the samples were geographically close, and these ratios were calculated between abundance of females in 5-mm-CL bins and abundance of males that were 20 mm CL larger. We also ignored shell condition and depth because both could change between the time sampled and mating season, and we did not include year effects in order to preserve adequate sample sizes.

Sex ratios were generally biased toward males in the smaller size intervals, but for intervals larger than the SM_{50} for female red deepsea crab, all ratios were <0.7, and many ratios were much lower. These data indicate that male mating partners for females become exceedingly scarce as females grow. Mating of male crab with multiple females has been observed for red deepsea crab (Elner, et al., 1987), southern

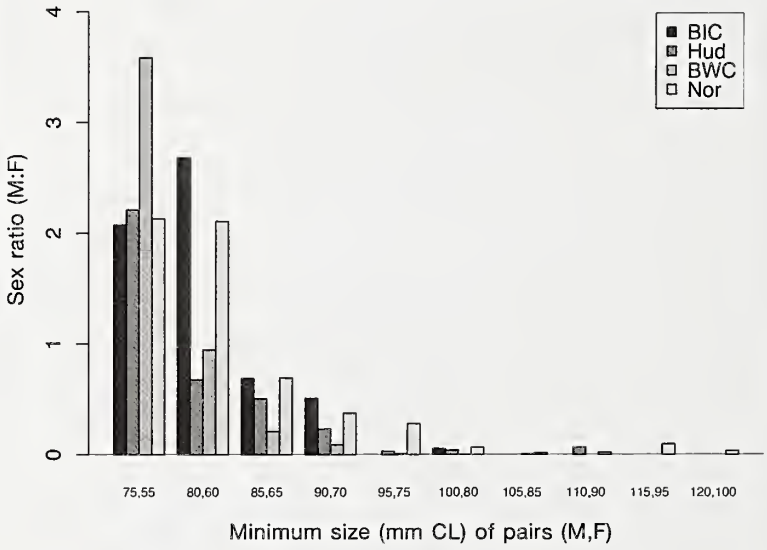

Figure 7

Sex ratio (M:F) of red deepsea crab (*Chaceon quinquedens*) at each of 4 sites sampled in the Mid-Atlantic Bight during 2011–2013, compared by offset 5-mm categories, for pairs in which the minimum size of males is 20 mm in carapace length (CL) greater than the minimum size of females. Missing bars indicate either a lack of males or females in one category. The 4 sites were Block Island Canyon (BIC), Hudson Canyon (Hud), Baltimore and Washington Canyons (BWC), and Norfolk Canyon (Nor)

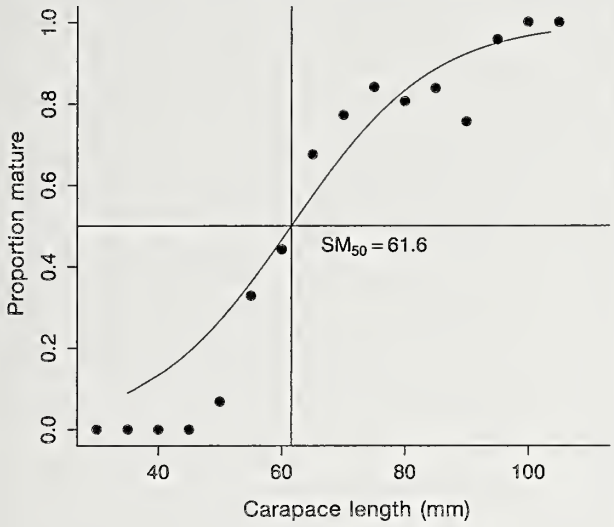

Figure 8

Proportion of female red deepsea crab (*Chaceon quinquedens*) that were mature (as defined by presence of eggs or condition of the gonopores) in each size group classified in intervals of 5 mm in carapace length [CL] (circles) and predicted maturity from logistic regression (line). The estimated size at 50% maturity (SM_{50}) was 61.57 mm CL

Tanner crab (Paul, 1984), and snow crab (Rondeau and Sainte-Marie, 2001). Male southern Tanner crab may mate with as many as 10 partners, but usually with less than 5 (Paul, 1984). Guarding time and the amount of sperm transferred by male snow crabs declines with sex ratio because males try to conserve sperm and, therefore, may leave females with inadequate supplies to fertilize a clutch of eggs (Rondeau and Sainte-Marie, 2001). Blue crab (*Callinectes sapidus*) show a marked decline in the rate of courtship initiation at sex ratios below 2 (Jivoff and Hines, 1998). The minimum sex ratio for successful fertilization of all females in a crab population is unknown, but may lie between 0.1 and 0.5; a conservative estimate would be 0.25, indicating that most females above the mean size in our study do not have access to an adequate number of males.

The crab in our study were considerably smaller than *C. affinis* from the Canary Islands (mean sizes of males and females were 130 and 120 mm CW) (Fernández-Vergaz et al., 2000) or the Azores (107 and 91 mm CL) (Pinho et al., 2001); however, crab in the Canaries and Azores were captured by traps, which are highly size selective; only 3 crab <80 mm CW were caught by Fernández-Vergaz et al. (2000).

Morphometrics

Sexual maturity in our sample of red deepsea crab cannot be inferred from morphometric characteristics. A variety of methods have been proposed for determining the maturity of crabs. Somerton (1980) described a computer technique that determined SM_{50} for male crabs by fitting morphometric data with a logistic regression. He defined 4 patterns of allometric growth, based on the relationship between chela and carapace measurements, and applied those relationships to determine size at sexual maturity for male snow crab in the Bering Sea (Somerton, 1981) and later for blue king crab (*Paralithodes platypus*; Somerton and MacIntosh, 1983). Allometric patterns in species of *Chionoecetes* are curvilinear, and variation increases with size, but patterns become linear when log-transformed. The slope of the log-transformed relationship is defined as the allometry coefficient.

The relationship between ChL and CL for our male red deepsea crab was linear, did not show increased variance with size, and did not require transformation. It has an allometry coefficient of 1.09, indicating isometric growth and has no inflection point that could be used to define the onset of sexual maturity. The relationship between ChL and CL for female crabs, however, indicated clear sexual dimorphism and was negatively allometric. The relationship between male ChH and CL was also isometric, with an allometry coefficient of 1.06. Similar to that of males, the relationship between female AW and CL was linear, had no apparent inflexion point corresponding to maturity, and did not differ between maturity types.

Similar results were obtained for *C. affinis* in the Azores; no inflections were found in the relationships between CL and CW, ChW (height), or female AW, and

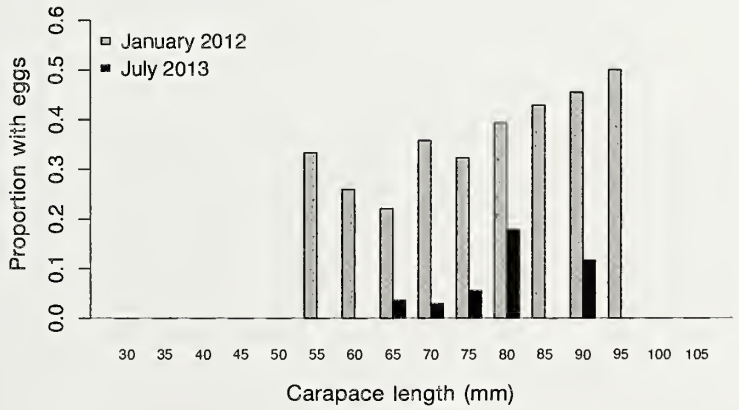

Figure 9

Proportion of mature female red deepsea crab (*Chaceon quinquedens*) with external eggs and captured in the Mid-Atlantic Bight in January 2012 and July 2011. Each size group is classified by intervals of 5 mm in carapace length (CL). Maturity was not recorded in 2011.

male:female dimorphism was present in the chelae but not in CW (Pinho et al., 2001). In contrast, allometric relationships for ChL and ChW in *C. affinis* from the Canary Islands were strongly positive (approximately 1.3–1.5) and were used in hierarchical cluster analysis to distinguish immature from mature individuals of both sexes (Fernández-Vergaz et al., 2000). Logistic regression of these crab indicated SM_{50} values of 129 mm CW for male *C. affinis*—a size that would be equivalent to103 mm CL for red deepsea crab if converted with the regression of CL on SW for the latter (Fernández-Vergaz et al., 2000).

Determination of sexual maturity on the basis of morphometrics works well for crabs of the families Oregonidae (*Chionoecetes* spp.) and Majidae. The spider crab (*Maja brachydactyla*) shows a typical curvilinear relationship between CL and ChH that becomes linear upon log-transformation, and Corgos and Freire (2006) used discriminant analysis to separate immature and mature male clusters. Their data were fitted even better by a 3-stage growth model, which included an inflection point between juveniles and adolescent males. Therefore, excluding one study on *C. affinis*, morphometric relationships have not proved useful for determining sexual maturity in the genus *Chaceon*.

Distribution by depth and temperature

At our sampling sites, highest abundance of red deepsea crab occurred at depths between 500 and 650 m, and few crab were captured at depths <400 m. Female red deepsea crab dominated catches taken at depths shallower than 600 m, and males were more prevalent at greater depths. Haefner et al. (1974) reported that the highest abundance occurred at depths between 265 and 512 m, and they observed that females dominated trawl catches above 400 m in and near Norfolk Canyon but that males became dominant below 400 m.

Our data show a slight but significant decline in size of crab with increasing depth—a drop that was much more apparent for females. This decline in size is consistent with other reports that indicate that juvenile red deepsea crab are more common at greater depths (Wahle et al., 2008). We also found that the proportion of males increased with depth. Off the Namibian coast, *C. maritae* (misidentified as *C. quinquedens*) show similar depth ranges; females predominate above 400 m at temperatures of ~8°C and males are more abundant down to 900 m and 4°C (Beyers and Wilke, 1980; as cited by Melville-Smith, 1989). In contrast, Kilgour and Shirley (2008) caught red deepsea crab by traps at depths of 533 to 1950 m in the Gulf of Mexico but found no significant relationships between depth and crab size or sex. Pinho et al. (2001) caught *C. affinis* with traps around the Azores Islands and found that the highest abundance occurred at depths between 700 and 900 m. In that study, size of both sexes decreased slightly with increasing depth, but the proportion of males declined with increasing depth, in contrast to our results.

Despite differences in depth distribution observed for red deepsea crab in our surveys, the differences in temperature distribution by sex were minor, and much overlap occurred between males and females. Similarly, differences in bottom temperature between years were minor despite sampling in either January or July, and differences weighted by crab catch were even less. These data indicate that temperatures at the depths sampled do not show great annual variation, and red deepsea crab tend to stay within a narrow range of preferred temperature. This information indicates that red deepsea crab recruit as juveniles to waters deeper than those sampled, move upslope during development, and become mature in the shallowest zones, after which they undergo an ontogenetic migration back to intermediate depths.

Female maturity and ovigerity

Our estimate of SM_{50} for female red deepsea crab (61.6 mm CL) was calculated by nonlinear logistic regression; therefore, a point estimate was possible. Haefner (1977) estimated female maturity on the basis of the relationship of AW to CL for females classified as mature or immature by gonopore condition, and he determined that maturity occurred over a size range of 65–75 mm CL. Haefner (1977) calculated 2 separate regression equations for females with mature or immature gonopores (total n=251) for the relationship between AW and CL that had similar slopes but different intercepts. However, the equation for immature females was influenced by 3 extremely small crab. Likewise, AW of *C. affinis* has been reported to change in intercept at maturity, between 95 and 105 mm CW (equivalent to 76–84 mm CL) (Fernández-Vergaz et al., 2000).

In contrast, covariance analysis of our data did not support the hypothesis that the 2 relationships were different, and there were no extreme outliers (total number of females analyzed=182). Abdomen morphometry indicated that *C. affinis* females become functionally mature (i.e., capable of bearing eggs) before reaching physiological maturity (which is assessed on the basis of apparent ovarian stage) (Fernández-Vergaz et al., 2000). Logistic regression indicated SM_{50} values of 108 mm CW (equivalent to 86.6 mm CL) for abdominal maturity and 113.4 mm CW (91 mm CL) for gonopore maturity of crab in the Canary Islands (Fernández-Vergaz et al., 2000), whereas the SM_{50} for female red deepsea crab in the Azores determined by gonopore condition was 83.1 mm CL (Pinho et al., 2001).

The presence of eggs on <50% of female crabs is a strong indicator that reproduction occurs at biennial (or longer) intervals. Haefner (1977) examined female red deepsea crab from the Norfolk Canyon, and reported that only 25.5% of females >71 mm CL were ovigerous in January 1976. He also reported that abraded gonopores were present in 93.5% of female red deepsea crab ≥71 mm CL but not in any crab <70 mm CL. In the Azores, ovigerous *C. affinis* were found only in the fourth and first quarters of the year, with a maximum

of 33% ovigerous crab. Lack of annual mating for red deepsea crab was previously hypothesized by other authors (Weinberg and Keith, 2003). Female *C. maritae* in South Africa were also reported to have asynchronous molting and aseasonal reproductive cycles (Melville-Smith, 1989).

Reproductive cycles >1 year may occur among crabs living at extremely low temperatures. Blue king crab in the Bering Sea living at temperatures ranging from −1°C to 4°C reproduce biennially (Somerton and MacIntosh, 1985; Jensen and Armstrong, 1989; Stevens et al., 2008), and approximately 50% of females bear fertilized embryos each spring. Female snow crab reproduce biennially in the Gulf of St. Lawrence at temperatures <1.0°C and have only 2 broods over their reproductive lifespan (Moriyasu and Lanteigne, 1998; Comeau et al., 1999), whereas snow crab living at higher temperatures (and greater depths) reproduce annually, potentially producing 4 lifetime broods (Kuhn and Choi, 2011).

Switching from biennial to annual reproduction can potentially halve or double lifetime reproductive output, depending on direction of change (Webb et al., 2007). A change of only 1°C can advance or delay hatching of red king crab (*Paralithodes camtschaticus*) by about 2 weeks, possibly contributing to year class failure from a mismatch between larval hatching and food sources (Stevens et al., 2008). Other crabs with reproductive cycles longer than 1 year include the golden king crab (*Lithodes aequispinus*) and others that live at depths >500 m and produce lecithotrophic larvae (Shirley and Zhou, 1997; Paul and Paul, 2001). Biennial spawning has been reported only for crab species living at temperatures <4°C, and for those with lecithotrophic larvae, but has not been reported for crabs with planktotrophic larvae living at temperatures >6°C. Therefore, crabs of the genus *Chaceon* are unusual in this respect.

The extremely low proportion of egg-bearing females and the advance stage of egg development observed in July 2013 indicate that hatching was nearly completed at that time, and some crab bore newly fertilized eggs in very early developmental stages. These observations indicate that hatching and ovulation events are separated by a time interval, possibly up to a year in red deepsea crab (Brachyura). This separation of events is in contrast with the reproductive strategy of red king crab (Anomura), which molt, mate, and extrude a new clutch of eggs within hours after releasing larvae (Stevens and Swiney, 2007). All species of king crab lack the ability to store sperm, however, and, as a result, comparisons to brachyurans are more appropriate. Snow crab (Brachyura) can store sperm, and multiparous crab may use stored sperm to produce additional clutches of eggs; however, those crab that re-mate must do so within 4–7 days after releasing larvae in order to produce viable clutches (Paul and Adams, 1984). Therefore, it appears that red deepsea crab differ from species of *Chionoecetes* in their ability to separate the process of larval release (and presumably mating) from that of ovulation and fertilization.

The current fishery for red deepsea crab is expanding into the southern portion of the Mid-Atlantic Bight, including the Norfolk and Washington Canyon areas. This expansion is a result of changing abundance, as well as of changes in the availability of processing facilities close to fishing grounds (Williams[7]). Therefore, the population targeted by the fishery is different from that fished 20 years or even 10 years previously. The results of this study lay a foundation for other synoptic studies on red deepsea crab in the Mid-Atlantic Bight. As we went to press (May 2016), we were continuing our work with red deepsea crab, analyzing tissue samples from crab collected during the cruises in 2011–2013, as well as from samples collected aboard commercial fishing vessels in 2014 and 2015. The results of this further analysis should reveal more details about the biology of the red deepsea crab, including size at maturity, reproductive cycles, fecundity, and embryonic and larval development.

Acknowledgments

This research was conducted with partial funding from the NOAA Living Marine Resources Cooperative Science Center, NOAA grant NA11SEC4810002. We gratefully acknowledge the assistance of the officers and crews of the NOAA Ships *Delaware II* and *Gordon Gunter*. We also appreciate the efforts of student participants on all 3 cruises, who were too numerous to name individually; still, major assistance to this project was provided by B.-J. Peemoeller, A. Stoneman, and I. Suyuheda. We thank R. Langton for his service as co-chief scientist in 2013 and to S. Smith and S. Van Sant for their participation as watch supervisors during the 2012 and 2013 cruises, respectively. Comments from L. Stehlik and anonymous reviewers helped improve the manuscript.

Literature cited

Beyers, C. J. D. B., and C. G. Wilke.
1980. Quantitative stock survey and some biological and morphometric characteristics of the deep-sea red crab *Geryon quinquedens* off South West Africa. Fish. Bull. (S. Afr.) 13:9–19.

Comeau, M., and G. Y. Conan.
1992. Morphometcry and gonad maturity of male snow crab, *Chionecetes opilio*. Can. J. Fish. Aquat. Sci. 49:2460–2468.

Comeau, M., M. Starr, G. Y. Conan, G. Robichaud, and J.-C. Therriault.
1999. Fecundity and duration of egg incubation for multiparous female snow crabs (*Chionoecetes opilio*) in the fjord of Bonne Bay, Newfoundland. Can. J. Fish. Aquat. Sci. 56:1088–1095.

Corgos, A., and J. Freire.
2006. Morphometric and gonad maturity in the spider

[7] Williams, J. 2014. Personal commun. The Atlantic Red Crab Co., New Bedford, MA 02740.

crab *Maja brachydactyla*: a comparison of methods for estimating size at maturity in species with determinate growth. ICES J. Mar. Sci. 63:851–859.

Elner, R. W., S. Koshio, and G. V. Hurley.
1987. Mating behavior of the deep-sea red crab, *Geryon quinquedens* Smith (Decapoda, Brachyura, Geryonidae). Crustaceana 52:194–201.

Fernández-Vergaz, V., L. J. López Abellán, and E. Balguerías.
2000. Morphometric, functional and sexual maturity of the deep-sea red crab *Chaceon affinis* inhabiting Canary Island waters: chronology of maturation. Mar. Ecol. Prog. Ser. 204:169–178.

Haefner, P. A., Jr.
1977. Reproductive biology of the female deep-sea red crab, *Geryon quinquedens*, from the Chesapeake Bight. Fish. Bull. 75:91–102.
1978. Seasonal aspects of the biology, distribution and relative abundance of the deep-sea red crab *Geryon quinquedens* Smith, in the vicinity of the Norfolk Canyon, western North Atlantic. Proc. Natl. Shellfish. Assoc. 68:49–62.

Haefner, P. A., and J. A. Musick.
1974. Observations on distribution and abundance of red crabs in Norfolk Canyon and adjacent continental slope. Mar. Fish. Rev. 36(1):31–34.

Hastie, L. C.
1995. Deep-water geryonid crabs: a continental slope resource. *In* Oceanography and marine biology: an annual review, vol. 33 (H. Barnes, A. D. Ansell, and R. N. Gibson), p. 561–584. Univ. College London Press, London.

Hines, A. H.
1988. Fecundity and reproductive output in two species of deep-sea crabs, *Geryon fenneri* and *G. quinquedens* (Decapoda: Brachyura). J. Crustac. Biol. 8:557–562.

Hinsch, G. W.
1988a. Morphology of the reproductive tract and seasonality of reproduction in the golden crab *Geryon fenneri* from the eastern Gulf of Mexico. J. Crustac. Biol. 8:254–261.
1988b. Ultrastructure of the sperm and spermatophores of the golden crab *Geryon fenneri* and a closely related species, the red crab *G. quinquedens*, from the eastern Gulf of Mexico. J. Crustac. Biol. 8:340–345.

Jadamec, L. S., W. E. Donaldson, and P. Cullenberg.
1999. Biological field techniques for *Chionoecetes* crabs. Alaska Sea Grant College Program, AK-SG-99-02, 80 p. [Available at website.]

Jensen, G. C., and D. A. Armstrong.
1989. Biennial reproductive cycle of blue king crab, *Paralithodes platypus*, at the Pribilof Islands, Alaska and comparison to a congener, *P. camtschaticus*. Can. J. Fish. Aquat. Sci. 46:932–940.

Jivoff, P., and A. H. Hines.
1998. Effect of female molt stage and sex ratio on courtship behavior of the blue crab *Callinectes sapidus*. Mar. Biol. 131:533–542.

Kilgour, M. J., and T. C. Shirley.
2008. Distribution of red deepsea crab (*Chaceon quinquedens*) by size and sex in the Gulf of Mexico. Fish. Bull. 106:317–320.

Kuhn, P. S., and J. S. Choi.
2011. Influence of temperature on embryo developmental cycles and mortality of female *Chionoecetes opilio* (snow crab) on the Scotian Shelf, Canada. Fish. Res. 107:245–252.

López Abellán, L. J., E. Balguerías, and V. Fernández-Vergaz.
2002. Life history characteristics of the deep-sea crab *Chaceon affinis* population off Tenerife (Canary Islands). Fish. Res. 58:231–239.

McRae, E. D.
1961. Red crab explorations off the northeastern coast of the United States. Commer. Fish. Rev. 23:5–10.

Melville-Smith, R.
1989. A growth model for the deep-sea red crab (*Geryon maritae*) off South West Africa/Namibia (Decapoda, Brachyura). Crustaceana 56:279–292.

Moriyasu, M., and C. Lanteigne.
1998. Embryo development and reproductive cycle in the snow crab, *Chionoecetes opilio* (Crustacea: Majidae), in the southern Gulf of St. Lawrence, Canada. Can. J. Zool. 76:2040–2048.

Nevissi, A., J. M. Orensanz, A. J. Paul, and D. A. Armstrong.
1996. Radiometric estimation of shell age in *Chionoecetes* spp. from the eastern Bering Sea, and its use to interpret shell condition indices: preliminary results. *In* High latitude crabs: biology, management, and economics. Alaska Sea Grant College Program Rep. AK-SG-96-02 (B. Baxter, ed.), p. 389–396. [Available at website.]

Paul, A. J.
1984. Mating frequency and viability of stored sperm in the Tanner crab *Chionoecetes bairdi* (Decapoda, Majidae). J. Crustac. Biol. 4:375–381.

Paul, A. J., and A. E. Adams.
1984. Breeding and fertile period for female *Chionoecetes bairdi* (Decapoda, Majidae). J. Crustac. Biol. 4:589–594.

Paul, A. J., and J. M. Paul.
2001. The reproductive cycle of golden king crab *Lithodes aequispinus* (Anomura: Lithodidae). J. Shellfish Res. 20:369–371.

Pinho, M. R., J. M. Gonçalves, H. R. Martins, and G. M. Menezes.
2001. Some aspects of the biology of the deep-water crab, *Chaceon affinis* (Milne-Edwards and Bouvier, 1894) off the Azores. Fish. Res. 51:283–295.

R Core Team.
2013. R: a language and environment for statistical computing. R Foundation for Statistical Computing, Vienna, Austria. [Available from website, accessed 15 April 2016.]

Robinson, M.
2008. Minimum landing size for Northeast Atlantic stocks of deep-water red crab, *Chaceon affinis* (Milne Edwards and Bouvier, 1894). ICES J. Mar. Sci. 65:148–154.

Rondeau, A., and B. Sainte-Marie.
2001. Variable mate-guarding time and sperm allocation by male snow crabs (*Chionoecetes opilio*) in response to sexual competition, and their impact on the mating success of females. Biol. Bull. 201:204–217.

Sainte-Marie, B., N. Urbani, J.-M. Sévigny, F. Hazel, and U. Kuhnlein.
1999. Multiple choice criteria and the dynamics of assortative mating during the first breeding season of female snow crab, *Chionoecetes opilio* (Brachyura, Majidae). Mar. Ecol. Prog. Ser. 181:141–153.

Shirley, T. C., and S. Zhou.
1997. Lecithotrophic development of the golden king crab *Lithodes aequispinus* (Anomura: Lithodidae). J. Crustac. Biol. 17:207–216.

Somerton, D. A.
1980. A computer technique for estimating the size of sexual maturity in crabs. Can. J. Fish. Aquat. Sci. 37:1488–1494.
1981. Regional variation in the size and maturity of two species of Tanner crab (*Chionoecetes bairdi* and *C. opilio*) in the eastern Bering Sea, and its use in defining management subareas. Can. J. Fish. Aquat. Sci. 38:163–174.
Somerton, D. A., and R. A. MacIntosh.
1983. The size at sexual maturity of blue king crab, *Paralithodes platypus*, in Alaska. Fish. Bull. 81:621–625.
1985. Reproductive biology of the female blue king crab *Paralithodes platypus* near the Pribilof Islands, Alaska. J. Crustac. Biol. 5:365–376.
Steimle, F. W., C. A. Zetlin, and S. Chang.
2001. Essential Fish Habitat Source Document: red deep-sea crab, *Chaceon (Geryon) quinquedens*, life history and habitat characteristics. NOAA Tech. Memo. NMFS-NE-163, 27 p.
Stevens, B. G., and K. M. Swiney.
2007. Hatch timing, incubation period, and reproductive cycle for captive primiparous and multiparous red king crab *Paralithodes camtschaticus*. J. Crustac. Biol. 27:37–48.
Stevens, B. G., K. M. Swiney, and L. Buck.
2008. Thermal effects on embryonic development and hatching for blue king crab *Paralithodes platypus* (Brandt, 1850) held in the laboratory, and a method for predicting dates of hatching. J. Shellfish Res. 27:1255–1263.
Stevens, B. G., W. E. Donaldson, J. A. Haaga, and J. E. Munk.
1993. Morphometry and maturity of male Tanner crabs, Chionoecetes bairdi, from shallow- and deepwater environments. Can. J. Fish. Aquat. Sci. 50:1504–1516.
Tallack, S. M. L.
2007. Escape ring selectivity, bycatch, and discard survivability in the New England fishery for deep-water red crab, *Chaceon quinquedens*. ICES J. Mar. Sci. 64:1579–1586.
Wahle, R. A., C. E. Bergeron, A. S. Chute, L. D. Jacobson, and Y. Chen.
2008. The Northwest Atlantic deep-sea red crab (*Chaceon quinquedens*) population before and after the onset of harvesting. ICES J. Mar. Sci. 65:862–872.
Webb, J. B., G. L. Eckert, T. C. Shirley, and S. L. Tamone.
2007. Changes in embryonic development and hatching in *Chionoecetes opilio* (snow crab) with variation in incubation temperature. Biol. Bull. 213:67–75.
Weinberg, J. R., and C. Keith.
2003. Population size-structure of harvested deep-sea red crabs (*Chaceon quinquedens*) in the northwest Atlantic Ocean. Crustaceana 76:819–833.
Wenner, E. L., and C. A. Barans.
1990. In situ estimates of density of golden crab, *Chaceon fenneri*, from habitats on the continental slop, southeastern U.S. Bull. Mar. Sci. 46:723–734.
Wigley, R. L., R. B. Theroux, and H. E. Murray.
1975. Deep sea red crab, *Geryon quinquedens*, survey off northeastern United States. Mar. Fish. Rev. 37(8):1–21.

NOAA
National Marine
Fisheries Service

Fishery Bulletin
established 1881

Spencer F. Baird
First U.S. Commissioner
of Fisheries and founder
of *Fishery Bulletin*

Is the survey selectivity curve for Pacific cod (*Gadus macrocephalus*) dome-shaped? Direct evidence from trawl studies

Kenneth L. Weinberg[1]
Cynthia Yeung (contact author)[1]
David A. Somerton[1]
Grant G. Thompson[2]
Patrick H. Ressler[1]

Email address for contact author: cynthia.yeung@noaa.gov

[1] Resource Assessment and Conservation Engineering Division
Alaska Fisheries Science Center
National Marine Fisheries Service, NOAA
7600 Sand Point Way NE
Seattle, Washington 98115

[2] Resource Ecology and Fisheries Management Division
Alaska Fisheries Science Center
National Marine Fisheries Service, NOAA
7600 Sand Point Way NE
Seattle, Washington 98115

Abstract—Survey selectivity can be viewed as a function of the availability of the stock to the sampling gear and the sampling efficiency of the gear. A dome-shaped survey selectivity function is one in which survey selectivity decreases with larger and older fish. Such a function is estimated for eastern Bering Sea (EBS) Pacific cod (*Gadus macrocephalus*) in the NOAA National Marine Fisheries Service stock assessment model, which would be appropriate if large (≥55 cm in fork length) Pacific cod avoid capture by the EBS survey bottom trawl. To test this assumption, a field study was conducted to determine whether large Pacific cod escape capture by either outswimming the survey trawl or by swimming above the trawl. Our results show that large Pacific cod do not outswim the trawl because catches did not increase when we increased towing speed. Additionally, large Pacific cod do not routinely swim above the trawl because analysis of acoustic backscatter collected concurrently with trawl hauls indicated that only 4% of the acoustic backscatter attributed to Pacific cod occurred at heights above the headrope. We found no evidence that survey-gear efficiency decreased with increasing fish length either because large fish outswam the trawl or because they tend to occur further from the bottom. Therefore the results of our experiment do not support the use of a dome-shaped survey selectivity function in the EBS Pacific cod assessment model.

Manuscript submitted 16 June 2015.
Manuscript accepted 20 May 2016.
Fish. Bull. 114:360–369 (2016).
Online publication date: 14 June 2016.
doi: 10.7755/FB.114.3.8.

Fisheries stock assessment surveys are intended to produce an index of relative stock abundance that varies over time in constant proportion to the true stock abundance. In stock assessment models, the scaler that relates modeled abundance to a survey index is often considered a product of a constant catchability and of a fish age- or length-dependent survey selectivity function (which, hereafter, for reasons of simplicity, we refer to as *length-dependent functions*, but the same concept applies to age-dependent functions). Both catchability and selectivity are typically estimated when a stock assessment model is fitted to data (Maunder and Piner, 2015), although, in some cases, the catchability coefficient is fixed a priori (Thompson[1,2,3]). The selectivity of a survey can be viewed as a function of the availability of the various biological components of the fish stock to the sampling gear and of the sampling efficiency of the gear (i.e., the proportion of encountered animals that are captured; Maunder et al., 2014). However, the relative

[1] Thompson, G. G. 2013. Assessment of the Pacific cod stock in the eastern Bering Sea. *In* Stock assessment and fishery evaluation report for the groundfish resources of the Bering Sea/Aleutian Islands regions, p. 239–380. North Pacific Fishery Management Council, Anchorage, AK. [Available at website.]

[2] Thompson, G. G. 2014. Assessment of the Pacific cod stock in the eastern Bering Sea. *In* Stock assessment and fishery evaluation report for the groundfish resources of the Bering Sea/Aleutian Islands regions, p. 255–436. North Pacific Fishery Management Council, Anchorage, AK. [Available at website.]

[3] Thompson, G. G. 2015. Assessment of the Pacific cod stock in the eastern Bering Sea. *In* Stock assessment and fishery evaluation report for the groundfish resources of the Bering Sea/Aleutian Islands regions, p. 251–470. North Pacific Fishery Management Council, Anchorage, AK. [Available at website.]

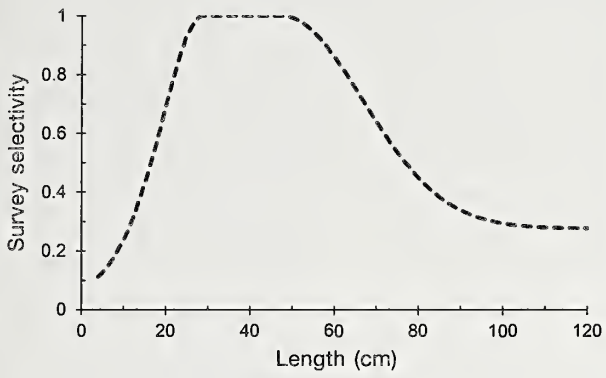

Figure 1

Length-based survey selectivity curve derived from the stock assessment of Pacific cod (*Gadus macrocephalus*) for the Bering Sea region in 2013. Lengths are given in fork lengths.

importance of availability (e.g., Do small fish occur at depths shallower than those of surveys?) and sampling efficiency (e.g., Do small fish pass through trawl mesh?) in determining the shape of a selectivity function is difficult to determine without additional information.

The shape of the survey selectivity function is at issue for the model used for stock assessment of Pacific cod (*Gadus macrocephalus*; Thompson[1,2,3]) in the eastern Bering Sea (EBS). The assessment model, conducted with the Stock Synthesis package, vers. 3.24q (Methot and Wetzel, 2013), is fitted to commercial catch data dating back to 1977, as well as to fisheries-independent data from the National Marine Fisheries Service annual bottom trawl survey of demersal fishes in the EBS (hereafter referred to as *the survey*). The survey provides estimates of relative abundance and length compositions dating back to 1982 and age compositions from 1994 onward (Lauth and Nichol, 2013).

The current assessment model accepted by the NOAA National Marine Fisheries Service for fishery management, in addition to several historical model configurations, includes a flexible survey selectivity function that, after being fitted to the data, decreases at larger (≥55 cm in fork length [FL]) fish sizes (Thompson[1,2,3]; Fig. 1). This dome-shaped functional form has rising and descending limbs to either side of the top. The descending limb on the right side suggests that larger fishes are less vulnerable to the survey in some way, perhaps because they are better able to escape the trawl or are separated spatially from smaller fishes. In contrast, the more traditional asymptotic, survey selectivity function implies that the survey is sampling a greater proportion of the large fishes in the population. If an assessment model is not well informed by the data, there will be uncertainty about whether the shape of the estimated function accurately reflects the survey sampling processes or whether it reflects parameter confounding in the model (Maunder and Punt, 2013). The difference between interpretations of the shape of the estimated function with regard to these 2 types of uncertainty may have a pronounced effect on the determination of stock size and recommended harvest rates.

Field studies designed to describe survey-gear efficiency and stock availability provide a source of "direct" evidence and can be useful in the fitting of the selectivity function (Cadrin et al., 1999; Weinberg et al., 2004; Clark and Kaimmer, 2006; Nichol et al., 2007; Somerton et al., 2007; Somerton et al., 2013). We present the results from a new study and review results from previous works to determine whether direct evidence from field studies corroborates the dome-shaped survey selectivity function estimated by the current assessment model used for Pacific cod. Although we focus on Pacific cod, the concept that field experiments can better inform assessment models is applicable worldwide for multiple species.

If it is assumed that the survey covers the entire geographic range of Pacific cod in the EBS, a dome-shaped selectivity function could result from a progressive decrease in trawl sampling efficiency for larger fish sizes. Sampling efficiency is dictated by 3 processes: vertical herding, horizontal herding, and escapement, all of which are dependent on trawl design, fishing procedures, fish behavior, and swimming endurance. Together, these processes play an important role in estimates of abundance and size composition of groundfish resources (Godø and Walsh, 1992).

Although studies on the behavior of Pacific cod are scarce, evidence has been collected from various field and laboratory experiments on other cold-water gadids and various demersal species, clearly showing that fish swimming stamina and reactions to trawling are species specific (He and Wardle, 1988; Winger et al., 1999), size dependent (Main and Sangster, 1981; He and Wardle, 1988; Winger et al., 1999), temperature affected (He, 1991; Winger et al., 1999), light responsive (Glass and Wardle, 1989; Walsh, 1991), and often density dependent (Godø et al., 1999; Kotwicki et al., 2014). Not all studies have come to the same conclusions for all species, or even within the same species in all cases, but the most universal observation is the inverse relationship between swimming speed and endurance. The faster a fish swims, the more energy required and the less time it is capable of sustaining such speed. If, however, a fish is able to swim fast enough and long enough to outpace a survey trawl, sampling efficiency will be reduced. Likewise, if large Pacific cod, more so than smaller Pacific cod, have the strength and stamina to outswim the survey trawl, survey selectivity will be reduced for the larger animals.

In addition to the possibility that larger Pacific cod avoid capture by outswimming the trawl, it is also possible that larger Pacific cod occur higher in the water column and are more likely to swim over the headrope of the survey trawl. The presence of fish in the water column can be documented by using acoustic data collected at the time of trawling. Analysis of acoustic

data to estimate abundance has not been attempted for Pacific cod because of concerns stemming from the confounding of backscatter signals close to the seabed (i.e., separating the weaker fish signal from the stronger seabed signal), in the area known as the *acoustic dead zone* (Ona and Mitson, 1996), and from the difficulty of separating species-specific backscatter when multiple species with swim bladders, such as Pacific cod and walleye pollock (*Gadus chalcogrammus*), co-occur.

Our objective was to report the results of an experiment aimed at examining whether survey trawl efficiency decreases for large-size Pacific cod because they outswim the trawl or because they pass over its headrope. If such size-specific trawl efficiency can be demonstrated, it would support the application of a dome-shaped function in the stock assessment model for Pacific cod.

Table 1

Survey selectivity (rounded to one decimal place) by length group based on the length-based schedule of the 2013 assessment model used for Pacific cod (*Gadus macrocephalus*) in the eastern Bering Sea. Ranges for length groups are provided in fork lengths (FLs).

Survey selectivity	Length group (cm FL)
1.0	34–54
0.9	55–60
0.8	61–65
0.7	66–69
0.6	70–74
0.5	75–79
0.4	80–88
0.3	89–105

Materials and methods

Experimental design

Our experiment was designed to test the hypothesis that a substantial proportion of large Pacific cod avoid capture by outswimming the survey trawl under standard survey protocols (Stauffer, 2004). Secondarily, we were also able to provide a test of the hypothesis that a substantial proportion of Pacific cod are unavailable to the trawl because they are in the water column above the headrope of the survey trawl. A Pacific cod was considered large if its FL was ≥55 cm, a definition based on lengths at the right tail of the selectivity schedule estimated in the 2013 stock assessment of EBS Pacific cod (Thompson[1]), for which estimated survey selectivity was less than 100.0 percent (Table 1, Fig. 1).

The experiment took the form of paired parallel tows: one vessel trawled at the survey standard speed of 1.5 m/s (3 kn, *slow*), while the other vessel towed at a faster speed of 2.1 m/s (4.0 kn, *fast*). Various Bering Sea fishermen of Pacific cod have reported tow speeds that range from 1.25 to 2.25 m/s (2.5–4.5 kn), depending on vessel power, mesh size, and other trawl design features (senior author, personal commun.). We felt the upper limit for towing the survey trawl should be no more than 2.1 m/s in order to maintain proper fishing configuration (Weinberg, 2003). At such a speed, we were 0.15 m/s short of the fastest speeds for commercial trawling. If the number of large Pacific cod captured in the standard slow tows is no different from the number caught in the faster tows, we would conclude that Pacific cod did not outswim the survey trawl.

Field operations

The experiment was conducted during 3–5 August immediately following the 2013 NOAA EBS bottom trawl survey aboard the 2 trawlers used for the survey. An 83-112 eastern trawl (standard for the EBS survey) was used in this experiment. The 83-112 eastern trawl is a 2-seam flatfish trawl with a 25.3 m (83 ft) long headrope and a 34.1 m (112 ft) long footrope (more details are provided in Weinberg, 2003; Lauth and Nichol, 2013). The simple 5.2 cm diameter footrope is weighted with 75 kg of chain hung in equal loops along its length from which the nylon netting is attached. Mesh size varies from a maximum of 10.2 cm in the wings and throat to a minimum of 3.2 cm for the liner in the codend. Each side of the net is attached to a steel V-door (1.8×2.7 m) that weighs approximately 816 kg by a pair of 54.9-m-long, 1.6-cm-diameter bare wire bridles. Because faster trawling has been shown to exacerbate inconsistencies in seabed contact of this trawl (Weinberg, 2003), an additional 34 kg of weight was secured to the footrope, then monitored with a bottom contact sensor for all tows in this experiment.

The major difference between tows of our experiment and standard survey tows was towing speed. All other trawling procedures followed those used during the survey (e.g., straight-line towing, locked winches with equal lengths of warp, standard warp length to depth ratios, and setting and retrieval methods designed to lower the net down on the seabed in fishing configuration quickly at the start of a tow and to raise it off the seabed quickly at the end of a tow). Our balanced-pair design called for repetitive parallel towing and vessels safely separated by no more than 463 m (0.25 nmi). On odd-numbered pairs, one vessel was randomly selected to tow at the standard survey speed of 1.5 m/s, while the other vessel towed at the faster speed of 2.1 m/s. On even-numbered pairs, the vessels switched towing speeds. To reduce potential bias from sea conditions, the faster boat was randomly appointed to fish either the port or starboard side of the slower boat.

When fishing with 2 boats at different speeds, we had a choice of enforcing either consistent tow duration (time) or consistent tow length (distance). Because it has been shown that variation in tow durations (15.0

and 30.0 min) did not affect the size distribution of catches for some Atlantic species, including Atlantic cod (*Gadus morhua*; Godø et al., 1990; Walsh[4]), we elected to reduce the duration of the faster tows so that the distance fished and swept area of tows were similar between the 2 speeds (Wileman et al., 1996). Hence, the duration of the slow (1.5 m/s) and fast (2.1 m/s) tows were set at 30.0 and 22.5 min, respectively, measured from the time the nets were on bottom and the winches were locked to the time when trawl retrieval was initiated.

Towing occurred at 2 independent sites, one at a depth of 136 m and the other at a depth of 86 m. Ten successful pairs of fast and slow tows were made at the deep site, and 14 pairs were completed successfully at the shallow site. All captured Pacific cod (sex not determined) were measured to the nearest centimeter (FL).

Data analysis

Swept area Swept area for each haul was estimated as the average net width from data collected with a Marport[5] acoustic net mensuration system (Marport Stout Inc., Snohomish, WA), multiplied by the length of the tow path, derived from GPS data of vessel locations at first and last contact of the footrope with the seabed; seabed contact was determined with a bottom contact sensor (Somerton and Weinberg, 2001). Outlier measurements of net width were removed by using a sequential outlier rejection algorithm, and the remaining data were fitted with a smoothed spline from which the average net width was calculated for each tow (Kotwicki et al., 2011).

Measuring the swept area of each tow was complicated by instrument failure during some tows. Therefore, only a subset of all tows produced valid net width data. Paired *t*-tests were used to test for a difference in the swept area between the fast and the slow tows of each pair where net widths were available for both tows. If the difference was found not to be significant ($P>0.05$) in this subset of tows after the data from our bottom contact sensors were examined thoroughly for anomalies that would indicate the likelihood of high variability in net width during a tow, we assumed the swept area was not different for any paired tows and used the raw catch (counts) from all tows as the dependent variable in subsequent analyses.

Effect of towing speed on catch The null hypothesis that the catch of large Pacific cod at a fast towing speed (c_f) was no different than the catch of large Pacific cod at a slow towing speed (c_s) was tested by using paired-sample tests, against the one-sided alternative that c_f was greater than c_s. First, the probability of either towing speed being equally likely to obtain greater catch was calculated with a sign test: the binomial probability that c_f was greater than c_s in x pairs (successes) out of the total y pairs of tows (trials) observed if the null hypothesis of no effect of speed on catch was true. A paired *t*-test was then conducted to further confirm the result of the less-sensitive, but more robust, sign test. The null hypothesis of the *t*-test was that there was no mean difference ($\bar{d}$) between $\ln(c_f)$ and $\ln(c_s)$ of the paired tows (H_0: $\bar{d}=0$, i.e. the mean ratio $\overline{c_f/c_s}=1$), assuming that the differences between pairs were normally distributed. The power ($1-\beta$) of the *t*-test was calculated for a 1-sided (H_a: $\bar{d}>0$) alternative hypothesis on the basis of the *t*-distribution, observed standard deviation (SD) of $\ln(c_f) - \ln(c_s)$, sample size (n) of 24 pairs of tows, and significance level (α) of 0.05. The power was calculated for a range of $\bar{d}$ for H_a from 0.1 to 1.0, where $e^{\bar{d}} \doteq c_f/c_s$.

Finally, we estimated $\bar{d}$ on the basis of the length-derived, double normal, survey selectivity schedule from the stock assessment model for Pacific cod in the EBS (see appendix A in Methot and Wetzel, 2013; Thompson[1]). For our study, we assumed that at the fast towing speed, no large Pacific cod can escape the net and all available fish are caught and that at the slow towing speed, the large Pacific cod available can escape the net in the proportion indicated by the survey selectivity function. To increase our sample size, we pooled the numbers of fish caught in this experiment into length groups with the same survey selectivity, rounded to the first decimal place (Table 1). The total expected catch in a tow based on the curve (c_e) was calculated as the sum of the catch in each length group in the slow tow (c_{s-l}) divided by the survey selectivity for that length group (s_l): $c_e = \sum_{l=1}^{L} c_{s-l}/s_l$. On the basis of the assumptions, c_e would be the expected catch in a fast tow. Therefore, the mean ratio of expected catch to the catch of the slow tow for the n pairs of tows, $\frac{\sum_{i=1}^{n} c_{e-i}/c_{s-i}}{n}$, would be the expected mean ratio of catch in the fast tow over the slow tow.

Vertical distribution Simrad ES60 echosounders were used in both survey vessels (Kongsberg Maritime AS, Kongsberg, Norway) and operated at frequencies of 38 and 120 kHz with a sampling rate of 1–2 pings/s to collect acoustic backscatter data. The sampling resolution of these data was approximately 0.2 m vertically and 0.8–2.1 m horizontally at ship speeds of 1.5 and 2.1 m/s (at 3 and 4 kn). Given nominal beam widths of 7° at both frequencies, depth of the hull-mounted transducers (4 m), and depth of the seafloor at the deep study site (136 m), the extent sampled by each ping was a circle with a diameter of approximately 16 m (close to the 18-m average net width for this depth) and an area of 205 m^2. These data were analyzed with Echoview, vers. 5.4.90 (Echoview Software Pty. Ltd., Hobart, Australia), which afforded us the opportunity to detect whether Pacific cod occurred above our net opening at

[4] Walsh, S. J. 1991. Effect of tow duration on gear selectivity. NAFO SCR Doc. 91/84, 9 p. [Available at website.]

[5] Mention of trade names or commercial companies is for identification purposes only and does not imply endorsement by the National Marine Fisheries Service, NOAA.

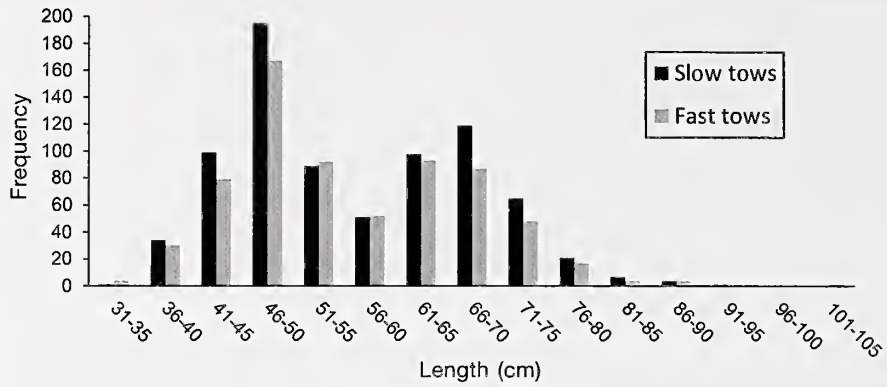

Figure 2

Length-frequency distribution of Pacific cod (*Gadus macrocephalus*), by towing speed, determined from 48 tows conducted for this study in the eastern Bering Sea during August 2013. Slow tows had a speed of 1.5 m/s, and fast tows had a speed of 2.1 m/s. Length intervals are given in fork lengths.

the moment they were sampled by the echosounder on the vessel.

The difference between frequencies (120 and 38 kHz) in mean volume backscattering strength (S_v, dB re 1/m; cf. MacLennan et al., 2002) was used to identify backscatter consistent with that of fishes with swim bladders. For analysis, backscatter data were grouped in bins, each of which had a resolution of 20 pings (horizontal) by 5 m (vertical). Bins for which the difference between S_v at 120 kHz and S_v at 38 kHz was between −10 and 8 dB were classified as backscatter that indicated fish (De Robertis et al., 2010). Only bins for which the backscatter had a signal-to-noise ratio of at least 10 dB (De Robertis and Higginbottom, 2007) were included in the analysis.

Fish backscatter per unit of area (s_A, m^2/nmi^2) was then integrated by using an S_v integration threshold of −70 dB in several depth layers referenced to a 0.25-m backstep above the seabed echo (0.25–2.0, 2.0–2.5, 2.5–3.0, 3.0–7.0, and 7.0–16.0 m). The upper bound of the first depth interval matched the mean headrope height of this experiment. Similarly, a height of 2.5 m corresponds to a survey-wide average headrope height for the 83-112 eastern trawl used to assess Pacific cod in the EBS (Nichol et al., 2007), a height of 7.0 m corresponds to a survey-wide average headrope height for the poly-Noreastern trawl used by the NOAA Alaska Fisheries Science Center to assess Pacific cod in the Gulf of Alaska region (Nichol et al., 2007), and a height of 16.0 m corresponds to an estimated effective fishing height for the 83-112 eastern trawl that is used to assess walleye pollock in the EBS (Kotwicki et al., 2013) and that perhaps may apply to Pacific cod as well.

The results of this analysis of backscatter data were examined for evidence of fish above the headrope height (mean: 2.0 m) during the time the demersal trawl was in contact with the seabed, after accounting for horizontal setback of the trawl behind the vessel (approximately 3–4 min depending on vessel speed). The acoustic assessment was restricted to the deep study site because catches there consisted almost exclusively of Pacific cod and flatfishes and, therefore, it was reasonable to assume that any backscatter that indicated fish with swim bladders was a result of the presence of Pacific cod. It was not possible to make such an assumption for data collected at the shallow study site because the catches there were dominated by walleye pollock, which cannot be acoustically distinguished from Pacific cod.

Results

Summary of catches

During the 48 experimental tows, 1462 Pacific cod, ranging in size from 34 to 105 cm FL, were caught, but only 2 fish were larger than 90 cm FL (Fig. 2). Of the captured fish, 701 individuals were large (≥55 cm FL) and included in further analyses. The bottom temperatures during the experiment ranged between 2.6°C and 2.7°C.

Swept area

Of the 24 paired tows, 16 pairs had reliable net mensuration data with which we could test differences in swept area by pair. The mean difference in swept area between paired tows (fast and slow) was −0.072 ha, a variance that was not significant (t=−0.492, df=15, P=0.63). The fast tows swept a greater area than that swept by the slow tows during half of the pairs (8 of 16 tows). Conversely, the slow tows swept a greater area than that swept by the fast tows during the other half of pairs. Bottom contact sensors provided reliable data

Table 2

Catch of large (≥55 cm in fork length) Pacific cod (*Gadus macrocephalus*) at fast (c_f) and slow (c_s) towing speeds for each pair of tows conducted for this study in the eastern Bering Sea in August 2013. Pairs 1–10 were deep tows. Pairs 11–24 were shallow tows. The expected catch (c_e) was calculated on the basis of the length-based selectivity curve from the 2013 National Marine Fisheries Service stock assessment as described in the *Materials and methods* section.

Tow pair	c_f	c_s	c_f/c_s	c_e	c_e/c_s
1	17	22	0.8	33	1.5
2	16	6	2.7	8	1.4
3	14	10	1.4	19	1.9
4	11	15	0.7	26	1.8
5	5	12	0.4	18	1.5
6	7	26	0.3	42	1.6
7	5	5	1.0	8	1.5
8	7	9	0.8	15	1.7
9	9	9	1.0	15	1.6
10	15	13	1.2	19	1.5
11	14	14	1.0	20	1.4
12	19	42	0.5	57	1.4
13	22	10	2.2	14	1.4
14	17	15	1.1	19	1.3
15	17	16	1.1	22	1.4
16	22	36	0.6	50	1.4
17	11	27	0.4	38	1.4
18	22	19	1.2	31	1.6
19	16	23	0.7	32	1.4
20	16	15	1.1	20	1.4
21	15	8	1.9	13	1.6
22	7	7	1.0	10	1.5
23	6	7	0.9	9	1.3
24	16	9	1.8	13	1.4

on all tows, indicating that trawl footropes were firmly in contact with the substrate and providing evidence for our decision to use all 24 pairs of data in subsequent analyses.

Effect of towing speed on catches

Fast tows had larger catches of large Pacific cod in only 10 of 24 paired tows. In those 10 pairs, the catches from fast tows were 1.1 to 2.7 times (mean: 1.6 times) greater than the catches from slow tows (Table 2). A sign test indicated that larger catches were not significantly more frequent in fast tows (successes=10, trials=24, P=0.924); larger catches in at least 18 of the 24 pairs would be required for significance ($P \leq 0.05$).

The mean difference $\bar{d}$ between $\ln(c_f)$ and $\ln(c_s)$ of −0.08 (SD 0.55) was approximately normally distributed according to a χ^2 goodness-of-fit test ($\chi^2_{5\text{-}2\text{-}1}$=1.226, P=0.54; Fig. 3). The mean of c_f/c_s was 1.1 (SD 0.58) (range: 0.3–2.7; Table 2). A paired t-test indicated that the difference in ln(*catch*) between fast and slow tows was not statistically significant (t_{23}=−0.69, P=0.50). The expected mean ratio of the catch of large Pacific cod in fast tows over slow tows (c_f/c_s) was 1.5 (range: 1.3–1.9). If the expected ratio of 1.5 were true, then the power of a 1-sided t-test (H_a: $\bar{d}>0$) would be 97% in rejecting H_0 (Table 3).

Vertical distribution

Demersal fish backscatter was fairly low, as would be expected given the low numbers of Pacific cod captured. The strongest demersal fish backscatter (S_v ~−45 dB) appeared very close to the acoustically detected seabed; fish backscatter farther off the seabed was generally weaker in comparison (S_v ~−65 dB). The demersal fish backscatter observed below the average headrope height of 2.0 m during this study was a very large fraction of fish backscatter integrated over all depth layers examined (median proportion: 0.96; Fig. 4). In an absolute sense, the highest demersal fish backscatter values were found within the depth layer of 0.25–2.0 m (Fig. 5); the median fish s_A in this layer was more than 14 times that in any other depth layer.

Discussion

We failed to detect a difference between slow (1.5 m/s) and fast (2.1 m/s) towing speeds in the rates at which

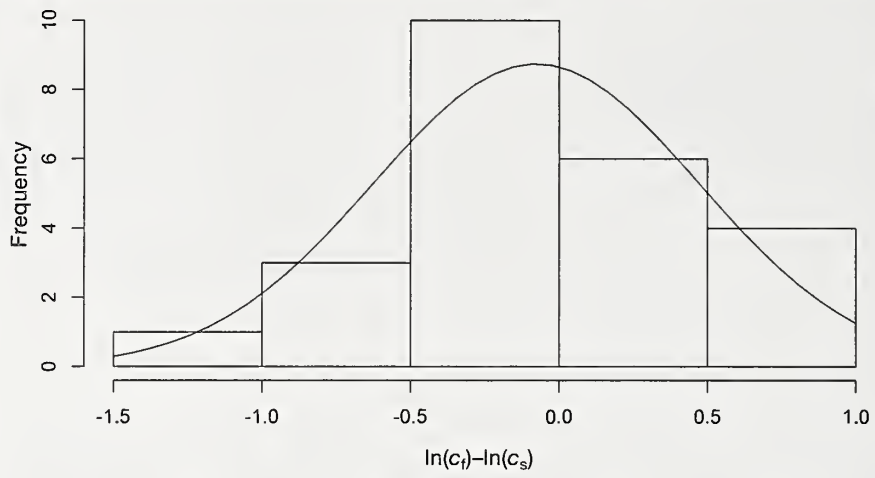

Figure 3

Normal distribution curve fitted to a histogram of the differences in ln(*catch*) of large Pacific cod (*Gadus macrocephalus*) between fast and slow towing speeds (goodness-of-fit: $\chi^2_{5\text{-}2\text{-}1}$=1.226, P=0.54) from this study conducted in 2013 in the eastern Bering Sea. ln(c_f)=catch at the fast towing speed of 2.1 m/s; ln(c_s)=catch at the slow towing speed of 1.5 m/s.

Table 3

Power of t-test (probability of rejecting H_0 when it is false) for the mean difference $\bar{d}$ between ln(c_f) (c_f=catch of fast tows) and ln(c_s) (c_s=catch of slow tows), where H_0: $\bar{d}$=0, against one-sided H_a: $\bar{d}$>0 alternative hypothesis. The t-distribution was used with a degree of freedom of 23 and a significance level (α) of 0.05.

$\bar{d}$	$e^{\bar{d}}=c_f/c_s$	Power
0.1	1.1	0.21
0.2	1.2	0.53
0.3	1.3	0.83
0.4	1.5	0.97
0.5	1.6	0.99
1.0	2.7	1.00

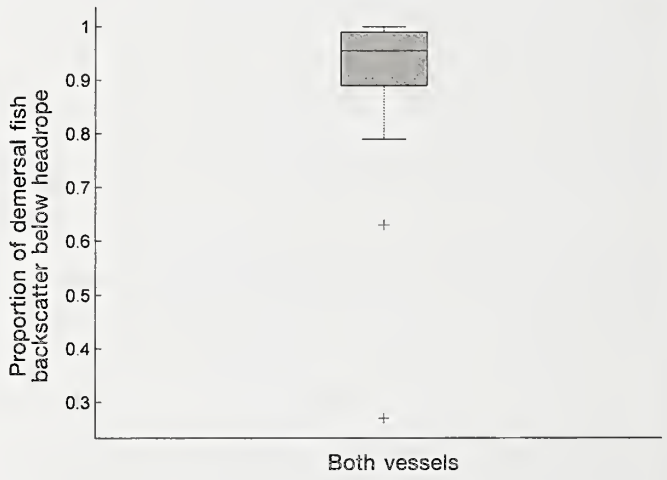

Figure 4

Boxplot indicating the proportion of demersal fish backscatter, in all depth layers examined (0.25–16.0 m above the sounder-detected bottom echo), found below the average headrope height but above the 0.25-m dead zone (0.25–2.0 m; n=20 tows), for this study conducted in August 2013 in the eastern Bering Sea. The line within the shaded box indicates the median value, the shaded box indicates the first and third quartiles, the horizontal lines outside the shaded box indicate a distance of 1.5 times the interquartile range above the third quartile and below the first quartile, and the plus marks indicate outliers outside these lines.

large Pacific cod (≥55 cm FL) were caught with the 83-112 eastern trawl. Therefore, we surmise that if the dome-shaped selectivity estimated in recent stock assessments (Thompson[1,2,3]) is due to a decrease in trawl efficiency for large Pacific cod, that decrease is not attributable to fish outswimming the net. We are unaware of other direct studies on the swimming behavior of Pacific cod in relation to trawling activity. Consequently, to make inferences, we must draw upon the conclusions from research conducted on other, similar species.

Of the many species studied for their swimming capabilities, the Atlantic cod is most closely related to Pacific cod. Winger et al. (2000) performed a comprehensive tank study on the swimming stamina of At-

lantic cod and deduced that changes in towing speed would affect the catching efficiency of this species. In their study, Atlantic cod were subjected to water velocities that were slower than our towing speeds, but water temperatures were close to those in our study (2.6°C). At the towing speeds used by fishermen in the northeast Atlantic (1.0 m/s), Atlantic cod were able to maintain sustained swimming speeds for 10 min, but at a speed of 1.5 m/s (the slow towing speed in our study), they could maintain swimming speed for only 1 min. If Pacific cod swimming abilities are indeed similar to those of Atlantic cod, then, given the towing speeds of 1.5 m/s or greater used in our experiment, we expect that Pacific cod maximum sustained swimming speeds would not be enough to elude capture even during a haul lasting 22.5 min, the shorter tow duration used in our experiment.

Large Pacific cod do not escape capture by outswimming the survey trawl, as indicated by our study results: catches when towing at the fast speed were no different than catches when towing at the slow speed. This result indicates that, once Pacific cod reach the trawl mouth, they lack the means to swim fast enough or long enough to escape forward around the wing ends. In situ video evidence shows that this species tends to hold station in front of the footrope for only brief periods before slipping back into the net (Rose[6]). Large Pacific cod are unlikely to swim over the net because acoustic backscatter indicates that most Pacific cod, when in the presence of a trawler, occur very close to the bottom within the vertical fishing dimensions of the trawl. In addition, findings from previous studies on gadid behavior indicate that trawl gear elicits a diving response in fish, not a rising response. The remaining avenues for escapement that could explain lowered trawl efficiency are 1) large Pacific cod could swim through the small mesh of the survey net, an option that is physically impossible and 2) they could escape beneath the footrope, the frequency of which has been previously shown to be negligible (Weinberg et al., 2002).

If large Pacific cod are not outswimming the trawl, perhaps they are swimming over the headrope—a notion that would also explain a drop in selectivity for large fish related to both trawl sampling efficiency and availability. Here, we used fish backscatter to within 0.25 m of the seabed to assess the vertical distribution of Pacific cod near the seafloor during our experiment. This process discards potential backscatter from fish in the acoustic dead zone (Ona and Mitson, 1996), which is located very close to the seabed and could be an area of concern for an absolute estimate of all fish s_A. However, the distribution of fishes within the dead zone is less important for our main interest of detecting Pacific cod occurrence in relation to the headrope height of the trawl; indeed, if most Pacific cod are in the acoustic dead zone, they clearly are not above the headrope height during vessel passage.

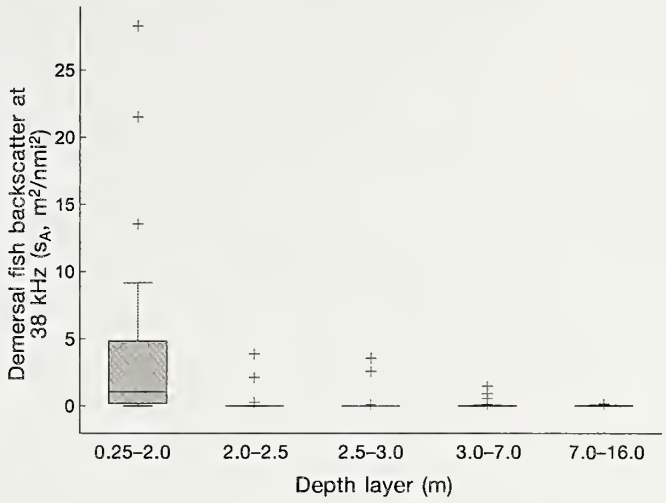

Figure 5

Boxplots of demersal fish backscatter per unit of area (s_A) at 5 depth layers within 16 m of the sounder-detected bottom (n=20 tows), determined from acoustic data collected at a frequency of 38 kHz in August 2013 in the eastern Bering Sea. The horizontal line across the shaded box indicates the median value, the shaded box indicates the first and third quartiles, the lines outside the shaded box indicate a distance of 1.5 times the interquartile range above the third quartile and below the first quartile, and the plus marks indicate outliers outside these lines.

Analysis of acoustic backscatter collected during towing indicated that only 4% of the total backscatter attributed to Pacific cod occurred above the height of the survey headrope, although the backscatter was measured at the vessel rather than at the net itself, meaning that any upward movement of fish after vessel passage would be undetected. Again, there are no previous studies on the vertical swimming behavior of Pacific cod in relation to trawls from which we can draw inferences. Studies of walleye pollock (Kotwicki et al., 2013) and Atlantic cod show that these 2 commercially important gadids were stimulated to dive, rather than rise; their response to trawl warps may be both acoustically, as well as visually, driven according to Handegard and Tjøstheim (2005). This behavior is also acknowledged by commercial fishermen who tend to drag their nets below semipelagic schools. There is, therefore, little reason to believe that Pacific cod swam over the headrope during this experiment.

Nichol et al. (2007) did, however, on the basis of 11 archival tags, provide evidence of an off-bottom portion of the Pacific cod vertical distribution during daylight hours (the time during which the EBS survey is conducted) when the fish were in an undisturbed state

[6] Rose, C. R. 2010. Unpubl. data. Resour. Assess. Conserv. Eng. Div., Alaska Fish. Sci. Cent., NOAA, Seattle, WA 98115.

(i.e., tags were deployed in the absence of vessel noise or oncoming trawl gear). They postulated that large Pacific cod swim above the survey-wide average height of the headrope (2.5 m) approximately 53% of the time and within 10 m of the seabed 95% of the time. Although their study was based on an interpretation of estimated tidal activity, their work has had a pronounced impact on the current stock assessment model, such that the catchability coefficient was fixed so that the average product of catchability and selectivity size range (60–81 cm FL) equaled 47% (Thompson[1,2,3]).

We agree with Nichol et al. (2007), in that it seems unlikely for the survey trawl to catch 100% of the Pacific cod in its path 100% of the time; however, we cast doubt on the conclusion that more than 50% of large fish swim above the trawl in the presence of trawling activity. Nichol et al.'s study was based on a very small sample, and one could argue that our study similarly lacked broad geographical range, over areas with varying habitat complexity, light intensity, and temperatures that (although never shown) may all have an effect on Pacific cod vertical distributions or perhaps even swimming speeds (Ferno et al., 2011). Additional experiments focusing on these factors would shed additional light on the matter.

Survey selectivity functions in stock assessment models are designed to be a parsimonious representation of the relative size dependency of the survey sampling process. However, stock assessment models can be quite complex, often including hundreds of parameters that must be estimated when the models are fitted to data (Maunder and Punt, 2013; Methot and Wetzel, 2013), and such complexity can lead to parameter correlation and confounding during model fitting. One example of this confounding is the correlation between survey selectivity parameters and the natural mortality rate (Thompson, 1994), a relationship that can lead to ambiguity in ascribing unexpectedly low catches at a particular fish length to either reduced survey selectivity or to an underestimated natural mortality rate.

We are, therefore, unable to corroborate the dome shape for the selectivity function of the survey of Pacific cod in the EBS by using direct evidence from this and other field studies in which trawl sampling efficiency has been examined. If the estimated survey selectivity function determined from the model is indeed correct, then the mechanisms that explain the steep descent of the right-hand tail must consist of something other than sampling efficiency. Four possible explanations for this steep descent of the right-hand tail are that 1) large fish migrate out of the survey grid, hence becoming unavailable to the survey; 2) sampling effort in preferred habitat of large fish embedded within the EBS survey area is not sufficient; 3) large fish prefer the small areas of rough, untrawlable bottom embedded within the EBS survey area; and 4) the relationships between availability and efficiency, on the one hand, and between catchability and selectivity, on the other, are complicated enough that studies of availability or efficiency alone are insufficient to explain catchability or selectivity (see Suppl. Text [Online]). If something is misspecified in the assessment model (e.g., perhaps the natural mortality rate is too low or varies with fish size), the selectivity of the survey for large Pacific cod would be closer to unity and could lead to a change in the harvest quotas. Therefore, further research on these subjects is needed to clarify the mechanisms responsible for the selectivity of the survey.

Acknowledgments

Funding for this project was provided by the National Marine Fisheries Service, National Cooperative Research Program with Industry. We are grateful for the advice provided by A. De Robertis on echo-integration techniques and for the helpful comments from our reviewers D. Nichol and S. Kotwicki. In addition, we thank our anonymous reviewers who sacrificed their valuable time to contribute to the advancement of fisheries science.

Literature cited

Cadrin, S. X., S. H. Clark, D. F. Schick, M. P. Armstrong, D. McCarron, and B. Smith.
1999. Application of catch-survey models to the northern shrimp fishery in the Gulf of Maine. N. Am. J. Fish. Manage. 19:551–568.

Clark, W. G., and S. M. Kaimmer.
2006. Estimates of commercial longline selectivity for Pacific halibut (*Hippoglossus stenolepis*) from multiple marking experiments. Fish. Bull. 104:465–467.

De Robertis, A., and I. Higginbottom.
2007. A post-processing technique to estimate the signal-to-noise ratio and remove echosounder background noise. ICES J. Mar. Sci. 64:1282–1291.

De Robertis, A., D. R. McKelvey, and P. H. Ressler.
2010. Development and application of empirical multifrequency methods for backscatter classification in the North Pacific. Can. J. Fish. Aquat. Sci. 67:1459–1474.

Ferno, A., T. Jørgensen, S. Løkkeborg, and P. D. Winger.
2011. Variable swimming speeds in individual Atlantic cod (*Gadus Morhua* L.) determined by high-resolution acoustic tracking. Mar. Biol. Res. 7:310–313.

Glass, C. W., and C. S. Wardle.
1989. Comparison of the reactions of fish to trawl gear, at high and low light intensities. Fish. Res. 7:249–266.

Godø, O. R., and S. J. Walsh.
1992. Escapement of fish during bottom trawl sampling—implications for resource assessment. Fish. Res. 13:281–292.

Godø, O. R., M. Pennington, and J. H. Vølstad.
1990. Effect of tow duration on length composition of trawl catches. Fish. Res. 9:165–179.

Godø, O. R., S. J. Walsh, and A. Engås.
1999. Investigating density-dependent catchability in bottom-trawl surveys. ICES J. Mar. Sci. 56:292–298.

Handegard, N. O., and D. Tjøstheim.
2005. When fish meet a trawling vessel: examining the behaviour of gadoids using a free-floating buoy and

acoustic split-beam tracking. Can. J. Fish. Aquat. Sci. 62:2409–2422.

He, P.
1991. Swimming endurance of the Atlantic cod, *Gadus morhua* L., at low temperatures. Fish. Res. 12:65–73.

He, P., and C. S. Wardle.
1988. Endurance at intermediate swimming speeds of Atlantic mackerel, *Scomber scombrus* L., herring, *Clupea harangus* L., and saithe, *Pollachius virens* L. J. Fish. Biol. 33:255–266.

Kotwicki, S., M. H. Martin, and E. A. Laman.
2011. Improving area swept estimates from bottom trawl surveys. Fish. Res. 110:198–206.

Kotwicki, S., A. De Robertis, J. N. Ianelli, A. E. Punt, and J. K. Horne.
2013. Combining bottom trawl and acoustic data to model acoustic dead zone correction and bottom trawl efficiency parameters for semipelagic species. Can. J. Fish. Aquat. Sci. 70:208–219.

Kotwicki, S., J. N. Ianelli, and A. E. Punt.
2014. Correcting density-dependent effects in abundance estimates from bottom-trawl surveys. ICES J. Mar. Sci. 71:1107–1116.

Lauth, R. R., and D. G. Nichol.
2013. Results of the 2012 eastern Bering Sea continental shelf bottom trawl survey of groundfish and invertebrate resources. NOAA Tech. Memo. NMFS-AFSC-256, 162 p.

MacLennan, D. N., P. G. Fernandes, and J. Dalen.
2002. A consistent approach to definitions and symbols in fisheries acoustics. ICES J. Mar. Sci. 59:365–369.

Main, J., and G. I. Sangster.
1981. A study of the fish capture process in a bottom trawl by direct observations from a towed underwater vehicle. Scott. Fish. Res. Rep. No. 23, 23 p.

Maunder, M. N., and K. R. Piner.
2015. Contemporary fisheries stock assessment: many issues still remain. ICES J. Mar. Sci. 72:7–18.

Maunder, M. N., and A. E. Punt.
2013. A review of integrated analysis in fisheries stock assessment. Fish. Res. 142:61–74.

Maunder, M. N., P. R. Crone, J. L. Valero, and B. X. Semmens.
2014. Selectivity: theory, estimation, and application in fishery stock assessment models. Fish. Res. 158: 1–4

Methot, R. D., Jr., and C. R. Wetzel.
2013. Stock synthesis: a biological and statistical framework for fish stock assessment and fishery management. Fish. Res. 142:86–99.

Nichol, D. G., T. Honkalehto, and G. G. Thompson.
2007. Proximity of Pacific cod to the seafloor: using archival tags to estimate fish availability to research bottom trawls. Fish. Res. 86:129–135.

Ona, E., and R. B. Mitson.
1996. Acoustic sampling and signal processing near the seabed: the deadzone revisited. ICES J. Mar. Sci. 53: 677–690.

Restrepo, V. R., J. Ortiz de Umbra, J.-M. Fromentin, and H. Arrizabalaga.
2007. Estimates of selectivity for eastern Atlantic bluefin tuna from catch curves. Collect. Vol. Sci. Pap. ICCAT. 60:937–948.

Somerton, D. A., and K. L. Weinberg.
2001. The affect of speed through the water on footrope contact of a survey trawl. Fish. Res. 53:17–24.

Somerton, D. A., P. T. Munro, and K. L. Weinberg.
2007. Whole-gear efficiency of a benthic survey trawl for flatfish. Fish. Bull. 105:278–291.

Somerton, D. A., K. L. Weinberg, and S. E. Goodman.
2013 Catchability of snow crab (*Chionoecetes opilio*) by the eastern Bering Sea bottom trawl survey estimated using a catch comparison experiment. Can. J. Fish. Aquat. Sci. 70:1699–1708.

Stauffer, G.
2004. NOAA protocols for groundfish bottom trawl surveys of the nation's fishery resources. NOAA Tech. Memo. NMFS-F/SPO-65, 205 p.

Thompson, G. G.
1994 Confounding of gear selectivity and the natural mortality rate in cases where the former is a nonmonotone function of age. Can. J. Fish. Aquat. Sci. 51:2654–2664

Walsh, S. J.
1991. Diel variation in availability and vulnerability of fish to a survey trawl. J. Appl. Ichthyol. 7:147–159.

Weinberg, K. L.
2003. Change in the performance of a Bering Sea survey trawl due to varied trawl speed. Alaska Fish. Res. Bull. 10:42–49.

Weinberg, K. L., D. A. Somerton, and P. T. Munro.
2002. The effect of trawl speed on the footrope capture efficiency of a survey trawl. Fish. Res. 58:303–313.

Weinberg, K. L., R. S. Otto, and D. A. Somerton.
2004. Capture probability of a survey trawl for red king crab (*Paralithodes camtschaticus*). Fish. Bull. 102: 740–749.

Wileman, D. A., R. S. T. Ferro, R. Fonteyne, and R. B. Millar (eds.).
1996. Manual of methods of measuring the selectivity of towed fishing gears. ICES Coop. Res. Rep. 215, 126 p.

Winger, P. D., P. He, and S. J. Walsh.
1999. Swimming endurance of American plaice (*Hippoglossoides platessoides*) and its role in fish capture. ICES J. Mar. Sci. 56:252–265.
2000. Factors affecting the swimming endurance and catchability of Atlantic cod (*Gadus morhua*). Can. J. Fish. Aquat. Sci. 57:1200–1207.

NOAA
National Marine
Fisheries Service

Fishery Bulletin
established 1881

Spencer F. Baird
First U.S. Commissioner
of Fisheries and founder
of *Fishery Bulletin*

A comparison of circle hook and J hook performance in the recreational shark fishery off Maryland

Angel L. Willey (contact author)
Linda S. Barker
Mark Sampson

Email address for contact author: angel.willey@maryland.gov

Fisheries Service
Maryland Department of Natural Resources
580 Taylor Avenue
Annapolis, Maryland 21401

Abstract—The purpose of this study, conducted from 2012 through 2014, was to gather data on the different effects of circle and J hooks on hooking outcome, frequency of deep hooking, and catch rate in the recreational shark fishery off Maryland. Circle hooks clearly outperformed J hooks. Interactions of sharks with circle hooks resulted in a 91% hooking rate (of which 3% were deep hookings), an 88% capture rate, and a catch rate of 0.9 sharks/hook interaction. The hooking rate for J hooks was 75% (of which 6% were deep hookings), a capture rate of 68%, and a catch rate of 0.7 sharks/hook interaction. These results indicate that circle hooks can improve fishing success and serve as a conservation measure by maximizing the probability of survival for sharks during recreational shark fishing.

Manuscript submitted 31 August 2015.
Manuscript accepted 6 June 2016.
Fish. Bull. 114:370–372 (2016).
Online publication date: 21 June 2016.
doi: 10.7755/FB.114.3.9

Numerous studies of the recreational use of circle hooks in teleost fisheries and the commercial pelagic longline fishery indicate that fewer fish are "deep hooked" on circle hooks and that catch efficiency with circle hooks is equal to, or better than, that with J hooks (Cooke and Suski, 2004; Serafy et al., 2012). These studies have helped circle hooks gain acceptance and have provided the data used to set forth regulatory requirements for some fisheries and tournaments (Cooke and Suski, 2004). In the recreational shark fishery, some anglers have been reluctant to switch to circle hooks because of concerns about catch efficiency and doubts about the applicability of the results of teleost studies to the catchability of sharks (Prince et al., 2002; Lucifora et al., 2009; Serafy et al., 2012). Therefore, scientific evidence that supports the benefits of circle hooks is needed to convince recreational shark anglers to voluntarily switch hook types and support regulatory measures that require circle hook use in their fishery. We undertook this study from 2012 through 2014 to gather data on the effects of circle and J hooks on hooking outcome, frequency of deep hooking, and catch rate in the recreational shark fishery off Maryland.

Materials and methods

Field methods

All data were collected by a charter captain that specialized in shark fishing off the Atlantic coast of Maryland. He fished as he normally did but dedicated 2 surface lines to our study, set with a circle hook and a comparable-size J hook. Circle hooks were limited to Mustad[1] 39960D hooks in sizes 16/0 when fishing occurred offshore and 13/0 when fishing occurred nearshore (O. Mustad & Son A.S., Gjovik, Norway). Bait type was identical in size and species for both lines and was refreshed at the same time.

The outcome of each shark interaction with the line (called a *strike*) was recorded as a *bite*, as *lost*, or as *captured*)—terminology similar to that of Skomal et al. (2002). A *bite* was defined as a strike that resulted in the shark taking the bait but not being hooked. An event was not recorded if the captain or mate

[1] Mention of trade names or commercial companies is for identification purposes only and does not imply endorsement by the Maryland Department of Natural Resources.

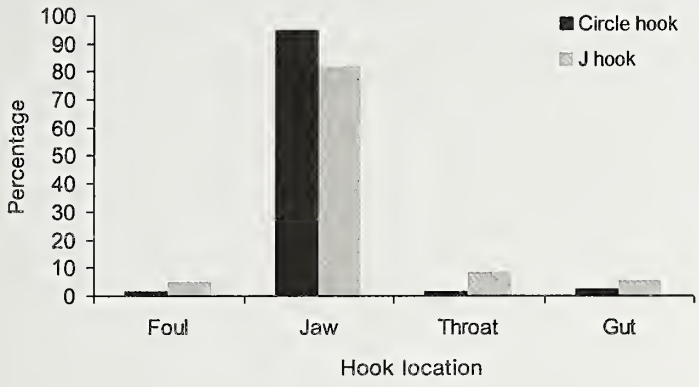

Figure 1

Hook locations (n=622) observed, 2012–2014, during a study of interactions of sharks with circle and J hooks in the recreational shark fishery off Maryland. Data for 2 landed sharks were not included in this figure because either a hook location was not recorded or the shark had become entangled in the line and a hooking event did not occur. A location at *throat* or *gut* was considered a deep hooking.

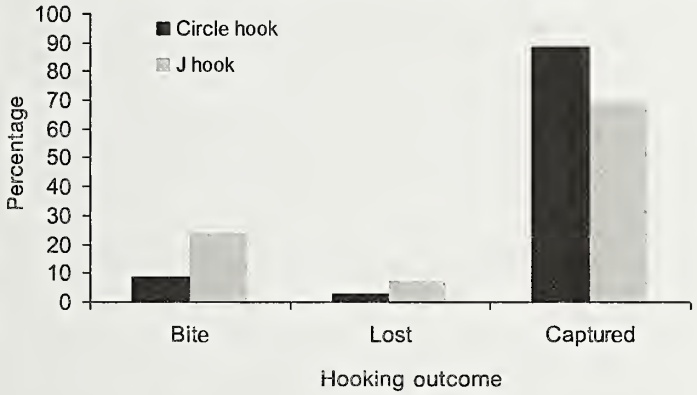

Figure 2

Outcomes of hooking events (n=781) observed during 2012–2014 as part of a study of interactions of sharks with circle and J hooks in the recreational shark fishery off Maryland, classified into 3 categories: 1) bite, when a shark took the bait but was not hooked; 2) lost, when a hooked shark became unhooked before the mate could grab the leader; and 3) captured, when a shark was fully played to the boat and the mate grabbed the leader.

could not confirm that it was a shark bite. A *lost* classification was defined as the outcome where a hooked shark became unhooked before the mate could grab the leader. A *captured* classification was the outcome when a shark was fully played to the boat and the mate grabbed the leader. Hook location was recorded as *jaw*, *throat*, *gut*, or *foul (external)*. Entangled fish were documented but excluded from the analysis because they were not actually hooked. *Deep hooking* was defined as hooking in the throat or gut.

Statistical methods

Trips were identified as nearshore or offshore because of differences in species composition and tackle requirements. Nearshore trips occurred in waters within 32.2 km (20 mi) of land, and offshore trips took place in waters 32.2 or more kilometers from land. Most of the nearshore fishing occurred within 1.6–9.7 km (1–6 mi) of the beach, and the majority of offshore fishing took place between 32.2 and 48.3 km (20 and 30 mi) from the beach.

Data were pooled across years, and the following tests were performed. Chi-square analysis was used to determine whether nearshore and offshore trip data could be pooled. Hypothesis tests of proportions were conducted to compare hooking outcomes and to compare rates of deep hooking between hook types. Catch rate was defined as the number of sharks captured per interaction and calculated as the mean of trip values. Student's t-test was used to compare catch rates between hook types.

Results

Data were collected during 24 offshore and 180 nearshore trips, and the results of chi-square analysis indicated that nearshore and offshore data could be pooled for all analyses (all P>0.10). During this study, 624 sharks representing 10 shark species were captured, primarily dusky shark (*Carcharhinus obscurus*; n=235), spinner shark (*Carcharhinus brevipinna*; n=180), sandbar shark (*Carcharhinus plumbeus*; n=89), and Atlantic sharpnose shark (*Rhizoprionodon terraenovae*; n=70). The other species caught were the blue shark (*Prionace glauca*; n=15), blacktip shark (*Carcharhinus limbatus*; n=13), tiger shark (*Galeocerdo cuvier*; n=7), shortfin mako (*Isurus oxyrinchus*; n=7), scalloped hammerhead (*Sphyrna lewini*; n=5), and smooth hammerhead (*Sphyrna zygaena*; n=3).

There were 438 shark interactions with circle hooks and 343 interactions with J hooks. Interactions with circle hooks resulted in a 91% hooking rate of which 95% of sharks were hooked in the jaw and only 3% were deep hookings (Fig. 1). Circle hooks had an 88% capture rate (Fig. 2) and a catch rate of 0.9 sharks/hook interaction. For J hooks, the hooking rate was 75% of which 82% of sharks were hooked in the jaw and 6% deep hookings. The capture rate was 68% and the catch rate was 0.7 sharks/hook interaction. All differences were significant with P<0.01.

Discussion

The data clearly indicate that circle hooks outperform J hooks. Circle hooks had both a higher hooking rate and capture rate than J hooks. Circle hooks had a lower deep-hooking rate and a higher proportion of sharks hooked in the jaw—results that are consistent with those of many teleost studies (Prince et al., 2002; Skomal et al., 2002). Both the higher catch rate and the lower deep-hooking rate indicate that circle hooks can improve fishing success and serve as a conservation measure for recreational shark fishing. In addition, the results of this study indicate that the use of circle hooks could increase adherence to the federal regulations regarding prohibited shark species—regulations that are outlined in a compliance guide for highly migratory species (NMFS[2]). These regulations require that shark species for which retention is prohibited be released in a manner that maximizes the probability of their survival.

[2] NMFS (National Marine Fisheries Service). 2015. HMS recreational compliance guide: guide for complying with the Atlantic billfishes, swordfish, sharks, and tunas regulations, p. 30. Off. Sustainable Fish., Highly Migratory Species Manage. Div., Natl. Mar. Fish. Serv., NOAA, Silver Spring, MD. [Available at website, accessed June 2016.]

Acknowledgments

We would like to thank the 3 anonymous reviewers for their constructive comments at the manuscript stage.

Literature cited

Cooke S. J., and C. D. Suski.
2004. Are circle hooks an effective tool for conserving marine and freshwater recreational catch-and-release fisheries? Aquat. Conserv. 14:299–326.

Lucifora, L. O., V. B. Garcia, and A. H. Escalante.
2009. How can the feeding habits of the sand tiger shark influence the success of conservation programs? Anim. Conserv. 12:291–301.

Prince, E. D., M. Ortiz, and A. Venizelos.
2002. A comparison of circle hook and "J" hook performance in recreational catch-and-release fisheries for billfish. Am. Fish. Soc. Symp. 30:66–79.

Serafy, J. E., S. J. Cooke, G. A. Diaz, J. E. Graves, M. Hall, M. Shivji, and Y. Swimmer.
2012. Circle hooks in commercial, recreational, and artisanal fisheries: research status and needs for improved conservation and management. Bull. Mar. Sci. 88:371–391.

Skomal, G. B., B. C. Chase, and E. D. Prince.
2002. A comparison of circle hook and straight hook performance in recreational fisheries for juvenile Atlantic bluefin tuna. Am. Fish. Soc. Symp. 30:57–65.

Fishery Bulletin

Guidelines for authors

Contributions published in *Fishery Bulletin* describe original research in marine fishery science, fishery engineering and economics, as well as the areas of marine environmental and ecological sciences (including modeling). Preference will be given to manuscripts that examine processes and underlying patterns. Descriptive reports, surveys, and observational papers may occasionally be published but should appeal to an audience outside the locale in which the study was conducted.

Although all contributions are subject to peer review, responsibility for the contents of papers rests upon the authors and not on the editor or publisher. *Submission of an article implies that the article is original and is not being considered for publication elsewhere.*

Plagiarism and double publication are considered serious breaches of publication ethics. To verify the originality of the research in papers and to identify possible previous publication, manuscripts may be screened with plagiarism-detection software.

Manuscripts must be written in English; authors whose native language is not English are strongly advised to have their manuscripts checked by English-speaking colleagues before submission.

Once a paper has been accepted for publication, online publication takes approximately 3 weeks.

There is no cost for publication in *Fishery Bulletin.*

Types of manuscripts accepted by the journal

Articles

Articles generally range from 20 to 30 double-spaced typed pages (12-point font) and describe an original contribution to fisheries science, engineering, or economics. Tables and figures are not included in this page count, but the number of figures should not exceed one figure for every four pages of text. Articles contain the following divisions: **abstract, introduction, methods, results, and discussion.**

Short contributions

Short contributions are generally less than 20 double spaced typed pages (12-point font) and, like articles, describe an original contribution to fisheries science. They follow the same format as that for articles: **abstract, introduction, results and discussion, but the results and discussion sections may be combined**. They are distinguished from full articles in that they report a noteworthy new observation or discovery—such as the first report of a new species, a unique finding, condition, or event that expands our knowledge of fisheries science, engineering or economics—and do not require a lengthy discussion.

Companion articles

Companion articles are presented together and published together as a scientific contribution. Both articles address a closely related topic and may be articles that result from a workshop or conference. They must be submitted to the journal at the same time.

Review articles

Review articles generally range from 40 to 60 double-spaced typed pages (12-point font) and address a timely topic that is relevant to all aspects of fisheries science. They should be forward thinking and address novel views or interpretations of information that encourage new avenues of research. They can be reviews based on the outcome from thematic workshops, or contributions by groups of authors who want to focus on a particular topic, or a contribution by an individual who chooses to review a research theme of broad interest to the fisheries science community. **A review article will include an abstract, but the format of the article *per se* will be up to the authors**. Please contact the Scientific Editor to discuss your ideas regarding a review article before embarking on such a project.

Preparation of manuscript

Title page should include authors' full names, mailing addresses, and the senior author's e-mail address.

Abstract should be limited to 200 words (one-half typed page), state the main scope of the research, and emphasize the authors conclusions and relevant findings. Do not review the methods of the study or list the contents of the paper. Because abstracts are circulated by abstracting agencies, it is important that they represent the research clearly and concisely.

General text must be typed in 12-point Times New Roman font throughout. A brief introduction should convey the broad significance of the paper; the remainder of the paper should be divided into the following sections: Materials and methods, Results, Discussion, and Acknowledgments. Headings within each section must be short, reflect a logical sequence, and follow the rules of subdivision (i.e., there can be no subdivision without at least two subheadings). The entire text should be intelligible to interdisciplinary readers; therefore, all acronyms, abbreviations, and technical terms should be written out in full the first time they are mentioned. Abbreviations should be used sparingly because they are not carried over to indexing databases and slow readability for those readers outside a discipline. They should never be used for the main subject (species, method) of a paper.

For general style, follow the U.S. *Government Printing Office Style Manual* (2008) [available at website] and *Scientific Style and Format: the CSE Manual for Authors, Editors, and Publishers* (2014, 8th ed.) published by the Council of Science Editors. For scientific nomenclature, use the current edition of the American Fisheries Society's *Common and Scientific Names of Fishes from the United States, Canada, and Mexico* and its companion volumes (*Decapod Crustaceans, Mollusks, Cnidaria and Ctenophora*, and *World Fishes Important to North Americans*). For species not found in the above mentioned AFS publications and for more recent changes in nomenclature, use the Integrated Taxonomic Information System (ITIS) (available at website), or, secondarily, the California Academy of Sciences *Catalog* of *Fishes* (available at website) for species names not included in ITIS. Common (vernacular) names of species should be lowercase. Citations must be given of taxonomic references used for the identification of specimens. For example, "Fishes were identified according to Collette and Klein-MacPhee (2002); sponges were identified according to Stone et al. (2011)."

Dates should be written as follows: 11 November 2000. Measurements should be expressed in metric units, e.g., 58 metric tons (t); if other units of measurement are used, please make this fact explicit to the reader. Use numerals, not words, to express whole and decimal numbers in the general text, tables, and figure captions (except at the beginning of a sentence). For example: We considered 3 hypotheses. We collected 7 samples in this location. Use American spelling. Refrain from using the shorthand slash (/), an ambiguous symbol, in the general text.

Word usage and grammar that may be useful are the following:

- *Aging* For our journal the word *aging* is used to mean both age determination and the aging process (senescence). The author should make clear which meaning is intended where ambiguity may arise.

- *Fish and fishes* For papers on taxonomy and biodiversity, the plural of *fish* is *fishes,* by convention. In all other instances, the plural is *fish.*
  Examples:
  The fishes of Puget Sound [biodiversity is indicated];
  The number of fish caught that season [no emphasis on biodiversity];
  The fish were caught in trawl nets [no emphasis on biodiversity].
  The same logic applies to the use of the words *crab* and *crabs, squid* and *squids,* etc.

- *Sex* For the meaning of male and female, use the word *sex*, not *gender.*

- *Participles* As adjectives, participles must modify a specific noun or pronoun and make sense with that noun or pronoun.
  Incorrect:
  Using the recruitment model, estimates of age-1 recruitment were determined. [Estimates did not use the recruitment model.]
  Correct:
  Using the recruitment model, we determined age-1 estimates of recruitment. [The participle now modifies the word *we,* i.e., those who were using the model.]
  Incorrect:
  Based on the collected data, we concluded that the mortality rate for these fish had increased. [*We* were not based on the collected data.]
  Correct:
  We concluded on the basis of the collected data that the mortality rate for these fish had increased. [Eliminate the participle and replace it with an adverbial phrase.]

Equations and mathematical symbols should be set from a standard mathematical program (MathType) and tool (Equation Editor in MS Word). LaTex is acceptable for more advanced computations. For mathematical symbols in the general text (α, χ^2, π, $\pm$, etc.), use the symbols provided by the MS Word program and italicize all variables, except those variables represented by Greek letters. Do not use photo mode when creating these symbols in the general text.

Number equations (if there are more than 1) for future reference by scientists; place the number within parentheses at the end of the first line of the equation.

Literature cited section comprises published works and those accepted for publication in peer-reviewed journals (in press). Follow the name and year system for citation format in the "Literature cited" section (that is to say, citations should be listed alphabetically by the authors' last names, and then by year if there is more than one citation with the same authorship. A list of abbreviations for citing journal names can be found at website.

Authors are responsible for the accuracy and completeness of all citations. Literature citation format: Author (last name, followed by first-name initials). Year. Title of article. Abbreviated title of the journal in which it was published. Always include number of pages. For a sequence of citations in the general text, list chronologically: (Smith, 1932: Green. 1947; Smith and Jones, 1985).

Digital object identifier (doi) code ensures that a publication has a permanent location online. Doi code should be included at the end of citations of published literature. Authors are responsible for submitting accurate doi codes. Faulty codes will be deleted at the page-proof stage.

Cite all software, special equipment, and chemical solutions used in the study within parentheses in the general text: e.g., SAS, vers. 6.03 (SAS Inst., Inc., Cary, NC).

Footnotes are used for all documents that have not been formally peer reviewed and for observations and personal communications. These types of references should be cited sparingly in manuscripts submitted to the journal.

All reference documents, administrative reports, internal reports, progress reports, project reports, contract reports, personal observations, personal communications, unpublished data, manuscripts in review, and council meeting notes are footnoted in 9 pt font and placed at the bottom of the page on which they are first cited. Footnote format is the same as that for formal literature citations. A link to the online source (e.g., [http://www/..... , accessed July 2007.]), or the mailing address of the agency or department holding the document, should be provided so that readers may obtain a copy of the document.

Tables are often overused in scientific papers; it is seldom necessary to present all the data associated with a study. Tables should not be excessive in size and must be cited in numerical order in the text. Headings should be short but ample enough to allow the table to be intelligible on its own.

All abbreviations and unusual symbols must be explained in the table legend. Other incidental comments may be footnoted with italic numeral footnote markers. Use asterisks only to indicate significance in statistical data. Do not type table legends on a separate page; place them above the table data. *Do not submit tables in photo mode.*

- Notate probability with a capital, italic *P*.
- Provide a zero before all decimal points for values less than one (e.g., 0.07).
- Round all values to 2 decimal points.
- Use a comma in numbers of five digits or more (e.g., 13,000 but 3000).

Figures must be cited in numerical order in the text. Graphics should aid in the comprehension of the text, but they should be limited to presenting patterns rather than raw data. Figures should not exceed one figure for every four pages of text and must be labeled with the number of the figure. Place labels **A, B, C,** etc. within the upper left area of graphs and photos. Avoid placing labels vertically (except for the y axis).

Figure legends should explain all symbols and abbreviations seen in the figure and should be double-spaced on a separate page at the end of the manuscript.

Line art and halftone figures should be submitted as pdf files with >800 dpi and >300 dpi, respectively. Color is allowed in figures to show morphological differences among species (for species identification), to show stain reactions, and to show gradations in temperature contours within maps. Color is discouraged in graphs, and for the few instances where color may be allowed, the use of color will be determined by the Managing Editor. Approved color figures should be submitted as TIFF or JPG files in CMYK format.

- Capitalize the first letter of the first word in all labels within figures.
- Do not use overly large font sizes in maps and for units of measurements along axes in graphs.
- Do not use bold fonts or bold lines in figures.
- Do not place outline rules around graphs.
- Place a North arrow and label degrees latitude and longitude (e.g., 170°E) in all maps.
- Use symbols, shadings, or patterns (not clip art) in maps and graphs.

Supplementary materials that are considered essential, but are too large or impractical for inclusion in a paper (e.g., metadata, figures, tables, videos, websites), may be provided at the end of an article. These materials are subject to the editorial standards of the journal. A URL to the supplementary material and a brief explanation for including such material should be sent at the time of initial submission of the paper to the journal.

- **Metadata, figures, tables** should be submitted in standard digital format (Word docx, pdf) and should be cited in the general text as (Suppl. Table, Suppl. Fig., etc.).
- **Websites** should be cited as (Suppl. website) in the general text and be made available with doi code (if possible) at the end of the article.
- **Videos** must not be larger than 30 MB to allow a swift technical response for viewing the video. Authors should consider whether a short video uniquely captures what text alone cannot capture for the understanding of a process or behavior under examination in the article. Supply an online link to the location of the video (e.g., YouTube).

Copyright law does not apply to *Fishery Bulletin,* which falls within the public domain. However, if an author reproduces any part of an article from *Fishery Bulletin*, reference to source is considered correct form (e.g., Source: Fish. Bull. 97:105).

Failure to follow these guidelines and failure to correspond with editors in a timely manner will delay publication of a manuscript.

Submission of manuscript

Submit manuscript online at the ScholarOne website. Commerce Department authors should submit papers under a completed NOAA Form 25-700. For further details on electronic submission, please contact the Associate Editor, Kathryn Dennis, at

kathryn.dennis@noaa.gov

When requested, the text and tables should be submitted in Word format. Figures should be sent as separate PDF files (preferred), TIFF files, or JPG files. Send a copy of figures in the original software if conversion to any of these formats yields a degraded version of the figure.

Questions? If you have questions regarding these guidelines, please contact the Managing Editor, Sharyn Matriotti, at

sharyn.matriotti@noaa.gov

Questions regarding manuscripts under review should be addressed to Kathryn Dennis, Associate Editor.

Fishery Bulletin

Subscription form

Superintendent of Documents **Publications** Order Form

*5178

☐ YES, please send me the following publications:

____ Subscriptions to *Fishery Bulletin*
for $32.00 per year ($44.80 foreign)

The total cost of my order is $ _____ . Prices include regular domestic postage and handling and are subject to change.

_____
(Company or Personal Name) (Please type or print)

_____
(Additional address/attention line)

_____
(Street address)

_____
(City, State, ZIP Code)

_____
(Daytime phone including area code)

_____
(Purchase Order No.)

Charge your order. IT'S EASY!

VISA

MasterCard

Please Choose Method of Payment:

☐ Check payable to the Superintendent of Documents
☐ GPO Deposit Account ☐☐☐☐☐☐☐–☐
☐ VISA or MasterCard Account
☐☐☐☐☐☐☐☐☐☐☐☐☐☐☐☐
☐☐☐☐ (Credit card expiration date)

To fax your orders (202) 512-2104

_____
(Authorizing Signature)

Mail to: Superintendent of Documents
P.O. Box 979050, St. Louis, Missouri 63197
Tel. no. (U.S. callers): 866-512-1800
Tel. no. (International callers): 1-202-512-1800

Thank you for your order!

Also available online at
http://bookstore.gpo.gov/actions/GetPublication.do?stocknumber=703-023-00000-2
email: ContactCenter@gpo.gov